UNIVERSITY OF CALABRIA

Department of Cell Biology

**Ph.D. in Molecular Bio-Pathology**
(Disciplinary Field BIO18-Genetics)

# Membrane Bio-Artificial Systems for Liver and Neuronal Tissue Engineering

Candidate
Antonella Piscioneri

Supervisor
Dr. Loredana De Bartolo

Co-ordinator
Prof. Giuseppe Passarino

CICLO XXIII

2010

# *INDEX*

# Sommario

I notevoli progressi nel campo dei biomateriali hanno reso possibile l'impiego di polimeri sintetici e naturali in svariate applicazioni dell'ingegneria tissutale e della medicina rigenerativa.

Il microambiente tridimensionale che circonda le cellule in vivo esercita un ruolo fondamentale nei processi di rigenerazione, mantenimento e riparazione tissutale, pertanto una dettagliata conoscenza a livello strutturale e funzionale del tessuto di interesse è fondamentale per un efficente contributo dell'ingegneria tissutale.

Un approccio interessante nell'ambito della medicina rigenerativa è rappresentato dall'uso di diversi biomateriali, costituiti da componenti biologiche, sintetiche, o da entrambre, capaci di agire come "materiali instruttivi" simulando e ricreando il naturale microambiente cellulare. L'impiego delle membrane polimeriche nell'ambito dell'ingegneria tissutale, grazie alle loro caratteristiche di stabilità, biocompatibilità nonchè di permeabilità selettiva, suscita notevole interesse e si rivela particolarmente promettente.

Il vantaggio fornito dalle membrane polimeriche consiste infatti, nella capacità di simulare la matrice extracellulare, consentendo e promuovendo il ripristino di una citoarchitettura tridimensionale ed il trasporto selettivo di metaboliti e nutrienti verso il compartimento cellulare e l'allontanamento dei cataboliti dallo stesso.

È importante sottolineare come, nell'ambito delle applicazioni dell'ingegneria tissutale, il tipo di membrana polimerica da adoperare dipende strettamente dalle proprietà e caratteristiche istologiche, fisiologiche e biomeccaniche possedute dal tessuto da ingegnerizzare. Le membrane polimeriche semipermeabili forniscono un adeguato supporto meccanico e chimico, capace di modulare i processi fondamentali alla base della rigenerazione tissutale quali l'adesione, la proliferazione e la differenziazione cellulare; esse infatti, agendo come barriere selettive, garantiscono un trasferimento altamente controllato di materia, da e verso il compartimento cellulare, ricreando un microambiente *in vitro* le cui caratteristiche riproducono la peculiarità del microambiente presente *in vivo*.

All'interno del nostro corpo le cellule sono naturalmente circondate dalla matrice extracellulare, la quale fornisce al tessuto, mediante segnali chimici e topografici,

l'idoneo supporto fisico e meccanico per il mantenimento di un'architettura tridimensionale; pertanto, riproducendo il ruolo svolto dalla matrice extracellulare, le membrane polimeriche possono fornire alle cellule gli stessi segnali chimici, fisici e topografici forniti in vivo dalla complessa matrice extracellulare. Ciò che rende ancora più vantaggioso l'impiego delle membrane polimeriche è la possibilità di modificare ed ingegnerizzare le loro superfici mediante legame di sequenze peptidiche, proteine e specifici fattori di riconoscimento, al fine di migliorare l'interazione cellula-substrato, elicitando così le specifiche risposte cellulari, con conseguente mantenimento delle integre funzionalità del distretto tissutale. Il punto focale delle applicazioni a lungo termine di ingegneria tissutale e medicina rigenerativa è, quindi, lo sviluppo di nuovi biomateriali capaci di consentire il differenziamento cellulare così come di evocare specifiche risposte cellulari.

Le acquisite e sempre crescenti conoscenze nell'ambito delle tecniche di preparazione delle membrane polimeriche e la capacità di monitorare e variare le loro caratteristiche in funzione del tipo di applicazione hanno reso possibile la realizzazione di nuove membrane da impiegare per l'allestimento di colture cellulari in sistemi bioibridi a membrana; tali dispositivi, definiti biobridi perchè costituiti da una componente biologica quali le cellule, ed una sintetica, cioè la membrana, possono essere utilizzati per fini terapeutici, o come ottime piattaforme in vitro per studiare l'effetto di diversi farmaci e sostanze xenobiotiche sul metabolismo cellulare.

Sulla base delle precedenti considerazioni il principale obiettivo di questa tesi è stato lo sviluppo di diversi sistemi bioibridi a membrana per applicazioni nel campo dell'ingegneria tissutale epatica e nel campo delle neurobiotecnologie. Come componente cellulare sono stati usati rispettivamente progenitori epatici e cellule neuronali, allo scopo di sottolineare l'ampio spettro di applicazione e il grande contributo dato dai sistemi a membrana nel campo della medicina rigenerativa.

Nella prima parte del lavoro sperimentale (capitoli 4 e 5), sono stati impiegati diversi tipi di membrane per l'espansione e la differenziazione di progenitori epatici, mentre nella seconda parte (capitolo 6) è stato realizzato un sistema bioibrido a membrana, in due diverse configurazioni, per la crescita ed il mantenimento in coltura di neuroni piramidali isolati dall'ippocampo. Per la realizzazione del sistema bioibrido riguardante l'impiego di progenitori epatici, sono state utilizzate cellule embrionali di ratto (RLC-

18) come modello di studio alternativo all'impiego di cellule progenitrici umane il cui utilizzo avrebbe sollevato problematiche dal punto di vista etico. Il primo stadio della strategia sperimentale è stato focalizzato all'espansione e differenziazione di cellule epatiche embrionali di ratto su membrane polimeriche di nuova sintesi. In particolare, è stata adoperata una membrana bioattiva sviluppata a partire da un blend di soluzione polimerica costituita dal polietereterchetone modificato (PEEK-WC) e Poliuretano (PU). L'impiego di questa membrana è doppiamente vantaggioso grazie alla combinazione delle ottime proprietà dei polimeri utilizzati (biocompatibilità, resistenza termica e meccanica, elasticità) con quelle intrinseche delle stesse membrane (permeabilità, selettività e geometria ben definita).

Poichè i progenitori epatici sono cellule ancoraggio-dipendenti e, pertanto, altamente sensibili al milieu fornito dalla matrice extracellulare, è stata messa a punto una modifica della superficie della suddetta membrana al fine di migliorare l'adesione cellulare e, conseguentemente la vitalità. In letteratura sono riportate diverse tecniche per la modifica delle superfici delle membrane; esse spaziano dal semplice coating con proteine della matrice extracellulare, alla coniugazione di molecole peptidiche o galattosio, fino al grafting superficiale con specifici gruppi funzionali.

In questo studio, la superfice della membrana di PEEK-WC-PU è stata funzionalizzata con un coating stabile di gruppi $NH_3$ mediante tecnica di deposizione al plasma, al fine di investigare se la biofunzionalizzazione della mebrana potesse elicitare l'espansione, il differenziamento e, pertanto l'acquisizione delle funzionalità specifiche tipiche delle cellule epatiche adulte. Tra le varie modifiche di membrana la funzionalizzazione mediante gruppi $NH_3$, consente di aumentare la polarità della superfice e di avere su di essa e quindi a diretto contatto con le cellule in coltura, gruppi chimici, tipici delle proteine, capaci di favorire l'adesione e le funzioni cellulari. La membrana di PEEK-WC-PU modificata e non modicata, è stata utilizzata su scala di laboratorio in un bioreattore piano permeabile all'ossigeno al fine di valutare la morfologia e le specifiche attività funzionali delle cellule epatiche una volta a contatto con le diverse membrane. Per testare la validità delle due membrane nel mantenere cellule adese e vitali.sono stati effettuati la quantizzazione della lattato deidrogenasi (LDH), e l'analisi al microscopio a scansione elettronica (SEM).

L'acquisita capacità delle cellule progenitrici di svolgere specifiche funzioni tipiche del tessuto epatico è stata investigata in termini di produzione di albumina e sintesi di urea. Al fine di valutare se i progenitori epatici abbiano effettivamente raggiunto un fenotipo prossimo a quello delle cellule epatiche mature è stata investigata l'espressione genica dell'alfafetoproteina (AFP) e dell'albumina. L'effetto del nuovo microambiente, rappresentato dalla membrana, è stato ulteriormente approfondito mediante la valutazione della senescenza e dell' invecchiamento cellulare attraverso monitoraggio dell'attività telomerasica, mentre l'influenza esercitata sulla proliferazione è stata valutata mediante analisi del ciclo cellulare (FACS). Tutte le operazioni sperimentali sono state parallelamente condotte su substrati di riferimento, quali il collagene e le tradizionali piastre di polistirene. I dati ottenuti in questa prima parte, hanno evidenziato che i bioreattori adoperanti sia la membrana nativa che quella funzionalizzata sono capaci di supportare l'espansione dei progenitori epatici e soprattutto di indurre e sostenere la loro integrità funzionale. Le cellule hanno mostrato un incremento dell'attività telomerasica su entrambe le membrane, acquisendo peculiari caratteristiche delle cellule epatiche come evidenziato dai livelli di produzione di albumina e sintesi di urea. Inoltre, l'analisi dell'espressione genica ha evidenziato un incremento dell'espressione del gene dell'albumina parallelamente ad un decremento osservato per l'AFP, indicando chiaramente l'acquisizione di un fenotipo diffrenziato durante il periodo di coltura.

Nelle moderne applicazioni dell'ingegneria tissutale, i polimeri biocompatibili e, soprattutto, biodegradabili sono stati proposti come materiali innovativi capaci di promuovere e supportare la crescita e la differenziazione cellulare, contribuendo, auspicabilmente, alla realizzazione di un costrutto epatico ingegnerizzato da impiegare in applicazioni cliniche e farmaceutiche. A tale scopo durante questo lavoro di tesi, è stata realizzata una membrana biodegradabile di chitosano. In particolare è stata investigata e messa a confronto la capacità delle membrane di chitosano e PEEK-WC di agire come materiale "instruttivo", che fornendo alle cellulle embrionali di ratto gli idonei stimoli chimici e fisici, ne sostiene l'espansione e ne guida la diffrenziazione funzionale. Il collagene e le tradizionali piastre di polistirene sono stati utilizzati come substrati di riferimento. Il chitosano è composto da residui di N-acetilglucosammina uniti tra di loro da legami β-1,4; si tratta di un polisaccaride naturale sintetizzato da

diversi organismi viventi (lo si ritrova per esempio nell' esoscheletro dei crostacei) ed è naturalmente degradato dagli enzimi del nostro corpo. Questo biopolimero è stato ampiamente utilizzato nel campo delle applicazioni biomedicali per le sue caratteristiche di biocompatibilità, rivelandosi particolarmente vantaggioso per la coltura di cellule epatiche grazie alla sua similarità strutturale con i glicosamminoglicani, componenti fondamentali della matrice extracellulare epatica. Le membrane di chitosano e di PEEK-WC hanno subito una caratterizzazione chimico fisica; lo swelling e il grado di dissoluzione sono state parallelamente analizzati poichè queste due proprietà sono di fondamentale importanza per una buona performance a lungo termine di un costrutto ingegnerizzato.

Per il mantenimento di cellule in coltura vitali e funzionalmente attive è necessario che esse mantengano una morfologia simile a quella posseduta in vivo ed, a tal fine, i cambiamenti morfologici delle cellule in coltura sono stati monitorati mediante microscopia a scansione elettronica (SEM) e, più approfonditamente mediante microscopia confocale (LCSM) in seguito ad immunofissazione di proteine del citoscheletro e della matrice extracellulare (ECM). Gli effetti dei diversi substrati sono stati anche analizzati in termini di incidenza sulla proliferazione cellulare, tramite analisi quantitativa della stessa. Attraverso la determinazione della produzione di albumina e sintesi di urea è stata valuata l'acquisizione della differenziazione funzionale da parte delle cellule progenitrici epatiche. Poichè il fegato èl'organo deputato alla detosifficazione delle sostanze xenobiotiche, come ulteriore funzione specializzata è stata indagata la capacità delle cellule di metabolizzare il Diazepam; a tal fine le cellule sono state incubate con Diazepam (10 μg/ml) in diverse fasi della coltura, e successivamente ne è stata valutata l'eliminzione e la formazione dei suoi metaboliti. La differenziazione funzionale è stata ulteriormente investigata attraverso tecnica di Western Blot che ha consentito di identificare il profilo di espressione proteico di alcuni markers epatici, come l'albumina, espressa dagli epatociti maturi, l'alfafetoproteina (AFP) che è tipicamente espressa dagli epatoblasti, ed infine la citocheratina 18 (CK18) una proteina espressa in diverse cellule del tessuto epatico. Dalla conduzione di questi esperimenti sono stati ottenuti risultati promettenti come si evince dall'osservazione della ricreazione di una citoarchitettura ben organizzata e dal mantenimento di una morfologia cellulare simile a quella del parenchima epatico; le cellule hanno esibito

infatti, una morfologia poligonale tipicamente posseduta dagli epatoci in vivo. Tali evidenze sottolineano che le membrane impiegate hanno fornito ai progenitori un ottimo microambiente nel quale riorganizzarsi secondo una morfologia consona al mantenimento della funzionalità cellulare. L'elevata attività metabolica in termini di produzione di albumina e sintesi di urea, osservabile specialmente sulla membrana di chitosano, ha indicato inoltre come questa membrana abbia effettivamente indirizzato le cellule verso la differenziazione. Tale evidenza è stata avvalorata dall'abilità delle cellule di metabolizzare il diazepam; é bene evidenziare come solo le cellule piastrate su chitosano e su collagene, il substrato naturale delle cellule epatiche, siano state capaci di formare l'intero pool di metaboliti del diazepam sin dalla prima somministrazione. L'ulteriore conferma dell'acquisite funzionalità specifiche del tessuto epatico, è stata dimostrat dalla forte espressione, evidenziata mediante western blot, della proteina albumina. Negli ultimi anni la ricerca nel campo della bio-ingegneria si è concentrata sulla realizzazione di sistemi artificiali costituiti da scaffold e cellule, da impiegare in fenomeni altamenti complessi come la riparazione e rigenerazione neuronale.

L'ultima fase del lavoro sperimentale è consistito nella realizzazione di un sistema bioibrido a membrana per applicazioni nel campo delle neurobiotecnologie. Le membrane polimeriche semipermeabili giocano un ruolo fondamentale in questo settore poichè che costituiscono un valido supporto per le cellule all'interno del sistema bioibrido. Esse contribuiscono, quindi, in maniera sostanziale alla realizzazione di dispositivi per la ricostruzione in vitro di un network neuronale che esibirà le tipiche caratteristiche morfologiche e funzionali delle cellule neuronali e potrà essere utilizzato come modello per lo studio della fisiologia neuronale. È in questo contesto che si inserisce la fase finale del lavoro sperimentale, che mira, pertanto, alla realizzazione di un sistema bioibrido a membrana per la coltura di neuroni piramidali isolati dall'ippocampo, regione cerebrale coinvolta in importanti funzioni neurofisiologiche, quali l'apprendimento e la memoria. L'utilizzo di membrane in configuarazione differente ha permesso di confrontare in vitro la crescita assonale e la ricostruzione di un network neuronale in sistemi bidimensionali (membrane piane) e tridimensionali (membrane in configurazione a fibra cava, HF ) e di confrontare lo sviluppo e la direzionalità dei processi neuritici nei due sistemi. Le membrane sia in configurazione piana che a fibra cava sono state realizzate attraverso la tecnica dell'inversione di fase a

partire da due differenti polimeri: il poliacrilonitrile (PAN) e il polietereterchetone modificato (PEEK-WC). Le membrane così realizzate sono state caratterizzate allo scopo di valutare le loro proprietà morfologiche, chimico-fisiche e di trasporto, e previo piastramento cellulare, sono state modificate con un coating di poli-L-lisina (PLL) allo scopo di favorire l'adesione cellulare e ricreare superfici aventi gli stessi gruppi funzionali a contatto con le cellule. Per valutare la validità del sistema bioibrido a membrana e paragonare gli effetti del sistema bidimensionale e tridimensionale, sono stati investigati lo sviluppo, il differenziamento e l'attività metabolica dei neuroni ippocampali isolati. Lo sviluppo ed il differenziamento delle cellule in coltura sono stati valutati attraverso l'osservazione dei possibili cambiamenti morfologici. L'analisi al microscopio a scansione elettronica ed al microscopio confocale all'ottavo e dodicesimo giorno di coltura, ha fornito importanti informazioni sui meccanismi di adesione al substrato, così come sull'organizzazione spaziale delle cellule in coltura. L'adeguato sviluppo del network neuronale è stato monitorato mediante localizzazione, distribuzione e quantizzazione di marcatori strutturali come la β-tubulina III, una proteina associata al citoscheletro e presente nel soma e in tutti i peolungamenti neuronali, e la GAP43, una proteina specifica dei prolungamenti assonali. La valutazione della morfologia è stata completata mediante analisi morfometrica per quantizzare la lunghezza assonale e dendritica e valutare la l'area della membrana ricoperta dalle cellule. La vitalià ed il metabolismo cellulare è stato indagato in termini di consumo di glucosio e produzione di lattato nel mezzo di coltura; la specifica attività funzionale è stata studiata mediante quantizzazione della secrezione di un fattore neurotrofico specifico, quale il Brain Derived Neurotrophic Factor (BDNF). Infine mediante real time PCR è stato studiato il profilo di espressione genica della MAP2 (microtubule-associate protein) e del GluR2 (glutammate receptor subtype 2), la cui regolazione è altamente critica per lo sviluppo dei neuroni ippocampali, intervenendo nel corretto sviluppo citoscheletrico e nel processo di formazione sinaptica rispettivamente.

I risultati conclusivi di questo lavoro evidenziano come sia le membrane in configurazione che a fibra cava sono in grado di supportare l'adesione e la crescita dei neuroni ippocampali, inducendone la loro differenziazione e polarizzazione. In particolare i migliori risultati sono stati ottenuti utilizzando la membrana di PAN a

configurazione tubulare; le prestazioni superiori del PAN HF, rispetto alle altre membrana in configurazione piana sono probabilmente da addurre alla sua geometria tridimensionale. A parità di conformazione, il PAN HF è risultato superiore al PEEK-WC HF, per la sua maggiore permeabilità, caratteristica, questa, che favorisce lo scambio e la diffusione di metaboliti e cataboliti, promuovendo l'adesione e la crescita delle cellule piramidali.

Un innovativo approccio nel campo delle neurobiotecnologie è basato sull'introduzione di specifiche modifiche strutturali al fine di ricreare un microambiente che possa fornire gli adeguati stimoli topografici, promuovendo l'adesione, la crescita e la polarizzazione dei neuroni. Poiché i neuroni in coltura sono capaci di modulare la loro risposta al variare dello stimolo topografico fornito, nell'ultima parte del lavoro sperimentale (capitolo 7) e' stato indagato il comportamento di neuroni piramidali ippocampali coltivati su membrane di acido polilattico le quali presentano sulla superficie specifici e ripetuti micropattern strutturali. La citoarchitettura e l'attività metabolica dei neuroni e' stata esaminata e messa a confronto sia coltivando le cellule su membrane strutturalmente modificate sia su membrane non modificate, utilizzando il polistirene come substrato di riferimento. L'acido polilattico e' un polimero biodegradabile, ampiamente utilizzato per le applicazioni biomedicali grazie alla sua comprovata biocompatibilità. Le membrane strutturalmente non modificate esibiscono una superfice piane, quelle invece modificate possiedono una superficie tridimensionale in seguito alla presenza di unità strutturali ripetute sulla loro superficie, quali canali e righe canali interconnessi. La morfologia e l'adesione cellulare e' risultata essere particolarmente suscettibile ed influenzabile dalla forma della ripetizione strutturale presente sulle diverse superfici di membrana. Infatti, sui substrati strutturalmente omogenei e, quindi piani, non si osserva una specifica direzionalità dei neuriti, che invece risultano omogeneamente distribuiti su tutta la superficie, al contrario, sui substrati strutturalmente modificati i neuriti si distribuiscono linearmente lungo le scalanature presenti sulla superfice. Questa differenza è essenzialmente dovuta alla presenza dei ripetuti microelementi sotto forma di canali, solchi e righe e canali interconnessi, che in seguito alla loro presenza riduco l'area di adesione cellulare e inducono il preciso orientamento dei microtubuli e dei filamenti di actina, direzionando lo sviluppo dei prolungamenti neuronali. L'organizzazione spaziale e l'area ricoperta

dalle cellule sui diversi substrati e' stata investigata mediante microscopia confocale e microscopio a scansione elettronico, rivelando una significativa crescita con il progredire dei giorni di coltura. La localizzazione e quantizzazione della GAP 43, uno specifico marker assonale, ha consentito di valutare la crescita assonale. La vitalità e la funzionalità cellulare è stata investigata in termini di consumo di glucosio, produzione di lattato e secrezione della neurotrofina BDNF. I risultati ottenuti, stabiliscono il prominente ruolo svolto dalle unità microstrutturali ripetute presenti sulle membrane nell'indurre un preciso orientamento neuronale lungo le suddette, indicando che queste membrane sono capaci di ricreare in vitro una matrice neuronale altamente ordinata.

Alla luce delle considerazioni riportate, si evince il vantaggio dell'impiego dei sistemi a membrana ed il potenziale contributo che questi sistemi possono offrire nella risoluzione di diversi problemi di interesse nel campo della tissue engineering e della medicina rigenerativa.

# Summary

In recent years, rapid progress has been made in the field of the biomaterials, which utilize both natural and synthetic polymers in a variety of application in tissue engineering and regenerative medicine.

It became clear over the years that functional tissue engineering requires detailed knowledge on the structure and function of the tissue of interest at various length scales varying from the subcellular (nm-μm) to the tissue (mm-cm) level. In particular, the importance of the three-dimensional (3D) microenvironment of the cells is emphasized nowadays as key-regulator of tissue generation, maintenance and repair.

A promising approach for the in vitro re-creation of the cell-niche can be achieved by using different biomaterials, composed of either biological compounds, synthetic polymer, or a combination thereof, that acts as "INSTRUCTIVE MATERIAL", inspired by the nature. Among polymeric materials, membranes are the most attractive in the use of bioartificial systems for their characteristics of stability, biocompatibility and selective permeability.

Polymeric membranes could mimic the extracellular matrix with which cells interact allowing the organization of the cells into a three-dimensional architecture, and the selective transport of metabolites and nutrients to cells and the removal of catabolites and specific products from cells.

The suitability of polymeric membranes for tissue engineering purposes is highly dependent on the histological, physiological and biomechanical properties of the tissue that needs to be engineered. The membranes would be able to modulate the adhesion, proliferation and differentiation of cells, which are fundamental processes for tissue regeneration by governing the mass transfer of molecules that generate a precisely controlled microenvironment that mimic the specific features of in vivo environments.

In vivo cells are surrounded by the extracellular matrix (ECM) that provides physical architecture and mechanical strength to the tissue through patterns of chemistry and topography from macroscale to nanoscale. Bioactive membranes should provide to the cells chemical, physical and topographical features similar to those of the complex in vivo ECM. In addition, the membrane surface can be tailored with proteins, peptides and cell-specific

recognition factors by modification processes in order to stimulate specific cell responses and maintain differentiated functions.

The development of new biomaterials able to activate specific response of the cells and to maintain cell differentiation for long time is one of the most pertinent issues in the field of tissue engineering and regenerative medicine. Progress in polymeric membrane preparation and in the understanding and control of their properties make possible the design of novel membranes to be used for cell culture in biohybrid systems such as therapeutic device or as in vitro model systems for studying the effects of various drugs and chemicals on cell metabolism.

On the basis of these considerations, the main objective of this thesis is the development of membrane bio-hybrid systems for the realization of tissue engineered constructs by using progenitor liver cells and neuronal cells, demonstrating the wide range of applications of membrane systems, as well as their contribution, in the field of tissue engineering and regenerative medicine. In particular, in the first part, two different kinds of membrane approaches were used for the expansion and differentiation of progenitor liver cells, while in the second part, a membrane bio-hybrid system in two different configurations was used for the maintenance and growth of neuronal cells isolated from hippocampus.

As a first step of the experimental work, the expansion and differentiation of rat embryonic liver cells on novel bioactive membranes was carried out. Rat embryonic liver cells (17 day embryos) (RLC-18) were used in this study as an alternative model of human liver progenitor cells, since using cells from the foetal human liver is limited by major ethical issues.

A novel bioactive membrane has been developed from a polymeric blend of modified polyetheretherketone (PEEK-WC) and polyurethane (PU) as support for liver cell culture. This membrane combines advantageous properties of both polymers (biocompatibility, thermal and mechanical resistance, elasticity) with those of membranes (permeability, selectivity and well defined geometry).

Since the progenitor liver cells are anchorage-dependent cells and are highly sensitive to the Extra Cellular Matrix (ECM) milieu, a modification of the membrane surface with specific functional groups have been used to improve cell adhesion and viability. Several surface modification techniques have been proposed to optimize specific interactions between cells and substrates including coating substrates with ECM proteins (e.g., collagen, laminin,

fibronectin), conjugation with peptide or galactose moieties, or grafting with functional groups.

For this study PEEK-WC–PU membranes were modified with an NH3 glow discharge plasma, aiming to graft nitrogenated functionalities at their surface, in order to investigate whether the biofunctionalized membrane could elicit the expansion as well as to induce and maintain the differentiated specific function of the progenitor liver cells. Among several surface modification strategies, grafting of N-containing functional groups allows to increase the polarity of the surface and to have chemical groups typical also of proteins that could support cell adhesion and functions.

Both native and plasma-grafted membranes were used in a small-scale gas-permeable flat membrane bioreactor in order to compare the morphological behavior and specific functions of the liver cells on the modified and unmodified membranes. LDH assay and SEM analyses were used to verify if the membranes were useful for the maintenance of viable cells attached to the membranes. In particular, the ability of the progenitor cells of gaining the ability to perform their specific liver functions was investigated in terms of albumin production and urea synthesis. To further investigate if the cells were able to reach a differentiated state, losing their progenitor phenotype, alpha-fetoprotein (AFP) and albumin gene expressions of cells, expanded in the different investigated systems, was also carried out. The effect of the new microenvironment provided by the membranes on cellular behaviour was further investigated. The cellular senescence and aging, that are critical for cell viability, were measured through the evaluation of the telomerase activity of embryonic liver cells, employing a PCR–ELISA technique; finally the ability of the substrate to influence cell proliferation was evaluated by means of cell cycle analysis. In this work all the evaluations have been done in parallel with conventional substrates such as collagen and polystyrene culture dishes (PSCD) representing the reference substrates.

The complete pool of the obtained data, in this first part, showed that the bioreactors with the native and plasma grafted PEEK-WC-PU membranes were able to support the expansion of the progenitor liver cells and above all to induce and sustain their differentiated functional integrity. In fact, the cells displayed an increased telomerase activity on both membranes as well as a the gain of different liver features, as showed by the levels of albumin synthesis and urea production. Furthermore, the increased gene expression of albumin and the decresead of

AFP ones, proved that on the membranes, the progenitor liver cells were able to acquire a differentiated phenotype during the investigated culture time.

Nowadays biocompatible and biodegradable materials have been proposed to support cells and promote their differentiation, and proliferation towards the formation of an engineered liver tissue is desired in clinical and in pharmaceutical applications. To match this demand in this thesis a new biodegradable membrane made up of chitosan was realized. The ability of chitosan and PEEK-WC membranes to promote the expansion and functional differentiation of rat embryonic liver cells was investigated; these two membranes, providing the right physical and chemical signals can act as instructive material. Also in this case traditional systems such as polystyrene culture dishes (PSCD) and natural substrate were used as references.

Chitosan is the N- deacetylated derivative of chitin, a cationic polysaccharide composed of glucosamine and N-acetylglucosamine residues with 1,4-β-linkage, that is a component of the shell of crustacean, such as crab, shrimp, cuttlefish and is naturally degraded by the body enzymes.

Due to its excellent biocompatibility and bioadsorbility, chitosan has been used in biomedical applications (e.g., artificial skin, drug delivery vehicles, hemodialysis, nerve), and therefore membranes prepared from chitosan can be advantageous for liver tissue engineering because of their similar structure of glycosaminoglycans, which are components of the liver extracellular matrix. Furthermore, chitosan's positive surface charge and biocompatibility enable it to effectively support the cell growth.

For the pivotal role played by the cell-membrane interaction, both membranes were fully characterized in terms of chemical and physical properties; the swelling behaviour and the degree of dissolution of the chitosan membrane were also evaluated since these parameters are crucial to achieve an efficient long-term performance of tissue-engineered construct. It is well established that the maintenance of a cell morphology similar to that in vivo is of primary importance for the development, expression and maintenance of hepatic differentiated functions, therefore the structural and morphological changes of the cells were monitored by SEM images and more deeply by LCSM after cytoskeleton and ECM protein immunostaining. The effect of the different substrates was also determined by quantitative analysis of cell proliferation. In order to determine if both chitosan and PEEK-WC membranes could commit the functional differentiation of the rat embryonic liver cells, liver-

specific functions were investigated in terms of albumin production and urea synthesis. The ability of the cells to perform drug biotransformation was evaluated after providing them diazepam (10 μg/ml), and evaluating its elimination and the formation of its metabolites over time. The functional differentiation of the progenitor liver cells was further assessed by Western Blot analysis, through the study of the expression pattern profile of some different specific proteins such as albumin, that is a typical marker of mature hepatocytes, the AFP, a marker of hepatoblast that are bipotent cells, and the CK18 a marker expressed by several liver cell type.

From these experiments promising results were obtained; indeed, the tissue architecture distribution and the maintenance of a parenchimal cell morphology with a polygonal shape typical of the hepatocytes in vivo, underlining that the membranes provided an optimal microenvironment to the progenitor liver cells. The high rate of metabolic activity of the specific liver functions performed by the cells, showed that the intrinsec characteristics of the chitosan membrane favoured and guided the cells towards the differentiations. This evidence is strongly supported by the ability of the cells to biotrasform the diazepam; moreover, this latter is worth to note that only the cells cultured on the chitosan membrane and on collagen, which is the natural hepatocytes substrate, were able to produce the complete pool of the diazepam metabolites from the first administration. The urea synthesis and albumin production was maintained at high levels, especially on the chitosan membrane. The functional differentiation is further confirmed by the strong immunodetection of albumin, that is a key features of the hepatic differentiation.

In the second part of the thesis the use of membrane system as a tool for neurobiotechnology application is proposed and developed. At present a great deal of attention is given towards the possibility of replacing or restoring the structural organization of damaged neural regions by developing artificial systems based on biomaterials scaffold and cells. In this context, once again the polymeric semi-permeable membrane could be the right support for the maintenance of the cell growth in a bio-hybrid system, representing also a valuable tool to be used as a physiological model in neuronal study. With this aim, taking into account, the highly structural anatomical organization in the nervous system, in this thesis the attention has been focused on the potential value of this biotechnological approach to a functionally key region of the brain such as the hippocampus, that is involved in several important neurophysiologic functions, such as learning and memory. Therefore, a membrane bio-hybrid system,

constituted of isolated pyramidal neurons and membranes, has been developed. New polymeric membranes in different configurations have been used in two- and three-dimensional culture systems in order to compare their performance in favouring and enhancing the reconstruction of a highly branched neuronal network as well as in inducing their orientation and the neuronal outgrowth. The membranes were prepared through the phase inversion technique by using two different polymer solutions made of the modified polyetheretherketone (PEEK-WC) and polyacrilonitrile (PAN) membranes, in both flat and hollow fiber configurations. These membranes were characterized evaluating the morphological, physico-chemical and transport properties, and were modified by coating with poly-L-lysine (PLL), in order to have the same functional groups interacting with the cells. In order to evaluate the suitability of the membrane bio-hybrid system for the reconstruction of the neuronal network and to compare the performance of the bidimensional and threedimensional system, the growth and the differentiation as well as the specific metabolic functions of the hippocampal neurons were investigated. The determination of structural and functional cell features have been carried out through the observation of possible morphological changes. Indeed, the electronical microscopy analysis gave interesting information on both the adhesion mechanisms to the substratum and space organization of neuronal cells. The morphological behaviour of hippocampal neurons was evaluated by SEM and confocal microscopy after 8 and 12 days of culture. The correct and stable hippocampal neuronal formation was supported by the evaluation, distribution and quantification, through LCSM analysis, of specific structural markers, such as GAP-43 and β-III tubulin. To further explore cell morphological features was performed a morphometric analysis in order to establish the axonal length as well as evaluating the membrane surface covered by the cells. The viability and metabolic functions were evaluated in quantitative terms via the determination of glucose consumption and lactate production. As specific differentiated activity was traced the secretion of the brain derived neurotrophic factor (BDNF), a neurotrophin that is an important indicator of the survival and differentiation of specific neuronal populations. Finally, through qRT-PCR, the expression of microtubule-associated protein (MAP2) and glutamate receptor subtype 2 (GluR2) gene expression were evaluated, which are known to be critically regulated for hippocampal neurons during the development of cytoskeleton and synaptic formations, respectively.

As a result from this study, it is possible to conclude that both 2D and 3D membranes support the adhesion and growth of hippocampal neurons, enhancing as well the neuronal differentiation and neurite alignment. In particular the best results were obtained by using the 3D PAN HF; this is probably due both to its geometry, with respect to the 2D membrane, and its higher permeability, with respect to the PEEK-WC HF membrane, that favours the diffusive exchange of metabolites and catabolites, enhancing the adhesion and outgrowth of the pyramidal cells.

Recent developments in biomaterial modifications are aimed to stimulate the microenvironment in which cells are cultured, in order to promote neuron adhesion, growth and especially polarization. The neurons have the ability to respond to topographical stimuli, and a particular application is represented by nano- and microtopographical features that can be incorporated into tissue-engineering design strategies to provide contact guidance for nerve regeneration. In the last part of the thesis, the behavior of hippocampal neuronal cells in terms of polarization and orientation on nonpatterned and micro-patterned biodegradable poly ($_L$-lactic acid) (PLLA) membranes was investigated. The PLLA is a biocompatible and biodegradable polymer, widely used in biomedical application thanks to its adjustable degradation rate that can match that one of the tissue formation. The non patterned membranes exhibit a flat structure, whereas the patterned membranes have a tree-dimensional one with channels plus ridge and bricks. Changes in morphological and functional behaviors of cells were evaluated and compared on both patterned and non patterned surface as well as on the traditional polystyrene culture dishes (PSCD) used as reference systems. The shape of the membrane pattern strongly affected the morphology and the adhesion of the cells as showed by SEM and LCSM analyses. Neurites on all investigated patterned membranes linearly extended along the grooves of micropatterns whereas no guidance of neurite outgrowths was observed on PSCD and on non patterned membranes. These differences are determined by the presence of the channel an the ridge that limits the adhesion area available for the cells and establish a precise direction towards the microtubules and act in filaments can accumulate and orient the filopodia.

The spatial organization of the cells on the different substrates was further investigated by confocal microscopy analysis quantifying the fluorescence average intensity of stained cytoskeletal protein and nucleic acid. The use of SEM images after 8 and 12 days of culture allowed to measure the area covered by the cells that increased significantly with time. The

staining of a specific axonal marker, GAP 43, allowed to measure the axonal length over the entire culture period. The metabolic activity was evaluated in terms of glucose consumption, lactate production and BDNF secretion, in order to obtain information about the viable status of the hippocampal cells on the different substrates. The results obtained strongly showed that the neuronal orientation follows the patterned surface of the PLLA membrane, indicating that this membrane is able to recreate in vitro and highly ordered neuronal cell matrix.

Concluding it is clear how the overall strategy of the work, therefore, was performed in order to highlight the important advantages of each of these membrane systems that might help in solving different problems of interest in the field of tissue engineering and regenerative medicine.

# CHAPTER 1

# FUNDAMENTALS OF TISSUE ENGINEERING

## 1.1 INTRODUCTION

Tissue loss or end-stage organ failure caused by injury or other types of damage is one of the most devastating and costly problems in human health care.

Surgical strategies that have been developed to deal with these problems include organ transplantation from one individual to another, tissue transfer from a healthy site to the diseased site in the same individual, and replacement by using mechanical devices such as joint prosthesis or dialysis machines.

Although significant advances have been achieved in terms of health care by these therapeutic options, many limitations and unsolved issues remain [1]

Organ transplantation is extremely limited by a critical donor shortage and the necessity of lifelong immunosuppression, in addition of requiring complex surgical intervention. The difficulties encountered in repairing or replacing severely damaged tissue may be resolved through a new promising field called tissue engineering [2].

Tissue engineering is "an interdisciplinary field that applies the principles of engineering and of life science towards the development of biological substitutes that restore, maintain or improve tissue or organ function" [3].

There are three general strategies for the application of tissue engineering: (i) use of an instructive environment (eg. bioactive material) to recruit and guide host cells to regenerate a tissue, (ii) delivery of repair cells and/or bioactive factors into the damaged area and (iii) cultivation of cells on or within biomaterial matrices in a culture system (bioreactor), under conditions designed to engineer a functional tissue [4].

All these strategies have the common and fundamental goal of reproducing an engineered environment that is able to recreate the structure and function of a specific tissue.

Currently, tissue engineering allows for several exciting possibilities, including the following three: (i) to create functional grafts for implantation and repair of failing tissues, (ii) to study the behavior and developmental processes of stem cells in the context of controllable three-dimensional (3D) models of engineered tissues, and (iii) to employ engineered tissues as models for physiology and disease studies [5–6].

The recreation of an experimental platform as a model system for studying biological mechanisms and testing the efficacy of potential therapies is a very promising

application that involves the *in vitro* seeding and attachment of cells. These cells then proliferate, migrate, and differentiate into the specific tissue while secreting the extracellular matrix (ECM) components required to create the tissue. It is evident, therefore, that the choice of the material is essential for the development and replication of an appropriate microenvironment for controlling and directing the cellular behaviour and promoting specific cell interactions.

## 1.2 IMPORTANCE OF CELL-MATRIX INTERACTION

Cells are inherently sensitive to physical, biochemical and chemical stimuli from their surrounding. *In vivo*, the local cell environment or "niche" provides specific environmental cues that determine cell-specific recruitment, migration, proliferation, differentiation and the production of the numerous proteins needed for hierarchical tissue organisation.

As a consequence, tissue dynamics, that is, tissue formation, function and regeneration after damage, as well as its function in pathology, is the result of an intricate temporal and spatial coordination of numerous individual cell fate processes, each of which is induced by a myriad of signals originating from the extracellular microenvironment. The growth and differentiation of most cell types is regulated by the interplay of different major signaling, environmental stress and physical cues from the biological matrix which surrounds the cells *in vivo*. In particular the extracellular microenvironment is a highly hydrated network hosting three different main effectors: (i) insoluble hydrated macromolecules (fibrillar proteins like collagens, noncollagenous glycoproteins such as elastin, laminin or fibronectin, and hydrophilic proteoglycans with large glycosaminoglycan (GAG) side chains) called physical signals (Figure 1.1), (ii) soluble macromolecules (growth factors, chemokines and cytokines), and (iii) proteins on the surfaces of the neighboring cells that establish the cell-cell interaction [7].

The biological response is influenced by multiple cellular interactions with the individual and specific ECM molecules and often with multiple sites within the same molecule as well as by a highly dynamic and complex array of biophysical an biochemical properties of the ECM. The cells are able to receive the external signals through different cell surface receptor of the integrin family and integrate it by an

intracellular signaling pathway that affect the cellular response in terms of gene expression, ultimately establishing the cell phenotype.

Thus, the final decision of a cell to differentiate, proliferate, migrate, apoptose, or perform other specific functions is a coordinated response to the molecular interactions with these ECM effectors [8]. It is worth to note that the flow of information between cells and their ECM is highly bidirectional, as, for example, observed in processes involving ECM degradation and remodeling. It is evident how native ECM exhibits macroscale to nanoscale patterns of chemistry and topography [9], and it is therefore somewhat unsurprising that cells respond to these various scales of chemically and/or topographically patterned features.

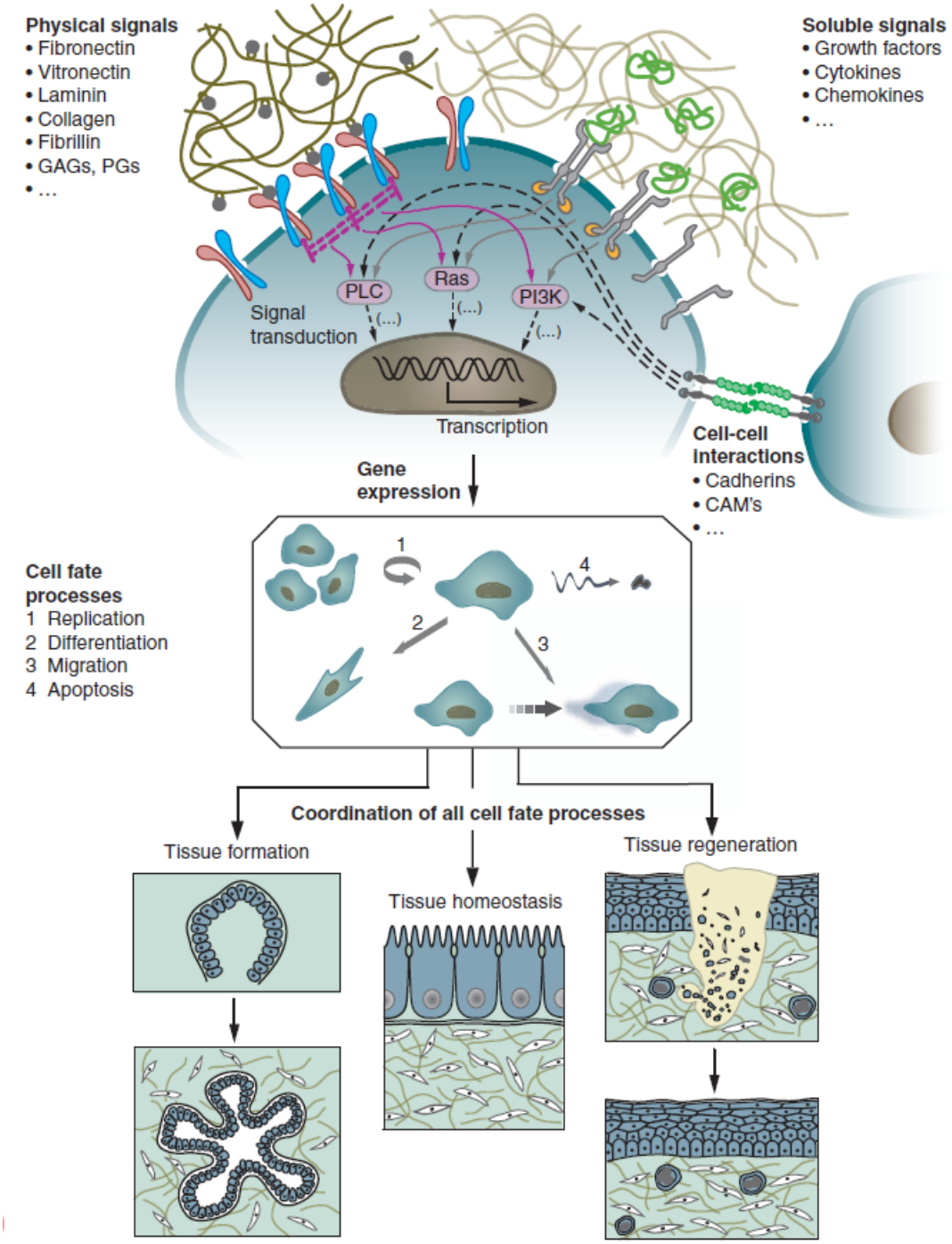


**Figure 1.1** The behavior of individual cells and the dynamic state of multicellular tissues is regulated by intricate reciprocal molecular interactions between cells and their surroundings. This extracellular microenvironment is a hydrated protein and proteoglycan-based gel network comprising soluble and physically bound signals as well as signals arising from cell-cell interactions. Adapted from : M P Lutolf and J A Hubbell Nature Biotechnology 2005; 23 (19) , 47-55 [7].

However, when cells are cultured *in vitro* or when materials are implanted into the body, cells encounter very different, unfamiliar surfaces and environments.

Since the ECM is the optimized milieu that nature has been developed for maintaining homeostasis and directing tissue development, a great effort has been made to mimic the ECM to guide morphogenesis in regenerative medicine. In this context the biomaterials play a pivotal role in the field of tissue engineering as designable biophysical and biochemical enviromental conditions that direct cellular behaviour and functions [10-11].

The guidance provided by biomaterials may facilitate restoration of the structure and function of damaged or dysfunctional tissues. Such materials should provide a provisional three dimensional (3D) support for a biomolecular interaction with cells to control their function, guiding the spatially and temporally complex multicellular processes of tissue formation and regeneration.

Different biomaterials have been proposed to support cells and promote their differentiation and proliferation toward the formation of a new tissue. Clearly, the design and selection of a biomaterial is of critical importance in the development of a construct for tissue engineering application.

An appropriate biomaterial must exhibit good biocompatibility with extremely low inflammatory, immunogenic, and cytotoxic responses, promoting favourable cellular connection and tissue development. In addition, it should be biodegradable and bioresorbable with the ideal rate of the new tissue formation, having at the same time good mechanical and chemical properties in order to promote an adequate cell-substrate interactions. Figure 1.2 shows the various characteristics desired for an ideal scaffold for tissue regeneration [12]. All these requirements can be achieved by innovative nanotechnology approaches, which allow the design and the modification of suitable biomaterials controlling and directing the cellular behaviour. Therefore, the development of biomaterials currently does, and will continue to, impose significant challenges in the field and history of tissue engineering

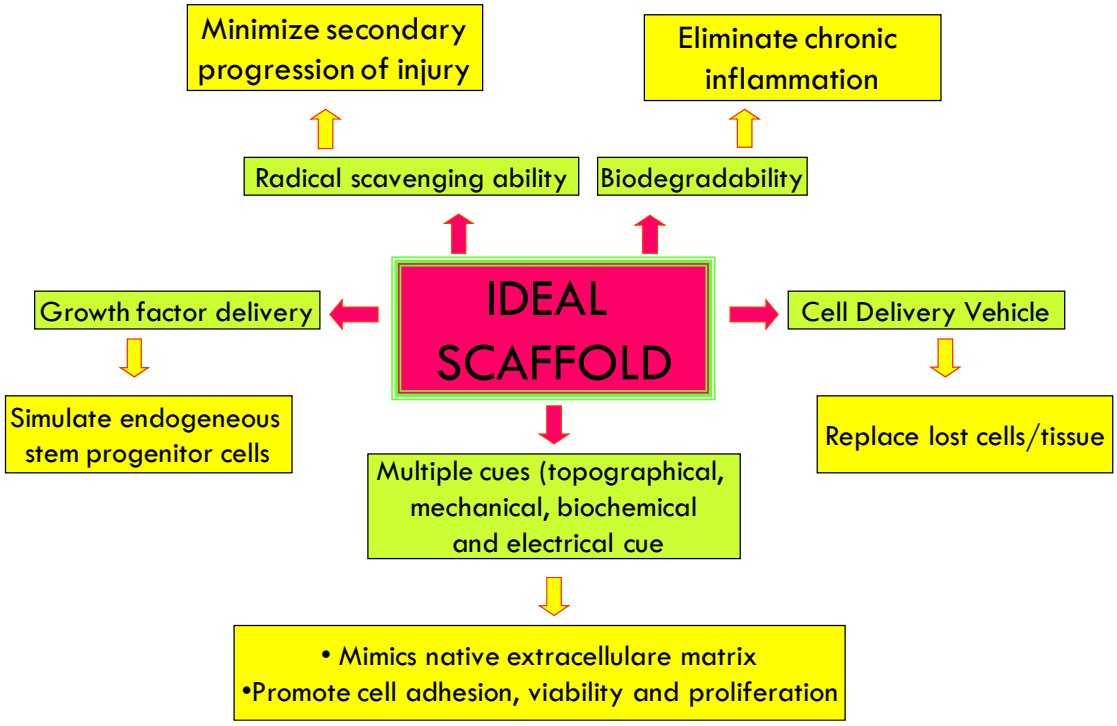


**Figure 1.2** Ideal properties of scaffold. Adapted by Subramanian et al. [12].

## 1.3 BIOMATERIALS IN TISSUE ENGINEERING APPLICATION

The early or *first-generation* of biomedical materials, during the 1960s and 1970s, were developed for use inside the human body with a common feature of biological "inertness" for reducing the immune response to the foreign body to the minimum possible. The original goal was to obtain a suitable combination of physical properties that match those of the replaced tissue.

With the *second-generation* of biomaterials the field began to shift from achieving a bioinert tissue responses to instead producing bioactive components that could elicit a controlled action and reaction in the physiological environment. By the mid-1980s, bioactive materials had reached clinical use in a variety of different applications. A further improvements in this second generation was the development of resorbable biomaterials exhibiting clinically relevant, controlled chemical breakdown and resorption. In this manner, the interface problem is resolved, because the foreign material is ultimately replaced by regenerating tissue, and eventually there is no discernable difference between the implant site and the host tissue [13].

Improvements of first- and second–generation biomaterials are limited in part because all man-made biomaterials used for repair or restoration of the body represent a compromise. In fact, living tissue can respond to changing physiological loads or biochemical stimuli, a property not shared by synthetic materials. This limits the lifetime of artificial body parts, motivating the introduction of more biologically based method for the repair and regeneration of tissue: the third generation of biomaterials

The third–generation of biomaterials are being designed to stimulate specific cellular responses at the molecular level, for instance activating genes that stimulate the regeneration of living tissue. The separate concepts of bioactive materials and resorbable materials have converged; resorbable materials are being made bioactive. Molecular modifications of resorbable polymer systems elicit specific interaction with cell integrins and thereby direct cell proliferation, differentiation, and extracellular matrix production and organization.

Polymeric materials have greatly contributed to the development of bioactive and biodegradable scaffold that can enhance tissue regeneration. Several classes of polymer have proved to be most useful in biomedical applications, but to select appropriate polymers for tissue engineering, it is necessary to understand the influence of the polymer in cell viability, growth and function.

Cell interaction with polymers are usually studied using cell culture techniques. Cells in culture are planted over a polymer surface and the extension of cell adhesion and spreading on the surface is evaluated. The maintenance of the cell culture for long periods is strongly influenced by the nature of the substrate that influence cell viability, function and motility. Most tissue-derived cells are anchorage-dependent and require attachment to a solid surface or viability and growth are compromised. For this reason, the initial events that occur when a cell approaches a surface are of fundamental interest. In tissue engineering cell-substrate adhesion is a multistep process that involves, in sequence: adsorption of an ECM onto the surface; recognition of the ECM components by cell receptors; cytoskeletal rearrangement. The proper accomplishment of these phases, leads the cells to gain the differentiated functions of the specific district with the subsequent tissue formation.

The biomaterials used for enhancement of tissue regeneration can be classified as natural, synthetic, and semi-synthetic materials.

Natural polymers can be considered as the first biodegradable biomaterials used clinically, possessing several properties that make them attractive for tissue engineering application. Natural materials such as collagen, gelatin, elastin, fibronectin, the linear glycosaminoglycan hyaluronic acid (HA), as well as carbohydrate polymers like chitosan, have been used for tissue engineering and as vehicles for cell delivery. Since ECM plays an instructive role in cell activities, such biomolecules would mantain the biological information and other physico-chemical features; exhibiting similar properties to the tissue replaced by them. Natural ECM polymers possess several inherent advantages such as bioactivity, the ability to present receptor-binding ligands to cells and the susceptibility to cell-triggered proteolytic degradation and natural remodeling.

Plant, animal, and insects components have also been explored to develop natural biomaterials such as silk, chitosan, alginate and matrigel. These polymers possess several properties that make them attractive for tissue engineering applications; for instance the chitosan is a natural biopolymer that consists of glucosamine and N-acetylglucosamine with a structure similar to GAGs which are components of the liver ECM consequently is a biomaterial with promising aplications in liver tissue engineering [14].

However, the rate of in vivo degradation of these natural and therefore enzymatically degradable polymers varies significantly with the site of implantation depending on the availability and concentration of the enzymes. Chemical modification of these polymers also can significantly affect their rate of degradation. The inherent bioactivity of these natural polymers has its own downsides. Natural materials, depending of the extraction methodology and tha batch characteristics, may induce immunological and inflammatory responses due to undefined factors and pathogens, which may still be present, even after purification [15].

Synthetic biomaterials on the other hand are generally biologically inert, they have more predictable properties, batch-to-batch uniformity, high reproducibility and the unique advantage of having property profiles tailored for specific applications, devoid of many of the disadvantages of natural polymers. Clearly, synthetic biodegradable polymers are preferable to nonbiodegradable polymers because of the advantage of avoiding a second surgery to remove the device.

At the present the most common biodegradable polymers in use or being studied include polylactic acid (PLA), poly-L-lactic acid (PLLA), polyglycolic acid (PGA), polycaprolactones (PCL) and polycarbonates [16-17]. Another group of synthetic polymers attracting attention in the field of regenerative medicine is polyurethanes. These are one of the most broadly used polymers in implantable biomedical devices such cardiac pacemakers and structural tissue replacements. The greatest disadvantage of synthetic material, however is the lack of cell recognition signals, resulting therefore in few cellular interaction. To overcome this limitation many researchers are focusing their efforts on the creation of semi-synthetic biomaterials by modifying the synthetic biomaterials with cell recognition sites such as incorporating cell adhesion petides.

### 1.3.1 Design Criteria of Biomaterials

Current interest has been focused on attempts to find new biomaterials suitable for realizing novel designs of engineered tissue. There are key parameters in selecting and engineering biomaterials such us the bulk and the surface properties. Bulk material selection is the first consideration of a matrix design, from biological effect to processability. Several properties of bulk materials for new biomaterials design have to be taken into consideration, including biocompatibility, wettability, transparency, biodegradability, and other mechanical properties. As mentioned before, a critical and important parameter that must be considered is the biocompatibility of the bulk material, because it determines the ability of materials to perform their desired functions with appropriate cellular or host responses. The degree of biocompatibility can vary from the lack of toxicity with respect to cell culture to the lack of immunological systemic response of human body. The strictest requirements are applied to implantable scaffold for avoiding undesired responses, such as a strong immune reaction or fibrous encapsulation. Ideally, the body should be able to metabolize the degraded substance; obviously, natural materials tend to show better biocompatibility than synthetic materials. A more relaxed definition of biocompatibility is applied to devices or substrates that will be used *ex vivo,* but the more complex the cellular system is, the more stringent the compatibility requirements are. Because natural ECM is a fully hydrated gel, wettability is a key consideration [18]. Indeed, materials with more hydrophilic chemistry are better at mimicking the aqueous *in vivo* environment.

Transparency of bulk material is another important parameter for in vitro modelling application in which cellular behaviours within the new matrix require microscopic detection. Thus, transparent materials are advantageous for a better monitoring and evaluation of the cell state during the culture period.

Controlled biodegradability is an essential requirement for implantable matrix and scaffold because the ideal tissue engineered construct is generally designed to disappear through degradation at the rate that in-growing tissue replaces it. Generally, synthetic materials degrade hydrolytically, and natural materials undergo an enzymatic degradation process. Hydrolytic degradation is more predictable and adjustable than enzymatic degradation. For example, the degradation profile of a poly (lactic-co-glycolic acid) (PLGA) matrix can be manipulated by adjusting the composition and the molecular weight of poly(lactic acid) (PLA) and poly(glycolic acid) (PGA) polymers. On the other hand, enzymatic degradation of natural materials is more dependent on the local enzyme concentration secreted from cells. As a consequence the degradation profile and mechanism under physiological conditions for the engineered construct materials, as well as the implantation site and desired function, need to be carefully considered during the design of a new implantable device [19]. Mechanical properties of bulk materials represent an important set of characteristics to consider in a biomaterial design or in choosing the right one. Bulk materials are fundamental contributors to the mechanical integrity of the matrix structure. In addition, the microscale mechanical properties are critical for determining the cell behaviour, including directing stem cell differentiation, cell migration and tissue growth, therefore, the new tissue construct should have mechanical properties resembling those of healthy tissue over the period of tissue regeneration. Cells not only adhere to surfaces, but also "pull" on the surface substrate and adjacent cells. The bulk mechanical properties directly shape the mechanical properties of the surface, such as stiffness or elasticity, which elicit clear cellular response. The relative substrate resistance encountered by the cells activates various mechanotransduction and cellular pathways, which in turn trigger gene expression. In vivo micromechanical stimuli are important environmental cues that enable cell attachment, migration and organogenesis. Matching the mechanical surface properties of the engineered tissue to the particular mechanical characteristics of the specific tissue site is therefore vital for controlling the cell behaviour. Cells on 2D

cultures initially recognize adhesive proteins on the substrate through the transmembrane integrin receptor receiving mechanical signals, which activate actin-filament polymerization and promote focal adhesion formation. Later, cells apply traction forces to pull the ligands from a substrate and sense the surface stiffness. For instance, it has been demonstrated that human mesenchymal stem cells (hMSCs) have a different phenotypic response on supports with different grades of elasticity. Human mesenchymal stem cells displayed a phenotype neurogenic lineage on the softest substrate, a myogenic phenotype on moderately stiff matrices, and an osteogenic phenotype on the stiffest substrates [20]. These results provide valuable informations for new biomaterial design introducing novel strategies suitable for many tissue regeneration applications.

Surface properties are also crucial in controlling the interaction between cells and a substrate. Although surface properties are often derived from the bulk properties of the materials, the bulk materials do not entirely define them, because the used substrates are coated with proteins almost immediately after implantation in the body or immersion in culture media. Surface chemistry and topography determine the identity, quantity, and conformational change of these adsorbed proteins. Surface properties include stiffness, charge, polarity, and chemistry, among a multitude of others. For example, the surface charge density determines the amount of protein adsorption and resultant cell adhesion. Greater surface charge brings a greater density of protein coating, which leads to better cell adhesion.

### 1.3.2 Surface Modification

When cells are cultured in vitro or when materials are implanted into the body, cells encounter very different and unfamiliar surfaces and environments. Several approaches have been introduced for modifying these unfamiliar substrates to promote desirable cell responses.

Surface modification of biomaterials, with the intent to improve not only biocompatibility but also the response of the target cell and/or tissue has been extensively studied to recreate the native tissue structure and to do it in the shortest time possible. Modifying material surface structures to mimic aspect of the ECM in order to provide the tissue-specific cues to direct cell behaviour and trigger tissue

regeneration, is an important aspect of many tissue-engineering strategies. Controlling the surface chemistry of materials enable, to some extent, to dictate the rate of protein absorption, the functionality of adsorbed proteins and subsequent cell adhesion.

The degree of biofunctional specificity exhibited on the material surface depends on the level and complexity of the surface-modification approach utilised [21].

One of the first approaches involves hybridizing natural and synthetic materials to improve the biological and physical properties of the substrate. For instance, limited bioactivity can be improved by covalently incorporating multifunctional ligands from natural materials, such as fibronectin, vitronectin, and laminin, onto synthetic polymers.

Another technique involves chemical modification of the polymer, confering charged end-groups to its surface that may lead to protein adsorption and structural rearrangements via electrostatic interaction. Indeed, the surface of biomaterials can be modified via chemical reactions, to confer upon the material precise surface energy, charge or functional groups and tailor their levels of interaction with proteins and cells. For example, the radiation grafting of chemical group such as –OH, -COOH and $NH_2$ onto the surface of relatively inert polymers has been used extensively to modify the surface of biomaterials. Energy sources like ionising radiation sources, ultraviolet radiation and high-energy electron beams are used to break the chemical bonds at the surface of the material to be grafted, allowing the formation of free radicals and other reactive species. The surface is then exposed to, and reacts with, molecules that will form the surface functional coating of the material.

Increasing biofunctionality can be achieved by attaching specific peptide motifs such as enzymes peptides, proteins which can bind to cell receptors inducing a "firm" cell anchorage. These biomolecules can be simply adsorbed onto the surface of the material, or covalently linked via chemical groups previously created on the surface. The biological response following the surface biomodification depends on structural parameter. The functionalisation of a material surface via absorption or chemical binding of other ECM elements is a common approach utilised to promote cell adhesion. For example a popular research strategy employed to improve the blood compatibility properties of vascular grafts comprises seeding endothelial cells onto their surface [22]. The complete coverage of the surface of the biomaterial by these cells (endothelialisation) inhibits thrombosis, prevents intimal hyperplasia, and thereby

increases the patency of vascular grafts. Furthermore, another example of mimickinng the natural ECM of surface modification is given by the incorporation of signal peptide such as RGD (Arg-Gly-Asp) which is found in many adhesion proteins and binds to many integrin receptors, modulating cell adhesion, and inducing cell migration. Finally, another approach is the incorporation of soluble signaling molecules within the scaffold, such as growth factor and deoxyribonicleic acid (DNA). For example, a larger biologically relevant protein can be produced using recombinant DNA technology incorporating the encoding sequence into the support.

On the basis of these important considerations it can be pointed out that the development of new biomaterials able to activate specific responses of the cells and to maintain cell differentiation for a long time is one of the most pertinent issues in the field of tissue engineering and regenerative medicine. Nowadays, it has been demonstrated that the suitability of polymers for tissue-engineering purposes is highly dependent on the tissue that needs to be engineered. The histological, physiological, and biomechanical properties of each tissue determine the success of the regenerative process, therefore restricting the choice of materials suitable for the specific application.

## 1.4 SEMIPERMEABLE POLYMERIC MEMBRANE AS A BIOMATERIAL

Among the biomaterials applied in the field of tissue engineering and regenerative medicine, polymeric semi-permeable membranes could provide the mechanical support required for the regulation of cell growth in bio-hybrid systems (Figure 1.3). The ultimate goal of this technique might be very well achieved by appropriate bio-interaction of desired cell responses which lead to the fabrication of the tissue structure. The realization of such bio-hybrid systems have a great impact in tissue engineering application since represent a key approach for studying both physiological and pathogenic states of the of the specific cells and tissue site as well as for the development of appropriate bio-molecules for therapeutic purposes. With the purpose of simulating *in vitro* biological phenomena, scientists have begun to construct artificial membranes that may be handled in both industrial and medical application. Artificial lungs (blood oxygenation) and kidneys (hemodialysis) are just the two oldest examples. The use of polymeric semi-permeable membranes with different physico-chemical and

transport properties is an appealing approach in the tissue and bio-artificial organ engineering field, since these bio-membranes share specific features such as the selective transport of molecules, resistance and protection. Furthermore, synthetic membranes are easily and readily produced in copious amount so that their morphological and physical-chemical properties can be modulated for numerous and specific application. This is of particular importance and augment the suitability of polymeric membranes for tissue engineering purpose because the membrane features can be adapted to the histological, physiological and biomechanical properties of the tissue that needs to be engineered. Indeed, the polymeric membrane are attractive for their characteristics of selectivity, stability and biocompatibility in the use of bio-hybrid systems for cell culture and therefore suitable a for the realization of an efficient in vitro model. They can act as support for cell adhesion of anchorage dependent cells and allow the specific transport of metabolites and nutrients to cells and the removal of catabolites and specific products. The surface and transport properties of the membranes play an important role in the promotion of cell adhesion, proliferation and viability. The material surface properties of the membrane, such as chemical composition, hydrophilicity/hydrophobicity, charge, free energy, and roughness, affect cell adhesion through the modulation of proteins secreted by cells or contained in the physiological liquids. In the next section particular attention is given to the specific membrane properties that need to be considered and achieved for polymeric semipermeable membrane used in bio-hybrid systems.

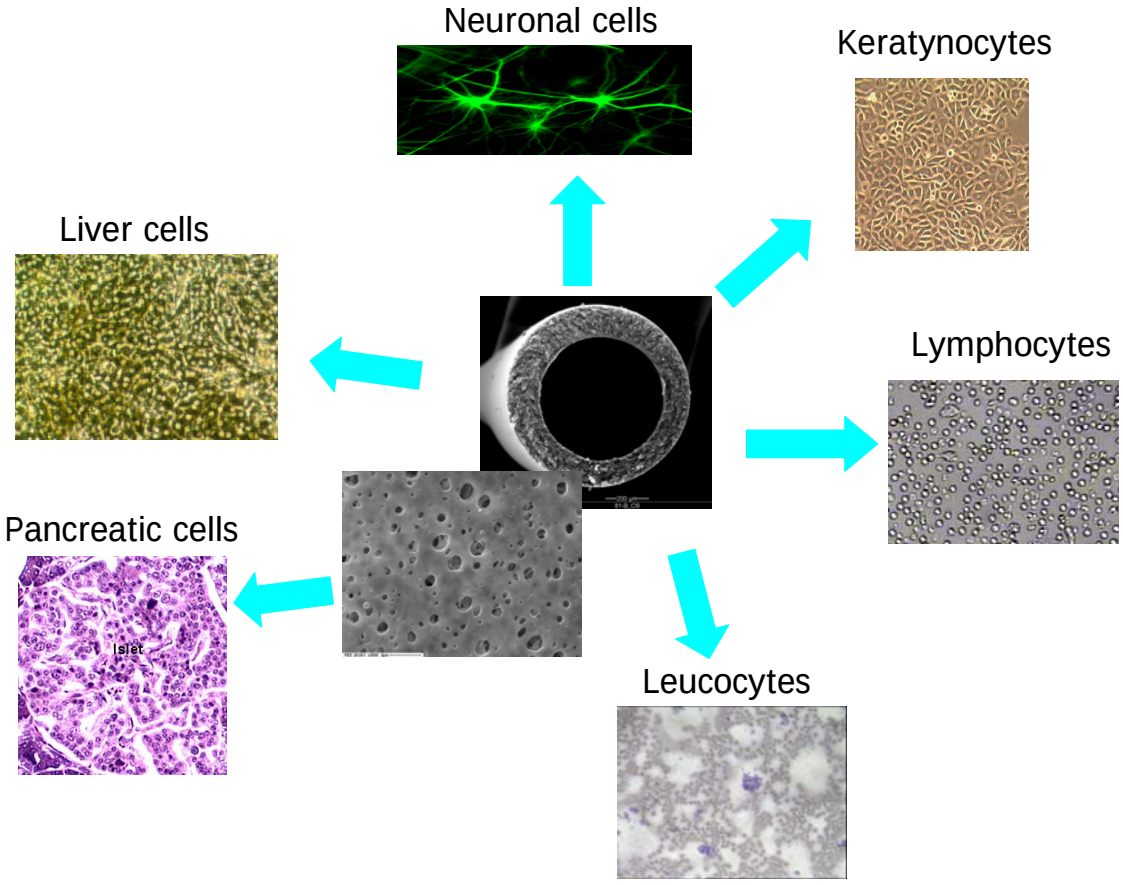


**Figure 1.3** Different applications of semipermeable polymeric membrane for cell growth in bio-hybrid systems.

### 1.4.1 Membrane properties in a bio-hybrid system

When designing a membrane, special attention should be paid to the acquisition of well-defined morphology (pore size, porosity, roughness, thickness, etc.) together with desirable mass transfer properties. Various possible transport mechanisms and their combinations in real systems (from adsorption-diffusion transport in dense membranes to molecular sieving transport, Knudsen diffusion transport, selective surface adsorption, etc.) have been studied to describe the selectivity and permeability in dense and microporous polymeric membranes. In membrane bio-artificial organs using isolated cells as biological component, semi-permeable membranes carry out several functions: they act as immune-selective barriers for the transport of metabolites and nutrients from the medium to the cell compartment and of metabolites and specific products from the cell to the medium compartment. As a consequence, the membranes

act as a physical and chemical support for cell adhesion, providing a large area for cell attachment, and also as a means of cell oxygenation [23, 24]. The transport of a chemical species across the membrane is a result of chemical potential differences (difference in temperature, pressure, concentration or combination of all these variables), which act on the various components of the system [25]. In accordance with the phenomenological approach of irreversible thermodynamics, the transport equations of solvent and solute can be expressed as the following:

$$Jv = Lp\ (\Delta P - \sigma\ \Delta\pi) \qquad \text{(Eq. 1.1)}$$

$$J\ s = cs\ (1-\sigma\ )Jv + \omega\Delta\pi \qquad \text{(Eq.1.2)}$$

Transport across a membrane is described by three parameters: hydraulic permeability Lp, solute permeability ω, and the reflection coefficient σ (eqs. 1.1 and 1.2). All these parameters are experimentally determined. The reflection coefficient is a measure of membrane selectivity and varies from 0 to 1 for a solute freely permeating and completely rejected by the membrane, respectively. The solute permeability coefficient is related to membrane solute diffusivity and thickness. In the absence of solutes, the equation becomes the following:

$$Jv = Lp\ \Delta P \qquad \text{(Eq.1.3)}$$

Lp is determined by measuring the solvent flux through the membrane under transmembrane hydrostatic pressure differences. Lp is related to membrane properties such as pore size and the distribution of the different pore size, as well as pore geometry, thickness, and tortuosity. In porous membranes the transport of chemical compounds depends not only on the trans-membrane pressure gradient but also on the size and shape of the solutes related to the pore size in the membrane. The porous membranes used in bio-artificial organs are generally micro-filtration and ultra-filtration membranes: the pore sizes of micro-filtration membranes range from 10 to 0.05 μm, whereas ultra-filtration is typically used to retain macromolecules from a solution, since its lower limit consists of solutes with a molecular weight of a few thousand Dalton. When the hydrostatic pressure difference is zero the transport of a chemical species through the membrane occurs across a concentration gradient according to the following formula:

$$Js = \omega \Delta C \qquad \text{(Eq.1.4)}$$

where $\omega = \frac{Deff}{l}$

As a result, the transport of solutes is obtained as a difference in diffusion rates across the membrane arising from differences in molecular size. Overall, the size range and physico-chemical properties of solutes, which must be transported through a membrane in bio-artificial organs, are extremely variable. Small solutes such as electrolytes, oxygen and high MW proteins (70,000 Da) must be efficiently transported through the membrane as well as both hydrophilic molecules dissolved in the plasma and hydrophobicmolecules. Hence, the transport of molecules across membranes depends not only on the size and physico-chemical properties of the molecules related to the pore size of the membranes, but also on the interactions between solute and membrane. In a tissue engineered neuronal construct, membranes can be used in a flat or hollow fiber (HF) configuration. In this case, hollow fiber membranes provide a wide area of cell adhesion in a small volume and a three-dimensional organization reminiscent of the tubular configuration of nerves (Figure 1.4). Microporous polyethersulfone HF membranes with 0.2 μm interconnecting pores, in fact, have been recently used as a scaffold to support the growth of human cells [26].

Flat membranes with a micro-porous structure are used not only for the adhesion of anchorage-dependent cells (e.g., neurons, endothelial cells, hepatocytes) but also for the transport of metabolites. On the other hand, dense membranes are useful to provide the cells with gas because of their permeability to oxygen, carbon dioxide and aqueous vapor (Figure 1.5). In these systems, cells come into contact with the membrane surface and this greatly influences the response of cell behavior towards the type of membrane used. For this reason, membranes should be chosen not only on the basis of their separation properties but also on the basis of physico-chemical and morphological surface properties. Cell-membrane interactions have to be closely investigated so that where it is possible membrane physico-chemical and morphological surface properties can be improved [27-28].

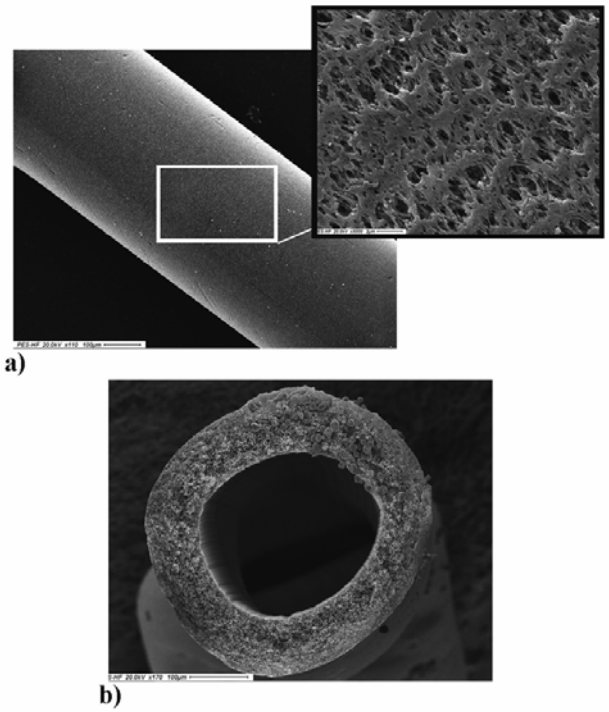


**Figure 1.4** Scanning electron micrographs of polyethersulphone hollow fiber membrane: a) outside surface, b) cross section of the membrane. Scale bars: (a) 100 μm, detail 2 μm; (b) 100 μm.

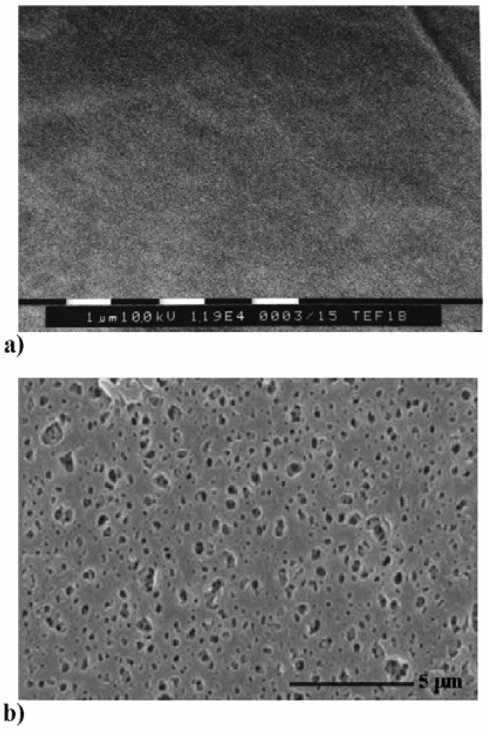


**Figure 1.5** Scanning electron micrographs of flat membrane surfaces: a) polytethrafluoroethylene dense membrane; b) polyethersulphone microporous membrane. Scale bars: 1μm (a); 5 μm (b).

It has been shown that the morphology of a cell tightly adhering to its substrate changes in relation to the properties of the substrate. As a consequence, the maintenance of cell morphology, in the same manner as that of in vivo conditions, is functionally vital to cells. In particular, the roughness and pore size of polymeric membranes seem to play an important role since they have been shown to influence the viability and metabolic rates of cells such as isolated hepatocytes [28]. The wettability of the membrane surface has proved to be another factor that affects the growth of neurons from PC-12 cells [29]. Although the basis for this difference is still poorly understood, this effect may be, in part, is due to the modification of the native substrate that anchors these cells, since the amounts and conformation of adhesion proteins contained in the culture medium vary. Currently, the contact angle is often used as a physical parameter indicative only of the wettability surface, but it allows more quantitative information concerning the energy parameters of the final surface material to be obtained [30]. The contact angle can be applied to characterize surface free energy parameters, the free energy of interfacial interactions in polymeric substrates. These measurements might be a predictive index of their cyto-compatibility and/or tissue biocompatibility. Therefore pre-treatment of surface material might enable the adaptation of its surface free energy to biological requirements. Modifications of surface membrane with the addition of well-defined molecules that are able to mimic the external cell environment shows great promise for the in vitro reconstruction of engineered tissues. Biomaterials are being designed to maintain specific cellular functions at the molecular level [31]. By immobilizing specific proteins, peptides, and other bio-molecules on a material, it is possible to mimic the extra-cellular matrix (ECM) environment thus providing a multifunctional cell-adhesive surface [32-33].

## EXPERIMENTAL DESIGN AND AIM OF THE WORK

The main focus of this work is to design and to realize membrane bioartificial systems for liver and neuronal tissue engineering constructs. To this purpose, different membrane systems have been considered in order to find adequate solutions to prominent problems and discover new insights in the area of tissue engineering. Several experiments have been designed, specifically targeted to highlight the advantages of each of the membrane bio-hybrid systems under consideration such as liver and neuronal tissue engineered alternative models.

Due to the increased requirements of new therapies for acute and chronic liver disease and the need to find an unlimited source of cells for transplantation therapy, in the first part of the experimental design, rat progenitor liver cells were used as alternative model of undifferentiated cells in a membrane system, in order to favor their expansion and functional differentiation. The use of polymeric semipermeable membranes with different physico-chemical and transport properties, is an appealing approach in bio-artificial organ systems since these bio-membranes share specific features, such as the selective transport of molecules, resistance and protection, recreating in vitro the peculiar microenvironment of the tissue that needs to be engineered. It should be feasible to design polymeric materials that elicit specific interaction with cell integrins and thereby direct cell prolifearation, differentiation and extracellular matrix production and organization. Taking into account these fundamental prerequisites, as culture substrate of the embryonic liver cells two different polymeric membranes made respectively of PEEK-WC-PU (a polymeric blend of modified polyetheretherketone and polyurethane) and chitosan have been used. The choice of employing the PEEK-WC-PU membrane was strictly related to the ability of this membrane to induce specific cellular response. To further improve cell-substrate interactions the membrane surface was functionalized with $NH_3$ groups. Cell morphology and adhesion of rat embryonic liver cells, as well as their capacity to perform specific liver functions were deeply analyzed since they are key points in the case of organ replacement or regeneration. A potential advantage offered by biodegradable materials is the disappearance from the implant site once regeneration has been completed. In this work a new chitosan film is proposed and used; chitosan is one of the most promising biomaterials in tissue engineering because it offers a distinct set of advantageous biological properties. The

ability of the chitosan membrane to recreate and provide a suitable microenviroment for enhancing and guiding functional differentiation of rat embryonic liver cells was validated by using the biohybrid system constituted by the progenitor liver cells and the chitosan membrane in culture for 21 days. The obtained data strongly demonstrates the role of the chitosan membrane in supporting the differentiation process of the rat embryonic liver cells that could be effectively used in liver tissue engineering and pharmaceutical application.

The second part of the thesis focuses on developing neural bio-hybrid systems as tools capable of regenerating a neuronal network, yielding an efficient approach for studying the behavior of neuronal populations in some of most common neurodegenerative disease such Parkinson's, or Alzheimer's or as an in vitro system for drug testing toxicology.

Engineering neural tissue is one of the most challenging goals of the tissue engineering. Neural tissue is highly complex and possesses an organized three-dimensional distribution that is essential for tissue function. An optimal scaffold for tissue engineering has to provide this distribution until the cells are able to activate their normal functions and develop neural connection.

Polyetheretherketone (PEEK-WC) and Polyacrilonitrile (PAN) in flat and hollow fiber configuration have been realized and employed for supporting the growth of hippocampal neuronal cells. The polymeric substrates were evaluated for their capacity to promote hippocampal neuronal cell adhesion and direct axon outsprouting as well as for the capacity to maintain cells metabolically active. These bioartificial systems produced a large number of neurite processes organized in a very complex network.

The incorporation of microscale and submicroscale topographies on biomaterial surfaces may enhance the biomaterials ability to modulate neuronal development and regeneration. To explore the effect of specific tographic signal on neuronal behavior in the last part of the experimental work, nonpatterned and micro-patterned biodegradable poly(L-lactic acid) (PLLA) membranes were used to study the response of the neurons to specific geometric features. New understanding of the neuronal behavior on topography in the early developmental stages may aid in designing surfaces for neuronal application, such as neural networks and advanced nerve guidance channel.

**REFERENCES**

[1] S.J. Shieh, J.P. Vacanti. State-of the-art tissue engineering: From tissue engineering to organ building. Surgery 2005;137(1):1-7

[2] Shyh-jou Shieh , Joseph P. Vacanti. State of the art tissue engineering: From tissue engineering to organ building. Surgery, 2005; 137 (1): 1-7.

[3] R. Langer, J.P. Vacanti. Tissue engineering. Science 1993; 260: 920-926.

[4] Jakab K., Norotte C, Marga F.,. Murphy K, Vunjak-Novakovic G. and Forgacs G.Tissue engineering by self-assembly and bio-printing of living cells. Biofabrication 2010, (2) 2 : 1-14.

[5] Grayson W L, Frohlich M, Yeager K, Bhumiratana S, Chan M E, Cannizzaro C, Wan L Q, Liu X S, Guo X Eand Vunjak-Novakovic G Regenerative medicine special feature: engineering anatomically shaped human bone grafts Proc. Natl Acad Sci., 2010. 107: 3299–3304

[6] W.L. Grayson, T.P. Martens, G.M. Eng, M.Radisic, V.Novakovic. Biomimetic approach to tissue engineering. Seminars in Cell & Developmental Biology, 2009; 20:665-673.

[7] M.P. Lutolf, J.A.Hubbel. Synthetic biomaterials as instructive extracellular microencironment for morphogenesis in tissue engineering. Nature Biotechnology, 2005; 23(1):47-55.

[8] H.K. Kleinman, D.Philip, M.P. Hoffman. Role of the extracellular matrix in morphogenesis. Current Opinion in Biotechnology, 2003;14:526-532.

[9] M.M. Stevens, J.H. George. Exploring and engineering the cell surface interface. Science, 2005;310 (5751):1135-1138.

[10] N. A. Peppas, R. Langer. New challenges in biomaterials. Science, 1994; 263:1715-1720.

[11] R.Langer, D.A. Tirrell. Designing materials for biology and medicine. Nature, 2004; 18:487-492.

[12] A. Subramanian, U.M. Krishnan, S.Sethuraman. Development of biomaterials scaffold for nerve tissue engineering: biomaterial mediated neural regeneration. Journal of Biomedical Science, 2009; 16:108-119.

[13] L.L. Hench. Biomaterials.Science, 1980; 208(4446):826-831.

[14] J.Li, J.Pan, L.Zhang, X. Guo, Y. Yu. Culture of primary rat hepatocytes within porous chitosan scaffold. Journal of Biomedical Materials Research Part A, 2003a; 67:938-943.

[15] L.S. Nair, C.T. Laurencin. Biodegradable polymers as biomaterials. Progress in Polymer Science, 2007; 32:762-798.

[16] H.Y. Cheung, K.T. Lau, T.P. Lu, D. Hui. A review on polymer based bio-engineered materials for scaffold development. Composites part B, 2007; 38(3): 291-300.

[17] C. Liu, Z. Xia, J.T. Czernuszka. Design and development of three dimensional scaffold for tissue engineering. Chemical Engineering Research and Design, 2007; 85(7):1051-1064.

[18] S. Zhang. Hydrogels: wet or let die. Nature Materials, 2004; 3:7-8.

[19] J. Lee, M. J. Cuddihy, N. A. Kotov. Three dimensional cell culture matrices: state of the art. Tissue engineering part B, 2008; 14(1):61-86.

[20] A.J. Engler, S.Sen, H.L. Sweeney, D.E. Discher. Matrix elasticity directs stem cell lineage specification. Cell, 2006; 126:677-689.

[21] I.C. Bonzani, J.H. George, M.M. Stevens. Novel materials for bone and cartilage regeneration. Current Opinion in Chemical Biology, 2006; 10:568-575.

[22] E. Rabkin, F.J. Schoen. Cardiovascular tissue engineering. Cardiovascular Pathology, 2002; 11:305-317.

[23] K.E. Dionne, B.M. Cain, R.H. Li, W.J. Bell, E.J. Doherty, D.H. Rein, M.J Gentile. Lysaght, Transport characterization of membranes for immunoisolation. Biomaterials, 1996; 17: 257-266

[24] E.Curcio, L. De Bartolo, G. Barbieri, M. Rende, L. Giorno, S. Morelli, E. Drioli. Diffusive and convective transport through hollow fiber membranes for liver cell culture. Journal of Biotechnology 2005; 117:309-321.

[25] Mulder, M. 1991, Basic principles of membrane technology, Kluwer Academic Publishers, Dordrecht/Boston/London.

[26] R.E. Unger, Q.Huang, K. Peters, D.Protzer, D. Paul, C.J. Kirkpatrick. Growth of human cells on polyethersulfone (PES) hollow fiber membranes. Biomaterials, 2005; 26:1877-1884.

[27] L. De Bartolo, S. Morelli, A. Bader and E. Drioli. Evaluation of cell behaviour related to physico-chemical properties of polymeric membranes to be used in bioartificial organs. Biomaterials 2002; 23(12): 2485-2497.

[28] L. De Bartolo, G. Catapano, C. Della Volpe, E. Drioli. The effect of surface roughness of microporous membranes on the kinetics of oxygen consumption and ammonia elimination by adherent hepatocytes. Journal of Biomaterial Science, Polymer Edition, 1999; 10 (6): 641-655.

[29] A.J. Lee, G. Knang, Y.M. Lee, H.B. Lee. The effect of surface wettability on induction and growth of neuritis from the PC-12 cell on a polymer surfaces, Journal of Colloid and Interface Science, 2003; 259: 228-235.

[30] C. J. van Oss. Interfacial Forces in Aqueous Media, Marcel Dekker, New York (1994).

[31]L.L Hench, J.M Polak. Third generation biomedical materials. Science, 2002; 295(5557):1015-1017.

[32] L. De Bartolo, S. Morelli, L. Lopez, L. Giorno, C. Campana, S. Salerno, M. Rende, P. Favia, L. Detomaso, R. Gristina, R. d'Agostino, E. Drioli. Biotransformation and liver specific functions of human hepatocytes in culture on RGD-immobilised plasma-processed membranes. Biomaterials, 2005; 26(21):4432-4441.

[33] L. De Bartolo, S. Morelli, M. Rende, S. Salerno, L. Giorno, LC Lopez, P. Favia, R. d'Agostino, E. Drioli. Galactose derivative immobilized glow discharge processed PES membranes maintain the metabolic activity of human and pig liver cells. Journal of Nanoscience and Nanotechnology 2006; 6: 2344–2353.

# CHAPTER 2

# MEMBRANE APPROACHES FOR LIVER TISSUE ENGINEERING: STATE OF THE ART

## 2.1 INTRODUCTION

The liver carries out a range of functions essential for bodily homeostasis. The impairment of liver functions has serious implications and is responsible for high rates of patient morbidity and mortality. Presently, liver transplantation remains the treatment of choice for patient with end-stage liver disease but is limited by both the high cost and severe shortage of donor organs; furthermore liver transplantation requires years of immunosuppression, which can cause long term to both the liver and Kidneys. These limitations have urgently increased the requirements for new therapies, for acute and chronic liver disease. With this aim, tissue engineering and regenerative medicine approaches, for the reconstruction of functional liver tissue, are being widely investigated and considerable work has been done over many years to develop effective liver-support devices. Various non biological approaches, represented by the classical extracorporeal detoxification system based purely on physical separation of toxins from the patient's blood , such as hemodialysis, hemoperfusion, and plasmapheresis, have limited success because considering the multiple and complex functions that liver performs [1-2]. On the other hand, extracorporeal biological treatment, including whole-liver perfusion, liver-slice perfusion, and cross-hemodialysis, have shown some beneficial results, but they are difficult to implement in a clinical setting [3]. Since the onset of liver failure is potentially reversible, many researchers have looked for an alternative option leading to development of external liver support devices known as **Bioartificial livers (BALs).** Generally, a BAL system consists of functional liver cells supported by an artificial cell culture material. In particular, it incorporates hepatocytes into a bioreactor in which the cells are immobilized, cultured, and induced to perform the hepatic functions by processing the blood or plasma of liver-failure patients. The BAL system acts as a bridge for the patients until a donor organ is available for transplantation or until liver regeneration [4]. In addition to cell therapeutic approaches, another important aspect of human liver cell biology is the testing and safe development of new drugs, as the liver plays a central role in the metabolism of the majority of drugs.

## 2.2 HEPATIC STRUCTURE AND FUNCTION: BAL ISSUES DESIGN

The development of constructs with metabolic functions equivalent to those of the liver, poses technical challenges for the complexity of liver cell physical-chemical requirements. The liver is a highly metabolic, complex array of vasculature, endothelial cells and parenchymal cells that performs many functions in the body. The bulk of the liver is primarily composed of parenchymal cells such as hepatocytes, hepatocyte precursor cells (oval cells or Ito cells), stellate cells, kuppfer cells, epithelial cells, sinusoidal epithelial cells, biliary epithelial cells, and fibroblasts [5,6]. The liver is involved in functions that remove toxins and provide metabolic activity such as cytochrome P-450 activity, glycogen storage, urea production, and release of proteins, carbohydrates, lipids, and metabolic wastes. The hepatocytes, composing 60% of the liver, primarily exhibit the characteristic hepatic functions and are widely studied in tissue engineering research. In addition, these cells clear the body of toxins and synthesis proteins such as albumin, alpha-fetoprotein (AFP), and transferrin. The hepatocytes used for tissue engineering purposes must be able to perform these basic functions. Hepatic cells are arranged in a highly intricate manner, allowing for optimal communication and attachment between cells. Communication through cellular junctions, gap junctions, chemical signals, and extracellular matrix (ECM) signals allow the cells to differentiate, grow, function, and apoptos [7–8]. Factors affecting the cellular environment control the size, shape and population of the colony. Structurally, hepatic cells are attached to a basal membrane composed of laminin and type IV collagen. They are connected to other cells through homotypic or heterotypic cellular junctions, alerted by the cell adhesion molecules (CAMS) binding to receptors, and surrounded by an extracellular matrix (ECM) that includes fibronectin and type I and III collagen [7-9-10]. Furthermore, hepatocytes exhibit a striking polarity that is expressed at multiple levels, in overall cell shape, distribution of the cytoskeleton and organelles, and in the division of the plasma membrane into three functionally and compositionally distinct domains: basolateral, canalicular, and lateral. At the basal surface the transport of small molecules across membranes and the exchange of metabolites with blood take place, whereas the secretion of bile acids and detoxification products occurs on the apical domain. Thus, the ability to modulate hepatocytes polarity and multicellular organization is important in developing an efficient in vitro system designed to perform

liver functions, and the development of a BAL system involves many design considerations. It must provide: (1) an adhesion support to the cells; (2) adequate mass transfer of oxygen, nutrients, and toxic substances from blood or plasma of patients to the cell compartments and proteins, catabolites, and other specific compounds produced by cells from the cell compartment to the blood or plasma; (3) immunoprotection of cells; and (4) biocompatibility. Attaining adequate cell seeding, nutrient and oxygen supply to cells , and control of biochemical signals gradients and concentrations in large scaffolds is not easily achievable. BAL devices are classified on the basis of cell source, type of culture system for the hepatocytes seeding, and on the basis of bioreactor configuration and operations.

### 2.2.1 Cell Source

In the field of liver therapeutic tissue engineering the choice of cell type and cell source is a key point, since the cellular component plays a critical role in the performance of a BAL device. The cells inside the BAL must retain their differentiated functions. Due to a lack of human-organ availability, one of main source of hepatocytes for bioartificial systems is xenogeneic material. Primary porcine hepatocytes, for example, which can be obtained in large quantities, have been widely used as the cell source for hybrid artificial livers. Porcine hepatocytes exhibit biotransformation functions, synthesis of urea, albumin, and other proteins, and are activated by growth factors that also activate human cells [11]. Although these cells are easily obtained in large quantities and demonstrate the same qualities and therapeutic effects of human hepatocytes, this type of cell source carries the risk of xenogeneic infections and and since they are not of human origin, they are not genetically matched, resulting in immune rejection by the patient [12]. An alternative approach is to use an immortalized hepatoblast carcinoma line which have the necessary functional and survival characteristics. The advantages of using established cell lines include the ability to culture large quantities of cells for an extended period of time and the ability to control the degree of hepatocyte function that is displayed [13-14]. However, because these cells are cancerous in nature, it is important to maintain safe handling practices when considering the possibility of using these cells clinically. Primary hepatocytes are harvested via perfusion and are the precursor cells to mature hepatocytes. Furthermore, primary human hepatocytes are

very difficult to culture, and human cells that are obtained via perfusion do not survive beyond several divisions. In addition, not only are human hepatocytes difficult to maintain in culture, they also do not perform normal functions or undergo differentiation [15]. Current attention is focused on finding a reliable sources of human hepatocytes. Stem cells have been suggested as interesting cell sources. These cells, found in sources such as bone marrow, are the most flexible cells in terms of being undetermined in their pathway and expressing a remarkable ability to differentiate into a desired cell type. Factors that contribute to a particular cell signalling pathway are currently being researched. These includes growth factor, cellular signalling within the interstitial fluid and extracellular matrix, and cues from other cells of either the same or different cell types. Hepatic progenitor cells (oval or Ito cells) found within the liver have already begun to differentiate, but still have several options before becoming destined to a specific cell line. These cells, will not necessarily become mature hepatocytes but could differentiate into other functional cells of the liver [16]. The generation of hepatic endoderm from pluripotent stem cells is now being identified as one resource to meet the big demand of functional human hepatocytes. Human embryonic stem cells are derived from the inner cell mass of preimplantation embryos and possess the ability to self-renew and differentiate to all cell types. These attributes in theory give them the potential to provide an unlimited supply of replacement cells for regenerative medicine [17]. Although the human embryonic stem cells could potentially provide an infinite source of hepatocytes, stem cells and somatic cells generally have limited function without the specialized tissue microenvironment. Thus, the recreation of a such niche is of primary importance for the development of scalable and high fidelity resources for drug testing or BAL reconstruction.

## 2.3 CULTURE SYSTEM

A successful BAL device requires a favourable culture model for the hepatocytes to maintain their viability and differentiated functions. Hepatocytes are involved in many important liver functions: blood detoxification; bile secretion; protein, steroid, or fat metabolism; and vitamin, iron, or sugar storage. This multifunctionality implies a great number of biological parameters, which are difficult to reproduce in vitro to maintain all the functionalities of the hepatocytes. Moreover, primary cultured hepatocytes rapidly

lose liver-specific functions when maintained under standard in vitro culture conditions. To overcome such limitations, several different culture models for maintenance of hepatocytes in vitro have been developed. As mentioned before, stationary suspension culture of isolated hepatocytes is ineffective, since in this circumstance hepatocytes lose differentiated function within hours. An alternative technique resulting in improved cell viability and functional activity is attachment culture. One example is given by the use of an overlying layer of collagen gel developed by Dunn et al., this culture model is described as a "collagen sandwich colture". In this model cells are spread on a monolayer and then covered with another collagen layer [18]. It has become increasingly clear that three dimensional rather than monolayer growth is particularly important for maintaining differentiated hepatocyte function in culture. One means of establishing three dimensional hepatocyte growth is the creation of multicellular spheroid aggregates. Early methods utilising stationary culture techniques had the disadvantage of requiring several days for spheroid formation [19], rendering this approach impractical for clinical use. More easily and rapidly hepatocyte spheroids-usually with diameters of 50–500 mm-can be formed from suspended isolated cells by spinner or rotational flask [20-21] or by incubation with a small number of collagen-coated dextran, polystyrene or glass microcarriers as a nidus for cell aggregation[22]. This induced hepatocytes aggregates maintain their specific functions and a their peculiar ultrastructure resembling that of a normal liver.

Another method of hepatocytes immobilization is the cell encapsulation within alginate-polylysine, polyacrylate or cellulose acetate also favours the development of three dimensional hepatocyte growth. The potential for three dimensional structure formation can be further enhanced by enriching the solution with natural extracellular matrix proteins prior to encapsulation or can include supplementation of factors in the culture medium and the co-cultivation of hepatocytes with other type of cells, the so called "feeder cells" [23]. With this technique cells are protected from mechanical damage, and additionally, immunoisolation from xenogenic cells, should be possible. In vivo studies have demonstrated that encapsulated hepatocytes transplanted in Gunn rats restored liver function without immunosuppression [24]. Between the technique for maintaining hepatocellular function there is also the use of artificial spherical bodies called microcarriers, that ensure a larger surface for cell adhesion. For instance cellulose

multiporous microcarrieers (MCs) are capable of immobilizing isolated cells in their micropores and thus they are a suitable extracellular matrix for maintenance of cellular function [25]. An example is given by Wu et al. that, by using chitosan as raw materials, fabricated a suitable size of porous microcarrier in which rat hepatocytes were cultured. The microcarrier was modified with lactose and maltose. The cells were able to maintain a morphologic structure similar to that in vivo and showed an higher metabolic activities on lactose-modified microcarriers [26]. Co-culture with non parenchymal cells significantly enhances hepatocytes viability and function, possibly due to the mixed effects of autocrine and paracrine stimulation by growth factors derived from the non parenchymal cells and the reproduction of extracellular matrix. In the liver, hepatocytes and endothelial cells are closely associated but separated by the extracellular matrix of the space of Disse. To establish the heterotypic cell-cell interaction that is essential for the maintenance of the proper liver function, Jindal et al. recreated an in vitro coculture system able to provide native cues, consisting of hepatocytes, collagen, and an overlaying endothelial monolayer. The authors demonstrated that this culture configuration induces the early recovery of hepoatocytes following cell isolation as evidenced by the increased albumin and fibrinogen protein secretion as well as gene expression [27].

Another study regarding the coculture system was carried out in order to maintain the differentiated status by means of hepatic stellate cells (HSCs), their soluble and particulate factors and lipid extracts. The central question of the study was to underlying that HSCs maintained hepatocytes functions and structure by multiple signals, preferentially cell bound, pointing in particular to non soluble membranous ligands contacts, showing once again the pivotal role played by the surrounding microenvironment for the maintenance of differentiated hepatocytes [28].

## 2.4 BIOREACTOR

Considering the several functions that the liver performs a hybrid liver-support device is one of the most complex bioreactors. Therefore, its design is optimized in order to ensure: the rapid detoxification of neural and hepatic toxins; the return of liver-specific hepatotrophic factors, as well as liver-specific coagulation factors, back into the patient’s blood; and the maintenance of liver-cell detoxification and synthetic functions

until liver tissue regeneration or organ transplantation. On the basis of these considerations, an efficient culture device must be designed considering the following important design criteria: i) to use a sufficient number of differentiated hepatocytes that can maintain the long-term functions; ii) to reduce mass transfer resistances and eliminate substrate limitations so that the device can function at maximum efficiency; iii) to minimize the dead volume in the device thereby reducing plasma dilution effects in the patient. The ideal bioreactor design would maximize mass transfer to the hepatocytes thereby allowing nutrients, including oxygen, and toxins from the patient's blood or plasma to reach the hepatocytes. The treated blood or plasma, including metabolites and synthetic products, would then be returned to the patient's circulation. To achieve this task a large surface area is important for cell adhesion. An ideal device should integrate efficient mass transport, scalability, and maintenance of hepatocyte functions. One of the most promising bioreactors is the membrane bioreactors. Membranes with suitable molecular weight cut-off (MWCO) have been proven to provide an effective immunoisolation barrier to immunocompetent species present in the patient's blood. Thus, xenogenic or allogenic implants may be used without need of immunosuppression therapy. Membranes permit also the transport of nutrients and metabolites to cells and the transport of catabolites and specific metabolic products to blood. In the case of anchorage-dependent cells, they offer high surface area available for cell attachment and culture. In these bioreactor designs mass transfer is determined by the molecular weight cut-off (MWCO) or pore diameter and occurs by diffusion and/or convection in response to existing transmembrane concentration or pressure gradients. Some bioreactors use membranes with MWCO ranging from 70 to 100 kDa that allow the transport of serum albumin but exclude proteins with high MW such as immunoglobulins and cells. The advantage to use these membranes is that to provide immunoprotection. Other bioreactors use microporous membranes with large pore diameter (0.2 μm) that allow the free passage of plasma proteins, toxins and clotting factors between blood or plasma and cells but they exclude the passage of cells. The advantage to use a membrane with large pore diameter is to increase the fluid convection in order to improve mass transfer conditions. Polymeric membranes with different morphology and chemical-physical properties have been used in BAL devices [29]. The majority of extracorporeal BAL have used cellulose and polysulfone

derivatives (Table 2.1 and Table 2.2). Morphological properties (e.g., pore size, pore size distribution and roughness) and physico-chemical properties (e.g., surface charge, wettability, surface free energy) affect all the adhesion and metabolic functions of hepatocytes [30-31]. However, most of the commercial membranes used for liver cell culture are developed for haemodialysis, which are optimised to be inert with blood proteins and cells. As a result membranes express poor properties regarding cell interactions and functions. Thus, the development of membranes that are able to favour the adhesion and the expression of liver specific functions is quite important for the design of a tissue-engineered liver bioreactor.

Another important issue in bioartificial liver design is the maintenance of sufficient oxygen supply to the hepatocytes. Since hepatocytes are highly metabolic with high oxygen uptake rates, in order to oxygenate the circulating blood or plasma some devices incorporate an oxygenator in the bioreactor, while other uses an inline oxygenator in the extracorporeal perfusion circuit. The modern bioreactor design should simulate the complex physiologic environments in vivo, such as physicochemical parameters (e.g. pH, temperature, concentration of nutrients and metabolites), mass transfer rates and biomechanical conditions. Various bioreactors have been designed to meet these demands. They range from rather simple hollow-fibre systems or semipermeable dialysers to more complex bioreactors that try to mimic the architecture of the liver. However, most of these systems have their limitations, either in that they offer a suboptimal environment for cell growth or their function is poorly reproducible. Hepatocytes have been cultured in membrane bioreactors in different configurations (Figure 2.1): (a) between flat-sheet membranes in a sandwich configuration; (b) in the lumen of hollow fibre membranes entrapped in a collagen layer; (c) in the shell of hollow fibre membranes in monolayer, (d) aggregate or spheroid structure and (e) attached to micro-carriers; (f) in a network of hollow fibre membranes with different functions; (g) in a spirally wound device in which hollow fibres are used to provide oxygen to the cells; (h) in multibore capillaries; (i) microencapsulated and (j) in a oxygen permeable membrane rotating system under microgravity conditions. In all of these bioreactor configurations, hepatocytes are cultured in contact with the membranes so that membranes with adequate surface and structural properties have to be used into the bioreactor [32].

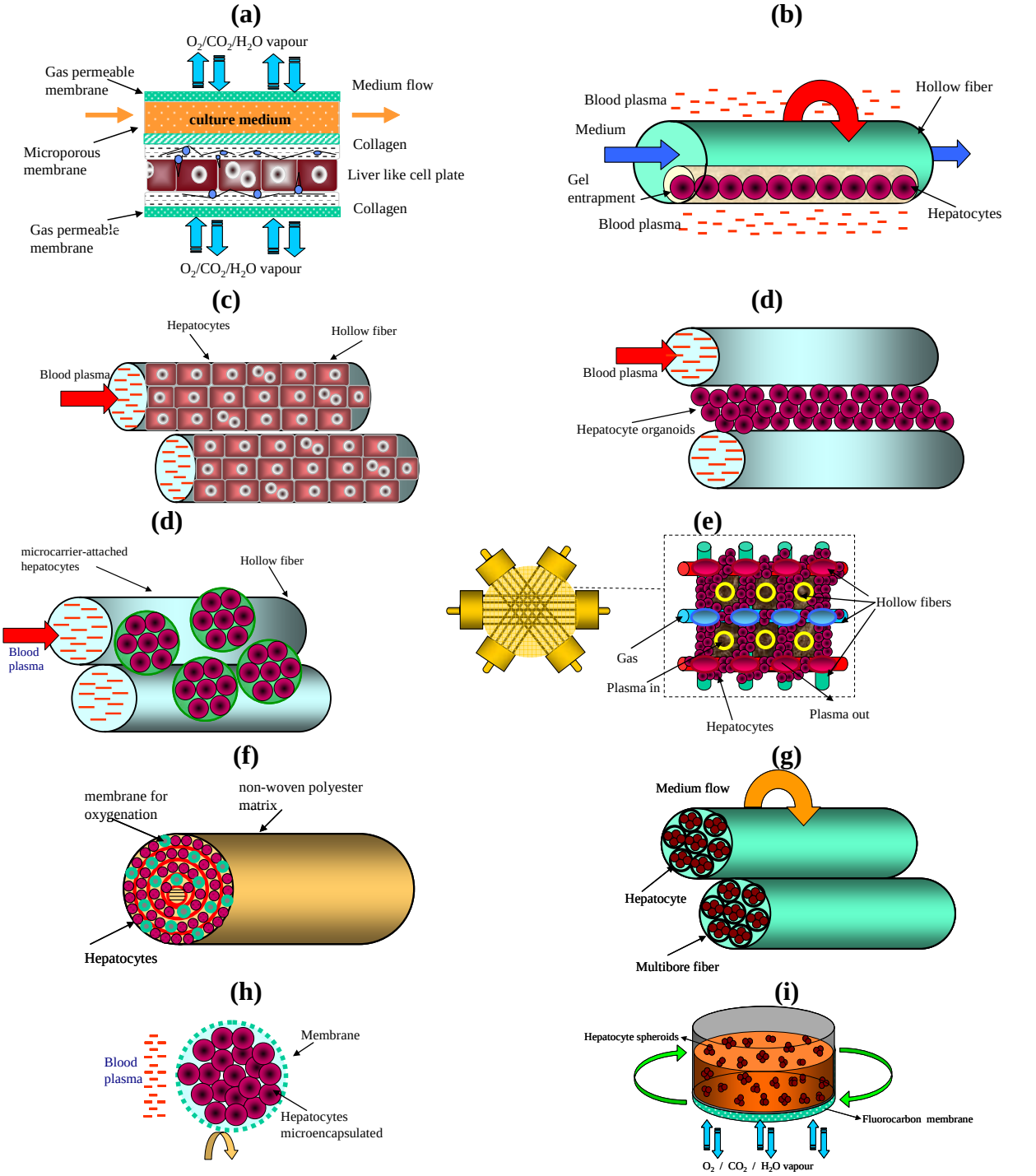


**Figure 2.1 –** Configuration of membrane bioreactors using hepatocytes cultured (a) between flat-sheet membranes; (b) entrapped in a three-dimensional contracted gel matrix inside of hollow fibre membranes; (c) outside of hollow fibre membranes in monolayer; (d) outside of hollow fibre membranes organised in organoids; (e) outside of hollow fibre membranes attached to microcarriers; (f) in a network formed by four capillary membranes with different functions; (g) in a spirally wound non-woven polyester matrix inside of hollow fibres; (h) in the intraluminal compartment of a multibore fibre bioreactor; (i) in microcapsules and (j) in a rotating-wall gas-permeable membrane system.

### 2.4.1 Membrane Bio-Hybrid Artificial Liver (BAL) Systems In Clinical Evaluation

Currently, several BAL devices are in various stage of clinical evaluation and are listed in Table 2.1. Many of these devices use hollow fibre membranes as supports the cultured hepatocytes and as immunoselective barriers between the plasma of patients and the hepatocytes used in the bioreactor [33]. In 1987 Matsumura et al., reported an early clinical trial of bioartificial liver [34]. The device was developed on the principle of hemodialysis against a suspension of functioning hepatocytes. The liver suspension was placed in a dialysate compartment on one side of a cellulosic semipermeable membrane. The blood flows through a compartment on the opposite side of the membrane. Afterwards, one of the first large clinical studies was performed by Margulis et al. in which 20 ml capsules filled with pig hepatocytes in suspension were used [35].

Since the 1990 several BALs were proposed. Sussman and colleagues developed an extracorporeal liver-assist device (ELAD) in which human hepatocyte cell line C3A, which is derived from hepatoblastoma cell line (HepG2) are located outside the hollow fibre and blood flows through the lumen of hollow fibres. A portion of the patient's plasma is ultrafiltrated through a cellulose acetate membrane (70kDa) and is in direct contact with the C3A cells [36]. This device is commercialized by the Amphioxus Cell Technology. A hollow fibre device that uses cryopreserved porcine hepatocytes attached to a collagen-coated dextran microcarriers that is called Hepatic Assist was developed by Demetriou and coworkers. In this system hepatocytes are loaded into the extracapillary space and patient plasma flows through the capillary lumina of membranes with pore size of 0.2 μm. This size is sufficiently small to block the passage of whole cells [37]. Plasma first passes through an activated charcoal column and flows through the lumen of the hollow fibres. A more complex system was proposed by Gerlach et al. The Liver Support System (LSS) or Modular Extracorporeal Liver System (MELS) consists of a bioreactor with four interwoven independent capillary membrane systems that serve different functions. The cells are cultured outer surface and among the capillaries. Each fibre type exhibits a different function: Silastic membranes for oxygen supply and removal of carbon dioxide, polyamide fibre for the plasma inflow, polyethersulfone fibre for the plasma outflow and hydrophilic polypropylene membranes for the sinusoidal endothelial co-culture [38]. With this capillary array

decentralised metabolite and gas exchange with small gradients are possible. Due to the independent plasma inflow and plasma outflow compartments, decentralised perfusion of cells between these capillaries is achieved. Additional functions could be integrated into the module.

The bioartificial liver support system (BLSS) is a hollow fibre device that uses porcine hepatocytes embedded in a collagen matrix. This system uses cellulose acetate hollow fibres with a 100 kDa MWCO containing greater than 70 g of primary porcine hepatocytes embedded in a collagen matrix. The patient' s blood is perfused through the capillary lumina [39]. In the circuit a flowing nutrient stream directly perfuses the hepatocytes providing specific nutrients. The Academic Medical Center Bioartificial Liver (AMC-BAL) developed by Flendrig and coworkers uses a three dimensional, spirally wound, non-woven polyester matrix for hepatocyte attachment with integrated hollow fibres for oxygen delivery to the cells [40]. In contrast with the other systems, the AMC-BAL uses direct contact between the patient's plasma and the matrix attached hepatocyte to improve bidirectional mass transfer.

Another BAL system that is currently in clinical testing is a bioreactor from TECA Corp. in which a polysulfone membrane with MWCO of 100 kDa compartimentalize pig hepatocytes [41].

**Table 2.1 –** Characteristics of membrane BAL systems in clinical evaluation

| References | Bioartificial System | Bioreactor Configuration | Membrane | Cell Source | Cell capacity | Culture technique | Cell position | Level of development |
|---|---|---|---|---|---|---|---|---|
| Matsumara et al., 1987 | Kiil dyalizer bioartificial liver | Plate | Cellulose (MWCO 20 kDa) | Primary rabbit hepatocytes | $1x10^{10}$ | suspension | Dalysate compartment | First clinical report |
| Margulis et al., 1989 | | Cartridge | Polyvinyl chloride | Porcine hepatocytes | $4x10^{7}$ | suspension | Shell | Phase II clinical trials |
| Sussman et al.1992 | ELAD Amphioxus cell Technology | Hollow Fibre | Cellulose acetate (MWCO=70 kDa) | Human cell line (C3A) | $2x10^{11}$ | Aggregates | Shell | Phase I clinical trial |
| Demetriou et al 1995 | Hepat Assist Circe Biomedical | Hollow Fibre | Polysulphone membranes (Pore size 0.2 μm) | Cryopreserved porcine hepatocytes | $5x10^{9}$ | Microcarrier attached irregular aggregates | Shell | Phase II/III clinical trial |
| Gerlach et al. 1994 | LLS Charite, Humboldt Univ Germany | Hollow Fibre | Polyamide (MWCO=100 kDa) Polyethersulfone (MWCO=80 kDa) Silastic Polypropylene (0.2 μm pore size) | Pig Primary hepatocytes - endothelial cells | $2.5x10^{9}$ | Aggregates | Shell | Phase I |
| Patzer et al 2002 | BLSS Excorp Medical Inc. | Hollow Fibre | Cellulose acetate (MWCO=100kDa) | Porcine Primary hepatocytes | 70-120g | Collagen gel entrapped | Shell | phase I/II clinical trials |
| Flendrig et al 1997 | AMC-BAL Univ. Amsterdam | Spirally wound | Non woven polyester matrix, polypropylene membranes (pore size 0.2 μm) | Pig primary liver cells | $1x10^{10}$ | Small aggregates | Shell/on the non-woven Polyester matrix | Phase I |
| Ding et al., 2003 | BAL TECA Corp. | Hollow Fibre | Polysulfone (MWCO=100 kDa) | Swine hepatocytes | $1x10^{10}$ | Aggregates | shell | Phase 0 |

### 2.4.2 Membrane BAL system in preclinical and in vitro evaluation

Several BAL systems have been evaluated preclinically *in vitro* experiments and in large animal models of liver failure.

In the Liverx2000 system of Hu and coworkers, the hepatocytes are suspended in a collagen gel and injected into the lumen of hollow fibre with a MWCO of 100kDa and the extracapillary compartment is perfused with a recirculating medium A media flow through the luminal space provides hepatocyte nutrients [42] (Table 2.2). A bioartificial liver support system consisting of hollow fibre cartridge using encapsulated multicellular spheroids of rat hepatocytes was developed by Shiraha et al. The spheroids, formed in a positively charged polystyrene dish were encapsulated into microdroplets of agarose that contained about $9 \times 10^7$ rat hepatocytes. The medium was circulated in a closed circuit in which the cartridge was inserted [43].

Several alternative device configurations have advanced to the stage of large animal, preclinical evaluation. Naka et al. have developed a system using primary porcine hepatocytes that is similar to the BLSS. The differences are in the use of microporous polysulphone hollow fibre membranes in the hepatocyte bioreactor and perfusion of plasma through the bioreactor. The system has shown some efficacy in support of ischemic pig liver failure model [44].

The flat membrane bioreactor (FMB) developed by De Bartolo and coworkers consists of primary porcine hepatocytes cultured between semipermeable flat membranes. This is a reproducible model with total hepatectomy in pigs, suitable to test the safety and efficacy of liver support system. Isolated hepatocytes were cultured within an extracellular matrix between oxygen-permeable flat-sheet membranes in the FMB. In particular both sides of the outside shell are constituted of PTFE membranes permeable to oxygen, carbon dioxide and aqueous vapour, which allow direct oxygenation of the cells, adhered to the surface and of the medium overlying the cells. Porcine hepatocytes are maintained in a three-dimensional co-culture with nonparenchymal cells. A microporous polycarbonate membrane separates the medium from cell compartment. The FMB maintained stable cell specific functions and is a safe and efficient device [45].

Nagaki and co-workers developed a hybrid liver support system which consists of plasma perfusion through porous hollow fibre modules inoculated with 10 billion of

porcine hepatocytes entrapped in a basement membrane matrix, Engelbreth-Holm-Swarm (EHS) gel. This system was applied to pigs with ischemic liver failure. It was demonstrated that the use of a BAL support device in combination with a hollow fibre module and hepatocytes entrapped in EHS gel has potential advantages for clinical use in patients with hepatic failure [46].

**Table 2.2** Membrane BAL systems in vitro and preclinical tests

| References | Bioartificial System | Bioreactor Configuration | Membrane material | Cell Source | Bioreactor cell capacity | Culture Technique | Cell position |
|---|---|---|---|---|---|---|---|
| Hu et al, 1997 | Liver x2000 | Hollow fibre | Polysulfone (MWCO 100 kDa) | Porcine hepatocytes | $1x10^8$ | Gel entrapment | Lumen |
| Shiraha et al., 1996 | BAL | Hollow fibre | Polysulfone (pore size 0.2 μm). Agarose microcapsule | Rat hepatocytes, HepG2 | $9x10^7$ | Multicellular spheroids | Extrafibre space |
| Naka et al., 1999 | BLSS | Hollow fibre | Polyethylene (Plasma Flo) (0.3 μm pore size) | Porcine hepatocytes | $5.4x10^9$ | Entrapment | Extrafibre space |
| De Bartolo et al., 2000 | FMB-BAL | Flat | Polyterafluoroethylene and Polycarbonate (pore size 0.2 μm) | Pig hepatocytes | $1x10^{10}$ | Sandwich | Between flat membranes |
| Nagaki et al., 2001 | BAL | Hollow fibre bioreactor | polyolefin fibre 0.4μm pore size | Rat hepatocytes, Hep G2 | $2x10^7$ | Entrapment | Extrafibre space |
| Roy et al., 2001 | Flat-plate | Microchannel bioreactor | polyurethane membrane dense | Rat hepatocytes | $2x10^6$ | Monolayer | Over the surface |
| Jasmund et al., 2002 | Oxy-HFB | Crosswise hollow fibre | Polyethylene (pore size 0.2 μm) polypropylene | Pig liver cells | $1\text{-}5x10^9$ | Aggregate | Extrafibre space |
| Mizumoto and Funatsu, 2004 | LLS HALLS | Hollow fibre Multicapillary | polyethylene coated with EVAL hollow fibre polyurethane foam and capillary | Porcine hepatocytes | 0.5-100 g | Organoids Spheroids | Extrafibre space |
| Curcio et al., 2007 | RWMS | Flat | Fluorocarbon dense membrane | Rat hepatocytes | $7.5\text{-}9x10^5$ | Spheroids | Over the surface |
| Schmtmeier et al., 2006 | Minibioreactor | Flat | polyterafluoroethylene membrane dense | Porcine hepatocytes | $6\ x10^6$ | Monolayer | Over the surface |
| Sauer et al., 2004 | Slide reactor | Hollow fibre | polyethersulfone membranes (pore size 0.2 μm) | Human hepatoma cells | $8x10^4$ | Aggregates | Between hollow fibres |
| Pless et al., 2006 | Microchannel bioreactor | Flat-plate | Polyurethane membrane dense | Rat hepatocytes | $2x10^6$ | Monolayer | Over the surface |
| Ostrovidov et al., 2004 | PDMS microbioreactor | flat | polydimethylsiloxane and polyester membrane (pore size 0.4 μm) | Rat hepatocytes | $5\ x10^5$ | Monolayer | Over the surface |

| | | | | | | | |
|---|---|---|---|---|---|---|---|
| De Bartolo et al., 2007 | Multibore fibre bioreactor | Multibore capillary | Modified polyethersulfone (pore size 0.2 μm) | Human hepatocytes | $7.5x10^6$ | Small Aggregates | Lumen |
| Lu et al., 2005 | PVDF-hollow fibre | Extracapillary space | polyvinylidene difluoride (pore size 0.5 μm) | Rat hepatocytes | $5\ x10^7$ | Aggregates | Extracapillary space |
| Memoli et al., 2007 | Membrane bioreactor | Flat | Galactosylated polyethersulfone (pore size 0.1 μm) | Human hepatocytes | $4.7\ x10^7$ | Small aggregates | Over the surface |
| De Bartolo et al. 2009 | Crossed hollow fibre membrane bioreactor | Extracapillary space | modified polyetheretherketone (MWCO 190 kDa)<br><br>polyethersulfone (pore size 0.2 μm) | Human hepatocytes | $15\ x10^6$ | Small aggregates | Extracapillary space |

An oxygenating hollow fibre bioreactor (OXY-HFB) BAL system was developed by Jasmund and coworkers and consists of oxygenating and integral heat exchange fibres with a simple design [47]. Primary liver cells are seeded on the surface of the fibres in the extrafibre space. Oxygen requirements are supplied and temperature is controlled via the fibres. Plasma from patient is perfused through an extrafibre space and brought into direct hepatocellular contact.

The liver lobule-like structure module (LLS) BAL system, has many hollow fibres that act as a blood capillary and are regularly arranged close to each other [48]. Hepatocytes are inoculated by a centrifugal force in the outer space of the hollow fibres.

The multicapillary polyurethane foam module (PUF) used as BAL system consists of a cylindrical PUF block with many capillaries in a triangular arrangement to form a flow channel [49]. The hepatocytes in the foam pores formed spheroids with a diameter of 100-150 μm. Based on the use of a gas permeable membrane a rotating-wall gas-permeable membrane system was developed by Curcio et al., and used for the formation and culture of hepatocyte spheroids. Microgravity conditions were obtained in rotating-wall systems in which hepatocyte aggregates were formed by cells protected from gravitational forces and acceleration. Owing to the high $O_2$ permeability of the rotating-wall membrane system the viability and functions of cells improved with respect to a polystyrene rotating wall system [50]. Schmitmeier and co-workers developed a new small-scale bioreactor with the hepatic sandwich model. It is of the same dimension as the conventional 24-well cell cultivation plate where the bottom is replaced by the gas-permeable polytetrafluorethylene (PTFE) membrane. Compared to hepatocytes cultured in conventional systems, primary porcine hepatocytes exhibited stronger liver-specific capacity and remained in a differentiated state in the small-scale bioreactor over a cultivation period of 17 days. This in vitro model could serve as a tool to predict the liver response to newly developed drugs [51]. Pless and co-workers evaluated the primary human liver cells in bioreactor cultures for extracorporeal liver support on the basis of urea production. In particular the long-term course of 47 bioreactor cultures of hepatocytes over a culture period of 21 days was investigated. The bioreactors based on the design developed by Gerlach et al. consist of three interwoven hollow fibre capillary boundless, forming four compartments, and integrated into a polyurethane housing. Two of the boundless are made of hydrophilic polyethersulfone membrane with a pore

size of 0.5μm, serving for medium supply during stand-by or for plasma perfusion during clinical application. The third bundle consists of hydrophobic multilaminate hollow fibre membranes and was perfused with a mixture of air and $CO_2$ supplying the cells with oxygen and carbon dioxide [52].

A simple hollow fibre based bioreactor that is suitable for light microscopy was developed by Sauer et al., to evaluate cell-cell and cell-membrane interactions [53]. The SlideReactor offers a cell compartment separated from a medium inflow and outflow compartment. Due to its simple design and the use of materials available in most laboratories, SlideReactor is a simple valuable tool to evaluate the cell-to-cell and cell-to-hollow fibre interaction and enables the comparison of different types or arrangement of hollow fibres, e.g., for use in bioreactor-based extracorporeal liver assist devices, or analysis of the influence of medium supplements on the cell viability and tissue integrity.

Flat plate microchannel bioreactor with an internal membrane oxygenator was designed to improve the oxygen supply to the cells. The hepatocytes are attached to a glass substrate and are in direct contact with the perfusing medium. A polyurethane gas permeable membrane separates the liquid compartment from the oxygenating gas compartment. This design allows oxygen delivery to the hepatocytes to be decoupled from the medium flow, thereby allowing oxygen delivery and flow to be studied independently. Hepatocytes with oxygen dependent functional heterogeneity may exhibit optimal function into the bioreactor [54]. Ostrovidov and coworkers developed two types of membrane-incorporating microbioreactors to improve the maintenance of primary rat hepatocytes: one with a commercially available polyester membrane and the other with a polydimethylsiloxane (PDMS) membrane. These microbioreactors closely mimic the in vivo liver architecture and revealed to be promising tools towards future application in drug screening or liver tissue engineering [55]. Recently, De Bartolo et al., developed a multibore fibre bioreactor as an in vitro liver tissue model to study disease, drugs and therapeutic molecules alternatively to animal experimentation [56]. This bioreactor, owing to the membrane configuration, combines the advantage of having 7 compartments represented by 7 capillaries arranged in one single fibre with high stability and mechanical resistance. Human hepatocytes were cultured in the intraluminal compartment of the multibore fibre bioreactor. The morphological,

physico-chemical and transport properties of the multibore fibre membranes favor cell adhesion and ensure a sufficient oxygenation process, nutrient feeding, end-product removal and distribution of fluid molecules inside the cell environment.

Membrane bioreactors using specific adhesive substrates such as galactosylated membranes were developed in order to improve the adhesion and specific functions of liver cells. A galactosylated polyvinylidene difluoride hollow fibre bioreactor provided specific adhesion and showed an enhanced albumin production of rat hepatocytes [57] It has been shown that a flat bioreactor using galactosylated-polyethersulfone membrane promoted the long-term maintenance of differentiated functions of human hepatocytes outside of the body [58]. This human hepatocyte bioreactor was applied to study IL-6 effects on the production of acute phase proteins and gave evidence that IL-6 down-regulated the gene expression and synthesis of fetuin-A by primary human hepatocytes. The human hepatocyte bioreactor behaves like the *in vivo* liver, reproducing the same hepatic acute-phase response that occurs during the inflammation process. Furthermore it's important to notice that in developing a three dimensional tissues, the problems of oxygen supply must to be addressed, particularly at the core of the construct. With this aim an engineered solution was proposed by De Bartolo et al. recreating an hollow fibre membrane bioreactor formed by two fibres set. In this bioreactor the extracapillary network, provided an high mass exchange through the cross-flow of the culture medium, mimicking closely the perfusion conditions found in vivo hepatic tissue. Thanks to this design and its good performance both the viability and the functional metabolic activity was maintained, addressing the mass transfer limitation currently seen in liver tissue engineered construct [59].

## 2.5 MEMBRANES FOR LIVER RECONSTRUCTION

Hepatocytes are anchorage dependent cells that require adhesive substrates for their functional and phenotypic maintenance. In the last few years, several studies have clearly estalished that semipermeable synthetic membranes can be used for the development of biohybrid systems for liver cell cultures [60]. It has been demonstrated that the morphological and physico-chemical properties of membranes, such as surface free-energy parameters, affect cell adhesion and specific metabolic functions of hepatocytes [30].

De Bartolo et al. developed a new membrane from polymeric blend of modified polyetheretherketone or PEEK-CW and polyurethane (PU) demonstrating that this membrane is able to support the long term maintenance of metabolic and biotransformation functions of human hepatocytes. Consequently, this membrane meets the criteria of an appropriate substratum for cell culture in a biohybrid system [61]. Furthermore, in the recent past, the in vitro use of membrane biohybrid systems contributed to provide important information about the effect of various drugs, such as diclofenac (DIC), rofecoxib and paracetamol , whose effects are not completely known, on the specific functions of human hepatocytes [62-63].

An interesting appeoach to the design of membrane able to activate specific biological responses of the cells is the surface-modification technique by biomolecule immobilization and plasma process. These modifications enhance the cytocompatibility of the membrane, leaving the bulk properties unaltered. It has been demonstrated that the immobilization of biomolecules on the membrane surface improves cell adhesion and the maintenance of differentiated functions [64]. In particular, the RGD amino acid sequence (arginine-glycine-aspartic acid) stimulate cell adhesion on synthetic surfaces, since this oligopeptide represents the minimal adhesion domain of the majority of extracellular matrix proteins ( e.g. fibronectin, vitronectin and collagen ). In the case of hepatocytes the immobilization of galactose motif on the surface enhances the specific interaction with cells owing to the specific binding between the galactose moiety and the asyaloglycoprotein receptor present on the cytoplasmatic membrane [65]. Another surface modification strategies was investigated in a recent work of Salerno et al. in which PEEK-WC–PU membranes were modified with an NH3 glow discharge process to graft N-containing functional groups at their surface in order to improve the maintenance of human hepatocytes. Indeed the cells reconstituted many of the liver features active in vivo and when cultured on NH3 plasma-grafted membranes they displayed higher metabolic activity in terms of albumin synthesis, urea production as well as for the biotransformation of diazepam as model drug [66].

## 2.6 CONCLUDING REMARKS

With the recent advances in the field of biomaterials, particularly in membrane systems, there is much promise of working toward functional tissue engineered constructs. Many strategies are being
developed to realize tailored synthetic and biodegradable membrane systems that are compatible with human cells and tissues. The preclinical development stage of some of these membrane systems demonstrates their potentiality in the tissue engineering field. Bioartificial membrane systems could not only have a role in the replacement of injured organ or tissue but also accelerate the development of new drugs that may cure patients as an alternative to animal experimentation. Many problems encountered with testing potential drugs can be overcome and redesigned on a quicker time scale and at lower cost utilizing a system that can effectively act as a functioning liver.

.

**REFERENCES**

[1] P.Opolon. High-permeability membrane hemodialysis and hemofiltration in acute hepatic coma: experimental and clinical results. Artificial Organs 1979, 3: 354–360

[2]A. J. Knell, D. C. Dukes. Dialysis procedures in acute liver coma. Lancet 1976, 2: 402–403.

[3]H.B. Stockman, C.A. Hiemstra, R. L. Marquet, J.N. Ijzermans. Extracorporeal perfusion for the treatment of acute liver failure. Annals of Surgery 1973, 231:460–470.

[4]A.J. Strain, J.M. Neuberger. A bioartificial liver-state of the art. Science 2002, 295: 1005–1009

[5 ] M.J. Powers, K. Domansky, M.R. Kaazempur-Mofrad, A.Kalezi, A. Capitano, A.Upadhyaya, P.Kurzawski, K. E. Wack, D. Beer Stoltz, R. Kamm, L.G. Griffith. A microfabricated array bioreactor for perfused 3D liver culture.Biotechnol Bioeng 2002;78 (3):257 –269.

[6] S. Gupta, H. Malhi, G.R.Gorla. Re-Engineering the liver with natural biomaterials. Yonsei Medical Journal 2000;41(6):814 –824.

[7] D. Mooney, L. Hansen, J. Vacanti, R. Langer, S. Farmer, D.Ingber. Switching from differentiation to growth in hepatocytes: control by extracellular matrix. Journal of Cellular Physiology 1992;151(3):497 –505.

[8]L.K. Hansen, D.J. Mooney, J.P. Vacanti, D,E Ingber. Integrin binding and cell spreading on extracellular matrix act at different points in the cell cycle to promote hepatocyte growth. Molecular Biology of the Cell 1994;5(9):967 –975

[9] K.L. Crossin. Cell adhesion molecules activate signaling networks that influence proliferation, gene expression, and differentiation. Annals of New York Academy Science 2003;961(1):159.

[10]G.K. Michalopoulos, W.C. Bowen, V.F. Zajac, D. Beer-Stolz, S. Watkins, V. Kostrubsky, S.C. Strom. Morphogenetic events in mixed cultures of rat hepatocytes and nonparenchymal cells maintained in biological matrices in the presence of hepatocyte growth factor and epidermal growth factor. Hepatology 1999;29(1):90 –100.

[11] A. A. te Velde, N.C.J.J. Ladiges, L.M. Flendrig, R.A.F.M. Chamuleau. Functional activity of isolated pig hepatocytes attached to different extracellular matrix substrates. Implication for application of pig hepatocytes in a bioartificial liver. Journal of Hepatology 1995; 3:184–192.

[12] A.Pasher, I.M. Sauer, P.Neuhaus. Analysis of allogeneic versus xenogeneic auxiliary organ perfusion in liver failure reveals superior efficacy of human livers. International Journal Artificial Organs 2002, 25: 1006–1012

[13] J.W. Allen, S. N. Bhatia. Engineering Liver Therapies for the Future. Tissue Engineering 2002, 8:725–737

[14]S. L.Nyberg, R. P. Remmel, H. J. Mann, M. V. Peshwa, W. S. Hu, and F. B. Cerra. Primary hepatocytes outperform Hep G2 cells as the source of biotransformation functions in a bioartificial liver. Annals of Surgery 1994, 220: 59–67.

[15]T. Mitaka, T. Mizuguchi F. Sato, C. Mochizuki, Y. Mochizuki. Growth and maturation of small hepatocytes. Journal of Gastroenterology and Hepatology 1998;13(Suppl.):S70 –S77.

[16]R.A. Faris, T. Konkin, G.Halpert. Liver stem cells: a potential source of hepatocytes for the treatment of human liver disease. Artificial Organs 2001;25(7):513 –521

[17] H. J. Rippon, A.E. Bishop. Embryonic stem cells. Cell proliferation 2004, 37 (1):23-34

[18] J.C.Y. Dunn, M.L.Yarmush, H.G. Koebe, R.G. Tompkins. Hepatocytes function and extracellular matrix geometry: long-term culture in a sandwich configuration. Faseb Journal 3:174-177.

[19]N.Koide, K. Sakaguchi, Y. Koide et al. Formation of mulncellular spheroids composed of adult rat hepatocytes in dishes with positively charged surfaces and under other non-adherent environments. Experimental Cell Researc 1990; 186: 227-35

[20] Hou D-X, Arimura M, Fukuda M, Oka T, Fujii M. Expression of cell adhesion molecule and albumin genes in primary culture of rat hepatocytes. Cell Biology International 2001;25/3:239–244.

[21]Yagi K, Tsuda K, Serada M, Yamada C, Kondoh A, Miura Y. Rapid formation of multicellular spheroids of adult rat hepatocytes by rotation culture and their immobilization within calcium alginate. Artificial Organs 1993;17(11):929–34.

[22] L.B. Kong, S. Chen, A.A Dememou, J.Rozga. Matrix-induced liver cell aggregates (MILCA) for bioartificial liver use. International Journal of Artificial Organs 1996; 19:72-78

[23] Z. C. Liu, T. M. S. Chang. Coencapsulation of hepatocytes and bone marrow cells: In vitro and in vivo studies. Biothecnology Annual Review, 2006; 12:137-151.

[24]V. Dixit, R. Darvasi, M. Arthur et al.Restoration of liver functions in gunn rats without immunosuppression using transplated microencapsulated hepatocytes. Hepatology, 1990; 12:1342-1349

[25]Y. Kino, M. Sawa, S. Kasai, M.Mito. Multiporous cellulose microcarrier for the development of a hybrid artificial liver using isolated hepatocytes. Journal of Surgical Research, 1998; 79:71-76

[26]C. Wu, J. Pan, Z. Bao, Y. YU. Fabrication and characterization of chitosan microcarrier for hepatocytes culture. Journal of Material Science Material in Medicine 2007; 18(11):2211-2214.

[27] R. Jindal, Y. Nahmias, A. W. Tilles, F. Bethiaume, M.L. Yarmush. Amino acid-mediated heterotypic interaction governs performance of hepatic tissue model. The Faseb Journal 2009; 23(7):2288-2298.

[28]P.Krause, F. Sagatolislam, S. Koenig, K. Unthan-Fechner, I. Probst. Maintening hepatocytes differentiation in vitro through co-culture with hepatic stellate cells.

[29]A. A. Demetriou, W. S Arnaout, G. Backfish, A. D. Moscioni In Artificial Liver Support, 2nd edn.; Brunner, G., Mito, M., Eds.; Springer: Berlin, 1993; pp 283–295.

[30]L. De Bartolo, S. Morelli, A. Bader and E. Drioli. "Evaluation of cell behaviour related to physico-chemical properties of polymeric membranes to be used in bioartificial organs", Biomaterials 2002; 23(12): 2485-2497

[31]L. De Bartolo, G. Catapano, C. Della Volpe, E. Drioli. The effect of surface roughness of microporous membranes on the kinetics of oxygen consumption and ammonia elimination by adherent hepatocytes. Journal of Biomaterial Science, Polymer Edition. 1999, 10: 641–655

[32] S. Morelli, S. Salerno, A. Piscioneri, C. Campana, E. Drioli, Loredana De Bartolo. Membrane bioreactors for regenerative medicine: an example of the bioartificial liver.

Asia-Pacific Journal of Chemical Engineering, 2010; 5: 146–159.

[33]W. S. Arnaout, A. D.Moscioni, R. L. Barbout, A. A Demetriou. Development of a bioartificial liver: bilirubin conjugation in Gunn rats. Journal of Surgical Research 1990, 48: 379–382.

[34]K. N. Matsumara, G. R. Guevara, H.Huston W.L. Hamilton, M. Rikimare, G. Yamasaki, M.S. Matsumura. Hybrid bioartificial liver in hepatic failure: preliminary clinical report.Surgery 1987, 101, 99–103.

[35] M. S. Margulis, E. A. Erukhimov, L. A. Andreiman, L.M. Viksna. Temporary organ substitution by hemoperfusion through suspension of active donor hepatocytes in a total complex of intensive therapy in patients with acute hepatic insufficiency. Resuscitascion,1989; 18, 85–94.

[36] N. L.Sussman, M. G. Chong, T.Koussayer, D. E.He, T. A. Shang, H. H.Whisennand, J. J. Kelly. Hepatology, 1992;16: 60–65.

[37]A. A. Demetriou, J. Rozga, L. Podesta, E. Lepage, E. Morsiani, A. D. Moscioni, A. Hoffman, M. McGrath, L. Kong, H. Rosen, F. Villamil, G. Woolf, J. Vierling ,L. Makowka. Scandinavian Journal of Gastroenterology, 1995; 208: 111–117.

[38]J. C. Gerlach, J. Encke, O. Hole, C. Muller, C. J.Ryan, P.Neuhaus. Bioreactor for larger scale hepatocyte in vitro perfusion. Transplantation, 1994; 58: 984–988.

[39] J. F. Patzer, G. V. Mazariegos, R.Lopez. Preclinical evaluation of the Excorp Medical, Inc, bioartificial liver support system. Journal of the American College of Surgeons, 2002; 195(3): 299–310.

[40]L. M. Flendrig, J. W. la Soe, G. G. Jorning, et al. In vitro evaluation of a novel bioreactor based on an integral oxigenator and a spirally wound non woven polyester matrix for hepatocyte culture as a small aggregate. Journal of Hepatology, 1997; 26:1379–1392.

[41]Y. T. Ding, Y. D. Qiu, Z.Chen, Q.X. Xu, H. Y. Zhang, Q. Tang, D.C. Yu. The development of a new bioartificial liver and its application in 12 acute liver failure patients. World Journal of Gastroenterology, 2003; 9 (4): 829–832.

[42]W. S. Hu, J. R. Friend, F. J.Wu, T. Sielaff et al. Development of a bioartificial liver employing xenogeneic hepatocytes. Cytotechnology 1997, 23:29–38.

[43]H. Shiraha, N.Koide, H.Hada, K. Ujike, M. Nakamura, T. Shinji, S. Gotoh, T. tsuji. Biotechnology and Bioengineering, 1996;50:416-421.

[44]S. Naka, , K.Takeshita, T.Yamamoto, , T. Tani, M.Kodama. Bioartificial liver support system using porcine hepatocytes in a three dimensional hollow fibre module with collagen gel : an evaluation in the swine acute liver failure model. Artificial Organs, 1999; 23: 822–828.

[45]L.De Bartolo, G. Jarosch-Von Schweder, A.Haverich, A.Bader. A novel full-scale flat bioreactor utilizing porcine hepatocytes:cell viability and tissue specific functions. Biotechnology Progress, 2000; 16: 102–108.

[46]M. Nagaki, K. Miki, Y.Kim, H. Ishijama, I. Hirahara, H. Takahashi, A. Sugiyama, H. Moriwaki. Digestive Diseases and Sciences, 2001; 46:1046–1056.

[47]L. Jasmund, A. Langsch, , R. Simmoteit, A.Bader.Cultivation pf primary porcine hepatocytes in an OXY-HFB for use as a bioartificial liver device. Biotechnology Progress, 2002; 18: 839–846.

[48]D. H. Lee, H. H. Yoon, J. K. Park. Hepatocytes culture technology and its application to bioartificial liver. Korean Chemical Engineering Research, 2004; 42: 129–138.

[49] H. Mizumoto, K. Funatsu. Liver regeneration using a hybrid artificial liver support system. Artificial Organs, 2004; 28:53–57

[50]E.Curcio, S.Salerno, G.Barbieri, L. De Bartolo, E. Drioli, A.Bader. Mass transfer and metabolic reaction in hepatocytes spheroids cultured in rotating wall gas-permeable membrane system. Biomaterials 2007. 28: 5487–5497.

[51] S. Schmitmeier, A. Langsch, I.Jasmund, A.Bader.Development and characterization of a small-scale bioreactor based on bioartificial hepatic culture model for predictive pharmacological in vitro screenings. Biotechnoogy and Bioengineering, 2006; 95: 1198–1206.

[52]G. Pless, I.Steffen, K. Zeilinger, I.M. Sauer, E. Katenz, D.Kehr, S. Roth, T. Mieder, R.Schartlander, C. Muller, B. Wegner, M.S. Hout, J.C. Gerlach. Evaluation of primary human liver cells in bioreactor cultures for extracorporeal liver support on the basis of urea production. Artificilals Organs 2006;30:686–694.

[53]I.M. Sauer, R. Scwartlander, J. Schmid, E. Efimova, F.W.R. Vondran, D. Kehr, G. Pless, A. Spinelli, B. Brandeburg, E. Hildt, P. Neuhaus. The SlideReactor-A Simple hollow fibre based bioreactor suitable for light microscopy. Artificial Organs, 2005; 29, 264–267.

[54] P.Roy, H. Baskaran, A. W Tilles, M.Yarmush, M. Toner. Analysis of oxygen transport to hepatocytes in a flat-plate microchannel bioreactor Annals of Biomedical Engineering,. 2001; 29, 947–955.

[55] S. Ostrovidov, J. Jiang, , Y. Sokai, , T. Fujii. Membrane-based PDMS microbioreactor for perfused 3D primary rat hepatocyte cultures. Biomedical Microdevices, 2004; 6: 279–287.

[56] L. De Bartolo, S. Morelli, M. Rende, C. Campana, S. Salerno, N. Quintiero, E. Drioli. Human hepatocyte morphology and functions in a multibore fibre bioreactor. Macromolecular Bioscience 2007, 7:671-680.

[57]H. F. Lu, W. S Lim, P.C Zhang, S.M. Chia, H. Yu, H.Q. Mao, K.W. Leong. Tissue Engineering, 2005 ; 11 : 1667–1677.

[58] B. Memoli, L. De Bartolo, P. Favia, S. Morelli, L.C. Lopez, A. Procino, G. Barbieri, E. Curcio, L. Giorno, P. Esposito,, M. Cozzolino, D. Brancaccio, V.E. Andreucci, R. d'Agostino, E. Drioli. Fetuin-A gene expression, synthesis and release in primary human hepatocytes cultured in a galactosylated membrane bioreactor. Biomaterials 2007; 28:4836-4844.

[59]L. De Bartolo, S. Salerno, E. Curcio, A. Piscioneri, M. Rende, S. Morelli, F. Tasselli, A. Bader, E. Drioli. Human hepatocyte functions in a crossed hollow fibre membrane bioreactor. Biomaterials, 2009;30: 2531–2543.

[60] L. De Bartolo, S. Morelli, M. Rende, A. Gordano, E. Drioli. "New modified polyet heretherketone membrane for liver cell culture in biohybrid systems: adhesion and specific functions of isolated hepatocytes" Biomaterials 2004, 25:3621-3629.

[61]L. De Bartolo, S. Morelli, M.C. Gallo, C. Campana, G. Statti, M. Rende, S. Salerno, E. Drioli. Effect of isoliquiritigenin on viability and differentiated functions of human hepatocytes on PEEK-WC-polyurethane membranes", Biomaterials 2005; 26:6625-6634.

[62]L. De Bartolo, S. Morelli, L.Giorno, C. Campana, M. Rende, S. Salerno, S. Maida, E. Drioli. Polyethersulfone membrane biohybrid system using pig hepatocytes: effect of diclofenac on cell biotransformation and synthetic functions. J. Membrane Science 2006; 278(1-2): 133-143

[63] L. De Bartolo, S. Salerno, L. Giorno, S. Morelli, G. Barbieri, E.Curcio, M. Rende E. Drioli. Membrane bioreactor using pig hepatocytes for in vitro evaluation of antinflammatory drug. Catalysis Today 2006; 118:172-180.

[64] L. De Bartolo, S. Morelli, L. Lopez, L. Giorno, C. Campana, S. Salerno, M. Rende, P. Favia, L. Detomaso, R. Gristina, R. d'Agostino, E. Drioli. Biotransformation and liver specific functions of human hepatocytes in culture on RGD-immobilised plasma-processed membranes. Biomaterials 2005; 26(21):4432-444.

[65]L. Ying,R. X., K. W. Leong, H.Q. Mao, E.T. Kang, K.G.Neoh. Immobilization of galactose ligands on acrylic acid graft-copolymerized poly(ethylene terephthalate) film and its application to hepatocyte culture. Biomacromolecules 2003;4(1):157-165.

[66] S. Salerno, A. Piscioneri, S. Laera, S. Morelli, P. Favia, A. Bader, E. Drioli, L. De Bartolo. Improved functions of human hepatocytes on $NH_3$ Plasma–grafted PEEK-WC-PU membranes. Biomaterials 2009, 30:4348-4356.

# CHAPTER 3

# MEMBRANE APPROACHES FOR NEURONAL TISSUE ENGINEERING: STATE OF THE ART

## 3.1 INTRODUCTION

In the numerous attempts to integrate tissue engineering concepts to repair all body parts, neuronal repair stands out. The nervous system consists of the central nervous system (CNS) which includes the brain and the spinal cord and the peripheral nervous system (PNS), which is composed of cranial, spinal, and autonomic nerves that connect to the CNS. The functional unit of the nervous system is the neuron that has a cell body and dendrites and axons. The dendrites serve as antennae to receive signals from the surroundings or other neurons whereas the axon that is longer than the dendrite is engaged in transporting impulses from the cell body to dendrites of other neurons through synapses. Electrical impulses can also pass from axon to axon, axon to soma, or from dendrite to dendrite.

In order to study how neuronal attachment and axon guidance can be accomplished using various surface cues cell line are often used for investigation of the nervous system due to their relatively low cost and simplicity compared to primary cell material. However it should be noted that cell lines can only be used as models and often do not show the same responses as primary material. PC-12 and C6 cell lines originally derived from neuronal rat tumors are often chosen as model cells for the investigation of nervous system for their characteristics.

Hippocampal neurons, as primary cells, are good models since they are derived from the hippocampus, a major component of the brain involved in long term memory and spatial awareness. The hippocampus, through the complex interaction with other limbic regions such as the cortex and amygdale is recognized for its highly remarkable synaptic plasticity. Here, the neuronal network is highly developed, being one of only few regions in the brain where new neurons continue to be created, furthermore hippocampal neuronal cell culture is the best characterized model for investigating polarization that occurs spontaneously during the first days of culture.

The effects of surface chemical cues on neuronal cell attachment, growth, migration and proliferation have been greatly studied by researchers; here follows a description of some advances in tissue engineering in the recreation of a neuronal bridging device.

## 3.2 NERVOUS SYSTEM: INJURY AND REPAIR

Damage to the nervous system, caused by mechanical, thermal, or ischemic factors, can impair various nervous system functions such as memory, cognition, language and voluntary movement. Most often, this is through crash or transaction of nerve tracts. This results in the interruption of communication between nerve cell bodies and their targets. However, other types of disruption of the interrelation between neurons and their supporting cells , and the destruction of the blood-brain barrier. Of all the types of injury, those to the CNS are among the most likely to result in death or permanent disability. Only in the United States, more than 3 million cases of traumatic brain injury are reported annually. These patients include anyone who has fallen, especially someone older than 64 years; a person who has been in a motor vehicle accident; someone with a gunshot wound or violence-related injury; or an adolescent or young adult who has a sports-related injury. Approximately 400 000 Americans suffer from neurological symptoms associated with multiple sclerosis (MS). Furthermore, over 5 million people in the United States and Europe alone suffer from the dementia associated with Alzheimer's disease. About 450 000 people in the United States live with spinal cord injury (one in 670), and there are about 11 000 new spinal cord injuries every year (one in 30 000) [1].

Following injury, the PNS and the CNS respond differently. While in the most cases, the severed axons of the PNS are able to re-extend and re-innervate their targets, eventually leading to a functional recovery [2], a rare return of damaged structures and functions is observed following injuries to the CNS. As a result, disorders or injuries of the CNS are often progressive, accompanied by permanent functional impairment. Studies have shown that the structural and functional recovery from nervous system depends upon a variety of factors, both intrinsic and extrinsic to the neurons [3].

In the peripheral nervous system after a nerve is severed, the distal portion begins to degenerate as a result of protease activity and separation from the metabolic resources of the nerve cell bodies. The cytoskeleton begins to breakdown, followed by the dissolution of the cell membrane. The proximal end of the nerve stump swells, but experiences only minimal damage via retrograde degradation. After the cytoskeleton and membrane degrade, Schwann cells surrounding the axons in the distal end shed their myelin lipids. Phagocytotic cells, such as macrophages and Schwann cells, clear

myelin and axonal debris [4]. In addition to clearing myelin debris, macrophages and Schwann cells also produce cytokines, which enhance axon growth [5]. Following debris clearance, regeneration begins at the proximal end and continues toward the distal stump. New axonal sprouts usually emanate from the nodes of Ranvier, nonmyelinated areas of axons located between Schwann cells. Functional reinnervation requires that axons extend until they reach their distal target, and in humans, axon regeneration occurs at a rate of about 2–5 mm/day; thus significant injuries can take many months to heal [Figure 3.1].

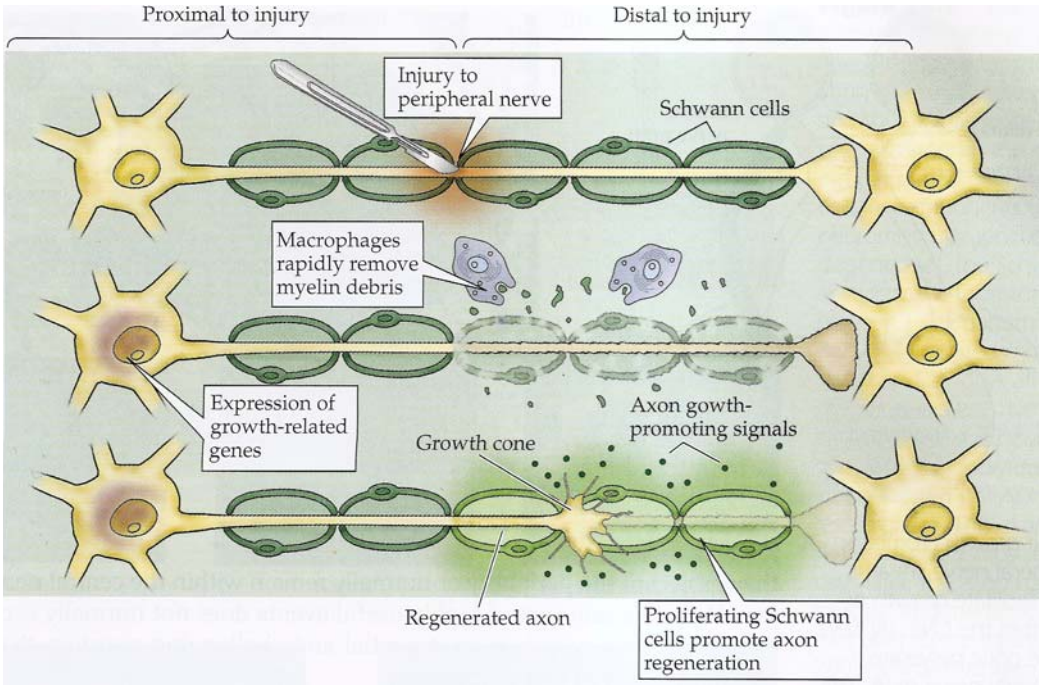


**Figure 3.1** Molecular and cellular responses that promote peripheral nerve regeneration. The Schwann cell is essential for this process. Once the macrophages have cleared the debries from the degenerating peripheral stump, the Schwan cell proliferate, express adhesion molecules on their surface, and secrete neurotrophins and other growth promoting signalling molecules. Adapted from D. Purves, Neuroscience, [6]

A key difference between the PNS and CNS is the capacity for peripheral nerves to regenerate; CNS axons do not regenerate appreciably in their native environment. Several glycoproteins in the native extracellular environment (myelin) of the CNS are inhibitory for regeneration. The outer myelin membrane contains non-permissive molecules, such as Nogo and myelin membrane associated glycoprotein (MAG) produced by the astrocytes and oligodendrocytes. Disruption of myelin following injury could expose such normally concealed inhibitory proteins to regenerative axons.
The physiological response to injury in the CNS is also different compared to that of the PNS. After injury in the CNS, macrophages infiltrate the site of injury much more slowly compared to macrophage infiltration in the PNS, delaying the removal of inhibitory myelin. This is largely a result of the blood-spine barrier, which limits macrophage entry into the nerve tissue to just the site of injury, where barrier integrity is weakened. In addition, cell adhesion molecules in the distal end of the injured spinal cord are not upregulated appreciably as they are in the PNS, limiting macrophage recruitment. Finally, astrocytes proliferate in a manner similar to that of Schwann cells in the PNS, but instead become "reactive astrocytes," producing glial scars that inhibit regeneration [Figure 3.2]. The dense scar tissue that forms following injury in the adult CNS is a formidable barrier to axonal outgrowth due, in part to its dense physical structure, and the upregulation of inhibitory extracellular matrix molecules secreted by several cell types within the scar. Thus, comparison between the PNS and the CNS environment following various lesions revealed that the CNS lacks several factors that are presented within the PNS. First, as mentioned above, there are Schwann cells in the PNS, that don't produce proteins inhibitory to axonal outgrowth and are able to provide nutrient support, guide and myelinate regenerating axons even after axotomy of peripheral neurons, and synthesize growth-promoting molecules and growth factors [7]. Second, a unique structure in the PNS called the Bands of Bungner, containing oriented arrays of Schwann cells and their processes within a basement membrane remains after axonal and myelin degeneration, which is believed to assist the regeneration process.

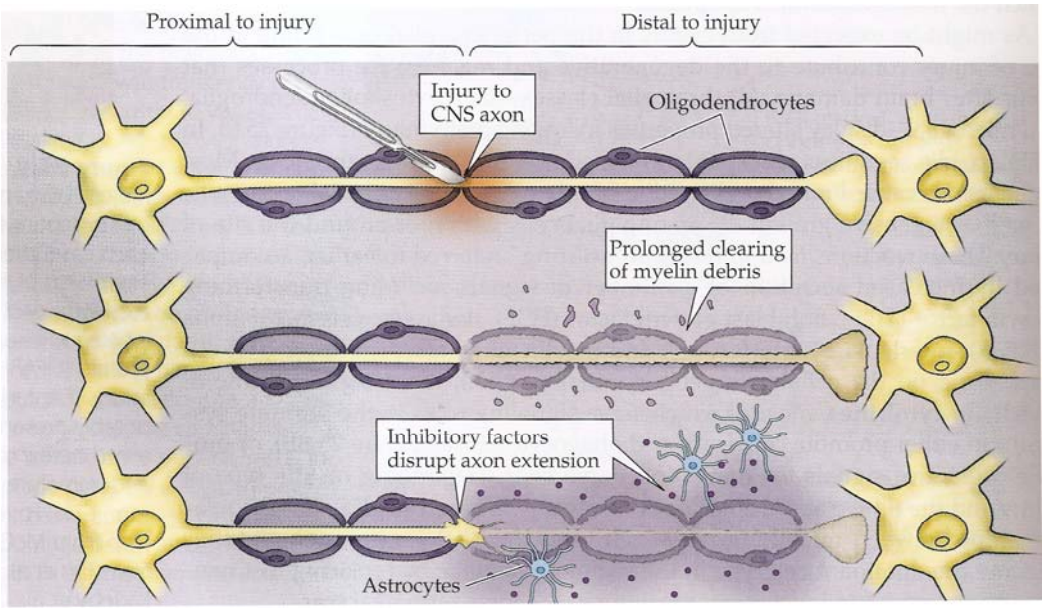


**Figure 3.2** Cellular response to injury in the central nervous system. In the absence of a glia scar, which are particular prominent in the long axon pathways in the brain, there is a series of local cellular changes at or near an injured site. These include the local degeneration of myelin as well as other cellular elements, the clearing of this debris by microglia that act as a phagocytic cell in the CNS, and the local production of inhibitory factors by reactive astrocytes and microglia. Adapted from D. Purves, Neuroscience [6].

### 3.2.1 Neurotrophic Factors to Promote Regeneration

The role of neurotrophic factors in neural regeneration has been the focus of extensive research. The influence of these factors in neural development, survival, outgrowth, and branching has been explored on various levels, from molecular interactions to macroscopic tissue responses. One family

of neurotrophic factors, the neurotrophins, has been heavily investigated in nerve regeneration studies. The neurotrophins include nerve growth factor (NGF), brain derived neurotrophic factor (BDNF), neurotrophin-3 (NT-3), and neurotrophin-4/5 (NT-4/5). Outside of the neurotrophin family, other factors of importance are ciliary neurotrophic factor (CNTF), glial cell line-derived growth factor (GDNF), and acidic and basic fibroblast growth factor (aFGF, bFGF).

NGF is vital to the development and regeneration of nervous system; this neurotrophin is expressed at low levels in healthy peripheral nerve and is upregulated in the distal stump upon injury [8]. On the cellular level NGF promote axonal growth from sensory

neurons through activation tyrosine kinase, TrKA. BDNF is known to enhance survival and promote axon growth of motor and sensory neurons and hippocampal neurons via its receptor TrKB. Has been shown that BDNF plays an important role in regulation of synapse structure and function.

NT3, like BDNF, promotes motor neuron survival and outgrowth as well as sensory axon growth. It has also been demonstrated that BDNF and NT-3 significantly influence axon path-finding, as well as aiding axonal regeneration in rats following spinal cord injury [9]. Recent studies also provide evidence that basic fibroblast growth factor (bFGF-2) and glial cell line-derived neurotrophic factor (GDNF) may play a role in facilitating nerve regeneration in the peripheral nervous system (PNS) and CNS. Both growth factors have been shown to influence neurons, Schwann cells, and oligodendrocytes toward axonal growth and remyelination following injury[10,11]. Ciliary neurotrophic factor (CNTF) has been shown to act primarily on neurons as a survival factor following injury in the PNS [12]. Taking in account the main role played by the ECM molecules and of the soluble factors (e.g. neurotrophins) in the maintenance of the integrity of the nervous system, it's necessary to steer engineering technique toward creating and modifying biomaterials to mimic the in vivo environment.

### 3.3 CLINICAL APPROACHES FOR TREATING PERIPHERAL NERVE INJURIES

For peripheral nerve injury, one of the current clinical treatments for nerve transaction is surgical end-to-end reconnection, which involves the suturing of individual fascicles within the nerve cable. End-to-end repair, however, is only effective if the nerve ends are directly adjacent and can be reconnected without causing tension. If the injury creates a gap in the nerve, autologous nerve grafts or autografts are used. For longer nerve gaps, this approach is not used because any tension introduced in the nerve cable would inhibit the regeneration while an autologous nerve graft from other donor sites is used. This technique has the disadvantage of the loss of function at the donor site and the need for multiple surgeries. There are a few devices that are now Food and Drug Administration (FDA) approved for relatively short nerve defects, including Integra Neurosciences Type I collagen tube (NeuraGen Nerve Guide) [13] and SaluMedica's

SaluBridge Nerve Cuff [14]. However, these treatments are reserved for small defects (several millimeters) and do not address larger peripheral verve injuries.

In the PNS the challenge is to find an alternative to autologous nerve graft and thus eliminate the need for two surgeries and the removal of tissue from the patient, improving also the recovery rates and functional outcome.

### 3.4 BIOENGINEERING STRATEGIES FOR NERVE REPAIR

For CNS injury, and particularly spinal cord injury, clinical treatment is less promising. Unfortunately, there is currently no treatment available to restore nerve function. The CNS is a greater challenge for new therapies. Already in 1981 was shown that the regenerative potential of the central neurons seemed to be expressed when the central nervous system glial environment was changed to that of the peripheral nervous system [15]. The precise regeneration of a lesioned projection, assuming that neurons survive of the transaction of their axons, regeneration processes include different events [16]. The damaged axon has to start a spontaneous sprouting, to go into and through the lesion site with the outgrowth in the correct direction to establish reconnection with their targets properly reinnervated. Therefore helping regenerating axons cross the lesion area represents an important step in the early regenerative process in which bioengineering approach may be effective. One way is to create a growth-permissive artificial substrate that connect the gap between damaged nerve tracts across the scar. This substrate works as a “bridge” that fills the lesion site. Owing to the profound impact of CNS damage, extensive studies have been carried out aimed at facilitating CNS repair. Many strategies have been developed to facilitate axonal reinnervation and to direct their outgrowth. Various devices using synthetic and biological substrates are being developed as biomaterial bridges for peripheral nerve grafts. In particular, membranes in tubular configuration act as a guidance channel to protect the regenerating axons in the lumen from the external environment. The membrane reduces the infiltration of fibrous tissue and provides a conduit for the diffusion of neurotrophic factors, increase the concentration of endogenous proteins inside the channel and allows the selective transport of molecules between the lumen and the surrounding environment [Figure 3.3].

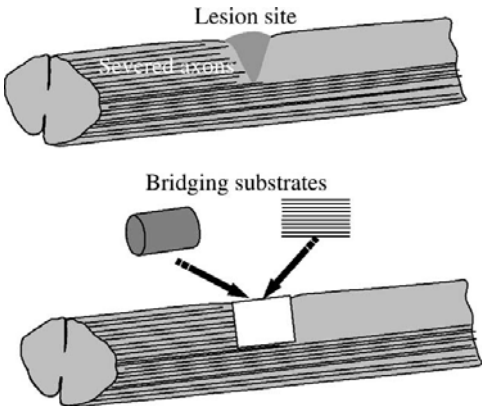


**Figure 3.3** Schematic diagram illustrating the concept of bridging following CNS injury**.**

Current attempts are focused on seeking new biomaterials, new cell sources, as well as novel designs of tissue-engineered neuronal bridging devices, to generate safer and more efficacious nervous-tissue repairs. Bioengineering efforts are focused on creating a permissive environment for regeneration and providing a seamless interface between the CNS and the PNS.

Many researchers are presently focusing efforts on creating physical or chemical pathways for regenerating axons for *in vivo* application or as *an in vitro* model. These devices include physical or mechanical guidance cues, cellular components, and biomolecular signals, as reviewed individually below. Future therapies will incorporate multiple cues into unique devices that more closely mimic native nerve. They will also be interactive and programmable, and thus capable of seamless communication with surrounding tissues.

### 3.4.1 Guidance therapies

For culturing neuronal cells is necessary to take in account that cell growth is strictly influenced by environmental cues. In particular the growth of cells and tissue is strongly influenced by environmental cues. In particular, topographical features, such as that created by cells, matrix proteins, and surface texture on biomaterials, influence cell and tissue growth. This phenomenon is termed as contact guidance. The physical guidance of axons is a vital component of nerve repair.

Since the 1960s, when Millesi et al. [17] pioneered microsurgical techniques to accurately align nerve fascicles in the direct resection of nerve ends, with improved functional outcomes, the need for physical guidance has been acknowledged as an essential element in nerve regeneration. The nerve guides or nerve-guidance channels serve to direct axons sprouting from the proximal nerve end, provide a conduit for the diffusion of growth factors secreted by the injured nerve ends, and reduce the infiltration of scar tissue. Past research in this area has focused either on existing natural or on synthetic materials; however, none of the materials studied to date have matched or exceeded the performance of the nerve autograft. As a result, researchers are now focusing on the combination of materials and desired biomolecules to create new composite materials that can actively stimulate nerve regeneration. Matrices are incorporated into the lumen of the guidance channel to enhance the organization of the regeneration environment and provide topographic-guidance cues via aligned textures, and biological-guidance cues by patterned biomolecules, to facilitate unidirectional outgrowth of the regenerating axons [18–19]. Cells [20], ECM molecules [21], or growth factors [22] can be incorporated into the tube to assist axonal sprouting and outgrowth. Among the variety of tubular structures used for guidance channels, semipermeable HFMs appear to be a favourable guide to regenerate neuronal tissue.

The most promising results were observed with a minichannel entubulation device in which Schwann cells were seeded into a semipermeable nondegradable HFM made of a random copolymer of acrylonitrile and vinylchloride (PAN–PVC) with an outer diameter comparable to that of the hemisected part of the right spinal cord [20-23] . A large number of both myelinated and nonmyelinated regenerating axons were discovered in the midpoint of the channel and some of the regenerating axons were able to traverse the bridge–host interface and reenter the host CNS environment. These axons terminated as button like structures in the gray matter. In order to confirm the efficacy of the minichannel design on CNS axon regeneration, further evaluations of functional recovery and synaptic reconnections are necessary. Topographic cues such as the surface microgeometry of the guidance channels and the morphology of the intraluminal matrices within the nerve bridging device may represent key elements in the successful guidance of regenerating axons.

## 3.5 TISSUE RESPONSE TO BRIDGING DEVICES

In a tissue-engineered construct, the response of tissue depends on the properties of the materials and the cells [24]. Material properties, including morphological, structural, mechanical, physicochemical [25], and electrical properties [26], affect tissue response. The cells within the construct interact with the material directly via physical contact or indirectly via the diffusion of cell-secreted soluble factors. In the case of a typical tissue-engineered neuronal bridging device, the properties of the material components relevant to the tissue response include the surface microgeometry, the MWCO, possibly the bioactive factors that are loaded and during the time released through the channel wall, and the degradation rate for biodegradable materials [27]. One particular advantage of tissue engineered platform of neural microenvironment is that they can present several types of cues in a synergistic or competitive manner to elucidate their relative importance. Axon guidance by concentration gradients of soluble guidance cues has been extensively studied *in vitro*. The modification of the surface with neuronal trophic factors has been found to elicit neuronal regeneration. The patterning of materials with chemical cues, such as ECM proteins (e.g., laminin, fibronectin, and RGD peptide), has been evaluated in the neurite outgrowth. Neurons from rat brainstem and cortices adhered to surfaces coated with laminin. DRG neurite attachment was found to be dependent on fibronectin strip width (30 mm). Hippocampal neurons adhered to and extended neurites on the pattern of poly-L-lysine and laminin. Different studies demonstrated that an applied electric field can accelerate neurite outgrowth and influence neurite orientation. In fact, the electric fields in the form of voltage gradients have been observed to polarize the nervous system along the rostral–caudal axis during the development (5–18mVmm$^{-1}$) and direct nerve growth and accelerate wound healing in the rat cornea (+40 mV/0.5 mm) [28].

Cues in three-dimension, such as matrigel, collagen, as well as synthetic polymer based scaffolds, support longer neurites outgrowth than in bidimensional culture systems.

Surface topography provides spatial and physical cues to the growth cone, influencing their regeneration and obviating the need for a cell-adhesive surface. Neurons have the capacity, in fact , to respond to topographical features in their microenviroments, and they have been shown to adhere, migrate, and orient their axons to navigate surface

features such as grooves in substrates in the micro- and nanoscales. Topographic guidance of neurite outgrowth has been explored *in vitro* with culture substrates that contained well defined micropatterned features such as etches, microchannels, nanotubes or microgrooves .

Mahoney et al. [29] studied the effects of polyimide microchannels in a range between 20-60 μm in width and 11 μm in depth on PC12 cell culture. Neurites were directed along the axis of the grooves with microchannel of 20-30 μm being the most effective at neurite direction.

More recently Morelli et al. [30] explored the polarization and orientation of hippocampal neuronal cells on nonpatterned and micro-patterned biodegradable poly(L-lactic acid) (PLLA) membranes, The micro-patterned membranes have a threedimensional structure consisting of channels plus ridges and bricks whereas the nonpatterned membranes have a flat surface. The most oriented neurons were observed specially on the patterned porous membranes with channel width of 20 μm and ridges of 17 μm, in which an higher frequency of neuronal orientations between -10° and 10° was observed too. These results demonstrated once again that the patterned microstructure is able to guide and enhance neurite extension and orientation.

Gomez et al. [31] studied the combined effect of NGF and microtopography of microchannels on axon initiation, polarization and elongation of hippocampal neurons. They observed that topography had a stronger effect on polarization but no effect on elongation, whereas NGF, and particularly a synergy of immobilized NGF plus topography, dominated axon length. These results revealed the synergies between the topographical and molecular cues, suggesting that both are required for maximal neurite growth.

Surface microgeometry of a nerve guidance channel affects the morphological patterns of neural regeneration. Aebischer et al. [32] demonstrated that varying only the luminal surface texture of otherwise identical guidance channels, the outcome of regeneration varies significantly. Smooth-walled tubes support the regeneration of a nerve cable containing numerous myelinated axons grouped into micro fascicles within an organized fibrin matrix. In contrast, rough-walled tube contain only a loose connective tissue stroma and few or no myelinated axons.

De Bartolo et al. [33] showed that hippocampal neurons exhibited a different morphology in response to varying the properties of the membrane surface. Indeed, cells grown on the smoother surfaces such as fluorocarbon (FC) and polyethersulfone (PES) membranes displayed a large number of neurites with consequent formation of bundles and a highly branched axonal network. When rougher membranes, as in the case the PEEK-WC, was used the neural cells formed aggregates and most of the processes were developed inside the pores of the membranes. Taken together these results suggest the pivotal role played by membrane surface properties in the adhesion and growth of the hippocampal neurons, which must be considered in the development of tailored membranes for neural tissue engineering.

Another approache to increase the efficiency of the guidance channel is the one proposed by Zhang et al.[34] that used highly aligned grooves on the inner surface of semipermeable HFMs produced from both nondegradable and biodegradable natural and synthetic polymers. In particular aromatic polyether based polyurethane (PU) was used as nondegradable and poly-$_{DL}$-lactide-coglycolide (PLGA) was employed as a degradable polymer. The studies using *in vitro* dorsal root ganglion (DRG) regeneration assay showed that both the alignment and the outgrowth rate of regenerating axons increased significantly in HFMs with aligned textures, more than those in HFMs with smooth inner surface.

Both surface and transport properties of the membranes play an important role in neuronal regeneration: the surface microgeometry of the membrane inner wall affects the orientation of the axonal growth, and the MWCO of the membrane affects axonal regeneration by governing the mass transfer of molecules between the controlled regenerating environment within the channel lumen and the external environment [35]. In Table 3.1, the main studies with neuronal cells using membrane systems for in vitro study are reported.

**Table 3. 1 – Characteristics of membranes for *in vitro* neuronal regeneration study**

| REFERENCE | MEMBRANE | CONFIGURATION | MATRICES | MEMBRANE PROPERTIES | CELLS | EFFECT |
|---|---|---|---|---|---|---|
| Li et al., 1999 | Polyacrylonitrile polyvinylchloride copolymer | Hollow fiber | Macroporous cellulosic microcarriers | Hydrogel | PC12 L-dopa secreting and C2C12 CNTF secreting | Cell proliferation, dopa and CNTF secretion |
| Manwaring et al., 2001 | Glass, CA, PES, PAN-PVC, PS, PP, PEVAC | Flat | - | Contact angle ranging from 35 to 95° | Dorsal root ganglion and cerebellar granule neurons | Cell proliferation on CA, PAN-PVC, PEVAC and glass |
| Broadhead et al., 2002 | Copolymer of acrylonitrile and vinylchloride | Hollow fiber | - | Cut-off 40,150 kDa | PC12 | Proliferation and maintanance of viability |
| Lee et al., 2003 | polyethylene | flat | Corona treated | Wettability gradient surfaces | PC-12 | Longer neurites on surface with contact angle of 55° |
| Zhang et al., 2005 | Aromatic polyether based polyurethane, Poly DL-lactide-coglicolide | Hollow fiber | Poly-L-lysine and laminin | Grooves on the lumen of width width of 38.5-91 μm | Dorsal root ganglion | High rate of neurite outgrowth on textured inner surface |
| Young et al., 2005 | Polyvinyl alcohol and polyethylene-co-vinyl alcohol | flat | - | Dense structure | Cerebral cortical stem cells | Differentiation in neurons/strocytes and proliferation |
| Lopez et al., 2006 | silicon | Flat | Laminin and collagen | Pore size ranging from 20 to 50 nm | PC-12 | The modification of collagen increase cell survival and functionality |

| | | | | | | |
|---|---|---|---|---|---|---|
| Chang et al., 2007 | Polyethyleneimine-polyethylenevinylalcohol | flat | - | Contact angle 23.2-84.9° | Rat cerebellar granule neurons | Increased cell viability on surface with 57.8° |
| De Bartolo et al., 2008 | Fluorocarbon, polyethersulfone, modifiedpolyetheretherketone, | flat | Poly-L-lysine | Roughness ranging from 6 to 200 nm | Hippocampal neurons | Surface with Ra up to 50 nm favoured the formation of longer neurites and BDNF secretion |
| Brayefield et al. 2008 | Polyethersulfone | Hollow Fiber | Laminin | Patterned with 5μm diameter channels. | PC12 and NPCs | Spontaneous cell process growth into the channels of the scaffold. |
| He et al. 2009 | Chitosan | Flat and Hollw fiber | Poly-L-lysine | Biodegradable | Hippocampal neurons | Adhesion and cellular growth. Expression of specific proteins. |
| Morelli et. al 2010 | PolyL-lactic acid (PLLA) | Flat | Poly-L-lysine | Micro-Patterned Non-patterned | Hippocampal neurons | Patterned membrane improved guidance and extension of the neurite. |

Young et al. [36] studied the effect of different membranes made of polyvinyl alcohol (PVA) and poly (ethylene-co-vinyl alcohol) (EVAL) on the proliferation and differentiation of neural stem cells isolated from embryonic cerebral cortex. Single neural stem cells seemed to remain dormant on the EVAL. Conversely, the development of cell clusters (neurospheres) was in a density-dependent manner on EVAL. Neurospheres proliferated under high-density culture condition, but differentiated into neurons and astrocytes under low-density culture condition. However, regardless of single cells or neurospheres, cultured cells could not survive on the PVA. These in vitro results are very encouraging since this information should be useful for the development of strategies in the biomaterial field for regulating the preservation, proliferation and differentiation of neural stem cells. The use of HFMs was employed by Yamazoe et al. [37] to induce the differentiation in dopaminergic neurons from mouse embryonic stem (ES) cells enclosed in hollow fibers using conditioning medium from PA6 cells, the stromal cells derived from skull bone marrow. With this system, dopaminergic neurons were efficiently obtained in HFMs and the dopamine release was observed; at the same time, hollow fibers membranes offered a protection to the dopaminergic neurons from mechanical disturbances and attacks by the host immune system. Although there are many issues that have to be addressed, this study showed that the differentiation of ES cells within hollow fibers is one of the most promising approach so that cell therapy of Parkinson's desease can be realized. Controllable 3-D neuronal networks in vitro, provide tools for studying neurobiological events. On this purpose, Brayefield et al. [38] recreated a scaffold constituted of polyethersulphone (PES) microporous hollow fibers ablated with excimer laser in order to generate specially designed channels. Such modification, was made in order to compartmentalize growth of neuronal cell body from their axonal processes and further facilitate directed process growth into the 3-D space of the fiber lumens. These laser-created channels within the PES fiber walls appear to enhance PC12 cell adhesion as well as able to sustain the growth of rat adult neural progenitor cells (NPC). Compartmentalization of neuronal cell bodies from their axons allowed a direct method for analyzing neurite outgrowth within a 3-D space at high densities that more accurately mimics the *in vivo* environment.

The physico-chemical properties of the membrane surface are also important in the interactions with cells. Manwaring et al. cultured cells derived from meningeal tissue on surfaces with different wettability: poly(vinylchloride)-poly(acrylonitrile) (PAN–PVC), polyethylene vinyl acetate (PEVAC), polypropylene (PP), polystyrene (PS), and Tecoflex (TECO). The hydrophilic materials supported the highest level of cell attachment while the hydrophobic materials supported less cell adhesion [39].Surface wettability plays an important role for neurite formation on the polymer surfaces for axon regeneration as demonstred by other studies in which PC- 12 cells exhibited a differentiated neuronal phenotype with a long neurite on polyethylene surface with moderate wettability [40].

Chang et al. [41] have investigated the effect of blending polyethyleneimine (PEI) with polyethylene vinyl alcohol (EVAL) on the granule neuronal cell behaviour. The addition of PEI at increasing concentration resulted in a change in wettability properties of the membranes with contact angle ranging from 23 to 85°. An increased cell viability was observed on membrane surface at 57.8°. In understanding the interactions between microfabricated synthetic interfaces and cells, Lopez et al. investigated microfabricated nanoporous silicon membranes modified with collagen and laminin on the survival, proliferation, and differentiation of PC- 12 cells. The modification of the membrane with collagen was important to improve the adhesion of cells [42]. The tubular membrane can be engineered to allow adsorption of the bioactive factors to the channel walls during the fabrication process, which could be released within the lumen to favour nerve regeneration.

A previous study reported enhanced nerve regeneration in vivo by using collagen tubules filled with BDNF-enriched collagen gel. The obtained results appeared to be at least as good as autologous nerve grafts for bridging short facial nerve gaps.

Both nonbiodegradable materials, such as silicon, polyester (PE), Polyvinyl Cloride (PVC), polyvinylidene Difluoride ( PVDF), and polytetrafluoroethylene (PTFE), and biodegradable materials, such as collagen, chitosan, polycaprolactone (PCL), and polyglycolic acid (PGA), have been used to realize tube as nerve-guidance channels for repairing transected nerves.

Asymmetric HFMs of polyacrilonitrile an polyvinylchloride copolymer (PAN–PVC) were used as a method of controlling proliferation and delivering therapeutic molecules

within a dose range. The method entails encapsulation into a hollow fiber device of discrete numbers of cell-containing microcarriers. Ability to control dose released over a several-fold range was demonstrated with encapsulated PC-12 cells delivering neurotransmitters (L-dopa and dopamine**)** and C2C12 mouse myoblast cells delivering neurotrophic factors (CNTF) [43].

As mentioned previously, the MWCO of the the guidance channel affects the cellular behaviour by governing the mass transfer of molecules as evidenced also by Broadhead et al.[44]. The objective of their study was to evaluate the influence of HFM permeability on several biological parameters using a model cell line. The PC 12 were encapsulated within PAN-PVC HFM with widely different transport properties. The encapsulated cell biomass, the number of proliferating cells, and the quantity of dopamine released increased as a function of increasing HFM diffusive permeability. In this respect, membrane permeability plays a dual role by regulating the size of the cell mass that generates the product and by being able to restrict the diffusion of the product across the membrane into the surrounding environment. The percentage of viable cells and the overall appearance of the biomass architecture were not significantly influenced by differences in HFM permeability.

The use of biodegradable materials in guidance channels offers the advantage of timely disappearance from the implantation site without an additional surgical intervention once the regeneration process is completed and further allows connection of the regenerated axons with the host circuitry. The important characteristics of a biodegradable guidance channel include minimal tissue response following implantation, in vivo degradation at a rate that matches with the regeneration process, non-toxic and readily excreted degradation products, and the absence of toxic residual chemicals that may be contained in their preparation [27].

Between the biodegradable polymer, chitosan has proved to have good in vitro biocompatibility with peripheral nerve cells or tissue and can serve as a promising nerve conduit material to promote peripheral nerve regeneration. He et al [45] confirmed that chitosan is biocompatible to primary culture of hippocampal neurons. They prepared a substrate made up of chitosan fibers or membrane, and it was found to support the survival and growth of the attached hippocampal neurons without citotoxic effects on cell phenotype and functions.

Other biodegradable material are well tolerated in the CNS, such as polylactic, polyglycolic acid, and their various copolymers [46], for these polymer the tissue inflammatory response generally becomes stabilized and resolved as a function of material degradation. Biodegradable materials are often formulated into microspheres; this design is aimed for controlling drug delivery at a CNS tissue site.

## 3.5 MEMBRANES USED IN *IN VIVO* NEURONAL REGENERATION

Semipermeable membranes are also used for the cell encapsulation in order to immunoisolate the cells from the host by being permeable to molecules smaller than certain sizes, but restricting the passage of larger molecules, such as antibodies and complement components, from entering the membrane lumen and interacting directly with the encapsulated cells [47]. One of the applications of HFMs with encapsulated cells is with regard to implantation in the CNS for treatment of Parkinson's disease. Parkinson's disease is a neurological disease characterized by the progressive
loss of dopaminergic neurons, in the substantia nigra pars compacta, which are important to motor control. A treatment strategy under development involves the implantation of encapsulate dopamine-secreting cells, with the purpose being to alleviate at least some of the symptoms of Parkinson's disease through the targeted delivery of dopamine.

There are also other nervous system disorders where the delivery of missing factor(s), for example, neurotransmitters, neurotrophic factors, or enzymes, might compensate for a disease-caused deficiency and thus alleviate symptoms. Although approaches such as the use of pumps or slow-release polymer systems could be employed, the use of encapsulated secretory cells is a particularly attractive one for chronic implant therapies since the supply will last as long as the cells survive. There are two methods of encapsulation: micro- and macroencapsulation [47]. For macroencapsulation, cells are usually suspended in a matrix within an HFM. The open ends of the hollow fiber are sealed, thereby forming a capsule within which cells reside. In this case, the relatively thick fiber membrane represents a large diffusion distance for the release of catecholamine. This limit can be overcome by microcapsules. The thin membrane and spherical shape result in a high surface-to-volume ratio that facilitates transmembrane

diffusion and enhances cell viability. A disadvantage of the microcapsules is that they are fragile and cannot be retrieved easily. One of the first studies concerning the implantation of HFMs was that of Benveniste, who implanted a Diaflo HFM microdialysis tube in the rat hippocampus and studied the cellular reaction. Hypertrophic astrocyte processes invaded the spongy fiber wall 3 days after and late collagen deposits and occasional granuloma were formed. This study represents an initial attempt toward understanding the CNS tissue response to an HFM device [48].

Later, Winn et al. [49] encapsulated cells in a PAN–PVC HFM implanted into an adult male rat's right parietal cortex. A layer of reactive astrocytes mixed with other inflammatory cells including macrophages and microglia enveloped the membrane with some of the cells penetrating into the fiber wall. However, the response was benign due to a consistent absence of necrosis at or around the implant–brain interface over time. Semipermeable polysulfone tubular membranes with MWCO ranging from 100 to 1000 kDa were used in transacted hamster sciatic nerve model to support nerve regeneration in the absence of a distal nerve stump by Aebischer et al. [35]. The MWCO of the tubular membrane affected the outcome of regeneration. Only membranes with MWCO of 100 kDa supported the regeneration of well-differentiated peripheral nervous tissue containing a significant number of myelinated axons. In Table 3.2, several studies *in vivo* with neuronal cells using membrane systems are reported.

Li et al. [43] used asymmetric hollow fiber membranes of PAN–PVC copolymer to encapsulate PC-12 cells secreting L-dopa and dopamine attached to macroporous cellulosic microcarriers. PC-12 cells on microcarriers were embedded in polyethylene oxide (PEO) or agarose within hollow fiber devices. Devices were implanted into rodent striatum for 4 weeks and assayed for catecholamine release. Proliferation control is attained by embedding cell containing microcarriers in nonmitogenic hydrogels.

Glial-cell line derived neurotrophic factor (GDNF) was encapsulated in HFMs of Polyethersulfone (PES) previously filled with Polyvinyl Alcohol (PVA) cylindrical matrix and the fiber ends sealed with acrylic-based glue. The implantation of encapsulated cells by PES fibers in animal models of Parkinson's disease [50] leads to improvement of movement associated with striatal reinnervation of dopaminergic fibers. Microcapsules made of alginate–polylysine–alginate have been used by Xue et al. [51], to encapsulate bovine chromaffin cells that have been implanted into the brain

of hemiparkinsonian rats. The results of this study show great promise in the application of adrenal autograft tissue for the treatment of Parkinson's disease. Bovine chromaffin cells have also been encapsulated in microcapsules of alginate with 100–300 mm diameter covered by poly-L-lysine and implanted in the subarachnoid space of rats. The microcapsules reduced the symptoms of pain. The cells were morphologically normal and retained their functionality [52].

When a spinal cord injury (SCI) occurs, the primary mechanical damage is followed by a complex process of secondary damage due to inflammation, ischemia, free radical production, and apoptosis, among other processes. Because the pathophysiology of SCI is complex and involves many distructive processes, combination strategies have begun to be pursued and include the provision of cellular scaffolds to replace necrotic tissue, the delivery of neuroprotective agents to limit secondary injury, and the delivery of biomolecules to limit and neutralize the inhibitory environment present after injury.

The three-dimensional structure of biomaterial scaffold plays a significant role in neuron adhesion, as well as neurite outgrowth. As result, nerve guidance channels (NGCs), such as hollow fiber membrane, have been the subject of rigorous research aimed at promoting nerve regeneration in both the PNS an CNS.

Transplantation of porous tubes in poly(2-hydroxyethyl methacrylate-co-methyl methacrylate) was performed by Reynolds et al. [53]. The purpose of the study was to determine the effect of the surgical implantation of a porous tube into the lesion cavity following a complete spinal cord transaction on the weight and oxidative potential of muscles, and locomotor activity. The result suggested that the use of a biomaterial guidance transplantation can have a positive effects improving locomotor functions in the treated rats. While the initial strategy of developing NGCs was to bridge long gaps between nerve stumps, there is increasing evidence that suggests filling NGCs with growth factors or seeding with support (and/or stem) cells can promote superior axon growth into these channels for potential application in spinal cord repair. Recent studies have shown that neural stem/progenitor cells (NSPCs) delivered within a chitosan NGC can promote regeneration of a thick tissue bridge in a rat after a complete spinal cord injury[54,55]. Prior to culturing the NSPCs, chitosan tubes were coated with laminin to improve cell adhesion; in vivo these NGCs enhance cell survival (which is normally very poor when cells are delivered alone) and facilitate differentiation predominantly to

oligodendrocytes and astrocytes. Hence, NGCs not only serve as a support bridge between the two stumps of the spinal cord, but also protect the transplanted cells from the hostile environment following spinal cord injury. In this study, differentiated NPSCs may have secreted factors that attract host tissue and axons into the construct although this was not quantified. Moreover, recent findings also indicate that resident precursor cells proliferate and differentiate into oligodendrocytes and astrocytes following CNS injury to promote tissue repair [56]. An alternative nerve repair strategy is proposed by Clements et al [57] that utilized an internal scaffolding of polysulfone membrane to promote and enhance nerve repair. Using a 14mm tibial nerve gap model in rats, the regenerative potential of 1-film guidance channels, containing a single aligned thin-film, was compared to that of a 3-film design. Significantly greater regeneration was observed in the 1-film channel; furthermore regenerated nerve cables through the 1-film channels were structurally more akin to normal nerve in terms of patterns of cellular distribution and alignment. Thus, by providing minimal, yet appropriate topographic cues, a guidance channels ability to bridge critically sized nerve defects may be significantly enhanced.

**Table 3.2 - Characteristics of membranes for *in vivo* neuronal regeneration study**

| REFERENCE | MEMBRANE | CONFIGURATION | MATRICES | MEMBRANE PROPERTIES | CELLS | EFFECT |
|---|---|---|---|---|---|---|
| Benveniste et al., 1987 | Diaflo | Microdialysis tube | - | 50 kDa | | Cellular reaction to implant |
| Winn et al., 1989 | PAN-PVC | Capsules | - | | Giant cells | Immunoisolation form xenograft |
| Aebischer et al., 1989 | Polysulfone | Tubes | - | MWCO 10 and 100 kDa | Sciatic nerve | Regeneration of peripheral nerve with 10 kDa MW cut-off membrane |
| Li et al., 1999 | Polyacrylonitrile polyvinylchloride copolymer | Hollow fiber | Macroporous celulosic microcarriers | hydrogel | PC12 L-dopa secreting and C2C12 CNTF secreting | Cell proliferation in vitro and in vivo and release of L-dopa and CNTF |
| Sajadi et al., 2006 | Polyethersulfone | Fiber | Polyvinylalcohol | Inner diameter 500 μm | MDX12 secreting GDNF | Regeneration of nigrostrial dopaminergic fibers |
| Reynolds et al., 2008 | Poly-2-hydroxyethyl methacrylate-co-methyl methacrylate | Tube | - | Dense structure | | Improvement of locomotion function after spinal transection |
| Xue et al., 2001 | Alginate-polylysine-alginate | Microcapsules | Polylysine | Diameter 100-300μm | Bovine chromaffin cells | Reversion of behavioral deficits in hemiparkinsonian rats |
| Kim et al., 2004 | alginate | Microcapsule | Poly-L-lysine | Diameter 100-300μm | Chromaffin cells | Maintenance of cell viability after implantationand analgesic effect |
| Nomura et al.2008 | Chitosan | Channels | Laminin | 4.1mm in outer diameter. Wall thickness 0,2mm. | NSPCs | Many surviving transplanted cells and host axons. |

## 3.6 CONCLUDING REMARKS

The principal goal of regenerative medicine is to promote tissue regeneration and healing after injury or disease. This can be achieved through the delivery of cells and/or factors in a tissue engineered scaffold designed to provide a biomimetic microenvironment conducive to cell adhesion, proliferation, differentiation, and host tissue regeneration. Most biomaterial scaffolds are biodegradable, biocompatible, and provide a temporary niche for cell-replacement strategies. The bioartificial recreation of such niche can be tailored for neuronal tissue engineering with different strategies previously described in this chapter and in particular for maximizing the extent of regeneration and functional recovery of the damaged axons it is necessary a combined and synergistic interaction of different cues. With the recent advances in the field of biomaterials, particularly in membrane systems there is much promise of working toward neural functional tissue-engineered construct. Bioartificial membrane systems represent a valuable model to investigate the regenerative mechanism in a well-controlled microenvironment in which the high branched neuronal network can be recreated. Finally, a neural biohybrid system may offer an in vitro platform for the study of new strategies for delaying axonal degeneration or neuronal loss of activity in neurodegenerative disorders as well as the fundamental processes in neurobiology.

**REFERENCES**

[1] Centers for Disease Control and Prevention, http://www.cdc.gov

[2] J.S. Belkas, M.S. Shoicet, R. Midha, Peripheral Nerve regeneration through guidance tubes. Neurological research 2004, 26:151-160

[3] E. Fernandez, R. Pallini, L. Lauretti, A. Scogna. Neurosurgery of the peripheral nervous system: injuries, degeneration, and regeneration of the peripheral nerves, Surgical Neurology 1997,48:446– 447

[4] G. Stoll, J.W. Griffin, C.Y. Li, B.D. Trapp. Wallerian degeneration in the peripheral nervous system: participation of both Schwann cells and macrophages in myelin degradation. Journal of Neurocytology, 1989; 18:671–683

[5] V. Chaudhry, J.D. Glass, J,W.Griffin. Wallerian degeneration in peripheral nerve disease. Clinical Neurology and Neurosurgery. 1992;10:613–627

[6] D. Purves, G.J. Augustine, D. Fitzpatrick, W.C. Hall, A.S. LaMantia, J.O. McNamara, L.E.White. Neuroscience fourth edition. Sinauer Associate, Inc. Publishers.

Sunderland, Massachusetts USA.

[7] J.S. Taylor, E.T. Bampton. Factors secreted by Schwann cells stimulate the regeneration of neonatal retinal ganglion cells. Journal of Anatomy, 2004;. 204 :25– 31.

[8] Y. Murakami, S. Furukawa, A. Nitta, Y. Furukawa Accumulation of nerve growth factor protein at both rostral and caudal stumps in the transected rat spinal cord. Journal of Neurological Science 2002; 198:63–69

[9] Y. Nakahara, F.H. Gage, M.H. Tuszynski. Grafts of fibroblasts genetically modified to secrete NGF, BDNF, NT-3, or basic FGF elicit differential responses in the adult spinal cord. Cell Transplantation 1996, 5:191–204

[10] A. Blesch , M.H. Tuszynski. Cellular GDNF delivery promotes growth of motor and dorsal column sensory axons after partial and complete spinal cord transections and induces remyelination. Journal of Comparative Neurology 2003;467(3):403-417

[11] J. Jungnickel, K. Haase, J. Konitzer, M. Timmer, C. Grothe. Faster nerve regeneration after sciatic nerve injury in mice over-expressing basic fibroblast growth factor. Journal of Neurobiology 2006; 66 (9): 940-948.

[12] M. Sendtner, R. Götz, B. Holtmann, H. Thoenen. Endogenous Ciliary Neurotrophic Factor is a lesion factor for axotomized motoneurons in adult mice. The Journal of Neuroscience 1997; 17(18): 6999-7006.

[13] S.J. Archibald, J. Shefner, C. Krarup, R.D. Madison. Monkey median nerve repaired by nerve graft or collagen nerve guide tube. Journal of Neuroscience, 1995. 15:4109–23.

[14] G. Lundborg, L. Dahlin, D. Dohi, M. Kanje, N.Terada. A new type of "bioartificial" nerve graft for bridging extended defects in nerves. Journal of Hand Surgery [Br], 1997;22: 299–303

[15] S. David, A. J. Aguayo "Axonal Elongation into Peripheral Nervous System "Bridges after central nervous system injury in adult rats". Science 1981, 214: 931-933.

[16] C.C. Stichel, H.W. Muller, Experimental strategies to promote axonal regeneration after traumatic central nervous system injury, Prog. Neurobiol. 56 (1998) 119– 148

[17] H. Millesi, J. Ganglberger, A. Berger. Erfahrungen mit der Mikrochirurgie peripherer Nerven. Chir. Plast.1967. 3:47.

[18] F. Ferrari, A. D De Castro Rodrigues, C. K. Malvezzi, M. Dal Pai Silva, C. R Padovani.Inside-out vs. standard vein graft to repair a sensory nerve in rats. The Anatomical Record 1999, 256;227–232

[19] N. Zhang, H. Yan, X. Wen. Tissue-engineering approaches for axonal guidance. Brain Research Reviews, 2005; 49:48–64.

[20] C. H. Chau, D. K. Shum, , H.Li, J. Pei, Y.Y. Lui, L. Wirthlin, Y.S. Chan, X. M. XM. Condroitinase ABC enhances axonal regrowth trhough Schwann cell seeded guidance channels after spinal cord injury. The FASEB Journal, 2004; 18: 194–196.

[21] B. J. Dowsing, , A. Hayes, , T. M. Bennet, W. A. Morison, A. Messina. Effects of LIF dose and laminin plus fibronectin on axotomized sciatic nerves.

Muscle & Nerve 2000; 23:1356–1364.

[22] C. Iannotti, , H. Li, P. Yan, X.Lu, , L. Wirthlin, , X. M. Xu,. Experimental Neurology 2003; 183:379–393.

[23] X. M. Xu, V. Guenard, , N. Kleitman, , M. B. Bunge. Axonal regeneration into Schwann cell seeded guidance channels grafted into transacted adult rat spinal cord. The Journal of Comparative Neurology, 1995; 351: 145–160

[24] C.E. Schmidt, J.B. Leach. Neural tissue engineering: strategies for repair and regeneration, Annual Review of Biomedical Engineering, 2003; 5:293– 347.

[25] K.D. Chesmel, J. Black, Cellular responses to chemical and morphologic aspects of biomaterial surfaces. I. A novel in vitro model system, Journal of Biomedical Materials Research, 1995; 29:1089–1099.

[26] R.B. Borgens. Electrically mediated regeneration and guidance of adult mammalian spinal axons into polymeric channels. Neuroscience, 1999; 91:251– 264.

[27] V. Maquet, D. Martin, F. Scholtes, R. Franzen, J. Schoenen, G. Moonen, R. Jer me, Poly(d,l-lactide) foams modified by poly (ethylene oxide)-block-poly(d,l-lactide) copolymers and a-FGF: in vitro and in vivo evaluation for spinal cord regeneration.

Biomaterials 2001, 22 : 1137–1146.

[28] B. Song, M. Zhao, J.Forrester, , C. McCaig.Nerve regeneration and wound healing are stimulated and directed by an endogenous electric field in vivo. Journal of Cell Science, 2004; 117: 4681–4690.

[29] Mahoney M.J., R.R Chen., J.Tan, W.M. Saltzman. The influence of microchannels on neurite growth and architecture. Biomaterials 2005;26:771-778

[30 ] S. Morelli , S. Salerno, A. Piscioneri , B. J. Papenburg , A. Di Vito, G. Giusi, M. Canonaco , D. Stamatialis , E. Drioli , L. De Bartolo. Influence of micro-patterned PLLA membranes on outgrowth and orientation of hippocampal neurites. Biomaterials 2010, 31: 7000-7011

[31] N.Gomez, Y. Lub, S. Chenb, C. E. Schmidt. Immobilized nerve growth factor and microtopography have distinct effects on polarization versus axon elongation in hippocampal cells in culture. Biomaterials 2007, 28 (2): 271-284

[32] P. Aebischer, , V. Guenard, ,R. F. Valentini. The morphology of regenerating peripheral nerves is modulated by the surface microgeometry of polymeric guidance channels. Brain Research 1990, 531: 211–218

[33] L. De Bartolo, M. Rende, S. Morelli , G. Giusi, S. Salerno, A. Piscioneri, A. Gordano, A. Di Vito, M. Canonaco, E. Drioli. Influence of membrane surface properties on the growth of neuronal cells isolated from hippocampus. Journal of Membrane Science 2008, 325:139–149

[34] N. Zhang, C. Zhang, X. Wen. Fabrication of semipermeable hollow fiber membranes with highly aligned texture for nerve guidance. Journal of Biomedical Material Research 2005, 75A: 941–949

[35] P. Aebischer, V. Guenard, S. Brace. Peripheral nerve regeneration through blind-ended semipermeable guidance channels: effect of the molecular weight cut off. Journal of Neuroscience 1989, 9: 3590–3595.

[36] T.H. Young, C.H. Hung. Behaviour of embryonic rat cerebral cortical stem cells on the PVA and EVAL substrates. Biomaterials 2005, 26:4291–4299.

[37] H. Yamazoe, H. Iwata. Efficient generation of dopaminergic neurons from mouse embryonic stem cells enclosed in hollow fibers. Biomaterials 2006, 27:4871-4880.

[38] C.A. Brayefield, K.G. Marra, J.P. Leonard, X.T. Cui, J.C. Gerlach. Excimer laser channel creation in polyethersulfone hollow fibers for compartmentalized in vitro neuronal cell culture scaffolds. Acta Biomaterialia 2008, 4:244-255.

[39] M. E Manwaring, R.Biran, P.A. Tresco. Characterization of rat meningeal cultures on materials of differing surface chemistry. Biomaterials 2001, 22: 3155–3168.

[40] S. J. Lee, G. Khang, Y. M. Lee, H. B. Lee. The effect of surface wettability on induction and growth of neurites from the PC-12 cell on a polymer surface . Journal of Colloid and interface science Interface Science 2003, 259: 228–235.

[41] K.Y. Chang, L.W. Chen, , T.H.Young, K.H. Hsieh. PEI/EVAL blend membranes for granule neuronal cell culture. Polymer Research 2007, 14: 229–243.

[42] Lopez, C. A., Fleischman, A. J., Roy, S., Desai, T. A. Evaluation of silicon nanoporous membranes and ECM-based microenvironments on neurosecretory cells. Biomaterials 2006, 27: 3075–3083.

[43] R. H. Li, S. Williams, M. White, D. Rein. Dose Control with cell lines used for encapsulated cell therapy. Tissue Engineering, 1999. 5(5): 453-465.

[44] K. W. Broadhead, R. Biran, P. A. Tresco. Hollow fiber membrane diffusive permeability encapsulated cell biomass, proliferation, and small molecule release. Biomaterials 2002, 23: 4689–4699.

[45] Q. He, T. Zhang, Y. Yang, F. Ding. In vitro biocompatibility of chitosan-based materials to primary culture of hippocampal neurons. Journal of material science: material in medicine 2009, 20: 1457-1466

[46] D.F. Emerich, M.A. Tracy, K.L. Ward, M. Figueiredo, R. Qian, C. Henschel, R.T. Bartus, Biocompatibility of poly ($_{DL}$-lactide-*co*-glycolide) microspheres implanted into the brain, Cell Transplant 1999, 8 :47– 58.

[47] H. Uludag, P. De Vos, P. A. Tresco. Technology of mammalian cell encapsulation.Advanced Drug Delivery Reviews 2000, 42: 29–64.

[48] H. Benveniste, N.H. Diemer. Cellular reactions to implantation of a microdialysis tube in the rat hippocampus, Acta Neuropathologica 1987, 74 :234– 238.

[49] S.R. Winn, P. Aebischer, P.M. Galletti, Brain tissue reaction to permselective polymer capsules, Journal Biomedical Materials Research 1989, 23: 31– 44.

[50] A. Sajadi, J.C. Bensadoun, B.L. Schneider , C. Lo Bianco , P. Aebischer . Transient striatal delivery of GDNF via encapsulated cells leads to sustained behavioral improvement in a bilateral model of Parkinson disease. Neurobiology of disease 2006, 22(1):119-29

[51] Y. Xue, J. Gao, Z. Xi, et al. Microencapsulated bovine chromaffin cell xenografts into hemiparkinsonian rats: a drug-induced rotational behavior and histological changes analysis. Artificial Organs 2001, 25: 131–135

[52] Y. M. Kim, Y. H. Jeon, G. C. Jin, J. O. Lim, W. Y.Baek. Immunoisolated chromaffin cells implanted into the subarachnoid space of rats reduce cold allodynia in a model of neuropathic pain: a novel application of microencapsulation technology. Artificial Organs 2004, 28(12):1059-1066.

[53] L. F. Reynolds, M.C. Bren, B.C. Wilson, G.D. Gibson, M.S. Shoichet, R.J.L. Murphy. Transplantation of porous tubes following spinal cord transaction improves hindlimb function in the rat. Spinal Cord 2008, 46: 58–64.

[54] H. Nomura, T. Zahir, H Kim, Y. Katayama, I. Kulbatski, C.M. Morshead, M.S. Shoichet, C.H. Tator. Extramedullary chitosan channels promote survival of transplanted neural stem and progenitor cells and create a tissue bridge after complete spinal cord transaction. Tissue Engineering Part A 2008, 14( 5):649-665.

[55] T. Zahir, H. Nomura, X. D. Guo, H. Kim, C. Tator, C. Morshead, and M. Shoichet. Bioengineering neural stem/progenitor cell-coated tubes for spinal cord injury repair. Cell Transplantation 2008, 17: 245–254.

[56] J. Carmen , T. Magnus , R. Cassiani-Ingoni , L. Sherman , M.S. Rao, M.P. Mattson. Revisiting the astrocyte-oligodendrocyte relationship in the adult CNS. Progress Neurobiology 2007,82(3):151-162.

[57] I. P. Clements, Y.T. Kim, A.W. English, X. Lu, A. Chung, R. V.Bellamkonda. Thin-film enhanced nerve guidance channels for peripheral nerve repair. Biomaterials 2009, 30:3834-3846.

# CHAPTER 4

# RAT EMBRYONIC LIVER CELL EXPANSION AND DIFFERENTIATION ON NH3 PLASMA-GRAFTED PEEK-WC-PU MEMBRANES

Biomaterials 30 (2009) 6514–6521

Contents lists available at ScienceDirect

Biomaterials

journal homepage: www.elsevier.com/locate/biomaterials

# Rat embryonic liver cell expansion and differentiation on $NH_3$ plasma-grafted PEEK-WC-PU membranes

Sanja Pavlica [a,*], Antonella Piscioneri [b], Frank Peinemann [a], Mario Keller [a], Javorina Milosevic [c], Andrea Staeudte [d], Andreas Heilmann [d], Michaela Schulz-Siegmund [e], Stefania Laera [f], Pietro Favia [f], Loredana De Bartolo [b], Augustinus Bader [a]

[a] Department of Cell Technologies and Applied Stem Cell Biology, Biomedical-Biotechnological Center, Medical Faculty, University Leipzig, Deutscher Platz 5, Leipzig 04103, Germany
[b] Institute on Membrane Technology – National Research Council of Italy, c/o University of Calabria (ITM-CNR), 87030 Rende (CS), Italy
[c] Translational Centre for Regenerative Medicine – Leipzig (TRM-Leipzig), University of Leipzig, Germany
[d] Fraunhofer Institute for Mechanics of Materials, Walter-Huelse Straße 1, Halle D-06120, Germany
[e] Department of Pharmaceutical Technologies, University of Leipzig, Germany
[f] Department of Chemistry, University of Bari (UNIBA), via Orabona 4, Bari 70126, Italy

ARTICLE INFO

*Article history:*
Received 1 July 2009
Accepted 12 August 2009
Available online 2 September 2009

*Keywords:*
PEEK-WC-PU membranes
Plasma processing
Membrane bioreactor
Rat embryonic liver cells
Proliferation

ABSTRACT

Biomaterials can potentially influence stem and progenitor cell proliferation and differentiation in both a positive and a negative way. Herein, we report on the expansion and differentiation of rat embryonic (E17) liver (RLC-18) cells on new bioactive membrane made of PEEK-WC-PU, whose surface was grafted with nitrogen functionalities by means of $NH_3$ glow discharges. The performance of the developed membrane was evaluated by analyzing the expression of the liver specific functions of cells cultured in a 6-well gas-permeable bioreactor. It was found that native and $NH_3$ plasma-grafted PEEK-WC-PU membranes enabled expansion of liver cells in the bioreactor. Liver embryonic cells on the membranes exhibited higher functional activities compared to those cultured on conventional culture dishes as demonstrated by higher albumin and urea production. They showed gene expression of alpha-fetoprotein and albumin in a time-dependent manner of the hepatic differentiation process. LDH assay and SEM analyses revealed that a high number of viable liver stem cells attached to the membranes. Unexpectedly, liver progenitors cultured on membranes had higher telomerase activity than ones in the plates, preventing cell senescence. Thus, membranes are able to sustain *in vitro* the same *in vivo* liver functions and to allow the expansion of progenitor cells.



## 1. Introduction

Biomaterials are used in tissue engineering with the aim to repair or reconstruct tissues and organs. They can potentially influence stem cell proliferation and differentiation in both a positive and a negative way; their characteristics have been applied to attract or repel stem cells in a niche-like microenvironment [1]. Advances in biomaterials engineering and scaffold fabrication enabled the development of *ex vivo* cell expansion systems. In addition to delivering biochemical cues, various technologies have been developed to introduce micro- and/or nano-scale features onto culture surfaces to enable the study of stem cell responses to materials with different physico-chemical properties.

In the case of anchorage-dependent cells (e.g., hepatocytes) that are highly sensitive to the Extra Cellular Matrix (ECM) milieu, the modification of surface with specific molecules or functional groups could be used to improve cell adhesion and viability. Several surface modification techniques have been proposed to optimize specific interactions between cells and substrates including coating substrates with ECM proteins (e.g., collagen, laminin, fibronectin), conjugation with peptide or galactose moieties, or grafting with functional groups [2–6].

A polymeric membrane made of modified polyetheretherketone (PEEK-WC) and polyurethane (PU) has been developed as potential biomaterial to be used for liver tissue engineering [7]. Such PEEK-WC-PU membrane was also tested with primary human hepatocytes after being surface-modified with plasma-grafted nitrogen groups; this modification increased the surface energy and reactivity of the membrane resulting in improved interactions with cells [8].

Etching, deposition and grafting plasma processes are often used to modify the surface of biomaterials, including membranes,

* Corresponding author. Tel.: +49 341 9731354; fax: +49 341 9731359.
*E-mail address:* sanja.pavlica@bbz.uni-leipzig.de (S. Pavlica).

0142-9612/$ – see front matter © 2009 Elsevier Ltd. All rights reserved.
doi:10.1016/j.biomaterials.2009.08.024

with tunable density of surface functional groups, without altering their bulk [9,10], in solvent-less dry procedures.

Plasma grafting with $NH_3$ or $N_2$ feeds, and plasma deposition processes with N-containing monomer feeds (e.g., allylamine), can provide polymer surfaces with N-containing functional groups, whose distribution and density can be tuned with the plasma parameters, and depend also on ageing processes (hydrophobic recovery, surface oxidation, etc.). Polar O- and N-groups generated on polymer surfaces are pursued to confer and improve "biological activity" and cell adhesion to materials [11].

Herein, we examine the expansion of rat embryonic (E17) liver cells and the expression of their differentiated functions on PEEK-WC-PU membranes plasma-grafted in $NH_3$ radiofrequency (RF, 13.56 MHz) glow discharges. This cell line was used in this study as a model of liver progenitor cells since using cells from the fetal human liver is ethically problematic and great difficulties in obtaining such cells are expected. We hypothesize that nitrogen functionalities grafted over the surface of the membrane control adhesion, proliferation and differentiation of embryonic liver cells. Membranes were first plasma pre-treated in a $H_2$ RF glow discharge to cross-link and stabilize the surface of the membrane before performing the plasma-grafting of nitrogen groups in a $NH_3$ RF glow discharge [12]. The pre-treatment is needed to reduce the hydrophobic recovery ageing of the final surface.

Liver specific functions such as the synthesis of albumin and urea were investigated on cells cultured in a 6-well oxygen permeable bioreactor developed in our group [13]. The ability of the substrate membranes to influence cell proliferation was evaluated by means of cell cycle analyses and by measuring their telomerase activity. Gene expression for alpha-fetoprotein (AFP) and albumin was also established. Conventional substrates such as collagen and polystyrene culture dishes (PSCD) were used as reference substrates.

## 2. Materials and methods

### 2.1. RF glow discharge plasma processes

Plasma pre-treatments ($H_2$, crosslinking) and treatment ($NH_3$, grafting N-groups) modification processes of the PEEK-WC-PU membranes were performed in a pyrex glass "parallel plate" plasma reactor, described elsewhere [8,14], equipped with two internal steel electrodes. The $H_2$ pre-treatment is needed to control the ageing of the N-grafted membranes. Discharges were ignited between the upper electrode, connected to a radiofrequency (RF, 13.56 MHz, ENI-ACG-10) power supply through an impedance matching network, and the flat lower internal electrode 7 cm far (ground, substrate holder). $H_2$ (generated with a HG200 Claind Hydrogen Generator) and $NH_3$ (Air Liquid) were fed trough electronic MKS mass flowmeters. The pressure, kept constant at 200 mTorr with a rotary pump, was controlled with a MKS baratron. Plasma $H_2$ pre-treatment and $NH_3$ treatment processes were performed in sequence, without opening the reactor in between, as follows: 10 sccm $H_2$ flow rate, 30 Watt RF power, 1 min for pre-treatments; 10 sccm $NH_3$ flow rate, 20 Watt RF power, 1 min for treatments.

Plasma parameters were optimized in both processes to maximize the extent of grafting of N-groups, measured by the surface N/C ratio of the modified PEEK-WC-PU membrane, and to slow down its ageing by hydrophobic recovery [12]. Modified membranes were immediately stored in polystyrene boxes and used for cell culture experiments within 8 days.

### 2.2. Surface characterization

The surface chemical composition of unmodified and modified membranes was determined by means of X-ray Photoelectron Spectroscopy (XPS). A Thermo VG Scientific XPS instrument was used (monochromatic AlKα X-rays, 1486.6 eV, 100 W, 400 μm spot size). Membranes were examined within 1 h after being plasma processed and 7–15 days after. XPS measurements were performed at a take-off angle (TOA) of 37° with respect to the normal to the sample surface ($6 \pm 2$ nm sampling depth). Survey (0–1100 eV of Binding Energy, BE) and high resolution C1s, N1s, and O1s spectra were recorded.

Water Contact Angle (WCA) measurements were performed in static mode with a CAM 200 instrument equipped with a photocamera. 2 ml drops of double distilled water were used. WCA values were measured within 1 h after the surface modification process, and many times during 2–3 weeks, to evaluate the ageing of the treated surfaces. The CAM software of the instrument was utilized to fit the shape of the drop and determine the WCA tangent with the Young–Laplace equation.

### 2.3. Preparation for SEM investigations

Investigations of the membrane geometry and the cell morphology were done by high resolution scanning electron microscopy (SEM) using a Quanta 3D FEG instrument (FEI Company). Sample preparation procedure prior SEM investigation consists of five main steps. At the end of the culture period, the cells on the collagen coated cover slips and membranes were fixed with 2.5% gluthardialdehyde (Sigma–Aldrich, Taufkirchen, Germany) in PBS for at least 12 h. After rinsing the samples in PBS (ccpro, Germany) they were stained using 2% osmium tetroxide (ROTH, Karlsruhe, Germany) for a period of 45 min. Before starting dehydration, the samples were washed three times with PBS. The dehydration of the samples was realised by stepwise incubation in a rising series of ethanol solutions (10–100%, 10 min each). Afterwards, the samples were dried during three step incubation in hexamethyldisilazane (Sigma, Taufkirchen, Germany) solutions in ethanol (33%, 66%, 100%, 15 min each). At the end of this series the samples were air dried and placed on a SEM sample holder using carbon glue. The last step contains the coating of the samples with a thin layer of platinum made by magnetron sputtering (HVD, Dresden, Germany) to achieve a conducting surface.

### 2.4. Membrane bioreactor

Semipermeable membranes (PEEK-WC-PU) were prepared from modified polyetheretherketone (PEEK-WC), provided by Institute of Applied Chemistry, Changchun, China, and polyurethane (PU) in flat configuration; the phase inversion technique was used, as previously reported [7,8]. Native and plasma-grafted membranes were used in a small-scale gas-permeable flat membrane bioreactor, developed after [13,15]. The bioreactor consists of a polycarbonate six well shell, a six-hole silicon seal and metal base, a fluorocarbon gas-permeable ($CO_2$, $O_2$ and $H_2O$ vapour) bioFolie membrane fluorocarbon foil (IVSS GmbH, Germany) and the PEEK-WC-PU membrane.

### 2.5. Cell culture

The rat embryonic liver (E-17) cell line (RLC-18) commercially available (ACC 332) was utilized. This line is nontumorigenic in nude mice liver (Ref. [25]). Cells were maintained in RPMI medium containing 5% FCS (Biochrom AG, Berlin, Germany), l-glutamine, penicillin and streptomycin (Biochrom AG, Berlin, Germany) at 37 °C in a humidified $CO_2$ incubator (95% air, 5% $CO_2$) and subcultured twice a week by using trypsin (0.05%)/EDTA (0.025%) solution (Sigma–Aldrich, Munich, Germany). The cells were cultured for up to 4 days at 10–14 passages on native and modified PEEK-WC-PU membranes, collagen I (BD Biosciences, Germany) and PSCDs.

### 2.6. Biochemical assays

The rate of albumin secretion by hepatocytes was measured with an enzyme-linked immunosorbent assay (ELISA) previously described [15,16]. Urea concentration was assayed by the enzymatic urease method (Sigma–Aldrich, Munich, Germany). The lactate concentration was measured with an YSI 7100 MBS Analyzer (YSI Incorporated, Yellow Springs, OH, USA). All chemicals were of analytical grade and obtained from reputable sources.

### 2.7. Determination of telomerase activity

To measure and compare telomerase activities of cells grown on different substrates we used the Telomerase ELISA Assay Kit TeloTAGGG (Roche Applied Science, Cat. No. 11854666910). This photometric enzyme immunoassay utilizes the Telomeric Repeat Amplification Protocol (TRAP). After cultivation of cells on plates and membranes for 4 days, they were lysed and their telomerase activities determined according to manufacturer's instructions.

### 2.8. FACS analysis of cell cycle

To assess the percentage of cells in the G1, S + G2-M or sub-G1 phase (cell death), cell-cycle analysis was performed. During expansion at different plates and membranes, cultured cells frequently underwent cytofluorimetric analysis. DNA content/cell cycle analysis was performed by detecting propidium iodide (PI)-stained RLC-18 cell nuclei [17,18]. Nuclei were prepared by lysing $1 \times 10^5$ cells in 250 μL of hypotonic lysis buffer (0.1% sodium citrate, 0.1%Triton X-100, and 50 μg/mL PI) and were subsequently analysed by flow cytometry, using a FACScan (Becton Dickinson, Heidelberg,Germany). The sample flow rate during analysis did not exceed 500–600 cells/s. For data analysis and correction of the background noise histograms were processed with the ModFit LT software (Verity, Turramurra, Australia).

### 2.9. RT-PCR analysis of hepatocyte-specific markers

RNA was isolated from cells, 3 days after seeding, with the RNAeasy-Kit (Quiagen). cDNA was transcripted from RNA with MLV transcriptase (Promega), random primers and dNTP mix. Realtime PCR was performed with 5 μg cDNA, prepared from three independent isolations. TaqMan gene expression assays (fluorescent labeled, Applied Biosystems) were used with the following cDNA-specific primers and probes: alb (Rn01413932_m1) and AFP (Rn01413978_m1). The TaqMan gene expression assay was used as reference (endogenous control) for the eukaryotic 18sDNA.

### 2.10. Statistical analysis

For statistical determinations, three wells were usually examined per sample and the values were averaged. Data shown represent mean values ± SD of 3–6 independent experiments done with triplicate determinations. The results of the LDH, albumin and urea assays were analyzed using appropriate analysis of variance (two-way ANOVA; SigmaStat software package, Jandel Corp., San Rafael, CA) followed by Tukey test for multiple comparisons with substrate (different plates/membranes) and time (1–4 days) as two factors. One way ANOVA was used only to analyze data on cell cycle and telomerase activity. The paired Student's *t*-test was utilized to assess the significance of differences between substrates observed in RT-PCRs. ($^*P < 0.05$).

## 3. Results

### 3.1. Plasma processes on PEEK-WC-PU membranes

An $H_2$ plasma pre-treatment was performed in order to cross-link and stabilize the surface of PEEK-WC-PU membranes before grafting N-groups, thus reducing their hydrophobic recovery ageing [12]. Pre-treatments in Ar discharges were also performed, but they were found less efficient than $H_2$ discharges where UV emission is stronger, and affects deeper layers of the membrane.

Native PEEK-WC-PU membranes exhibited WCA values of $80 \pm 12^\circ$ and the following XPS composition: C% $80.9 \pm 4.0$; O% $17.0 \pm 1.0$; N% $2.1 \pm 0.1$; N/C $0.026 \pm 0.003$. The large WCA error bar is likely due to pore size distribution, roughness and surface chemical composition (e.g., due to uneven surface segregation of PU) of the membrane. Nitrogen atoms are found at the surface of the untreated membrane since PU is present in the PEEK-WC-PU composition.

Within 1 h after the $H_2/NH_3$ plasma process WCA values of $41 \pm 9^\circ$ were measured on modified membranes, and the following XPS composition: C% $67.2 \pm 3.4$; O% $12.9 \pm 0.6$; N% $19.9 \pm 1.0$; N/C $0.296 \pm 0.030$. Lowered WCA value, increased N% and increased N/C ratio attest clearly for the increased hydrophilic character of the modified membrane, due to the grafting of polar N-groups. 8 days of ageing in air result in stabilized WCA values of $61 \pm 3^\circ$, and XPS composition C% $67.5 \pm 3.4$; O% $12.3 \pm 0.6$; N% $17.5 \pm 0.9$; N/C $0.259 \pm 0.026$ (slightly lowered N% and N/C ratio), for the hydrophobic recovery of the uppermost moieties of the membrane. These values remain stable with time and represent the surface of the membrane where cells were grown in the bioreactor.

It is worth to stress here that the $H_2$ plasma pre-treatment is really useful to reduce the ageing of the membrane; $NH_3$ processed membranes with no pre-treatment exhibited leads almost to the complete recovery of its original surface properties, with WCA values of $51 \pm 3^\circ$ increasing to $75 \pm 3^\circ$ after 8 days. A more detailed description of surface analysis data, including Time-of Flight Secondary Ion Mass Spectrometry (ToF-SIMS) results are presented in our previous papers [8,19].

### 3.2. Cell viability, metabolic activity and morphology of embryonic liver cells cultured on different substrates

The high viability of rat embryonic liver cells cultured on native and $NH_3$-modified PEEK-WC-PU membranes as well as on collagen and PS culture dishes is presented in Fig. 1A. Results of LDH assay revealed a high number of viable liver cells attached to both membranes, both of which express excellent cell-growth conditions. As shown by SEM micrographs, cells easily adhered to the membranes, then proliferated during a 4 day culture period and spread to a confluent layer covering the membrane surface (Fig. 2A and B). After saturation of the space available cells tend to form cord-like structures formed by aggregates as a result of cell proliferation. On plasma-grafted membranes cells adhered and proliferated showing a polyhedral shape and a low spreading degree with respect to native substrate (Fig. 2C and D). Cells exhibited also a three-dimensional cell growth and tight cell–cell contact structure, very similar to what is found in the native liver. A different organization was displayed by cells cultured on collagen where spreading was observed and a two-dimensional surface layer was formed (Fig. 2E and F). As on the collagen, cells grown on traditional PSCD cells formed similar two-dimensional layers (data not shown).

Further, cells displayed enhanced metabolic activity which was maintained at high levels over the culture period. In particular, the liver-specific functions expressed in terms of urea synthesis (Fig. 1B) and albumin production (Fig. 1C) were maintained for 4 days. Interestingly, embryonic liver cells grown on modified membranes exhibited somewhat higher differentiated functional activities compared to those cultured on the other substrates as demonstrated by higher albumin and urea production. These findings demonstrate that PEEK-WC-PU membranes are able to support the differentiation of rat liver progenitors particularly when they are plasma grafted with nitrogen functionalities.

### 3.3. Gene expression in rat embryonic liver cells cultured on different substrates

Since albumin production rate is a crucial parameter of the liver function, in addition to the investigation of the capacity of albumin production of embryonic liver cells on different substrates, it was also our interest to examine their gene expression by means of RT-PCR analysis (Fig. 3A). The cells showed gene expression of albumin in a time-dependent manner of the hepatic differentiation process. High albumin gene expression was found on both native and plasma-grafted membranes, particularly on the last ones. These results correlate well with the enhanced albumin secretion of cells grown on modified PEEK-WC-PU membranes (Fig. 1C). Cells reached a differentiated state, as confirmed by the down-regulated expression of gene for AFP with respect to other substrates (Fig. 3B). On the other hand, positive gene expression for alpha-fetoprotein indicates the maintenance of the progenitor phenotype on PSCDs in contrast to the membranes where an AFP down-regulation was observed. So, cultivation of embryonic liver cells on PEEK-WC-PU membranes leads to their differentiation losing their progenitor phenotype. On the contrary, an up-regulation of AFP gene expression was maintained on PSCD substrates, demonstrating that cells were not still in a well-differentiated state.

### 3.4. Telomerase and cell cycle-proliferation capability

Since cellular senescence and aging are critically influenced by telomerase, which elongates telomeres, we measured telomerase activity of embryonic liver cells with a PCR–ELISA technique (Fig. 4A). Unexpectedly, the telomerase activities of rat liver progenitors grown in membrane bioreactors were significantly enhanced, exerting values similarly as in the positive control, in contrast to low values of telomerase activities of cells grown on collagen and PSCD, expressing similar values as in the negative control. In order to determine whether increased proliferation was

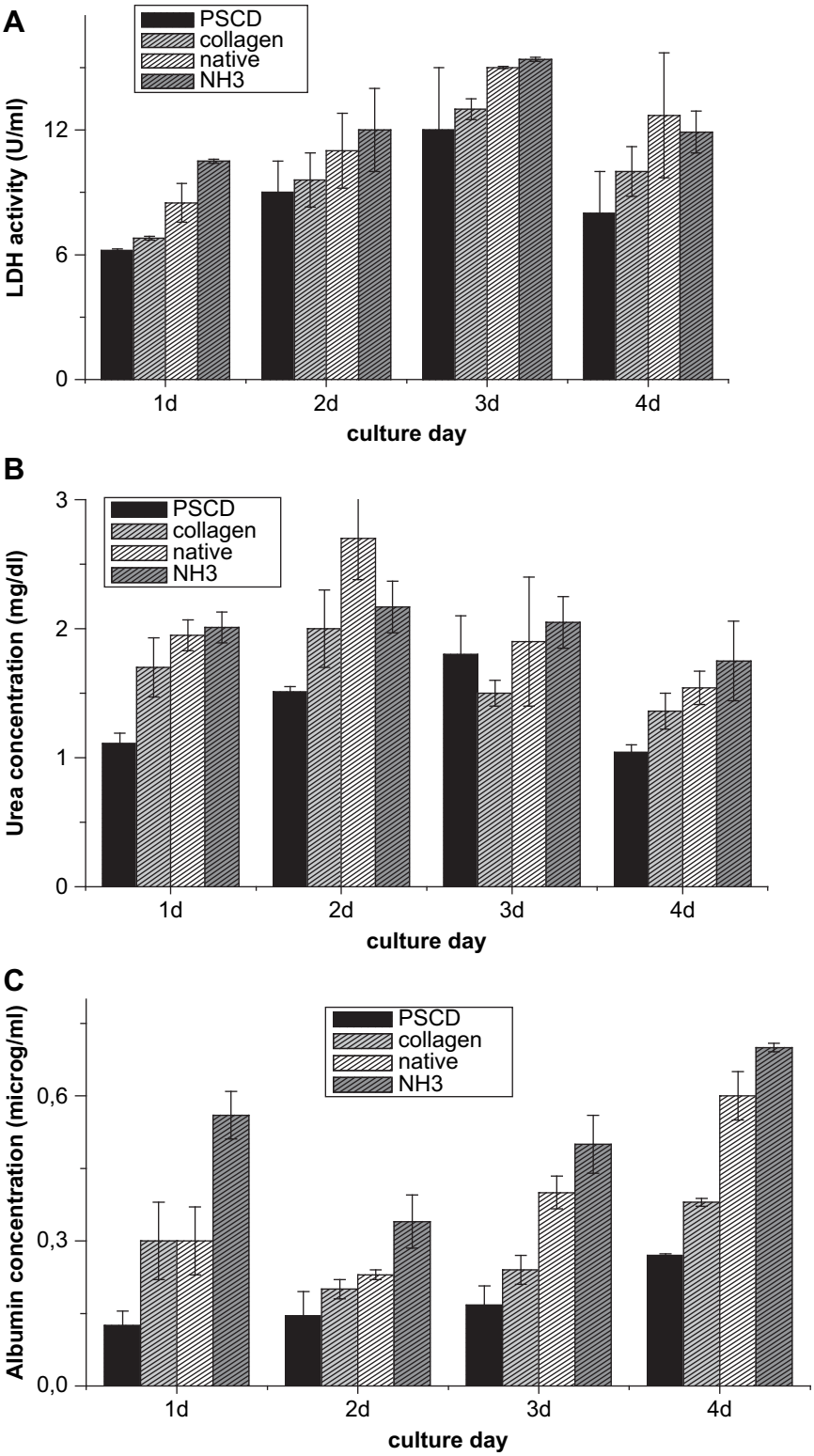


**Fig. 1.** Cell viability (A), Urea synthesis (B) and albumin production (C) of embryonic liver cells on PSCD, collagen, native and $NH_3$ plasma-grafted PEEK-WC-PU membranes. The values are the mean of five independent experiments ± standard deviation. In LDH, urea and albumin assays, two-way ANOVA test revealed a significant difference ($^*P < 0.001$). Interestingly, a statistically significant interaction between time (days) and support ($P = <0.001$) was found only in albumin assay. All pairwise multiple comparison procedures were done by Tukey test (at significance level 0.05). These findings showed a significant difference in cell viability, urea and albumin levels among cells grown on $NH_3$ vs. PSCD, NH3 vs. collagen, native vs. PSCD groups. Interestingly, only in albumin assay the significant differences were observed between $NH_3$ vs. native and collagen vs. PSCD groups.

involved in the augmentation of telomerase activity of embryonic liver cells grown in membrane bioreactors, FACS analyses were performed to see the differences in cell-cycle distribution (Fig. 4B). After 4 days of culture, most cells were found in G1-phase independently on the substrate, as result of their increase in size. 40–45% of cells were found in S-phase and only few cells were found in G2-phase and in the apoptotic state. On native and modified membranes, the percentage of cells in G1-phase was

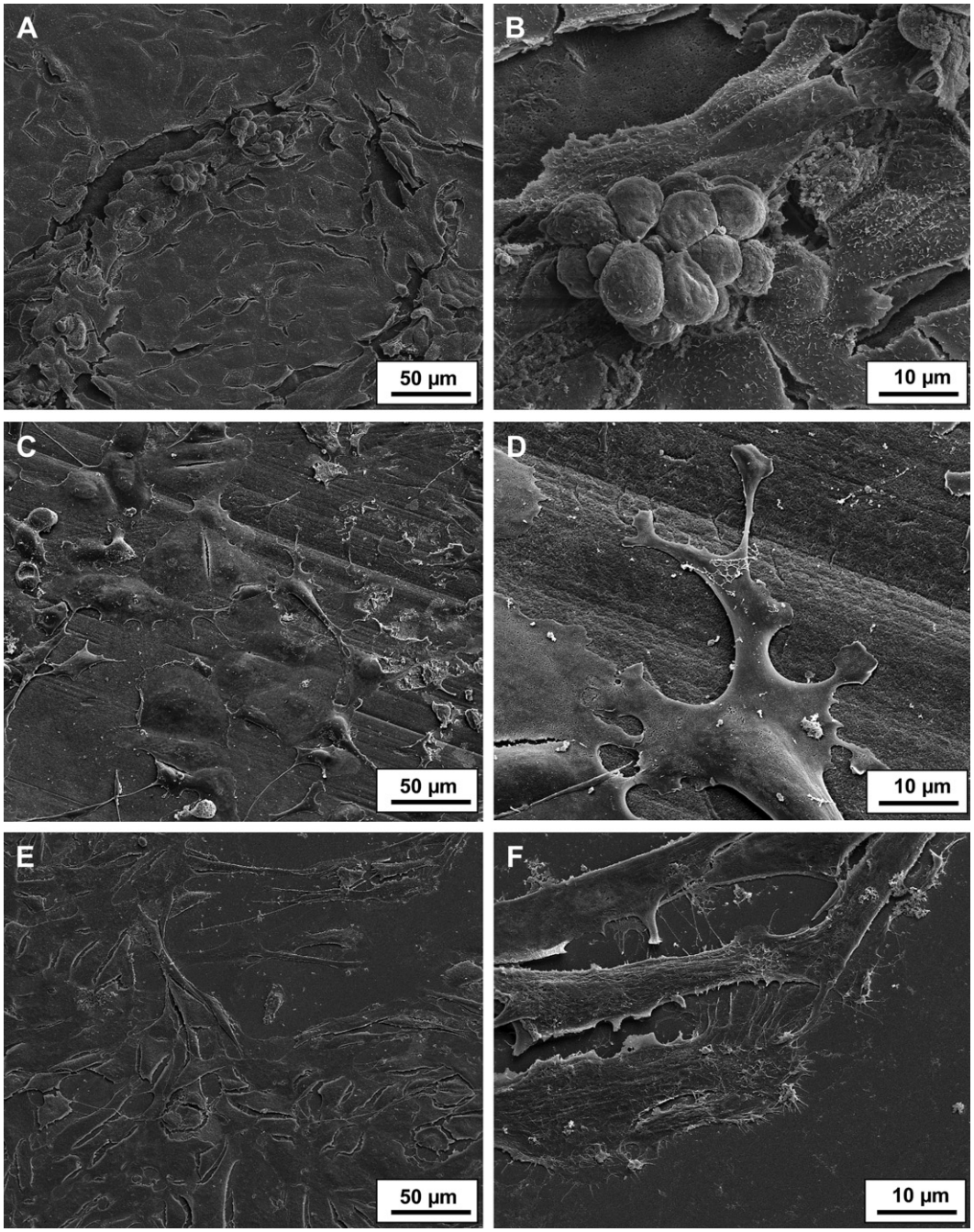


**Fig. 2.** SEM micrographs at different magnifications of embryonic liver cells grown on: (A,B) native PEEK-WC-PU membrane; (C,D) $NH_3$ plasma-grafted PEEK-WC-PU membranes; (E,F) collagen, each after 4 days of culture.

found higher with respect to collagen and PSCD. Coherently the telomerase activity increased on membranes.

## 4. Discussion

Proliferation, differentiation and morphology of liver cells on the different substrates were investigated in this study. We reported on the expansion of rat embryonic liver cells cultured on native and on $NH_3$ plasma -grafted PEEK-WC-PU membranes, to be possibly used in tissue engineering. We used RLC-18 rat embryonic liver cells that have been isolated and characterized by Takaoka et al. [20], who found activities of pyruvate kinase, glucose-6-phosphate dehydrogenase, hexokinase, gluco-kinase and catalase corresponding to values typical of liver tissues of rat embryos in the later stage of pregnancy.

Differences of cell adhesion and organization properties between embryonic liver cells cultured on native and N-grafted PEEK-WC-PU membranes surface, and on collagen, a natural ECM moiety were found. As expected, cells cultured on the collagen, proliferate and appear with flat and spread morphology. On the contrary, native membranes promote the continuous proliferation of cells that leads to the saturation area suitable for adhesion. As a result, cells tend to form aggregates in a cord-like structure although the cell spreading is also clearly visible on such membranes. It is well known that the morphology of cells adhering to a substrate is highly dependent on its physical structure and on

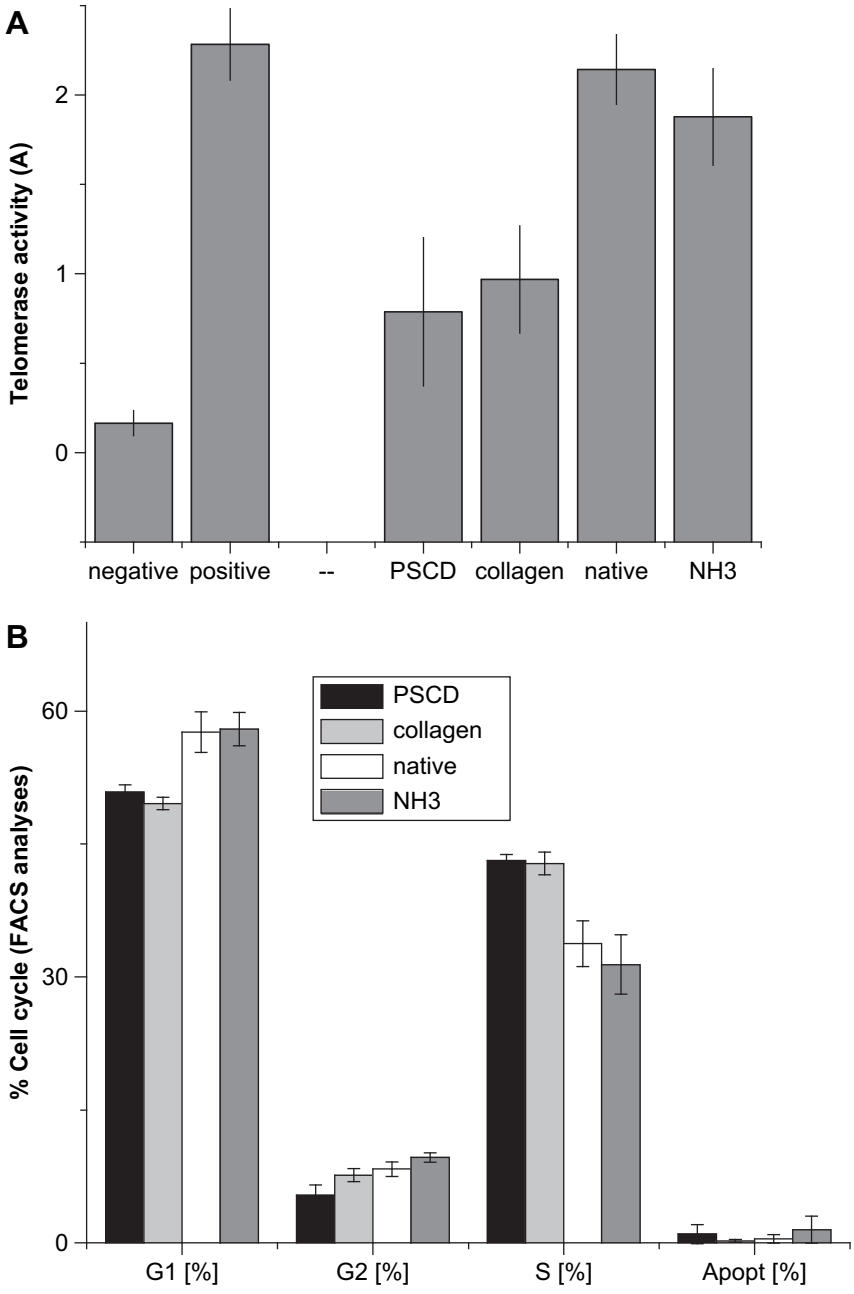


**Fig. 3.** Results of RT-PCR analysis: Gene expression of albumin (A) and AFP (B) in embryonic liver cells, 3 days after seeding on PSCD, collagen, native and $NH_3$ plasma-grafted PEEK-WC-PU membranes. Values in collagen are considered as 1. All other values were calculated relative to this. Data are adjusted to day0, $RQ = 2^{(-\Delta\Delta ct)}$, $RQ < 1 \rightarrow$ downregulation; $RQ > 1 \rightarrow$ upregulation. Data are presented as means ± SEM of three independent experiments. The paired Student's *t*-test was used to assess the significance of differences between observed data. ($^*P < 0.05$ vs. collagen populations).

chemical properties. Surface properties of (bio)materials, in fact, influence the adsorption of proteins (e.g., from the culture medium) at its surface thus, at last, drives the complex organization of cell–(protein)–substrate interactions and recognition processes to which cultured cells react with their morphological and physiological behaviour [21]. The formation of three-dimensional cord-like structure and cell spreading observed on native membranes is due to the physico-chemical properties of the surface that modulate the interactions with cells through protein adhesion and integrin receptors. Differently the grafted N-groups (amino-, amido-, cyano-, imino-groups) on modified membranes enhance the polarity of the membrane and boost the initial cell-membrane interactions through a direct interaction between the $-NH_2$ groups for example and the carboxylic groups of the pericellular components and proteins. Hence, cells exhibit a more polygonal shape and regular distribution in hepatic plates all over the whole surface of the membranes. Such organization can be considered an index of balanced cell-surface interactions that leads to form a 3D "liver-like" structure more easily than spread cells. Therefore, the cells cultured in the 3D are in tight contact with each other and their microenvironment resulting in a better communication and integration of gene expression [22].

We have shown that most cells grown on native and modified membranes are in the G1-phase, in agreement with the increase of their telomerase activity. A relationship seems to hold between the up-regulation of telomerase activity and the cell cycle progression.

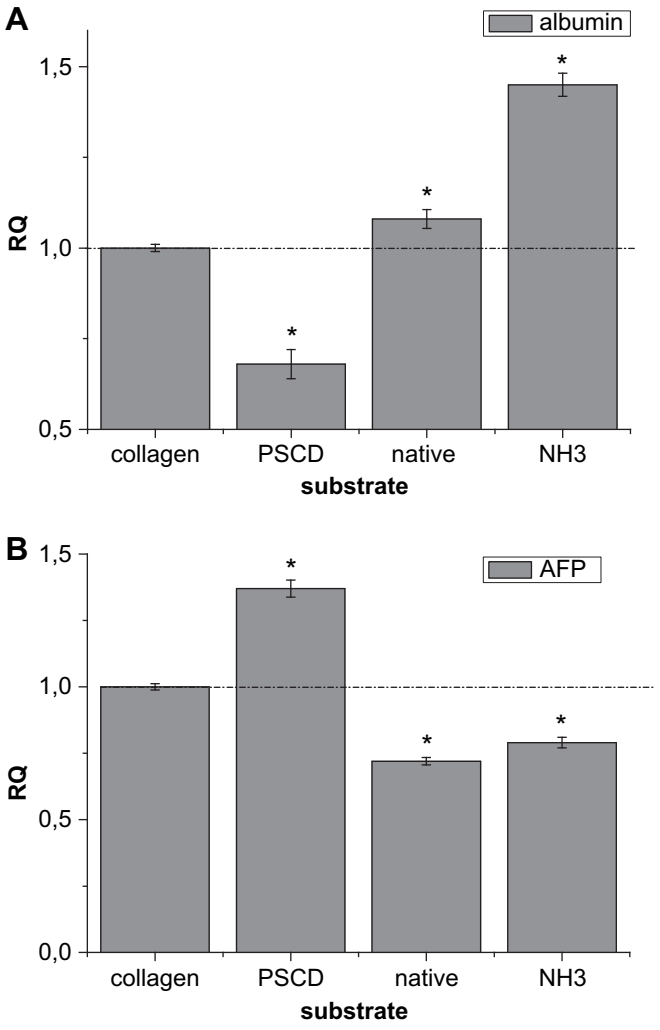


**Fig. 4.** (A) Telomerase activity of embryonic liver cells measured 3 days after seeding on PSCD, collagen, native and $NH_3$ plasma-grafted PEEK-WC-PU membranes. The values are the mean of three independent experiments ± standard deviation. One way analysis of variance (ANOVA) detected that the differences in the median values among the treatment groups are greater than would be expected by chance; there is a statistically significant difference ($P = 0.010$). Further, all Pairwise Multiple Comparison Procedures made by Tukey Test (at significance level 0.05) revealed only a significant difference between positive and negative controls, while not significant differences was found between 4 substrates used in this study. (B) Cell cycle analyses of embryonic liver cells cultivated on different supports for 3 days. Apoptotic, hypodiploid nuclei were measured as described in materials and methods and analyzed by flow cytometry. The values are the mean of four separate experiments ± standard deviation. One way ANOVA test was performed to analyze data of cell cycle analysis. The differences in the mean values among the substrate groups are greater than would be expected by chance; there is a statistically significant difference ($P = <0.001$) for G1, G2 and S phase, while $P = 0.013$ for apoptosis. Multiple Comparisons versus Control Group (Dunnett's Method, a significance level 0.05) revealed a significant difference between native vs. collagen and native vs. PSCD groups for G1, G2 and S phases. Very interestingly, Dunnett's test revealed only in apoptotic phase a significant difference ($P < 0.050$) between native vs. $NH_3$ group in contrast to other three phases where no difference between native and $NH_3$ group was observed.

Telomerase is well activated during the G1-phase, a phenomenon already observed during liver regeneration after partial hepatectomy [23]. Although the reason why telomerase should be activated during the process of normal liver regeneration is still unclear, the telomere dysfunction is associated with the defects in liver regeneration while it also accelerates the development of liver cirrhosis in response to chronic liver injury [24]. The up-regulation of the telomerase activity in regenerating hepatocytes may therefore play an important role in the maintenance of liver functions. In our study the high telomerase activity that was found on native and modified membranes with respect to other substrates reveals that cells reached a well differentiated state.

This is confirmed also by the different AFP and albumin gene expressions of cells expanded in the different investigated systems. Albumin-production is one of the main functions of the liver; at day 12 (E12) of the rat embryonic development the albumin-mRNA and AFP-mRNA, as well as their corresponding proteins, are expressed [25]. Ref. [26] demonstrated that in the developing liver AFP-mRNA reaches a peak at E16 and then decreases, while albumin-mRNA peaks at E18 and persists in the following adult stage [26]. We demonstrated that the synthesis of albumin (Fig. 1C) was low as found for other liver embryonic and fetal cells, significantly lower than in mature rat hepatocytes (data not shown).

$NH_3$ plasma-modification of PEEK-WC-PU membranes up-regulated and down-regulated the albumin and AFP gene expression respectively as result of their enhanced differentiation in contrast to the other substrates used. We can, thus, expect that the differentiation *in vitro* of liver progenitors grown on $NH_3$ plasma-grafted membranes, before being transplanted *in vivo*, would avoid spontaneous differentiation into undesired lineages at the transplantation site, as well as reduce the risk of teratoma formation, in the case of embryonic stem cells. We believe that the best condition to maintain a good bioactivity of the cells is an environment the closest possible similar to *in vivo* conditions, which the N-grafted PEEK-WC-PU membranes clearly seem to provide as a novel functional biomaterial. Therefore, the outcome of this study supports that this biomaterial enables cell expansion of embryonic liver cell model and might offer promising features as conduit additive in regard to liver regeneration according to its physiological properties and responsibilities during genesis and liver repair *in vivo*.

## 5. Conclusion

These results demonstrated that native and plasma-grafted PEEK-WC-PU membranes allow the expansion and differentiation of rat embryonic liver cells. Most of the cells grown on membranes as demonstrated by the increase of their telomerase activity and undergone a differentiation process. High albumin and low AFP gene expressions were found on both native and plasma-grafted membranes, particularly on the last ones. Similarly, the liver specific functions in terms of urea synthesis and albumin secretion were performed at high levels particularly on plasma-grafted membranes. Herein, we showed that plasma-grafted membranes are able to support the expansion and differentiation of embryonic liver cells. Further analysis of liver progenitor and stem cells (as well as of mature hepatocytes) by using the new bioactive membranes will aid new insights in the development of tissue engineered implantable liver systems.

## Acknowledgements

The work was funded by EU through the EU-project LIVE-BIOMAT NMP3-CT-013653. Prof. R. d'Agostino (Dept. Chemistry, Univ. Bari) is acknowledged for fruitful discussions. Mr Savino Cosmai (Dept. Chemistry, Univ. Bari) and Mrs. Angela Hennig (BBZ, University of Leipzig) are acknowledged for technical assistance.

## References

[1] Neuss S, Apel C, Buttler P, Denecke B, Dhanasingh A, Ding X, et al. Assessment of stem cell/biomaterial combinations for stem cell-based tissue engineering. Biomaterials 2008;29:302–13.
[2] Pierschbacher MD, Ruoslahti E. Cell attachment activity of fibronectin can be duplicated by small synthetic fragments of the molecule. Nature 1984;309:30–3.

[3] Hersel U, Dahmen C. RGD modified polymers: biomaterials for stimulated cell adhesion and beyond. Biomaterials 2003;24:4385–415.
[4] Yang J, Bei J, Wang S. Enhanced cell affinity of poly (D,L-lactide) by combining plasma treatment with collagen anchorage. Biomaterials 2002;23:2607–14.
[5] Memoli B, De Bartolo L, Favia P, Morelli S, Lopez LC, Procino A, et al. Fetuin-agene expression, synthesis and release in primary human hepatocytes cultured in a galactosylated membrane bioreactor. Biomaterials 2007;28:4836–44.
[6] De Bartolo L, Morelli S, Piscioneri A, Lopez LC, Favia P, d'Agostino R, et al. Novel membranes and surface modification able to activate specific cellular responses. Biomol Eng 2007;24:23–6.
[7] De Bartolo L, Morelli S, Gallo MC, Campana C, Statti G, Rende M, et al. Effect of isoliquiritigenin on viability and differentiated functions of human hepatocytes on PEEK-WC-polyurethane membranes. Biomaterials 2005;26: 6625–34.
[8] Salerno S, Piscioneri A, Laera S, Morelli S, Favia P, Bader A, et al. Improved functions of human hepatocytes on $NH_3$ plasma–grafted PEEK-WC-PU membranes. Biomaterials 2009;30(26):4348–56.
[9] Sardella E, Favia P, Gristina R, Nardulli M, d'Agostino R. Plasma-aided micro and nanopatterning processes for biomedical applications. Plasma Processes Polym 2006;3:456–69.
[10] Favia P, Sardella E, Lopez LC, Laera S, Milella A, Pistillo B, et al. Plasma assisted surface modification processes for biomedical materials and devices. In: Guceri S, Fridman A, editors. Plasma assisted decontamination of biological and chemical agents. NATO Science For Peace and Security Series; 2008. p. 203–26.
[11] Siow KS, Brichter L, Kunar S, Griesser HJ. Plasma methods for the generation of chemically reactive surfaces for biomolecule immobilization and cell colonization. Plasma Processes Polym 2006;3:392–418.
[12] Favia P, Milella A, Lacobelli L, d'Agostino R. Plasma pre-treatment and treatments on polytetrafluorethylene for reducing the hydrophobic recovery. In: d'Agostino R, Favia P, Wertheimer MR, Oehr C, editors. Plasma processes polym. Weinheim: Wiley-VCH, 2005. p. 271–80.
[13] Schmitmeier S, Langsch A, Jasmund I, Bader A. Development and characterization of a small-scale bioreactor based on a bioartificial hepatic culture model for predictive pharmacological in vitro screenings. Biotechnol Bioeng 2006;95:1198–206.
[14] Lopez LC, Buonomenna MG, Fontananova E, Iacoviello G, Drioli E, d'Agostino R, et al. Adv Funct Mater 2006;16:1417–24.
[15] Bader A, Frühauf N, Zech K, Haverich A, Borlak JT. Development of a small-scale bioreactor for drug metabolism studies maintaining hepatospecific functions. Xenobiotica 1998;28:815–25.
[16] Diekmann S, Glöckner P, Bader A. The influence of different cultivation conditions on the metabolic functionality of encapsulated primary hepatocytes. Int J Artif Organs 2007;30:192–8.
[17] Nicoletti I, Migliorati G, Pagliacci MC, Grignani F, Riccardi C. A rapid and simple method for measuring thymocyte apoptosis by propidium iodide staining and flow cytometry. J Immunol Methods 1991;139:271–9.
[18] Milosevic J, Schwarz SC, Krohn K, Poppe M, Storch A, Schwarz J. Low atmospheric oxygen avoids maturation, senescence and cell death of murine mesencephalic neural precursors. J Neurochem 2005;92:718–29.
[19] Laera S, Lopez LC, De Bartolo L, Morelli S, Salerno S, Piscioneri A, et al. $H_2$–$NH_3$ Plasma-grafting of PEEK-WC-PU membranes to improve their cytocompatibility with hepatocytes. Plasma Polymer and Processes 2009. doi:10.1002/ppap.200930307.
[20] Takaoka T, Yasumoto S, Katsuta H. A simple method for the cultivation of rat liver cells. Jpn J Exp Med 1975;45:317–26.
[21] Ye SH, Watanabe J, Takai M, Iwasaki Y, Ishihara K. Design of functional hollow fiber membranes modified with phospholipid polymers for application in total hemopurification system. Biomaterials 2005;26:5032–41.
[22] Stoehr SA, Isom HC. Gap junction-mediated intercellular communication in a long-term primary mouse hepatocyte culture system. Hepatology 2003;38:1125–35.
[23] Inui T, Shinomiya N, Fukasawa M, Kobayaski M, Kuranaga N, Ohkura S, et al. Growth-related signaling regulates activation of telomerase in regenerating hepatocytes. Exp Cell Res 2002;273:147–56.
[24] Rudolph KL, Chang S, Millard M, Schreiber-Agus N, DePinho RA. Inhibition of experimental liver cirrhosis in mice by telomerase gene delivery. Science 2000;287:1253–8.
[25] Shiojiri N, Lemire JM, Fausto N. Cell lineages and oval cell progenitors in rat liver development. Cancer Res 1991;51:2611–20.
[26] Muglia L, Locker J. Developmental regulation of albumin and alpha-fetoprotein gene expression in the rat. Nucleic Acids Res 1984;12:6751–62.

# CHAPTER 5

# BIODEGRADABLE AND SYNTHETIC MEMBRANES FOR THE EXPANSION AND FUNCTIONAL DIFFERENTIATION OF RAT EMBRYONIC LIVER CELLS

Acta Biomaterialia 7 (2011) 171–179

Contents lists available at ScienceDirect

Acta Biomaterialia

journal homepage: www.elsevier.com/locate/actabiomat

# Biodegradable and synthetic membranes for the expansion and functional differentiation of rat embryonic liver cells

Antonella Piscioneri [a,b], Carla Campana [a,c], Simona Salerno [a], Sabrina Morelli [a], Augustinus Bader [d], Francesca Giordano [b], Enrico Drioli [a,c], Loredana De Bartolo [a,*]

[a] Institute on Membrane Technology, National Research Council of Italy, ITM-CNR, c/o University of Calabria, via P. Bucci Cubo 17/C, I-87030 Rende (CS), Italy
[b] Department of Cell Biology, University of Calabria, via P. Bucci, 87030 Rende (CS), Italy
[c] Department of Chemical Engineering and Materials, University of Calabria, via P. Bucci, I-87030 Rende (CS), Italy
[d] Biomedical–Biotechnological Center, University of Leipzig, Leipzig, Germany

ARTICLE INFO

*Article history:*
Received 30 March 2010
Received in revised form 26 July 2010
Accepted 30 July 2010
Available online 4 August 2010

*Keywords:*
Membranes
Embryonic liver cells
Expansion
Functional differentiation
Tissue engineering

ABSTRACT

The insufficient availability of donor organs for orthotopic liver transplantation worldwide has urgently increased the requirement for new therapies for acute and chronic liver disease. The creation of an unlimited source of donor cells for hepatocyte transplantation therapy and pharmaceutical applications may be the isolation and expansion of liver progenitor cells or stem cells. Here we report the expansion and functional differentiation of rat embryonic liver cells on biodegradable and synthetic polymeric membranes in comparison with traditional substrates, such as collagen and polystyrene culture dishes. Membranes prepared from chitosan and modified polyetheretherketone were used for the culture of liver progenitor cells derived from rat embryonic liver. Cells proliferated, with a significant increase in their number within 8–11 days. The cells displayed functional differentiation showing urea synthesis, albumin production and diazepam biotransformation on all substrates investigated. In particular, on a chitosan membrane liver-specific functions were expressed at significantly higher levels for prolonged times compared with other synthetic membranes, utilizing traditional substrates (collagen and PSCD) as references. These results demonstrate that chitosan membranes offer cells favourable conditions to promote the expansion and functional differentiation of embryonic liver cells that could be effectively used in liver tissue engineering and in pharmaceutical applications.



## 1. Introduction

Liver disease is the eighth most frequent disease worldwide. Many patients die annually from liver disease. Many of those in need of a transplant suffer from full hepatic failure caused by disease, genetic complications or adverse drug reactions [1]. The European Liver Transplant Registry (ELTR) has accumulated data on 85,446 transplantations in 76,818 patients from 143 centres in 25 countries from May 1968 to December 2008 (<http://www.eltr.org>). In the USA 30,000 people die each year of end-stage liver disease [2]. Currently there are 105,328 patients on the waiting list for a donor organ, of whom 16,482 are candidates awaiting a liver transplant (United Network for Organ Sharing at <http://www.unos.org>). In 2006, 6649 liver transplants were performed in the USA and 1935 died while waiting for a liver transplant because of the shortage of organs (<http://www.unos.org>).

Insufficient donor organs for orthotopic liver transplantation worldwide have made the development of new therapies for acute and chronic liver disease an urgent requirement.

The ability to expand hepatic stem cells or embryonic liver cells is desirable to generate cells for liver tissue engineering in clinical and pharmaceutical applications. Conventional methods for expanding hepatic stem cells or progenitor cells comprise polystyrene culture dishes and components of the extracellular matrix (ECM) such as collagen [3]. Alternatively, biocompatible and biodegradable materials have been proposed to support cells in culture and promote their differentiation and proliferation towards the formation of liver tissue [4].

Natural polymers such as chitosan are advantageous for liver tissue engineering because of their structural similarity to glycosaminoglycans, which are components of the liver ECM. Chitosan is an N-deacetylated derivative of chitin and is naturally degraded by body enzymes. In addition, its reactive amino and hydroxyl groups provide many possibilities for covalent and ionic modification, which allows extensive adjustment of the mechanical and biological properties. Due to its excellent biocompatibility and bioadsorbility chitosan has been used in several biomedical

* Corresponding author. Tel.: +39 0984 492036; fax: +39 0984 402103.
*E-mail addresses:* l.debartolo@itm.cnr.it, loredana.debartolo@cnr.it (L.D. Bartolo).

1742-7061/$ - see front matter © 2010 Acta Materialia Inc. Published by Elsevier Ltd. All rights reserved.
doi:10.1016/j.actbio.2010.07.039

applications (e.g. skin, bone, cartilage, blood vessels, haemodialysis, nervous system and liver) [5–10]. Scaffolds constituted of chitosan cross-linked with other biomolecules have been applied in the culture of a liver cell line and primary hepatocytes [11,12]. Chitosan membranes modified with biomolecules have been used for the culture of a fibroblast cell line and, in the form of a galactosylated scaffold, chitosan has been used to induce the formation of rat hepatocyte aggregates [13,14].

Membranes prepared from chitosan could act as a synthetic ECM combining the advantageous properties of the polymer (i.e. biocompatibility, biodegradability and biofunctionality) with those of membranes, such as permeability, selectivity and a well-defined geometry [15,16]. Membranes would allow the organization of cells into a three-dimensional architecture, providing mechanical integrity and a space for the diffusion of nutrients and metabolites to and from the cells [17,18].

Synthetic polymeric membranes can also be used in the development of in vitro engineered constructs to reproduce a physiological tissue model for studying drugs and metabolic diseases. Modified polyetheretherketone (PEEK-WC) membranes have good stability, permeability and biocompatibility, as previous studies with rat hepatocyte cultures have demonstrated [19]. They can easily be mass produced with modified morphological and physico-chemical properties for specific applications, but are not degradable and so can be used only in in vitro systems.

In this study we have investigated the ability of chitosan and PEEK-WC membranes to promote the expansion and functional differentiation of rat embryonic liver cells, utilizing traditional substrates such as collagen and polystyrene culture dishes (PSCD) as references. The goal was to evaluate whether membranes could provide the cells with the necessary signals, derived from the biofunctional, biochemical and physical properties of the materials, to commit them to differentiation. Rat embryonic liver cells (17 day embryos) were used in this study as an alternative model of human liver progenitor cells [20,21], since using cells from the foetal human liver is limited by major ethical issues. Embryonic liver cells have many advantages over primary hepatocytes for proliferation in vitro and transplantation in vivo [22].

## 2. Materials and methods

### 2.1. Membrane preparation

Chitosan membranes were prepared by dissolving 4% (w/v) chitosan (Sigma, Milan, Italy) in acetic acid solution 2% (v/v). Then polyethylene glycol (PEG) with a molecular weight of 6000 Da (Merck-Schuchardt, Hohenbrunn, Germany) was added to the chitosan solution at a ratio of 4:1 and stirred for 2 h. The solution was cast on a glass plate using a commercial applicator (Adjustable Bird Applicator 0–250 μm, Elcometer) and dried at room temperature. The membrane was immersed in a solution of 1% NaOH after drying. Finally, the membrane was washed in deionised distilled water for the test.

Synthetic membranes were prepared from PEEK-WC or poly(oxa-1,4-phenylene-oxo-1,4-phenylene-oxa-1,4-phenylene-3,3-(isobenzofurane-1,3-dihydro-1-oxo)-diyl-1,4-phenylene) (patented by Zhang et al. [23] and provided by the Institute of Applied Chemistry, Changchun, China) by the inverse phase technique using the direct immersion–precipitation method as previously described [19]. The PEEK-WC was obtained by polycondensation reaction between 4,4-dichlorobenzophenone and phenolphthalein [23].

### 2.2. Membrane characterization

The wettability properties of all membranes were characterized using water contact angle (WCA) measurements obtained by the sessile drop method and water sorption at ambient temperature using a CAM 200 contact angle meter (KSV Instruments, Helsinki, Finland). Results are the means of 10 measurements of different regions of the sample surface. All measurements were repeated six times.

Swelling and dissolution tests were performed on the chitosan membranes. Membrane samples (1 × 1 mm) were weighed and then placed in 1 ml of phosphate-buffered saline (PBS) at 37 °C. Swollen membranes were withdrawn at various times and were weighed again. The swelling index (*SI*) was calculated as $\%SI = \frac{W_s - W_i}{W_i} \times 100$, where $W_i$ and $W_s$ are the sample weights before and after incubation in PBS, respectively. After drying at 37 °C for 48 h samples were weighed again and the solubility percentage was calculated as $\%S = \frac{W_i - W_d}{W_i} \times 100$, where $W_d$ is the dried sample weight after the dissolution test. Each test consisted of four replicate measurements.

### 2.3. Cell culture

Rat embryonic liver cells (17 day embryonic liver of Japanese albino rat) (RLC-18), consisting of parenchymal cells [20], were obtained from the DSMZ (Braunschweig, Germany). Cells were maintained in RPMI medium containing 10% foetal calf serum (Biochrom AG, Berlin, Germany), l-glutamine, penicillin and streptomycin (Biochrom AG) at 37 °C in a humidified $CO_2$ incubator (95% air, 5% $CO_2$) and subcultured twice a week using 0.05% trypsin/0.025% EDTA solution (Carl Roth GmbH, Karlsruhe, Germany and Sigma–Aldrich, Munich, Germany). The cells were cultured on the chitosan and PEEK-WC membranes and on collagen I (BD Biosciences, Germany) and PSCDs at passage 6. Cells were cultured for up to 24 days. The medium was changed every 48 h.

Experiments were performed in the presence of 10 μg ml$^{-1}$ diazepam in the culture medium to evaluate the ability of the cells to perform drug biotransformation functions, in particular the elimination of diazepam and the formation of its metabolites.

The morphology of cells cultured on the different substrates was assessed by means of scanning electron microscopy (SEM) and laser confocal scanning microscopy (LCSM).

Liver-specific cellular functions were investigated in terms of albumin production and urea synthesis.

### 2.4. Cell fixation for SEM

Cells cultured on membranes, collagen and PSCD were prepared on days 7 and 16 for SEM analysis by fixation in 3% glutaraldehyde and 1% formaldehyde in PBS, followed by post-fixation in 1% osmium tetroxide and progressive ethanol dehydration.

### 2.5. Cell staining for LCSM

The morphological behaviour of embryonic liver cells cultured on the substrates examined was investigated after 7 and 16 days culture by LCSM after cytoskeleton and ECM protein immunostaining. Samples were rinsed with PBS, fixed for 15 min in 3% paraformaldehyde in PBS at room temperature (RT), permeabilized for 5 min with 0.5% Triton-X100 and saturated for 15 min with 2% normal donkey serum.

Vinculin was visualized using a mouse monoclonal antibody raised against human vinculin (Santa Cruz Biotechnology, Santa Cruz, CA) with Cy3™-conjugated AffiniPure donkey anti-mouse IgG (Jackson ImmunoResearch Europe, Cambridge, UK) as the secondary antibody. Actin was stained with Alexa 488-conjugated phalloidin (Molecular Probes, Eugene, OR). All primary and secondary antibodies were incubated for 2 and 1.5 h at RT, respectively. Counterstaining for nuclei was performed with 0.2 μg ml$^{-1}$ DAPI (Molecular Probes) with incubation for 30 min. Finally, samples

were rinsed, mounted and observed with a laser confocal scanning biological microscope (Fluoview FV300, Olympus, Italy).

### 2.6. Biochemical assays

Samples from the culture medium were collected in pre-chilled tubes and stored at −20 °C until assayed. Albumin secretion was measured by ELISA. 96-well plates were coated with 50 μg ml$^{-1}$ chromatographically purified rat albumin (Sigma, Milan, Italy) and left overnight at 4 °C. After four rinses 100 μl of cell culture supernatant was added to the wells and incubated overnight at 4 °C with 100 μl of anti-rat albumin monoclonal antibody conjugated with horseradish peroxidase (Bethyl Laboratories, Montgomery, TX). After four rinses the substrate buffer containing tetramethylbenzidine and $H_2O_2$ (Sigma, Milan, Italy) was added for 7 min and the reaction was stopped with 100 μl of 8 N $H_2SO_4$. Absorbance was measured at 450 nm using a Multiskan Ex (Thermo Lab Systems).

The urea concentration was determined with a quantitative colorimetric urea assay kit QuantiChrom™ (Gentaur, Brussels, Belgium).

The statistical significance of the experimental results was established by ANOVA followed by a Bonferroni post hoc test ($P < 0.05$).

### 2.7. High performance liquid chromatography (HPLC) analysis of diazepam and its metabolites

Embryonic liver cells were incubated with 10 μg ml$^{-1}$ diazepam. HPLC was used to monitor the biotransformation of diazepam [24] into its metabolites. Aliquots of the culture medium were alkalinized with 20% 4 M NaOH, precipitated with isopropanol (1:10) and extracted with ethyl acetate (5:1) by gentle rocking for 10 min and subsequent centrifugation at 200 *g* for 15 min at RT. The ethyl acetate phase was then evaporated and dried under vacuum and the pellet dissolved in 96 μl of mobile phase consisting of acetonitrile/methanol/0.04% triethylamine, pH 7.04, in the proportions 25/35/40. The samples were analysed by HPLC using a 250 × 4.6 mm $C_{18}$-RP Purosphere Star 5 μm column equipped with a precolumn (Merck KGaA, Darmstadt, Germany). The sample injection volume was 20 μl. The mobile phase was delivered at 0.8 ml min$^{-1}$ and the column was operated at ambient temperature. Effluents were monitored with a UV detector at 236 nm. Besides diazepam, its metabolites temazepam, oxazepam and nordiazepam were investigated. For all substances calibration curves were regularly run for between 10 ng ml$^{-1}$ and 10 μg ml$^{-1}$.

## 3. Results

The chitosan membrane had a dense structure and a thickness of 5.5 ± 0.23 μm. In contrast, the PEEK-WC membrane had an asymmetrical structure with a gradient of porosity from one side to the other. The membrane had a porous surface with a mean pore size of 55 nm and a thickness of 66 ± 0.84 μm. Further information is included in Supplementary Data.

Fig. 1 shows the wettability properties of the chitosan and PEEK-WC membranes. The chitosan membrane surface displayed a hydrophilic character, as demonstrated by the time-related WCA and water sorption measurements (Fig. 1a). WCA decreased from 53.8 ± 5.6° at $t = 0$ to 42.17 ± 1.8° at $t = 2.88$ s, while the water sorption increased by 19%. The PEEK-WC membrane surface also showed a hydrophilic character, although the WCA value was higher (76 ± 5.1°) compared with chitosan and remained constant over time (Fig. 1b). The swelling and dissolution behaviour of the chitosan membrane changed with time (Fig. 2). The swelling index displayed a maximum at 3 h (about 366%), while dissolution

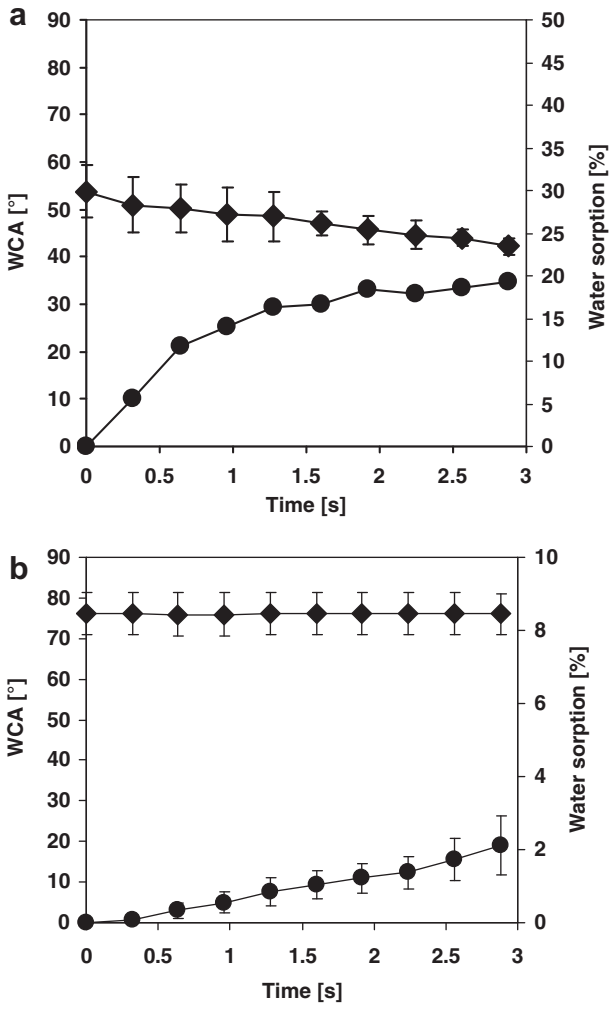


**Fig. 1.** Time related water contact angle (♦) and water sorption (●) of (a) chitosan and (b) PEEK-WC membranes. The values are the means of 10 measurements per sample ± SD.

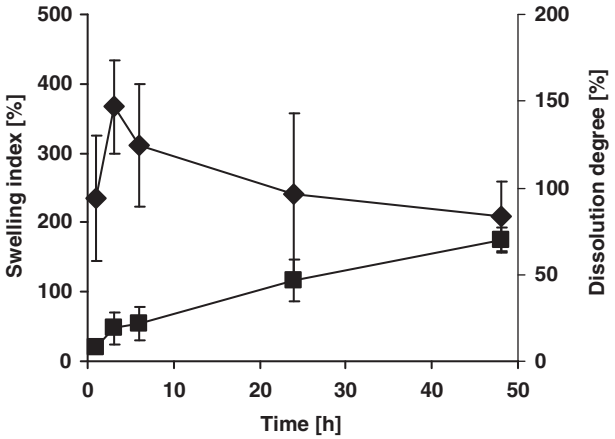


**Fig. 2.** Swelling (♦) and dissolution (■) behaviour of chitosan membrane as a function of time. The values are the means of 10 measurements per sample ± SD.

increased with increasing time, reaching a value of 69.7% after 48 h.

As shown by SEM, cells readily adhered to the chitosan membrane, then proliferated during the first days of culture and spread to form a confluent layer covering the membrane surface (Fig. 3a).

After complete coverage of the available space cells tended to form cord-like structures comprised of aggregates as result of cell proliferation (Fig. 3b). On PEEK-WC membranes cells adhered and proliferated, showing a polyhedral shape and a low degree of aggregation with respect to the chitosan membranes (Fig. 3c and d). The cells exhibited a cell growth morphology and tight cell–cell contact. A similar organization was displayed by cells cultured on collagen, on which the formation of cord-like structures was observed after 16 days culture (Fig. 3f). As on the collagen, cells grown on traditional PSCD formed similar two-dimensional layers (Fig. 3g and h). Further morphological investigations were performed by LCSM after 7 and 16 days culture (Fig. 4). Staining for actin and vinculin demonstrated the overall morphology of the cells cultured on chitosan and PEEK-WC membranes and the organization of the cytoskeletal proteins. After 7 days cells were found to typically have a distinct circumferential bundle of actin filaments immediately behind the free edges of lamellae, while straight, thin bundles of filaments were observed in the central regions of the cells (Fig. 4a). Numerous focal adhesions were observed under the circumferential bundles of actin and at the ends of the straight bundles of actin filaments (Fig. 4a, c, e and g). Cells grown on the chitosan (Fig. 4a) and PEEK-WC membranes (Fig. 4c) appeared well spread, with the typical polyhedral shape of parenchymal cells. After 16 days culture cells maintained the organisation of actin fibres radially oriented in the area of cell–cell contact and focal adhesion complexes (Fig. 4b, d, f and h).

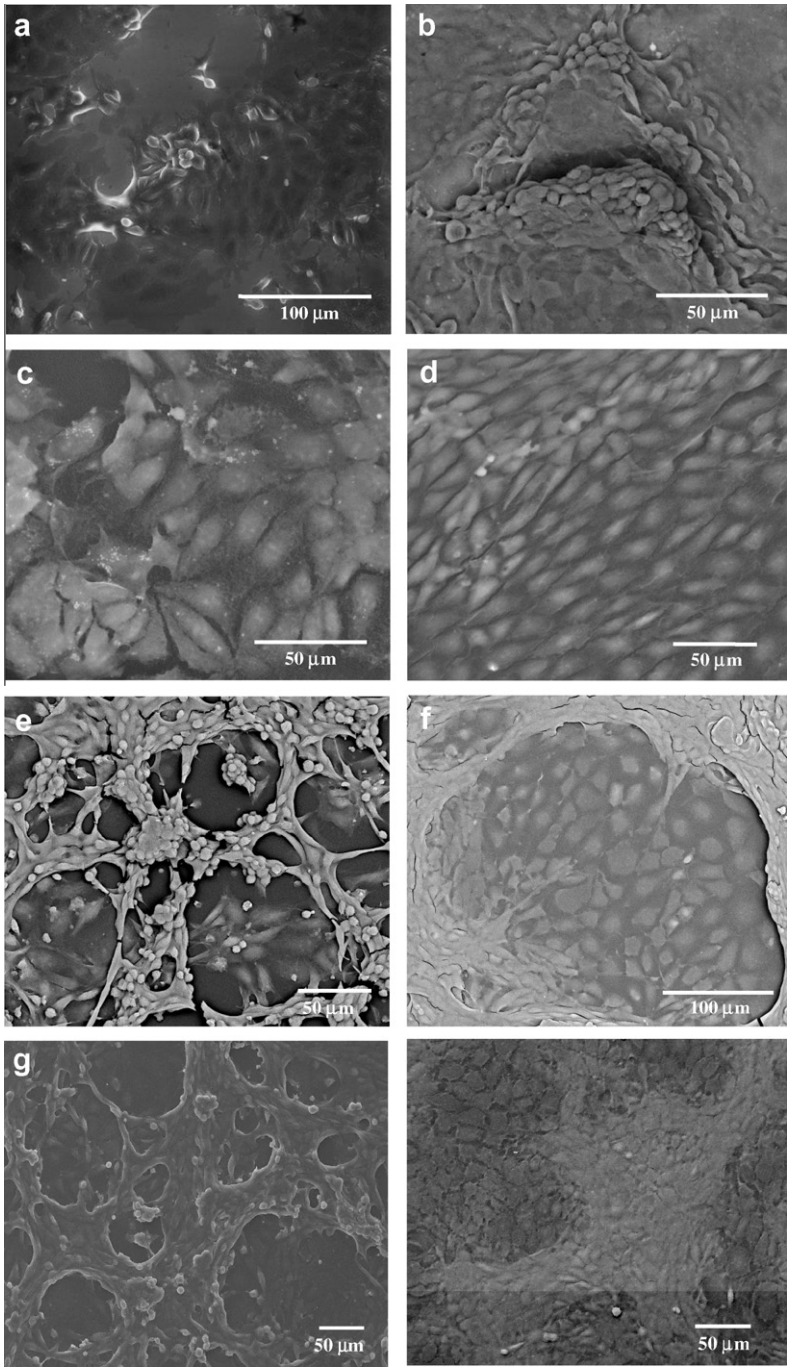


**Fig. 3.** SEM images of rat embryonic liver cells after 7 days (a, c, e, g) and 16 days (b, d, f, h) culture on: (a and b) chitosan membrane; (c and d) PEEK-WC membrane; (e and f) collagen; (g and h) PSCD. Images are at different magnifications.

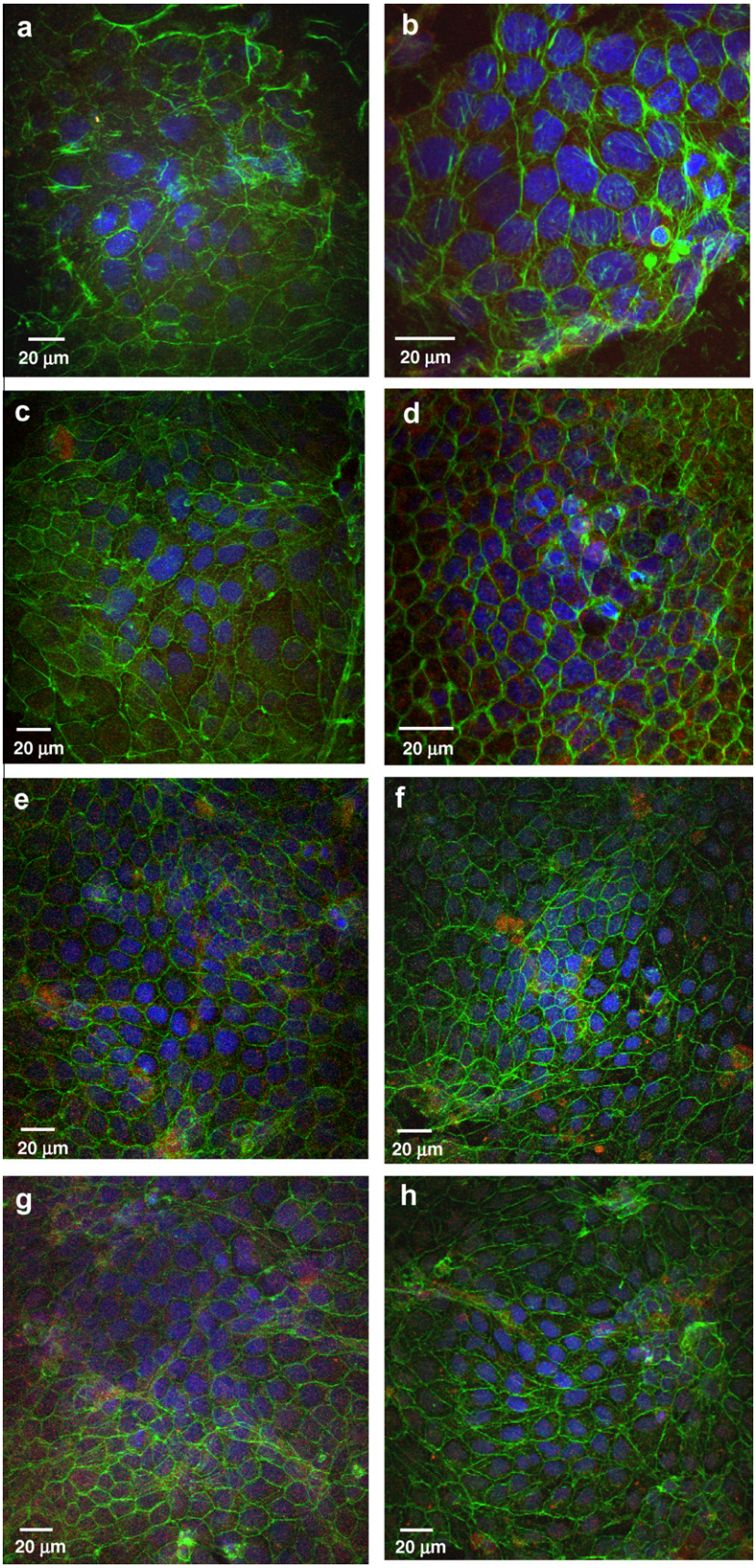


**Fig. 4.** Confocal images of rat embryonic liver cells after 7 days (a, c, e, g) and 16 days (b, d, f, h) culture on: (a and b) chitosan membrane; (c and d) PEEK-WC membrane; (e and f) collagen; (g and h) PSCD. Cells were stained for actin (green), vinculin (red) and nuclei (blue).

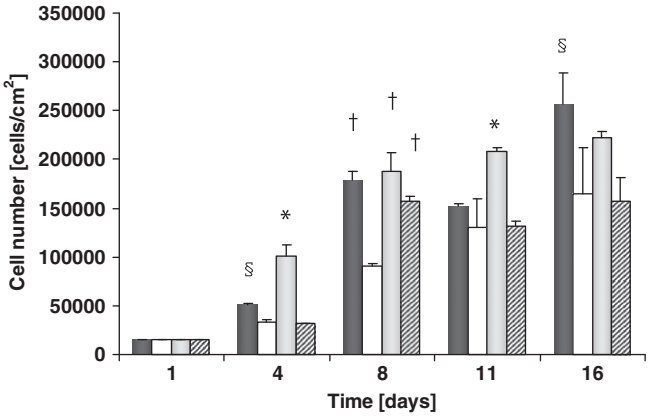


**Fig. 5.** Proliferation of rat embryonic liver cells on chitosan membrane (full bar), PEEK-WC membrane (white bar), collagen (grey bar) and PSCD (dashed bar). The values are the means of six experiments ± SD. *$P < 0.05$ vs. all; §$P < 0.05$ vs. PEEK-WC and PSCD; †$P < 0.05$ vs. PEEK-WC.

A quantitative analysis of cell proliferation is given in Fig. 5, which depicts the growth curves of rat embryonic liver cells on the different substrates. First observation of the cells was on day 4, at which time point about $5 \times 10^4$ and $10 \times 10^4$ cell cm$^{-2}$ were present on the chitosan membrane and on collagen, respectively. Cell numbers on the collagen and chitosan membranes were the same by day 8 and cell expansion with time was quite similar for the two substrates. On the PEEK-WC membrane and PSCD the cultures reached saturation with values of $13 \times 10^4$ cell cm$^{-2}$ on day 11, whereas maximum counts on the chitosan membrane and collagen were reached on day 16. At this time the number of cells approached $25 \times 10^4$ cell cm$^{-2}$ on the chitosan membrane and $22 \times 10^4$ cell cm$^{-2}$ on collagen. After 16 days culture on the different substrates cells were slowly lost to the medium due to complete coverage of the available space for adhesion.

Interestingly, the cells exhibited functional differentiation during culture, leading to the expression of liver-specific functions, such as albumin production, urea synthesis and drug biotransformation. Early during culture albumin production increased, reach-

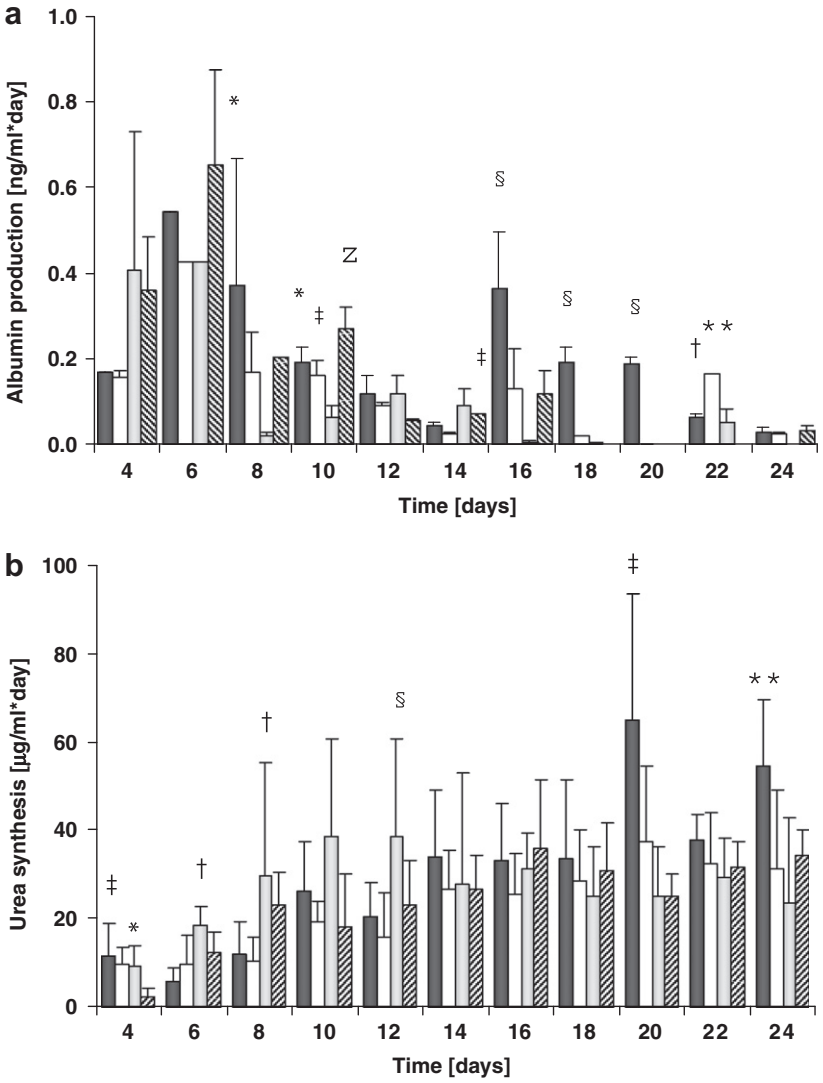


**Fig. 6.** Liver-specific functions of rat embryonic liver cells on chitosan membrane (full bar), PEEK-WC membrane (white bar), collagen (grey bar) and PSCD (dashed bar). (a) Albumin synthesis. The values are the means of six experiments ± SD. *$P < 0.05$ vs. collagen; §$P < 0.05$ vs. PEEK-WC, collagen and PSCD; †$P < 0.05$ vs. collagen and PSCD; ‡$P < 0.05$ vs. collagen; **$P < 0.05$ vs. chitosan, collagen and PSCD; ᶻ$P < 0.05$ vs. PEEK-WC and collagen. (b) Urea synthesis. The values are the means of six experiments ± SD. *$P < 0.05$ vs. CS, PEEK-WC and PSCD; ‡$P < 0.05$ vs. PSCD; †$P < 0.05$ vs. CS and PEEK-WC; §$P < 0.05$ vs. PEEK-WC; **$P < 0.05$ vs. collagen and PSCD.

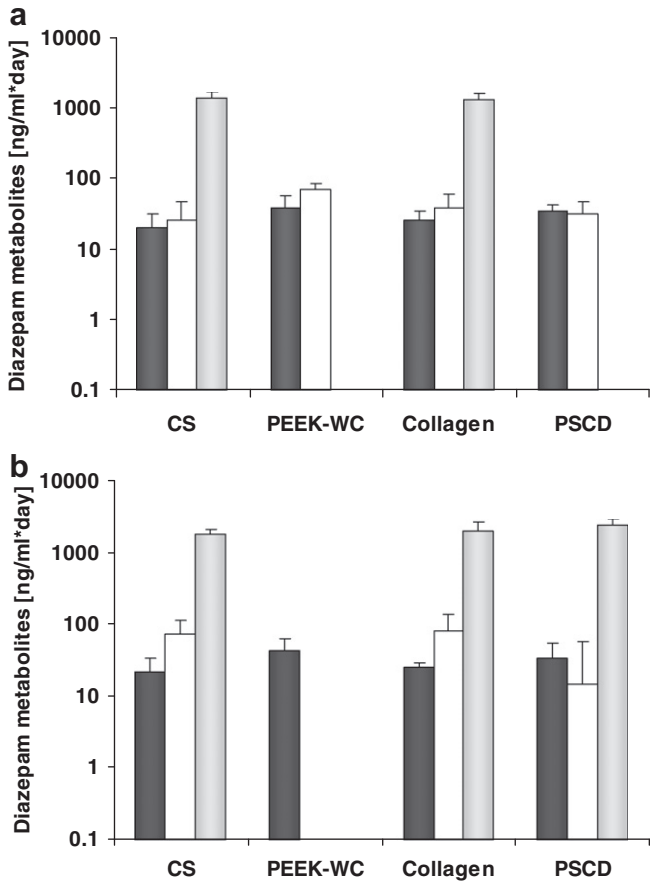


**Fig. 7.** Diazepam metabolite formation of rat embryonic liver cells after (a) 7 and (b) 16 days culture on membranes, collagen and PSCD. Full bar, oxazepam; white bar, nordiazepam; grey bar, temazepam. The values are the means of six experiments ± SD.

ing values of 0.543 ng ml$^{-1}$ per day on the chitosan membrane by day 6, after which secretion of albumin decreased up to 10–14 days on all substrates (Fig. 6a), although cells on the chitosan membrane continued to synthesise albumin at a higher rate (0.2 ng ml$^{-1}$ per day) compared with the other substrates. However, the level of albumin was lower compared with that produced by primary hepatocytes isolated from adult rats on collagen, which showed values of from 4.22 ± 0.15 (day 1) to 96 ± 0.7 μg ml$^{-1}$ per day (day 14).

Expression of mature hepatocyte markers such as albumin and cytokeratin 18 (CK18), as well as the hepatoblast marker α-fetoprotein (AFP), was detected by Western blotting. The initial cell suspension before seeding, which consisted of parenchymal cells, was AFP-positive, while only a faint band appeared for albumin. After 14 days culture on the different substrates the AFP band had disappeared, while distinct bands for albumin and CK18 appeared as a result of cell differentiation, especially on the membranes where more intensive and thicker bands were observed for albumin. Further information is included in Supplementary Data.

Urea was synthesised at rates that increased with time on all substrates (Fig. 6b). Cells on collagen displayed higher levels of urea synthesis from day 6 to day 10 and then remained stable, whereas on the chitosan membrane the synthesis of urea reached its highest value on day 20. At this time urea was synthesised at a rate 6-fold higher than the rate measured on day 4. Significant differences were observed for urea synthesis by primary rat hepatocytes, which exhibited values ranging from 219 ± 2.55 (day 1) to 138 ± 0.4 μg ml$^{-1}$ per day (day 24).

Biotransformation functions were tested by incubating cells with diazepam at a concentration of 10 μg ml$^{-1}$ on days 7 and 16 of culture (Fig. 7). Diazepam metabolites due to phase I reactions, including oxazepam, nordiazepam and temazepam, were detected. Differences were observed for metabolite formation by embryonic liver cells cultured on different substrates.

On collagen the rate of temazepam formation was higher compared with the other metabolites on both day 7 (Fig. 7a) and day 16 (Fig. 7b) with values of 1325.75 and 1895.50 ng ml$^{-1}$ per day, respectively.

Cells cultured on the chitosan membrane display an ability to biotransform diazepam, with the formation of all the metabolites involved in the pathways leading to its clearance.

In particular, the clearance of diazepam on the chitosan membrane occurred with the formation of a greater amount of the metabolite temazepam compared with oxazepam and nordiazepam, with values of 1340.99 on day 7 and 1737.19 ng ml$^{-1}$ per day on day 16.

Diazepam was also completely metabolized by cells cultured on PSCD after 16 days, whereas on the PEEK-WC membrane only one metabolite was detected. After the first administration the complete pool of metabolites was only obtained using the chitosan membrane and the natural substrate collagen, suggesting good performance of the chitosan membrane in maintaining cell functional integrity.

## 4. Discussion

A great deal of attention has been focused on liver progenitor cells for their therapeutic potential and their usefulness in toxicological testing after in vitro differentiation. The suitability of a matrix onto which cells can organise and develop in the proper environment is a key to the differentiation and maintenance of the differentiated phenotype at the morphological and functional level. One of the critical steps in the development of membranes for liver regeneration is the design and selection of the biomaterial. The choice of chitosan as a polymer is related to its intrinsic properties of excellent biocompatibility and biodegradability.

Chitosan membranes may act as a synthetic ECM providing a structure with a well-defined geometry and suitable physico-chemical properties. The degradation behaviour of the chitosan membrane is crucial to the long-term performance of tissue-engineered constructs. We evaluated the swelling behaviour and the degree of dissolution of chitosan with time (Fig. 2). It can be seen that the swelling index reached a maximum after 3 h and then decreased slowly. A similar swelling profile has been reported by others [25–27]. Since chitosan is hydrophilic and the diffusion of chitosan is fast, the films began to swell prior to degradation. During the initial stages of hydration bond cleavage and degradation of chitosan occurred, but swelling surpassed degradation [27]. The decrease in swelling can be attributed to buffer salts, residual acetic acid, etc. [26]. Furthermore, when swelling reached a maximum continuing degradation led to weight loss and the swelling index decreased to a value of 209 ± 50% at 48 h, while the degree of dissolution reached a value of 69.7 ± 7%.

The wettability of both membranes due to the presence of polar groups, particularly on chitosan membranes, promoted cell adhesion and proliferation on these substrates. As confirmed by LCSM observations on both membranes, cells maintained their polygonal shape with a clear reorganization in vitro of the cytoskeletal proteins over the entire culture period, forming a parenchyma-like structure. The adhesion and morphology of cells was strongly affected by the intrinsic physico-chemical properties of the substrate on which they were seeded, as has been shown in a previous work that showed a relationship between cell adhesion and membrane

surface hydrophilicity [28]. The membrane surface can elicit cell adhesion and functioning directly by modulating the interaction with cellular adhesion molecules and/or indirectly by inducing the secretion of ECM proteins. This is consistent with our experimental results regarding the cellular morphological analysis. Additionally, the chitosan membrane offers the cells a matrix that is similar to glycosaminoglycans in the liver ECM and favours the initial step of cell adhesion due to the presence of protonated amino groups at physiological pH, which interact with anionic functional groups on the cellular membrane in the early attachment phase until the cells have synthesised the ECM proteins that mediate contact with integrins.

Functional differentiation of rat embryonic liver cells on the chitosan and PEEK-WC membranes, as well as on collagen and traditional culture dishes, has been evaluated in terms of albumin production, urea synthesis and diazepam biotransformation. Differentiation of embryonic liver cells was traced by determining the expression of albumin, a typical marker of mature hepatocytes, of AFP, a marker of hepatoblasts, which are bipotent cells giving rise to hepatocytes and bile duct epithelial cells, and of CK18, a marker expressed by several liver cell types, including bile ductal epithelial cells and hepatocytes [29]. Cells that before seeding expressed AFP but little albumin and CK18 differentiated into hepatocytes, as demonstrated by the functional markers of mature hepatocytes CK18 and albumin and the loss of AFP expression, especially on chitosan membranes [30]. To test whether the cells possessed liver-specific functions we investigated urea synthesis, albumin production and diazepam biotransformation during culture time. It is interesting to note that cells maintained their liver-specific functions for the whole culture period. The rate of urea synthesis increased with time, with values ranging from 12 (day 4) to 55 $\mu g\ ml^{-1}$ per day (day 24). Similar values have been measured using human mesenchymal stem cells after differentiation [31]. In contrast, the synthesis of albumin was high on day 6 and then decreased concomitant with the increased proliferation (Fig. 6). The values for albumin produced by the cells in our study are comparable with those measured by Tai et al. using human mesenchymal stem cells in a polyelectrolyte fibrous scaffold, who found about 0.047 and 0.075 $ng\ ml^{-1}$ per day after 10 and 20 days culture, respectively [31], and by McClelland et al. using hepatic stem cells in a collagen substrate, which exhibited values ranging from about 0.1 to 0.25 $ng\ ml^{-1}$ per day [3]. However, the measured values for albumin synthesis were lower compared with those displayed by primary adult hepatocytes. This is not completely unexpected, because the differentiation process takes longer. In fact, Freeman et al. have shown that foetal liver cells synthesise albumin at a level of 10 $ng\ ml^{-1}$ only after 3 weeks culture and that albumin synthesis increased by two orders of magnitude only after 6 weeks [32].

The decrease in albumin synthesis that we observed during cell proliferation was probably due to down-regulation of albumin synthesis during proliferation. The transcription rate of the albumin gene is regulated by the interaction of a variety of promoter binding proteins, such as CCAAT/enhancer binding protein (C/EBP)-α, C/EBP-β. C/EBP-α is abundant in normal liver and is considered to regulate the expression of many genes and activate the promoter of the albumin gene. In the non-growing, actively metabolizing normal adult liver C/EBP-α expression is high and restricted to hepatocytes [33], while in rapidly growing cells C/EBP-α expression is extremely low [34]. Mischoulou et al. demonstrated that the expression of C/EBP-α is inversely related to the proliferative state of the cells and this is consistent with a role for C/EBP-α as a factor that can function to maintain the quiescent state [35]. In our study we observed a decrease in albumin synthesis during hepatocyte proliferation that in part recovered when cell proliferation began to slow down.

Another important result concerns the biotransformation activity of cells (Fig. 7). Diazepam is metabolised by liver cytochrome P450s (CYPs) to three major metabolites, N-desmethyldiazepam or nordiazepam, temazepam and oxazepam. The metabolic pathway of diazepam involves a variety of CYPs. Neville et al.(1993) reported that *p*-hydroxylation, 3-hydroxylation and N-desmethylation are the pathways of diazepam metabolism in rat liver microsomes and that they were catalyzed by the P450 isoforms CYP2D1, CYP3A2 and CYP2C11, respectively [36,37]. The production of all three metabolites on chitosan membranes, as well as on collagen, after 7 days culture demonstrated activity of the full range of phase I CYP isoenzymes was achieved on these substrates, while cells on PEEK-WC membranes and PSCD secreted only some diazepam metabolites, probably due to partial expression of the isoenzymes responsible for metabolism. Cells continued to produce the three major metabolites of diazepam over the period of culture and after 14 days showed complete biotransformation of diazepam through phase I reactions on chitosan membranes, as well as on collagen and PSCD, with a significant increase in the metabolic rates.

## 5. Conclusions

Here we have investigated the proliferation of rat embryonic liver cells and the expression of differentiated functions on chitosan and PEEK-WC membranes prepared by the phase inversion technique in comparison with collagen and PSCD. Cells proliferated, resulting in a significant increase in cell numbers, and formed a structure close to that of liver parenchyma. The chitosan membrane provided an optimal microenvironment for embryonic liver cells, giving them the means to acquire and maintain specific functions in a comparable way to those found in collagen, used as reference system. Cells underwent functional differentiation, showing urea synthesis, albumin production and diazepam biotransformation at significantly high levels, particularly on the chitosan membrane. On the basis of these results we hypothesise that the chitosan membrane was able to promote the proliferation and functional differentiation of embryonic liver cells, facilitating their use in liver tissue engineering applications where the membrane, thanks to its biofunctional, physico-chemical and degradable properties, may act as a carrier for the local delivery of cells promoting their differentiation into the terminal target cell type.

## Acknowledgement

This work was supported by grants from the European Commission through the Livebiomat project STREP NMP3-CT-013653 in FP6.

## Appendix A. Figures with essential colour discrimination

Certain figures in this article, particularly Figure4, is difficult to interpret in black and white. The full colour images can be found in the on-line version, at doi:10.1016/j.actbio.2010.07.039.

## Appendix B. Supplementary data

Supplementary data associated with this article can be found, in the online version, at doi:10.1016/j.actbio.2010.07.039.

## References

[1] de Rave S, Tilanus HW, van Der LJ, de Man RA, van der Berg B, Hop WCJ, et al. The importance of orthotopic transplantation in acute hepatic failure. Transpl Int 2002;15:29–33.

[2] Asonuma K, Gilbert JC, Stein JE, Tekada T, Vacanti JP. Quantitation of transplanted hepatic mass necessary to cure the Gunn rat model of hyperbilirubinemia. J Pediatr Surg 1992;27:298–301.
[3] McClelland R, Wauthier E, Zhang L, Melhem A, Schmelzer E, Barbier C, et al. Ex vivo conditions for self-replication of human hepatic stem cells. Tissue Eng Part C 2008;14:341–51.
[4] Kulig KM, Vacanti JP. Hepatic tissue engineering. Transpl Immunol 2004;12:303–10.
[5] Hirano T. Chitin biotechnology applications. Biotechnol Annu Rev 1996;2:237–58.
[6] Chandy T, Sharma CP. Chitosan as a biomaterial. Biomater Artif Cells Artif Organs 1990;18:1–24.
[7] Agnihotri SA, Mallikarjuna NN, Aminabhavi TM. Recent advances on chitosan-based micro-and nanoparticles in drug delivery. J Controlled Release 2004;100:5–28.
[8] Gingras M, Paradis I, Berthod F. Nerve regeneration in a collagen–chitosan tissue-engineered skin transplanted on nude mice. Biomaterials 2003;25:4273–8.
[9] Yuan Y, Zhang P, Yang Y, Wang X, Gu X. The interaction of Schwann cells with chitosan membranes and fibers in vitro. Biomaterials 2004;25:4273–8.
[10] Kim IY, Seo SJ, Moon HS, Yoo MK, Parl IY, Kim BC, et al. Chitosan and its derivative for tissue engineering applications. Biotechnol Adv 2008;26:1–21.
[11] She Z, Jin C, Huang Z, Zhang B, Feng Q, Xu Y. Sik/chitosan scaffold: preparation, characterization and culture with HepG2 cell. J Mater Sci: Mater Med 2008;19:3545–53.
[12] Li J, Pan J, Zhang L, Guo X, Yu Y. Culture of primary rat hepatocytes within porous chitosan scaffolds. J Biomed Mater Res 2003;67A:938–43.
[13] Karakecili AG, Satriano C, Gumusderelioglu M, Marletta G. Enhancement of fibroblastic proliferation on chitosan surfaces by immobilized epidermal growth factor. Acta Biomater 2008;4:989–96.
[14] Feng ZQ, Chu X, Huang NP, Wang T, Wanf Y, Shi X, et al. The effect of nanofibrous galactosylated chitosan scaffolds on the formation of rat primary hepatocyte aggregates and the maintenance of liver function. Biomaterials 2009;30:2753–63.
[15] Rathke TD, Hudson SM. Review of chitin and chitosan as fiber and film formers. J Macromol Sci Part C Polymer Rev 1994;34:375–437.
[16] Zhang M, Li XH, Gong YD, Zhao NM, Zhang XF. Properties and biocompatibility of chitosan film by blending with PEG. Biomaterials 2002;23:2641–8.
[17] De Bartolo L, Salerno S, Curcio E, Piscioneri A, Rende M, Morelli S, et al. Human hepatocyte functions in a crossed hollow fiber membrane bioreactor. Biomaterials 2009;30:2531–43.
[18] De Bartolo L, Morelli S, Piscioneri A, Lopez LC, Favia P, d'Agostino R, et al. Novel membranes and surface modification able to activate specific cellular responses. Biomol Eng 2007;24:23–6.
[19] De Bartolo L, Morelli S, Rende M, Gordano A, Drioli E. New modified polyetheretherketone membrane for liver cell culture in biohybrid systems: adhesion and specific functions of isolated hepatocytes. Biomaterials 2004;25:3621–9.
[20] Takaoka T, Yasumoto S, Katsuta H. A simple method for cultivation of rat liver cells. Jpn J Exp Med 1975;45:317–26.
[21] Pavlica S, Piscioneri A, Peinemann F, Keller M, Milosevic J, Staeudte A, et al. Rat embryonic liver cell expansion and differentiation on $NH_3$ plasma-grafted PEEK-WC-PU membranes. Biomaterials 2009;30:6514–21.
[22] Machaj EK, Grabwska I, Gaijkowska A, Jastrzewska M, Oldak T, Moraczewski J, et al. Differentiation potential of the fetal rat-liver derived cells. Folia Histochem Cytobiol 2005;43:217–22.
[23] Zhang HC, Chen TL, Yuan YG. Chinese patent no. 85108751; 1987.
[24] Bader A, De Bartolo L, Haverich A. High level benzodiazepine and ammonia clearance by flat membrane bioreactors with porcine liver cells. J Biotechnol 2000;81:95–105.
[25] Baskar D, Kumar TSS. Effect of deacetylation time on the preparation, properties and swelling behaviour of chitosan films. Carbohydr Polymer 2009;78:767–72.
[26] Azevedo EP, Saldanha TDP, Navarro MVM, Medeiros AC, Ginani MF, Raffin FN. Mechanical properties and release studies of chitosan films impregnated with silver sulfadiazine. J Appl Polymer Sci 2006;102:3462–70.
[27] Ren D, Yi H, Wang W, Ma X. The enzymatic degradation and swelling properties of chitosan matrices with different degrees of N-acetylation. Carbohydr Res 2005;340:2403–10.
[28] De Bartolo L, Morelli S, Bader A, Drioli E. Evaluation of cell behaviour related to physico- chemical properties of polymeric membranes to be used in bioartificial organs. Biomaterials 2002;23:2485–97.
[29] Schmelzer E, Zhang L, Bruce A, Wauthier E, Ludlow J, Yao HL, et al. Human hepatic stem cells from fetal and postnatal donors. J Exp Med 2007;204:1973–87.
[30] Zhao Y, Chen S, Cai J, Song Z, Che J, Liu C, et al. Derivation and characterization of hepatic progenitor cells from human embryonic stem cells. Plos One 2009;4:e6468.
[31] Tai BCU, Du C, Gao S, Wan ACA, Ying JY. The use of a polyelectrolyte fibrous scaffold to deliver differentiated hMSCs to the liver. Biomaterials 2010;31:48–57.
[32] Freeman AE, Engvall E, Hirata K, Yoshida Y, Kottel RH, Hilborn V, et al. Differentiation of fetal liver cells in vitro. Proc Natl Acad Sci USA 1981;78:3659–63.
[33] Birkenmeier EH, Gwynn B, Horward S, Jerry J, Gordon JI, Landschulz WH, et al. Tissue-specific expression, developmental regulation, and genetic mapping of the gene encoding CCAAT/enhancer binding protein. Genes Dev 1989;3:1146–56.
[34] Friedman AD, Landschulz WH, McKnight SL. CCAAT/enhancer binding protein activates the promoter of the serum albumin gene in cultured hepatoma cells. Gene Dev 1989;3:1314–22.
[35] Mischoulon D, Rana B, Bucher NLR, Farmer SR. Growth-dependent inhibition of CCAAT enhancer-binding protein (C/EBPα) gene expression during hepatocyte proliferation in the regenerating liver and in culture. Mol Cell Biol 1992;12:2553–60.
[36] Neville CF, Ninomiya S, Shimada N, Kamataki T, Imaoka S, Funae Y. Characterization of specific cytochrome P450 enzymes responsible for the metabolism of diazepam in hepatic microsomes of adult male rats. Biochem Pharmacol 1993;45:59–65.
[37] Konomu S, Noriaki S, Hyung Sub K, Mayumi I, Akio K, Shoichi F. Strain differences in diazepam metabolism at its three metabolic sites in Sprague-Dawley, brown Norway, dark agouti, and Wistar strain rats. Drug Metabol Disposit 2004;32:959–65.

**Supplementary data to:**
A. Piscioneri, C. Campana, S. Salerno, S. Morelli, A. Bader, F. Giordano,E. Drioli, L. De Bartolo, "Biodegradable and synthetic membranes for the expansion and functional differentiation of rat embryonic liver cells", *Acta Biomaterialia* 7 (2011) 171–179

## Western Blotting

For western blotting analysis the proteins were extracted according the following procedure. After 14 days of culture on different substrates the rat embryonic liver cells were washed once with cold PBS and then pelletted by centrifugation. The cell pellets were resuspended in ice-cold lysis buffer (50 mM Tris-HCl, 150 mM NaCl, 1% Triton X-100) supplemented with protease and phosphatase inhibitor cocktails, vortexed and incubated for 40 min at 4°C. During the incubation time, the samples have been sonicated for 30 s and centrifuged at 10,000 rpm for 20 min at 4 °C. The supernatants were transferred in new tubes and the protein concentration was determined by using the QBIT fluorometer (Invitrogen, Paisley, UK).

Western blotting was performed as previously described. Equal amounts of protein (50 μg) were boiled for 5 minutes, separated under denaturing conditions by SDS-PAGE on 8% polyacrylamide Tris-glycine gels and electroblotted to nitrocellulose membrane. Non-specific sites were blocked with 5% non fat dry milk in 0.1% Tween-20 in Tris-buffered saline (TBS-T) for 1 hour at room temperature and incubated overnight with monoclonal antibody against albumin (Santa Cruz Biotechnology, 1:500), cytokeratin 18 (CK18) (Santa Cruz Biotechnology 1:200) and Alpha-fetoprotein (AFP) (Santa Cruz Biotechnology 1:200). The antigen–antibody complex was detected by incubation of the membranes for 1 h at room temperature with a peroxidase-coupled anti-IgG antibody (1:3000) (Santa Cruz Biotechnology, Santa Cruz, CA) and revealed using the ECL Plus Western blotting detection system (Amersham, USA) according to the manufacturer's instruction. Each membrane was exposed to the film for 1 minutes.

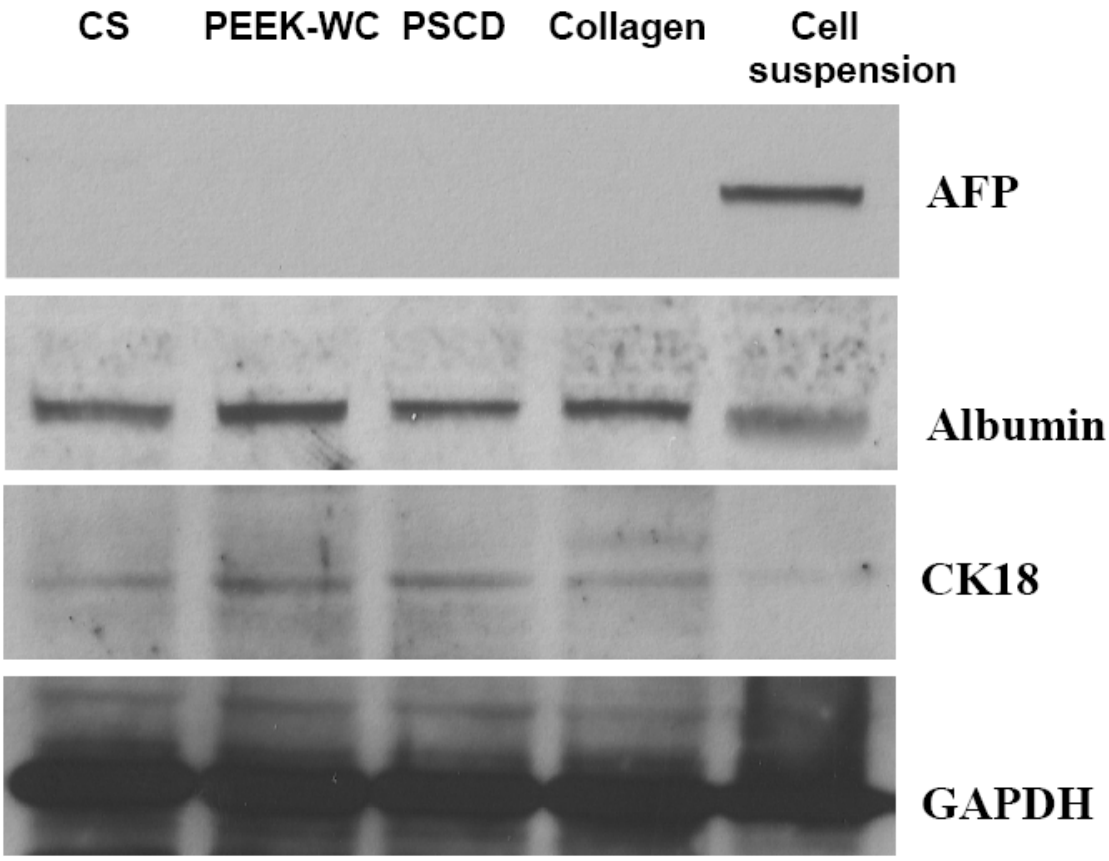


Western blotting analysis of AFP, albumin and CK18 in the rat embryonic liver cells before seeding (indicated as cell suspension) and after 14 days of culture on the investigated substrates. Detection of glyceraldehyde 3-phosphate dehydrogenase (GAPDH) is shown as an internal loading control. A typical experiment representative of ≥3 independent experiments, is shown.

# MANUSCRIPT SUBMITTED

# CHAPTER 6

## 2-D AND 3-D MEMBRANE SYSTEMS FOR THE RECONSTRUCTION OF HYPPOCAMPAL NEURONAL NETWORK

SABRINA MORELLI[1], ANTONELLA PISCIONERI[1], SIMONA SALERNO[1], MARIA RENDE[1], CARLA CAMPANA[1,2], FRANCO TASSELLI[1], ANNA DI VITO[3], GIUSEPPINA GIUSI[3], MARCELLO CANONACO[3], ENRICO DRIOLI[1,2] AND LOREDANA DE BARTOLO[1]

*[1]Institute on Membrane Technology, National Research Council of Italy, ITM-CNR, c/o University of Calabria, Via P. Bucci, cubo 17/C, Rende (CS), Italy*

*[2]Department of Chemical Engineering and Materials of University of Calabria, via P. Bucci cubo 45/A 87030 Rende (CS) Italy*

*[3]Comparative Neuroanatomy Laboratory, Department of Ecology, University of Calabria, via P. Bucci 4/B, 87030 Rende (CS), Italy*

**ABSTRACT**

The selection of appropriate biomaterials that promote cellular adhesion and growth is particularly important for the in vitro reconstruction of neuronal network.

This study focused on the development of new polymeric membranes in 2D and 3D configurations as novel biomaterials for neuronal outgrowth. Two membrane systems constituted of modified polyetheretherketone (PEEK-WC) and polyacrylonitrile (PAN) membranes in flat and hollow fiber (HF) configurations were developed and used for the culture of hippocampal neurons.

We demonstrated that all investigated membranes supported the adhesion and growth of hippocampal neurons enhancing neuronal differentiation and and neurite alignment. The differences in cell behaviours between cells cultured on 2D and 3D membranes were highlighted by the quantitative analysis of neuronal marker fluorescence intensity, morphometric analysis, RT-PCR analysis and also by metabolic activity measurements. In particular, the 3D PAN HF membranes showed ideal growth culture conditions guarantying good levels of metabolic features.

Primary hippocampal cells cultured on PAN HF membranes were able to recreate in vitro a 3D neural tissue-like structure that mimicking the hippocampal tissue, could be used as a tool for the study of natural and pathological neurobiological events.

## 6.1 INTRODUCTION

Each year, in the United States of America, more than 1.7 million cases of traumatic brain injury are reported. Approximately 400 000 Americans suffer from neurological symptoms associated with multiple sclerosis (MS). Interestingly, more than 5 milion people in the United States and Europe alone suffer from dementia associated with Alzheimer's disease. About 450 000 people (approximately 1 out of 670) in the United States live with spinal cord injury, with about 11 000 new spinal cord injuries being registered every year (1 out of 30 000) [1]. Owing to the profound impact of central nervous system (CNS) damage, extensive studies have been carried out in this field with the scope of discovering better therapeutic approaches aimed at facilitating CNS repair. Many strategies have been developed to improve, among others, axonal reinnervation and to direct its outgrowth on more advanced culture media, such as synthetic and biological substrates as biomaterial bridges [2] and as peripheral nerve grafts [3]. At date, many attempts have been focused on seeking not only new biomaterials, but also new cell source as well as novel designs of tissue-engineered neuronal bridging devices in order to generate safer and more efficacious nervous tissue repairs.

Biomaterials for neuronal bridging devices include polymeric materials for both non-biodegradable polymers (polyvinylchloride, silicone, polyethylene, polytetrafluroethylene), and biodegradable polymers (polyglycolic acid, poly(L-lactide-co-glycolide), alginate, collagen, chitosan). Indeed, recently numerous studies have demonstrated that polymeric semi-permeable membranes, in fiber and flat configurations, are excellent biomaterials for successfully *in vitro* reconstruction of neuronal tissue [4-5-6-7]. In particular, membranes in tubular configuration act as guidance channel to protect the lumen of regenerating axons from the external environment. Surprisingly, among the variety of tubular structures used for guidance channels, semi-permeable hollow fiber membranes appear to be considered a favorable guide for the regeneration of neuronal tissue [7-8-9].

In these past years the development of functional neuronal networks using 3D tissue constructs has become of great importance since it offers the advantage of *in vitro* neuronal reconstruction. Compared to traditional 2D culture systems, 3D *in vitro* cultures of neuronal cells appear to better mimic *in vivo* neuronal microenvironments [10] aside representing a great potential for building 3D neuronal circuits [11] as well as

for creating tissue-based biosensors [12-13], and for promoting systemic restoration of severe nerve injuries [14- 15]. In this context, studies aimed toward the determination of differences between 2D and 3D environments for neuronal function could very well have great beneficial bearings on neuroengineering applications.

At present, little is known about the possibility of developing an *in vitro* analogue of hippocampal tissue as a 3D tissue-engineered model, which could prove to be essential for a better definition of the molecular basis involved with physiological learning and memory processes. In addition, the effects of biomaterial configuration on growth and functional differentiation of primary hippocampal neurons are not yet fully known. As a consequence it is the aim of this study to evaluate the development of new polymeric membranes in 2D and 3D configurations as novel biomaterials for hippocampal neurons outgrowth. 2D membrane systems, constituted of modified polyetheretherketone (PEEK-WC) and polyacrylonitrile (PAN) membranes in flat and hollow fiber (HF) configurations with different morphological and permeable properties were developed and used for hippocampal neuronal culture systems. These neuronal systems are well known for their plasticity and regeneration properties [16] along with being considered the best-characterized model for investigating polarization that occurs spontaneously during the first few days of culture [17-18]. The membranes developed in the present study were modified by poly-L-lysine (PLL)-coating in order to minimize the different physico-chemical properties of the surfaces and to have the same functional groups interacting with the cells, as previously reported [6]. The morphological (growth and neurite length) and functional (glucose, lactate and neurotrophic factor production) properties exhibited by hippocampal neurons cultured on membranes with different configurations in comparison with traditional systems such as polystyrene culture dishes (PSCD) coated with PLL are discussed in this paper. Moreover, these morphological and metabolic properties were correlated to the transcriptional capacities of some developmental markers, such as the microtubule-associated protein (MAP2) gene, a cytoskeleton dendritic marker, plus glutamate receptor subtype 2 (GluR2) of acid α-amine-3 hydroxy-5 methyl-4 isoxiazode receptors (AMPARs).

## 6.2 MATERIALS AND METHODS

### 6.2.1 Preparation of flat and hollow fiber (HF) membranes

PEEK-WC and PAN membranes in flat configuration were prepared by inverse phase techniques by using the direct immersion precipitation method [19]. PEEK-WC or poly(oxa-1,4-phenylene-oxo-1,4-phenylene-oxa-1,4-phenylene-3,3(isobenzofurane-1,3-dihydro-1-oxo)diyl-1,4-phenylene), is a chemically stable polymer with excellent thermal and mechanical resistance [20]. PEEK-WC membranes were prepared from 15% (w/w) PEEK-WC polymer, 80% (w/w) poly(vinylpyrrolidone) (PVP) in dimethylformamide (DMF). After casting, polymeric films were coagulated in a water bath. The membranes were washed extensively with water and dried at room temperature. PAN membranes in flat configuration were prepared from a solution of PAN (15% wt/wt) and PVP (10 % wt/wt) in DMF under continuous stirring at 50 °C for 4h. There after, the polymer solution was cast to a 250- μm- thick film and then allowed to precipitate in water. After their formation, the membranes were rinsed with water for several hours.

PEEK-WC membranes in HF configuration were prepared according to the well-known dry-wet spinning method. Polymer solutions with 18% wt/wt of PEEK-WC in Dimethylacetamide (DMA) were prepared under continuous mechanical stirring at room temperature as previously described [21]. HF membranes were prepared by extruding the polymer solution through a spinneret in which dimensions (OD, ID, needle) were 800, 400 and 200 μm respectively. A 50/50 v/v mixture of DMA and pure water was used as the bore fluid and tap water as the external coagulant. Polymer solution and bore fluid flow rate were 3.0 and 3.5 g/min respectively. The air gap was 35 cm.

For the preparation of PAN HF membranes, a copolymer containing 92 and 8% wt/wt of acrylonitrile and vinyl acetate respectively with a viscosity average molecular weight ($M_V$) of 40 000 Da, (Montefibre SpA, Italy) was used. Porous membranes were prepared by using PVP (K17 by BASF) as the pore forming additive and DMF as the solvent. The weight ratio was 15/15/70 for PAN, PVP and DMF, respectively. Polymer solutions were prepared by dispersing the PAN powder in DMF in a glass flask at room temperature to prevent the formation of large clots and afterwards PVP was added. The solution was then heated at 70°C under mechanical stirring until a homogeneous

solution was obtained. The solution was then loaded onto a thermostated vessel, kept at 70°C. The spinning setup was the same for that used for PEEK-WC HF membranes. Polymer solution and bore fluid flow rates were 2.2 and 2.7 g/min respectively. For the bore fluid, a 60/40 v/v mixture of DMF and pure water was used and the air gap was fixed at 60 cm. The membranes were modified by coating with PLL (MW 30 000–70 000), dissolved in a boric acid/sodium tetraborate solution (1:1) to a final concentration of 0.1mg/mL, in order to have the same functional groups over the surfaces with a density of 40μg/cm$^2$. The membranes were coated with poly-l-lysine in PBS and incubated for 3 h and then the excess of PLL solution was removed and dried. Poly-l-lysine-coated PSCD were used as controls.

### 6.2.2 Membrane Characterization

The morphological properties of all membranes and precisely mean pore size, pore size distribution and thickness were characterized by scanning electron microscope (SEM). Dried membrane samples, in flat and HF configurations, were cut in cross-section, mounted with double-faced conductive adhesive tape, and analyzed by SEM (ESEM FEG QUANTA 200, FEI Company, Oregon, and USA) in order to establish cross-sectional structure and thickness, intra- and extra- lumen morphology and diameters, shape and sizes of the membrane pores as well as the distribution of pore size. Measurements of the inner and outer diameter and wall thickness derived from digital images using NIH Image.

The wettability of the native and modified membranes was characterized by means of water dynamic contact angle (DCA) measurements. The contact angle of water droplets was measured at room temperature with a CAM 200 contact angle meter (KSV Instruments, Ltd., Helsinki, Finland). DCA measurements were performed under standard conditions, which take into account various parameters (e.g., temperature, cleanliness of sample, drop volume). The instrument supported by video camera and software permitted us to obtain precise drop measurements and evolution in time. DCA measurements were performed on native and PLL-coated membranes. At least 30 measurements on different regions of each membrane sample were averaged for each DCA value. The permeability properties of HF membranes were characterized by pure water flux measurements in the absence of solutes and at different trans-membrane

pressures ($\Delta P^{TM}$). For each membrane, the hydraulic permeance $L_p$ was evaluated before and after modification process with PLL by applying the following equation (Eq. 6.1) [22]:

$$L_P = \left( \frac{J_{Solvent}}{\Delta P^{TM}} \right)_{\Delta c=0} \qquad \text{Eq. 6.1}$$

This equation provides a linear correlation between water flux and the convective driving force. FITC labeled PLL (Sigma, Italy) was used for the visualization and quantification of membrane coating. Imaging of the FITC labeled coated membranes were obtained by using an Olympus Fluoview FV300 Laser Confocal Scanning Microscope (LCSM) (Olympus, Italy). Quantitative analysis was performed on different sample areas for each investigated coated membrane (n=3) by measuring the average intensity of fluorescence through the application of a Fluoview 5.0 software (Olympus Corporation). A calibration curve of FITC labeled PLL was obtained by casting known quantities of the fluorescent protein on defined areas of polystyrene dishes and thereby calculating the surface concentrations on confocal images of dry samples. The thickness of the PLL coating resulted to be 1.2 ±0.09 μm, when measured with FITC labeled PLL by Z-direction scanning at the LCSM.

### 6.2.3 Cell isolation and culture

The hippocampus of both hemispheres was dissected from the brain of postnatal days 1-3 (PND1-3) hamsters (*Mesocricetus auratus*)(in accordance with the institutional and national guide for the care and use of laboratory animals), removed and collected in falcon tubes in Neurobasal medium A (Invitrogen Corporation, Milan, Italy) containing 0.02% BSA (Sigma, Milan, Italy). The tissue was digested in a Neurobasal medium A containing 0.1% papain (Sigma) and 0.02% BSA (Sigma) for 20 min at 37°C ([23]Xie *et al*., 2000). Ten minutes after digestion, the tubes containing the tissue was mixed and at the end of digestion, the supernatant containing papain was removed and Neurobasal medium A supplemented with B27 (2% v/v; Invitrogen Corporation, Milan, Italy) penicillin-streptomycin (100 U/mL), glutamine 0.5 mM (Biochrom AG), 5ng/mL basic fibroblast growth factor (b-FGF; Sigma) was added to the remaining pellet. Samples were gently triturated mechanical by using a sterile Pasteur pipette with a wide opening to dissociate larger aggregates. After sedimentation of the aggregates the supernatant

was removed and transferred into tubes containing 1% papain inhibitor in Neurobasal medium A and 1% BSA, as described elsewhere [5]. The samples were centrifuged at 1300 rpm for 10 min at room temperature and cell pellets were gently re-suspended in Neurobasal medium A containing B27 supplement, penicillin-streptomycin, 0.5 mM glutamine, 5ng/mL b-FGF. Serum-free B27 supplemented Neurobasal medium A seems to have a beneficial effect on the growth and differentiation of hippocampal neurons, as suggested by other researchers [18-24]. The viability of the cells after isolation was assessed by trypan blue test, which resulted to be 97±2%. Cells were seeded on the different membrane surfaces at $2.5x10^5$ cell/$cm^2$ density. Controls without cells were prepared for each type of substrate. Cells and controls were incubated at 37°C in an atmosphere containing 5% $CO_2$. Cultures were fed every 4 days replacing half of the medium during each feeding interval.

### 6.2.4 Immunostaining of neuronal cells and quantitative analysis

The morphological behaviour of neurons at 8 and 12 *in vitro* culture days (DIV8 and DIV12) on the different membranes were investigated and compared to PSCD as controls by observing them at a Laser Confocal Scanning Microscopy (LCSM, Fluoview FV300, Olympus, Milan, Italy) after the immunostaining of neuronal cytoskeleton and axon markers, βIII-tubulin and 43 KDa growth-associated protein (GAP-43), respectively [6]. Six samples for each substrate were analyzed. In particular, neuronal cells were rinsed with PBS, fixed for 15 min with paraformaldehyde (4%), permeabilized for 10 min with 0.25% Triton X-100 and subsequently blocked for 30 min with 1% BSA at room temperature. To visualize βIII-tubulin a rabbit polyclonal anti-βIII-tubulin (1:100; Sigma, Milan, Italy) and a goat anti rabbit IgG FITC-conjugated (1:100; Invitrogen) were used. To visualize GAP-43, a monoclonal mouse anti-GAP-43 (1:100; Sigma, Milan, Italy) and a goat anti-mouse IgG TRITC-conjugated (1:100; Invitrogen) were used. Primary antibodies were incubated overnight at 4°C, secondary antibodies for 60 min at room temperature. Nucleic acids were counterstained with DAPI (200 ng/mL; Sigma, Milan Italy). Finally samples were rinsed, mounted and observed with a LCSM. A quantitative analysis was performed on confocal microscopy images of neurons at DIV8 and DIV12 by using Fluoview 5.0 software (Olympus Corporation). The fluorescence average intensity for stained βIII-tubulin and GAP43

was calculated vs the z axis of acquired images of 0.5 μm optical thickness. Confocal images were also utilized to evaluate the axonal length stained with GAP43.

### 6.2.5 Sample preparation for SEM

Samples of neurons grown on the different 2D and 3D substrates were prepared for SEM by fixation in 2.5% glutaraldehyde, pH 7.4 phosphate buffer, followed by post-fixation in 1% osmium tetroxide and by progressive dehydration in ethanol. Samples were examined at SEM and representative images displaying both neuronal structural features and adhesive properties for the different membrane surfaces were obtained at DIV 8 and DIV 12. NIH-Scion Image software was used in order to perform quantitative evaluations of the area filled by neurons, expressed as percentage of the total membrane area for the two different developmental stages.

### 6.2.6 Metabolic assays

The metabolic activity of neuronal cells was evaluated by assessing glucose, lactate and the neuronal brain derived neurotrophic factor (BDNF) levels in the culture medium from 6 different isolations and cultures, previously collected and stored in tubes at -20°C until assays. The glucose concentration in the medium was detected by using Accu-Chek Active (Roche Diagnostics, Monza Italy). To assay BDNF secretion, a sensitive BDNF ELISAs immunoassay (Promega Corporation WI, USA) was carried out on samples collected at DIV8 and DIV12. BDNF Elisa was performed as follows: ELISA plates were coated with 100 μL of anti-BDNF monoclonal antibody overnight at 4°C. After washing, 100 μL of cell culture supernatant was added to the wells and left for 2 h at room temperature. Thereafter the wells were washed five times and incubated with 100 μL of anti-human BDNF for 2 h at room temperature. After washing, the wells were covered for 1h with anti-IgY horseradish peroxidase-conjugate and then 100 μl of Tetramethylbenzidine were added for 10 min. The reaction was blocked with 100 μl of 1N HCl and absorbance was measured at 450 nm using a Multiskan Ex (Thermo Lab Systems). Lactate content was determined using lactate oxidase enzymatic assay Lactate Dry-Fast (Sentinel, Milan, Italy) via spectrophotometer analysis. The statistical significance of all experimental results was established by using ANOVA test followed by Bonferroni *t*-test ($p < 0.05$).

### 6.2.7 Extraction of total RNA and preparation of cDNA

Total RNA was extracted from hippocampal cells grown on all membrane substrates considered for this study and on PSCD substrates. All samples processed for RNA extraction were collected at DIV8 and DIV12 and the extraction was carried out by using Trizol reagent (Invitrogen, Carlsbad, CA), according to the manufacturer's instructions for cell suspension. The quality of RNA samples was assessed by measuring optical density (OD, 260/280) absorption ratio of 1.7 (range 1.62 – 2.1) and their integrity was verified by the detection of 18S and 28S bands after agarose gel electrophoresis. Total RNA (2 μg) of each sample was used to synthesize cDNA according to indications of the High Capacity cDNA Reverse Transcription Kit (Applied Biosistem, Italy).

### 6.2.8 Quantitative real time PCR (qPCR)

Quantitative real-time PCR (qPCR) was performed on a Biorad Miniopticon (Biorad, Italy) single color thermocycler. The primer set used for qPCR analysis were designed using Primer Premier 3.0 and optimal primers were identified on the basis of the following parameters: a) robustness, consisting of a successful amplification over a range of annealing temperatures, b) specificity, since these primers were able to generate a single significant peak in the melting curve and c) consistency, which represents an high reproducibility of Quantification Cycle ($C_q$) values within the reactions of a triplicate. For the quantitative expression analysis, we selected two target markers on the basis of their morpho-functional properties in hippocampal cells and namely MAP2 gene, a cytoskeleton dendritic marker, plus GluR2 that represents a synaptic marker. The primers used for MAP2 are FW 5'TGACTTTGCACAGATGGCTTC and BW 5'CCACCTTCTCTTTGACTTCTG while the primers used for GluR2 are FW 5'GGTCAGCAGATTTAGCCCCTACG and BW 5' ACCACCACACACCTCCAACAAT.

The length of all PCR products ranged from 150 to 200 bp and the average amplification efficiency of each primer pair was optimized ranging between 0.95 and 1.00. After checking independent trials of several housekeeping genes, the β-actin proved to be an optimal housekeeping (HK) gene for brain tissue with respect to other

tested genes. β-actin reported the most reproducible results across the various cDNAs and so was selected as normalization gene by using the following primer pair: FW 5'TATCGGCAATGAGCGGTTCC and BW 5′AGCACTGTGTTGGCATAGAG G. An amplification reaction was prepared in a final volume of 25 μl by adding 12.5 μl of SYBR-Green Supermix, 0.3 μM of primers for target genes (MAP2 and GluR2) and 0.1 μM of primers for β-actin and 2 μl (10 ng) of cDNA. All reactions were run in triplicate according to the following cycling parameters: one cycle at 94°C for 3 min, 40 cycles of denaturation at 94°C for 10 s and annealing-extension at 58°C for 30 s. After the reaction, the existence of a unique PCR product was confirmed via the melting curve analysis [25], which was obtained by an increase of 0.5°C every 10 s from 58°C to 95°C. The presence of single PCR product was further verified by 1.5 % agarose gel-electrophoresis. The results of qPCR were analyzed using Opticon Monitor qPCR detection system (Biorad), with a program that permits the analysis of the reaction kinetic. Cycle threshold ($C_q$) values were obtained with Genex software (BIORAD) and all data were analyzed according to the method of standard curve [26] on the basis of gene expression levels calculated from three biological replications. Data obtained for all samples at DIV8 and DIV12 were reported as a proportion of the highest value after normalization with β-actin. Differences were statistically estimated by one-way ANOVA followed by a *post hoc* Bonferroni test when there was a significant $p$-value < 0.05.

## 6.3 RESULTS

### 6.3.1 Membrane properties

SEM micrographs of PEEKWC and PAN membranes in flat (2D) configuration revealed their morphological structure characterized by the presence of pores with mean diameter of 68.55 ± 9.5 nm and 19.45 ± 1.3 nm, respectively along with a thickness of 110 μm for PAN membrane (Figure 6.1a) and of 87 μm for PEEK-WC membrane (Figure 6.1b). The morphological properties of HF membranes are shown in Figure 6.2, in which it was possible to observe a greater porosity in the PAN HF membrane (Figure 6.2a) as compared to that of the PEEK-WC HF (Figure 6.2d). In particular, PAN membranes showed an internal and external diameter, respectively, of 688 ± 5 μm and

910 ± 13 μm as well as a wall thickness of 107 ± 12 μm (Figure 6.2 b,c) while PEEK-WC HF membranes displayed an inner and outer diameter, respectively, of 557 ± 7μm and 747 ± 9 μm and a wall thickness of 93 ± 8 μm (Figure 6.2e,f).

The effective coating of the membranes with PLL was detected in the absence of cells by a quantitative analysis using FITC-labeled PLL. As observed in Figure 6.3, the amount of PLL on the different membranes determined by measurements of the average fluorescence intensity was in the range of 40μg/cm$^2$ and this did not prove to statistically different than the others thus confirming the similar coating level of all membranes. Interestingly, PLL coating membranes seemed to modify their native physical and chemical properties as demonstrated by dynamic contact angle measurements (Figure 6.4). The advancing and receding contact angles of PEEK-WC and PAN membranes in flat and HF configurations decreased significantly after PLL coating, which tends to demonstrate the effective changes in surface wettability, especially the advancing and receding contact angles of PEEK-WC HF membranes as shown by the decreased values of θadv = 89° ± 3.4° and θrec 67° ± 3.9° to values of θadv =78° ± 2.9° and θrec 62° ± 4.7°, respectively, after coating (Figure 6.4b). The native PAN HF membranes have a high hydrophilic surface character and this tends to improve the advancing contact angle as shown by its lower value (59.54° ± 1.76°) measured on this type of membrane. Also the modified membranes displayed a marked wettability even if, in this case, it appeared that PLL coating induced a reduction of the surface hydrophilic character. Conversely, the wettability properties of PAN membranes in flat configuration decreased after PLL coating as well as for PEEK-WC membranes.

Surprisingly, all membranes exhibited different transport properties. The observed steady-state hydraulic permanence of the membranes was calculated according to the slope of the flux $J$ versus the transmembrane pressure ($\Delta P^{TM}$) supplied a straight line, which resulted to be 0.089 l/h*m$^2$ for PEEK-WC HF membranes and 0.240 l/h*m$^2$ in the case of PAN HF membranes (Figure 6.5). These results demonstrated that PAN HF membranes were more permeable with respect to PEEK-WC HF and the PLL coating thus reducing the hydraulic permanence to about 66% for PEEK-WC HF membranes (Figure 6.5b) and of about 11% for PAN HF membranes (Figure 6.5a).

### 6.3.2 Neuronal morphological and morphometric evaluation

After having obtained well appropriate morphological, physical-chemical and permeability properties for cell culture purposes, the membranes were used for hippocampal neurons *in vitro* culture assays. First of all, we performed SEM analysis to examine the adhesion and the cell growth of hippocampal neurons on PAN and PEEK-WC membranes in flat and HF configurations as compared to a PSCD substrate that was used as control for all experimental assays. In figure 6.6 it was possible to observe the morphological features of neurons seeded on the various substrates at DIV8 and DIV12 states. Indeed it seemed that primarily cultured hippocampal neurons were able to adhere and to grow on the different substrates as displayed by few if any visible cell differences between neurons grown on 2D and 3D membranes. At DIV8 (Figures 6.6a,c,e,g,i), a mature morphology of the neuronal cells was reached for all substrates, as demonstrated by the well-developed pyramidal soma along with significantly very long neuritis and elaborated dendritic arbors. It was evident that during this culture time period, neuronal cells were distributed uniformly on 2D PAN, 3D PAN HF, 3D PEEK-WC HF as well as on the control (PSCD), while at DIV12 neurons on 2D PEEK-WC membranes (Figure 6.6f) tended to aggregate into large groups. However, the density of axonal network increased after 12 days of culture for each kind of substrate as shown by a very high complexity with very branched neuritis being reached especially on 2D PAN, 3D PAN HF and 3D PEEKWC HF (Figure 6.6). It is worthy to note that hippocampal neurons at DIV12 on 3D membranes showed a very complex dendritic arborization exhibiting a 3D structure (Figures 6.6h, j). Quantitative analysis confirmed that the area covered by cells increased with time for all substrates, reaching maximal percentage values (about 80% ) at DIV12 on 2D and 3D PAN membranes (Figure 6.7). In contrast, neurons grown on the other membranes adhered to a lesser extend reaching values within the range of 50-60%.

From confocal microscope analysis it seemed that the neuronal marker β-III tubulin, which is a cytoskeleton protein distributed in the soma and in all neuronal processes, and GAP-43, which is a specific protein involved in the regulation of axonal outgrowth, were consistently expressed by hippocampal neurons cultured on the different substrates supporting correct neuronal differentiation events (Figure 6.8). In particular, a complex neuronal network was achieved at DIV12 on 2D PAN, 3D PAN HF and 3D PEEK-WC

HF membranes (Figures 6.8d,h,e). Of particular interesting is that cells cultured on 3D PAN HF at this culture time showed very long neuritis extending along these fibers and producing a three-dimensional structure, as shown by the relative strong green fluorescence emission signals (Figure 6.8h). Moreover, cells grown on 2D PEEKWC membranes for the same culture period exhibited a neurite outgrowth with dense fasciculation compared to the other membranes (Figure 6.8f). As far as the quantities are concerned it appeared that total β-III tubulin levels on both 2D and 3D membrane were significantly higher than the values of the PSCD (ANOVA followed by Bonferroni t-test), which tends to support a good level of polymerization of the cytoskeletal factors being correlated to the integrity of neuronal projections. From these results it is possible to suggest the following trends for DIV8: 3D PAN HF > 2D PAN >3D PEEK-WC HF≥ 2D PEEKWC>PSCD (Figure 6.9a). Furthermore, the signals of β-III tubulin increased within time for all substrates and at DIV12 a intensity peak was registered on 2D PEEKWC, which is tightly related to intense fasciculation processes observed at confocal microscope (Figure 6.8 f). On the other hand the specific marker of axonal growth cones, i.e. GAP-43, supplied highest fluorescent intensity values, independently of culture period, when neurons were cultured on 3D PAN HF membranes (Figure 6.9b).

In order to further substantiate the quantitative morphological features, axonal length of hippocampal neurons were determined at DIV8 and DIV12, periods in which the different neuronal elements and synaptic complexes, respectively, are fully formed. At DIV8 the longest axons (133 ± 35 μm) resulted to be typical for 3D PAN HF followed by 2D PAN (120 ± 23 μm), while in contrast the values resulted to be similarly lower (in the range of 92-100 μm) for the 3D PEEKWC and for the other 2D substrates. The axons continued to elongate with time and at DIV12 became significantly longer for 2D PAN (150 ± 14 μm) and on 3D PAN HF (147 ± 13 μm) with respect to those determined on the other membrane systems.

### 6.3.3 Neuronal metabolism

Coherently, cells exhibited different metabolic activities (glucose consumption, lactate production and BDNF secretion) for 2D and 3D membranes. The consumption of

glucose increased with time for all substrates (Figure 6.11). The highest values were measured for neurons cultured on 3D PAN HF membranes at DIV 12. During the early developmental stage (DIV4 and DIV8) there were no appreciable differences in glucose consumption for the different membranes, while at DIV12 glucose consumption was significantly higher for 3D PAN HF membranes with respect to the other substrates, reaching values of 1699 ± 21 pg/cell. The lactate production of neurons cultured on the different membranes was also investigated in order to evaluate cellular catabolism and anaerobic glycolysis events (Figure 6.12). During the early stages of culture (DIV4) this metabolic activity was significantly higher for PSCD than the other substrates. Even for DIV8 cells high levels of lactate production resulted for both 3D PAN HF membranes (197 ± 33 pg/cell) and for controls (258 ± 19 pg/cell). At DIV12 the highest value was obtained for 3D PAN HF substrates, which resulted to be significantly higher with respect to 2D PAN membranes. The other specific neuronal metabolic indicator evaluated for primarily hippocampal cells, i.e. the neurotrophin BDNF, which plays a fundamental role on neuronal outgrowth, differentiation, maintenance and survival events, supplied contrasting results as shown by higher BDNF levels on DIV4 for 2D substrates with respect to 3D membranes (Figure 6.13). At DIV8 these values increased for 3D PAN HF membranes reaching values of 5.7 ± 0.7 pg/milioncell, while BDNF values decreased for the other substrates. On both 2D and 3D PAN membranes, cells exhibited significantly high level of BDNF on DIV12 especially in the case of 3D PAN HF substrate where an evident peak of BDNF secretion resulted to be greater (+55%) with respect to that measured on DIV8. Overall these metabolic activities demonstrated that neuronal cells were viable and functionally active for all investigated membranes. Particularly at DIV12, metabolic cellular activities detected for 3D PAN HF membranes were higher than those reached for all other substrates independent of 2D or 3D configuration. These results tend to underlie the ability of 3D PAN HF membranes to assure both neuronal viability and functional activities at least for a 12 days culture period.

### 6.3.4 MAP2 and GluR2 mRNA expression

The morphological and metabolic hippocampal cellular properties were correlated with the transcriptional capacities of some of their developmental markers, such as MAP2

and GluR2. First of all, a single PCR product with the desired length was observed for target genes (MAP2 and GluR2) and the reference β-actin, while no band was observed in the negative control samples without RT (data not shown). The sequencing of these PCR products permitted us to obtain, for the first time, a partial coding sequence of the putative MAP2 (GU586150), GluR2 (GU586153) and β-actin (GU586151) in *Mesocricetus auratus* showing a high nucleotidic identity (>85%) to the corresponding sequence of other rodents such as *Rattus norvegicus* and *Mus musculus* [27-28]. However, in order to evaluate potential expression differences of the two target genes between the different membranes at DIV8 and DIV12, it was necessary to determine the PCR efficiency and linearity of template amplification via the optimization of standard curves for MAP2 and GluR2 plus for β-actin. PCR amplification efficiency for each primer pairs was calculated on the basis of the slope of the standard curve, which in most cases, was close to –3.4, indicating maximal PCR amplification efficiency with a highly correlation coefficient of amplification accuracy being within the range of 0.990 to 0.998. After the standardization of qPCR parameters, these optimal conditions were used to assess expression differences of MAP2 and GluR2, which are known to be tightly correlated to hippocampal cytoskeleton and synaptic formations, respectively. In a first result, a consistent expression of MAP2 was reported for neurons grown on 2D and 3D PAN membranes as well as for PSCD substrates that resulted to be greatly ($p<0.01$) increased at DIV8 with respect to the other substrate (PEEK-WC) (Figure 6.14a). At a later developmental stage (DIV12) both 3D PAN HF membranes and PSCD substrate resulted to be suitable for long-term *in vitro* growth, as shown by not only great MAP2 expression levels with respect to 2D and 3D PEEK-WC membranes, but also for a moderate ($p<0.05$) increase of this cytoskeletal factor with respect to neurons plated on 2D PAN membranes (Figure 6.14b). As far as the expression of GluR2, it was interesting to note that also in this case 3D PAN HF resulted to be the better substrate allowing neurons commence the formation of a dendritic complex network at DIV8, in a comparable manner to PSCD substrate. The expression of GluR2 for these two substrates resulted to be greatly enhanced when compared with 2D and 3D PEEKWC, while a moderate increase was observed with respect to 2D PAN (Figure 6.15a). At DIV12, when the synaptic complexity and dendritic arborization are completed, 3D PAN and 2D PAN continued to maintain a moderate GluR2 expression

level with respect to the other substrates in both flat and HF configuration and this appeared to occur in a similar manner to that of PSCD substrate that showed a moderate increase with respect to both 2D and 3D PEEK-WC membranes (Figure 6.15b).

## 4. DISCUSSION

The present work focused on the development of novel biomaterials in a different configuration as a potential tool for studying neuronal cell behavior. The *in vitro* investigation of hippocampal neuronal network reconstruction was carried out on a 2D membrane system with respect to that of a 3D. In particular, these two systems were evaluated in terms of outgrowth and polarization of axonal and dendritic processes as well as in terms of metabolic activity in order to better characterize the type of membrane that could be proposed for neuronal tissue engineering approaches. For these purposes, polymeric membrane structures and physical-chemical properties must be carefully considered for the designing of both 2D and 3D culture systems. In our study 2D and 3D membranes, prepared from two different polymers PAN and PEEK-WC exhibited different morphological, physical-chemical and transport properties and were modified by coating with PLL in order to enhance cell-adhesion as well as assuring comparable functional groups interacting with the cells. Since it has been well established that both surface and transport properties of membranes play an important role on neuronal regeneration [6-29-30-31], it was necessary to determine the changes of membrane properties after PLL-coating. Indeed, the advancing and receding contact angles, which are respectively a measure of the apolar and polar domains of the surface, displayed the different wettability of the native membranes and demonstrated the significant changes of this feature after PLL-coating. In particular, PLL surface modification minimized their native different physical-chemical properties, since the hysteresis, which represents the difference between advancing and receding contact angle, is maintained after PLL coating even if it results in a reduction, probably due to the morphological heterogeneity and to the different orientation of chemical groups on the membrane surface. Moreover, the membranes exhibited different permeability properties, which are important for membrane transport systems. Indeed, the hydraulic permanence measurements demonstrated that PAN HFs were more permeable with respect to PEEK-WC HF and this result is in a good agreement with their more

hydrophilic and porous character as. Interestingly, PLL coating strongly reduced the hydraulic permanence for PEEK-WC HF membranes while for PAN HF membranes this decrease was not appreciable.

Surprisingly this study reports, for the first time, new evidences on neuronal morphology, axonal outgrowth and metabolic activity of hippocampal neurons cultured on membranes in 2D and 3D configurations. It is well known that a good biomaterial for an *in vitro* study of neuronal survival and developmental properties permits the adequate condition for normal neuronal differentiation and outgrowth [32]. In this context, we demonstrated that both 2D and 3D membranes supported the adhesion and growth of hippocampal neurons enhancing neuronal differentiation and neurites alignment. At DIV8, cells grown on all substrates displayed long neurite processes outgrowth with numerous branches reaching a well-defined shape typical of the hippocampal neurons. This feature resulted to be important for *in vivo* studies due to their highly remarkable synaptic plasticity capacity, which proves to be essential for the induction of some key hippocampal neurophysiological functions such as memory and learning [33]. As demonstrated by SEM images and confirmed by quantitative analysis of the heavily covered cellular areas, at a later developmental stage (DIV12), neurons seeded on the different membranes formed a more complex neuronal network than that observed at DIV8. This evidence is confirmed by more extensive branching of the outgrowing neuritis, which are in line with the results reported for other biohybrid systems such as micro-patterned biodegradable poly(L-lactic acid) membranes [34]. Furthermore, a dense array of neurons connected to each other via their neuritis was observed along the HF membranes producing a 3D structure. The morphometric analysis displayed that at DIV12 neurons grown on the 3D PAN HF membranes adhered to a very high extend compared to the other substrates, reaching the 77% of coverage on the total membrane area.

It is noteworthy that the distribution of specific structural markers GAP-43 and βIII tubulin showed cell features along with the organization of neuronal network on membranes varied with the different configurations. As already pointed out both GAP-43, which is an axonal protein involved with neuronal outgrowth and synaptic plasticity of developing and regenerating neurons [35] and βIII tubulin, a cytoskeletal protein typical of the soma and neuronal processes [36] were expressed in a differential manner.

In particular, the expression of GAP43 increased during axonal development, so that the wide distribution of this structural protein on 3D PAN HF membrane suggests how this specific substrate is able to enhance the formation and arborization of neuronal processes especially in a 3D structure (Figure 6.8h). Indeed the neuronal network was highly complex with a lot of neuron-to-neuron connections and this represents a very important result since neuronal networks produced in cell cultures provide a great potential for investigation of synapse formation, development, and function [37- 38]. In addition the differences of cell behavior between 2D and 3D membranes were confirmed by the quantitative analysis of neuronal marker fluorescence intensity and axonal length. Moreover, MAP2 and GluR2 qPCR expression analysis and metabolic activity measurements further corroborate the suitability of 3D configuration for a long-term survival and differentiation of hippocampal neurons. The quantitative analysis of GAP-43 fluorescence intensity clearly indicated that the high levels of axonal outgrowth preferred 3D PAN HF membranes for both DIV8 and DIV12 cultures, which may turn out to be an essential factor for regulating interaction properties with other signaling proteins and for the dynamic assembly of synaptic membranes [39]. According to these morphometric data, DIV8 neurons cultured on 3D PAN HF membranes exhibited very extensive axons in comparison to those adhered on the other membranes, reaching the highest value on 3D PAN HF membranes at DIV12, similar to those obtained on 2D PAN membranes.

The ability of 3D PAN HF membranes to support and promote neuronal network was also confirmed and substantiated by the expression pattern of MAP2 and GluR2 genes which are, respectively, dendritic [40] and synaptic [41] markers of hippocampal neurons. MAP2 is the major microtubule associated protein of brain tissue which promotes microtubule assembly and forms side-arms on microtubules [42] and its expression during development is considered as a specific marker of neuronal cytoskeletal integrity [43]. In the case of the other developmental marker, e.g. GluR2, it represents a major receptor subunit involved with silent synaptic activation, the formation of hippocampal extrasynaptic spines and dendritic elongating processes [39-44]. The results of qPCR analysis provided strong evidence of both cytoskeletal integrity and synaptic activation in hippocampal neurons at different developmental stages on both 2D and 3D investigated membranes. The more consistent expression of

MAP2 and GluR2 genes was obtained for 3D PAN HF membranes, especially at DIV12, when the dendritic arborization and synaptic complexity were completed, suggesting that such a substrate resulted to be the more suitable for the realization of well-developed neuronal network resembling *in vivo* hippocampal neuronal properties as already shown for hamster neurons grown on other culture systems [6-34- 39]**.**

In line with this trend, the metabolic activities investigated in terms of glucose consumption, lactate production and BDNF secretion demonstrated that all the membranes used for the culture of neuronal cells supported the long-term maintenance of vital cell functions. Also in this case, the 3D PAN HF membranes continued to show the ideal growth culture conditions guaranteeing good levels of metabolic features. It is worthy to note that BDNF secretion is a critical factor for neuron integrity, since this neurotrophin is essential for neuronal survival and differentiation during development [45] and for synaptic function and plasticity in the mature brain [46]. As a consequence, the high values of BDNF secretion obtained in our experiments further confirm the viability and the differentiation of hippocampal neurons cultured in our 3D membrane systems. Previous reports have shown that BDNF may act on both presynaptic and postsynaptic cells [47] demonstrating that this neurotrophin is distributed not only along dendrites and therefore located postsynaptically but also presynaptically along the axon, where it induces the delivery of GluR2-containing AMPAR to the synapses [48]. Recently, Geremia et al. found that the immunoneutralization of BDNF resulted in a down-regulation of GAP-43 and Tα1-tubulin mRNA expression in both intact and injured sensory neurons and consequently a decrease of the intrinsic ability of these neurons to extend *in vitro* neurites [49], demonstrating that the endogenous BDNF plays a role on induction of the regenerative response. In accordance to these authors our findings suggest a correlation between BDNF secretion, axon length and GAP-43 expression. Indeed, the highest BDNF secretion (Figure 6.13) as well as the greatest axonal length (Figure 6.10), GAP-43 intensity (Figure 6.9b) and GluR2 expression (Figure 6.14) were all detected on 3D PAN HF membranes.

## 6.5 CONCLUSIONS

Overall in the present study, the performances of hippocampal neuronal processes grown on different 2D and 3D polymeric membranes permitted us to evaluate

biocompatible membrane systems with the intention of supplying optimal conditions for the creation of a biomimetic microenvironment for neural tissue engineering. The obtained data suggest that all investigated membranes may be useful biomaterials for the *in vitro* reconstruction of neuronal network and confirm that the relationship between the structure of the polymeric membranes and cell features, which is one of the major issue in biomaterial science and engineering. In this particular case, our study provided a complete 3D neural tissue-like structure assembled *in vitro* using primary hippocampal cells and PAN HF membranes. In particular, we assume that the better neuronal outgrowth on 3D PAN HF membranes is specifically due to its intrinsic geometry and the higher hydraulic permanence that enhance the mass transfer of nutrients and metabolites to the cells and the removal of catabolites. As a consequence, this advanced model system could allow the mimicking of hippocampal neuronal events in order to study natural neurobiological properties of these cells, such as memory and learning processes, or induction of disease pathologies allowing testing of new therapies on the resolution of these states.

## Figures

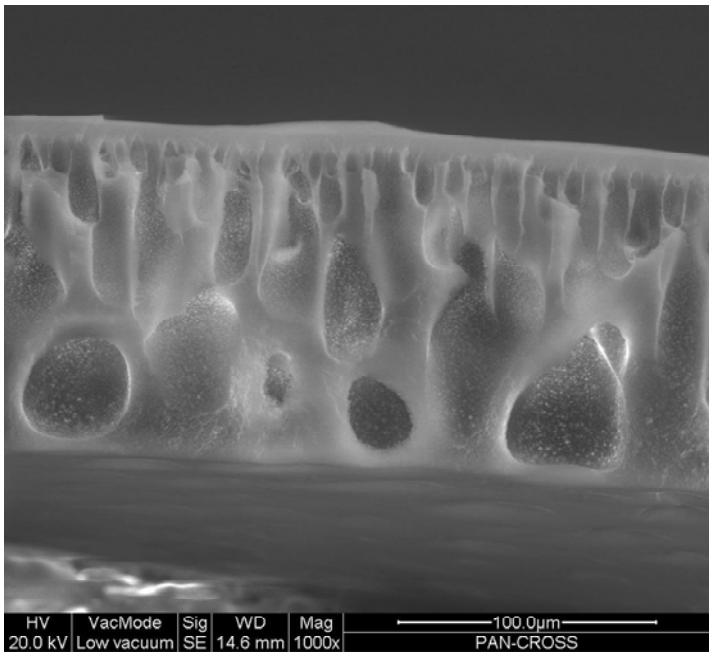


(a)

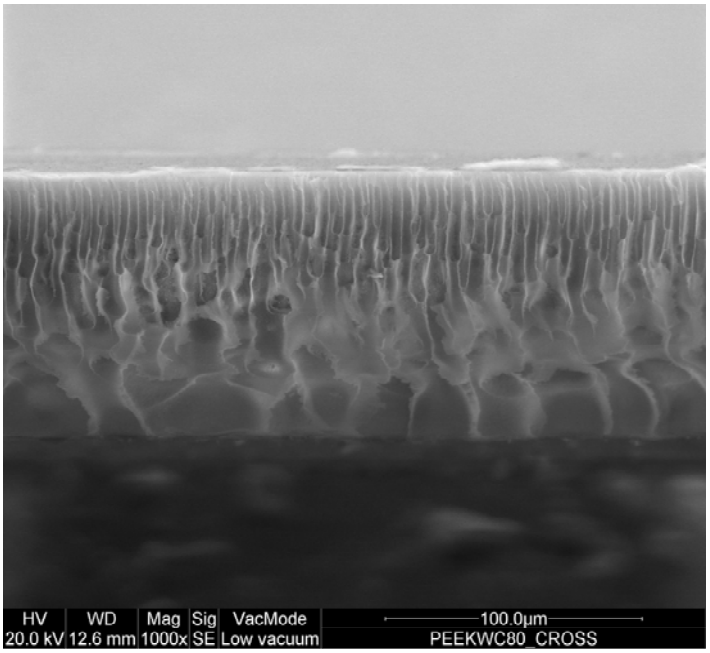


(b)

**Figure 6.1** SEM's images of the cross section of (a) 2D PAN and (b) 2D PEEK-WC membranes.

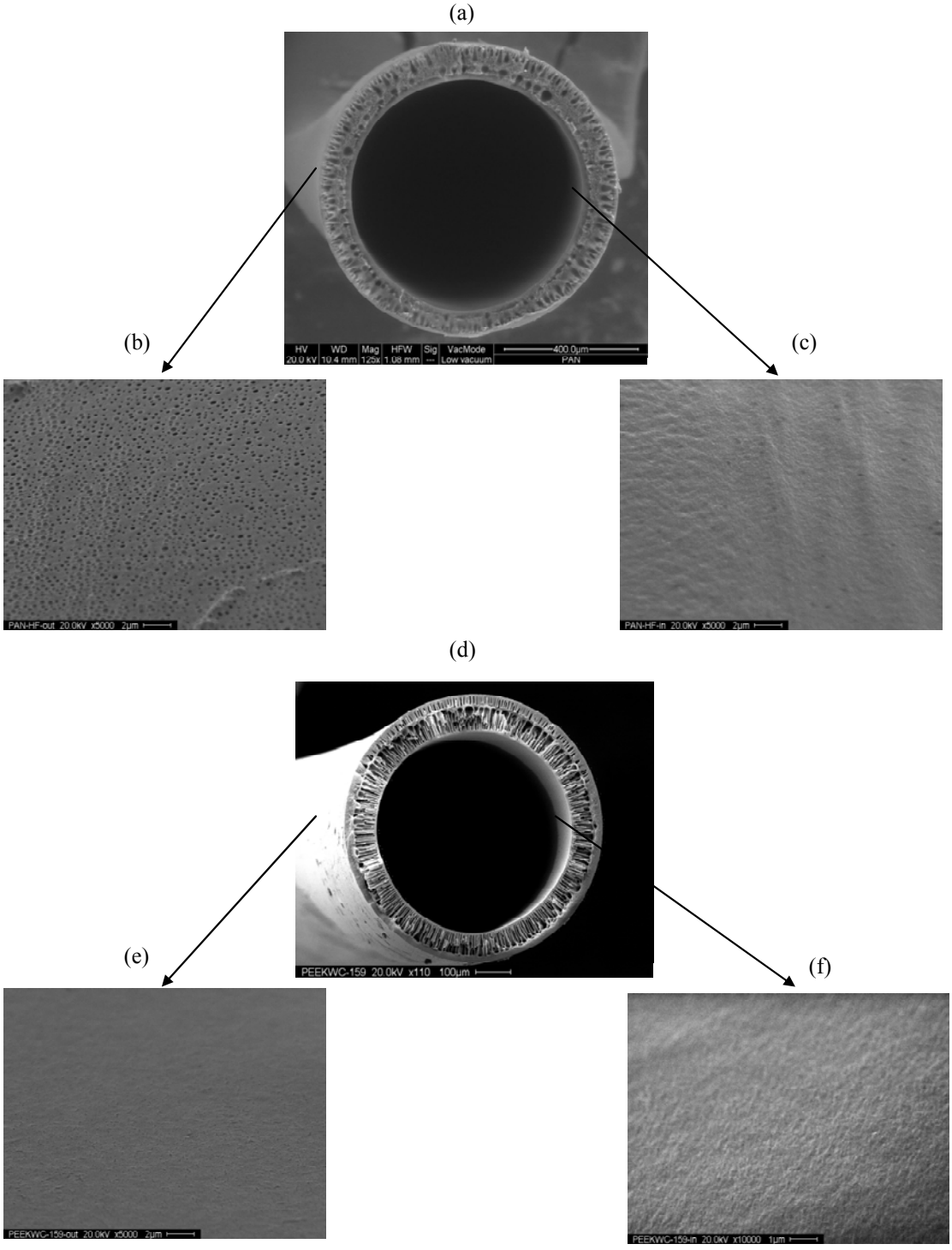


**Figure 6.2** SEM's images of the cross section of (a) 3D PAN HF and (d) 3D PEEKWCHHF membranes: (b) outer and (c) inner surface of 3D PAN HF, (e) outer and (f) inner surface of 3D PEEKWC HF membranes.

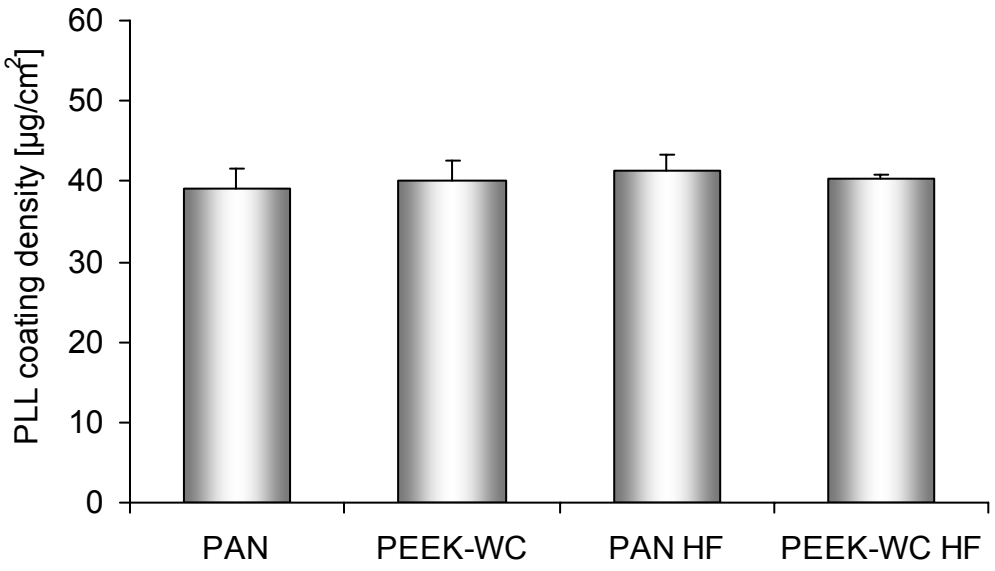


**Figure 6.3** Poly-l-lysine (PLL) density measured on the different substrates after coating with FITC labeled PLL. Data were expressed as $\mu g/cm^2 \pm$ S.E.M

**a)**

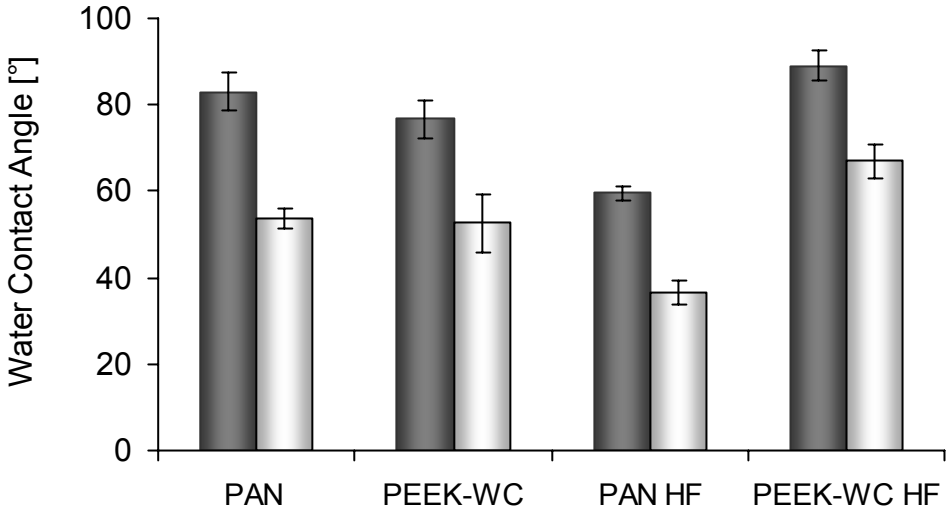


b)

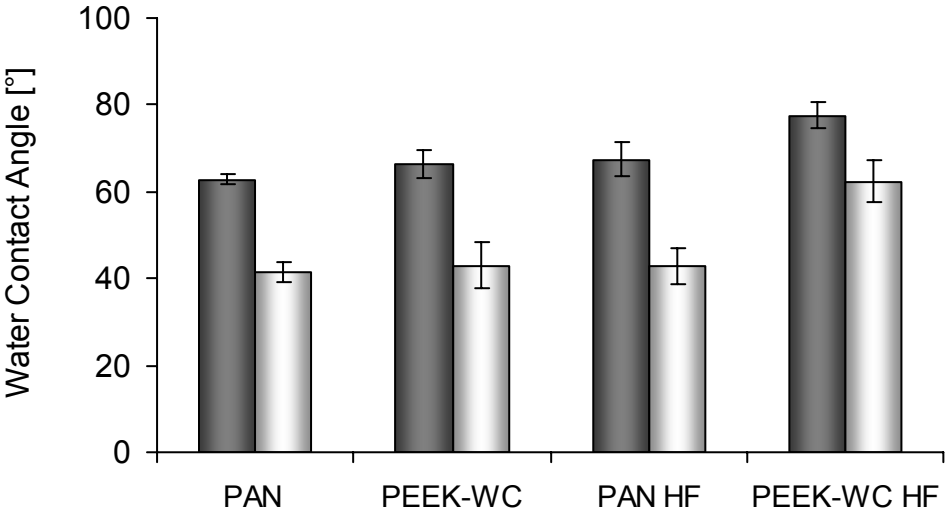


**Figure 6.4** Advancing (full bar) and receding (empty bar) contact angle measured on: (a) native membranes and (b) PLL-coated membranes.

**a)**

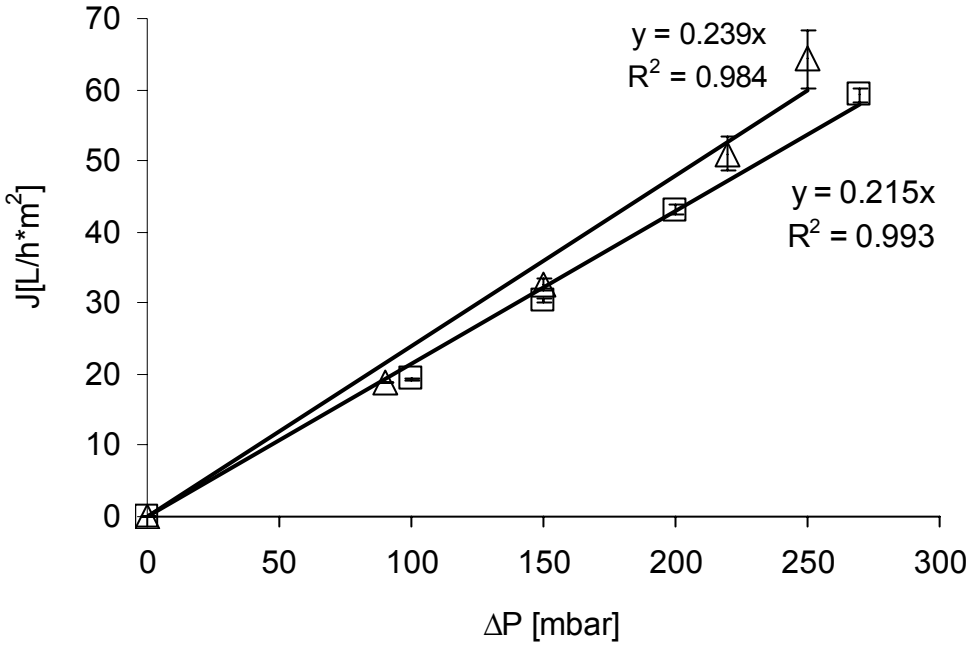


**b)**

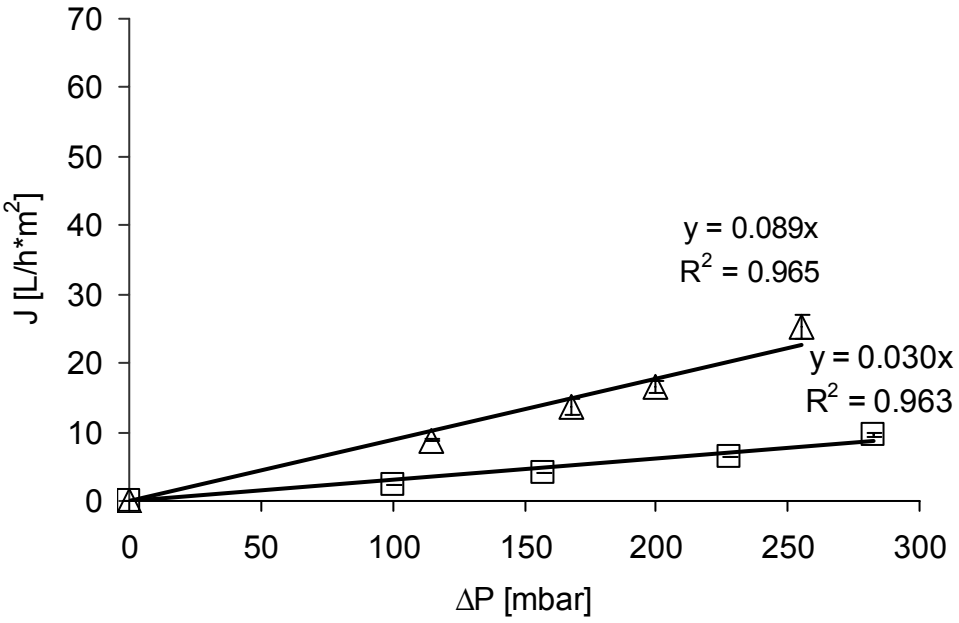


**Figure 6.5** Hydraulic permeation measurements of (a) 3D PAN HF and (b) 3D PEEKWC HF membranes: (Δ) native membranes, (□) PLL-coated membranes. Experimental values (symbols) represent the average of 10 measurements. The interpolation of experimental data is reported as a solid line.

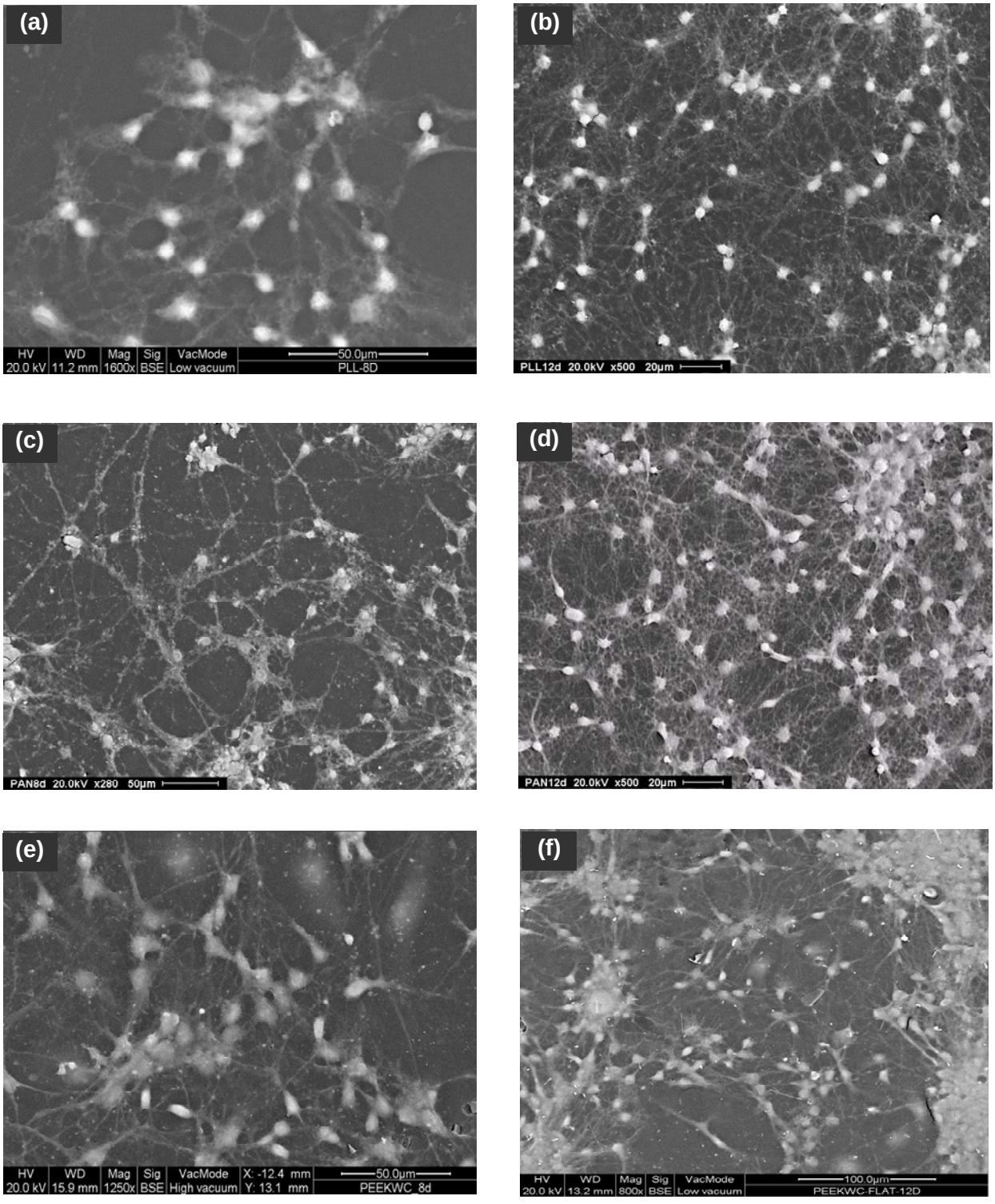
(a)
HV 20.0 kV | WD 11.2 mm | Mag 1600x | Sig BSE | VacMode Low vacuum
50.0µm
PLL-8D
(b)
PLL12d 20.0kV x500 20µm
(c)
PAN8d 20.0kV x280 50µm
(d)
PAN12d 20.0kV x500 20µm
(e)
HV 20.0 kV | WD 15.9 mm | Mag 1250x | Sig BSE | VacMode High vacuum | X: -12.4 mm Y: 13.1 mm
50.0µm
PEEKWC_8d
(f)
HV 20.0 kV | WD 13.2 mm | Mag 800x | Sig BSE | VacMode Low vacuum
100.0µm
PEEKWC-FLAT-12D

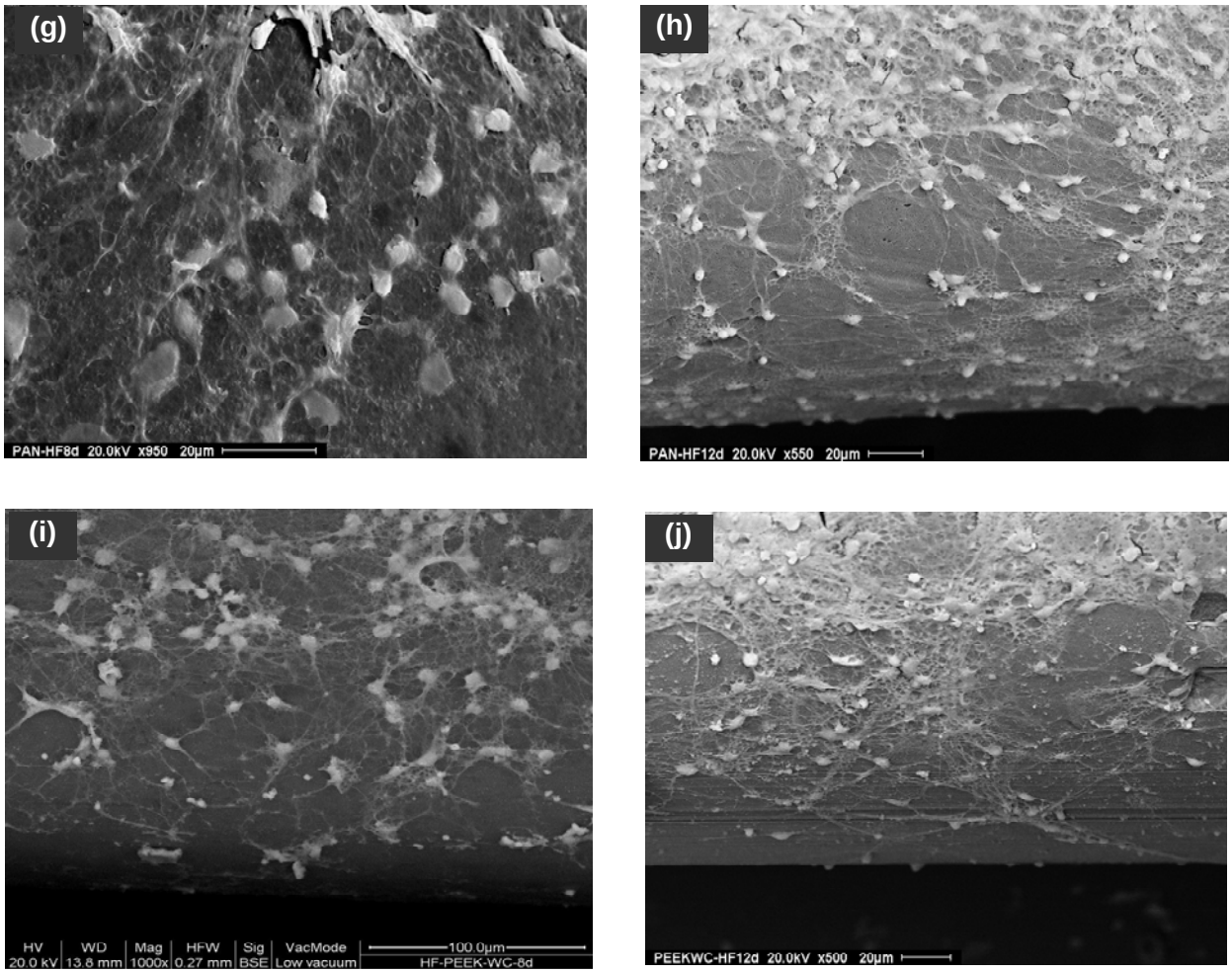


**Figure 6.6** SEM's images of hippocampal neurons at DIV8 (a, c, e, g and i) and DIV12 (b, d, f, h and j) on: (a and b) PSCD, (c and d) 2D PAN, (e and f) 2D PEEKWC, (g and h) 3D PAN HF and (i–j) 3D PEEKWC HF membranes.

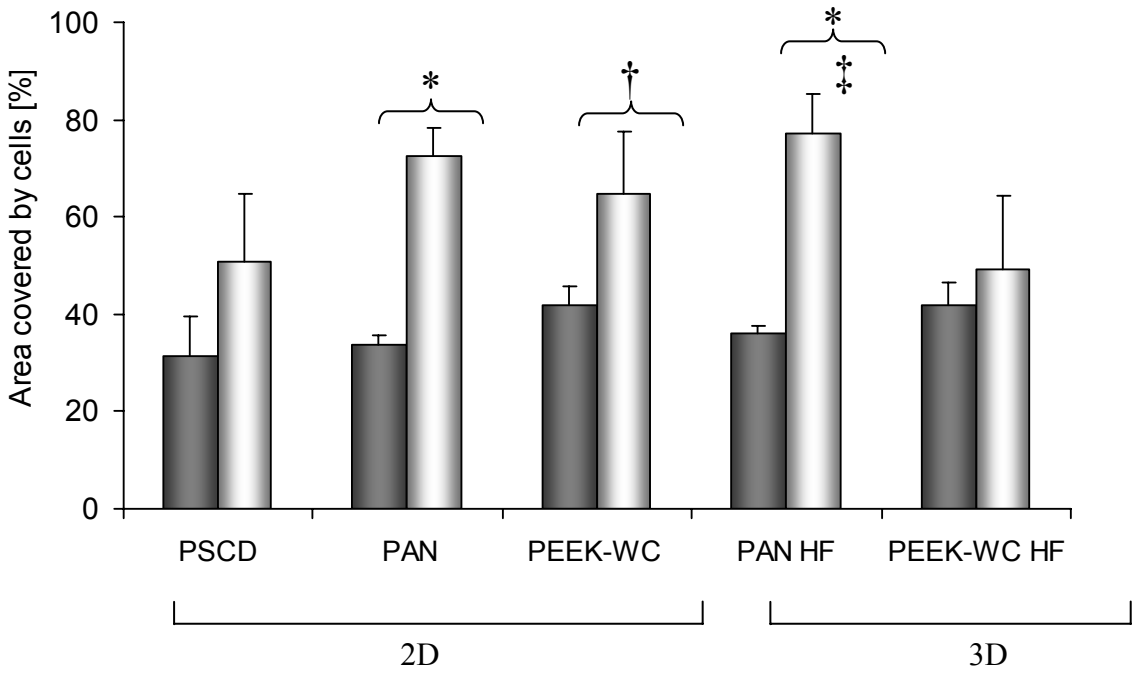


**Figure 6.7** Percentage of the area covered by hippocampal neurons at DIV8 (full bar) and DIV12 (empty bar) on the different membranes. The data were expressed as an average ± standard deviation and evaluated according to ANOVA followed by Bonferroni *t*-test. ‡$p < 0.05$ vs PEEK-WC HF and PSCD at DIV 12. Data statistically significant according to Student's t-test: *$p<0.001$; †$p<0.05$.

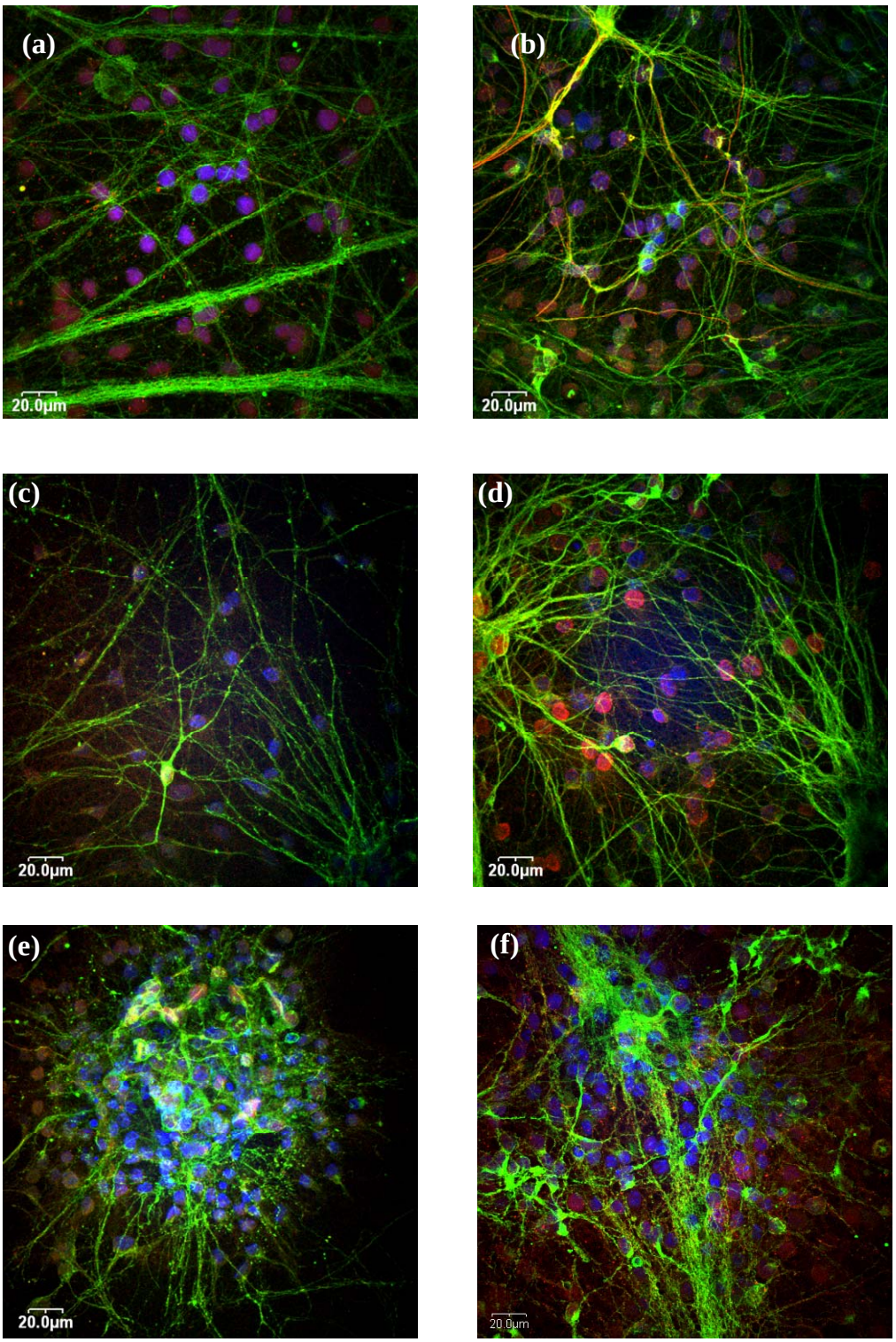
(a)
20.0µm
(b)
20.0µm
(c)
20.0µm
(d)
20.0µm
(e)
20.0µm
(f)
20.0µm

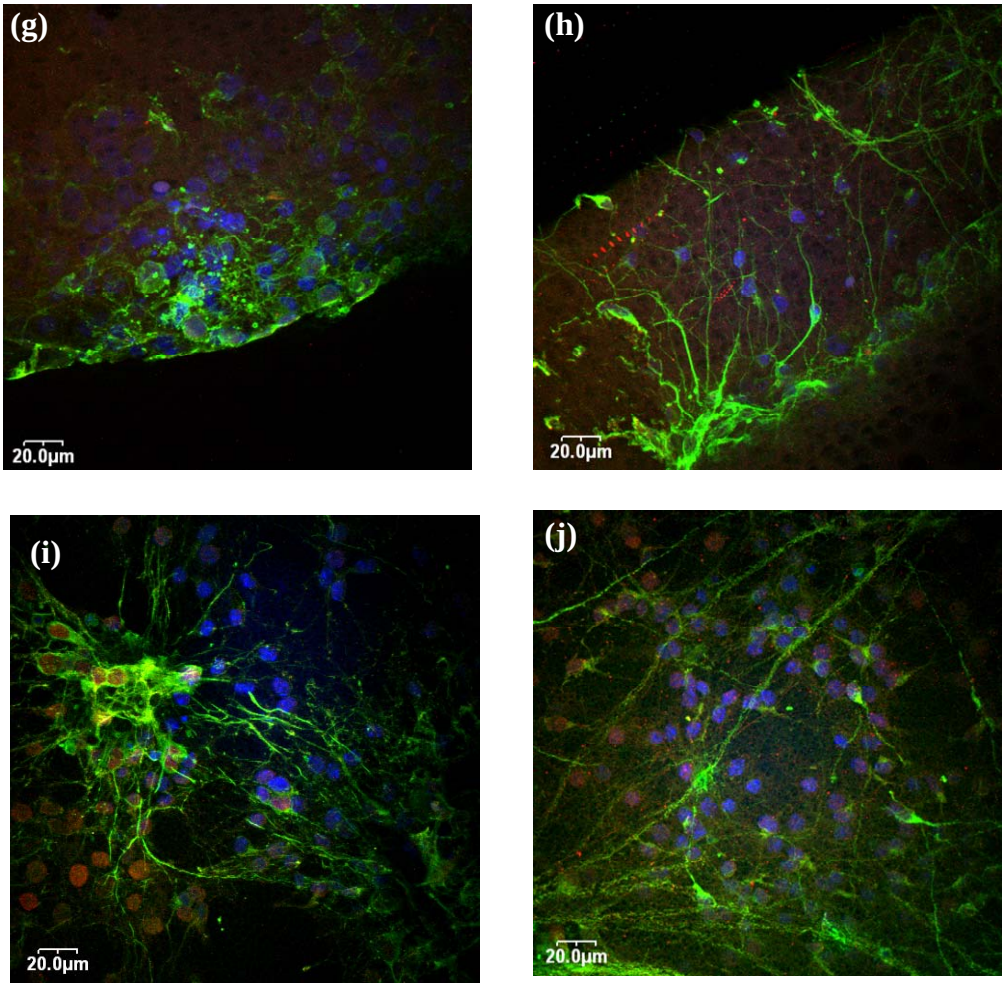


**Figure 6.8** Confocal laser micrographs of representative hippocampal neurons traced during the entire culture period at DIV8 (a, c, e, g and i) and DIV12 (b, d, f, h and j) on: (a and b) PSCD, (c and d) 2D PAN, (e and f) 2D PEEK-WC, (g and h) 3D PAN HF and (i–j) 3D PEEK-WC HF membranes. Cells were stained with βIII-tubulin (green), axonal marker GAP-43 (red) and nuclei (blue).

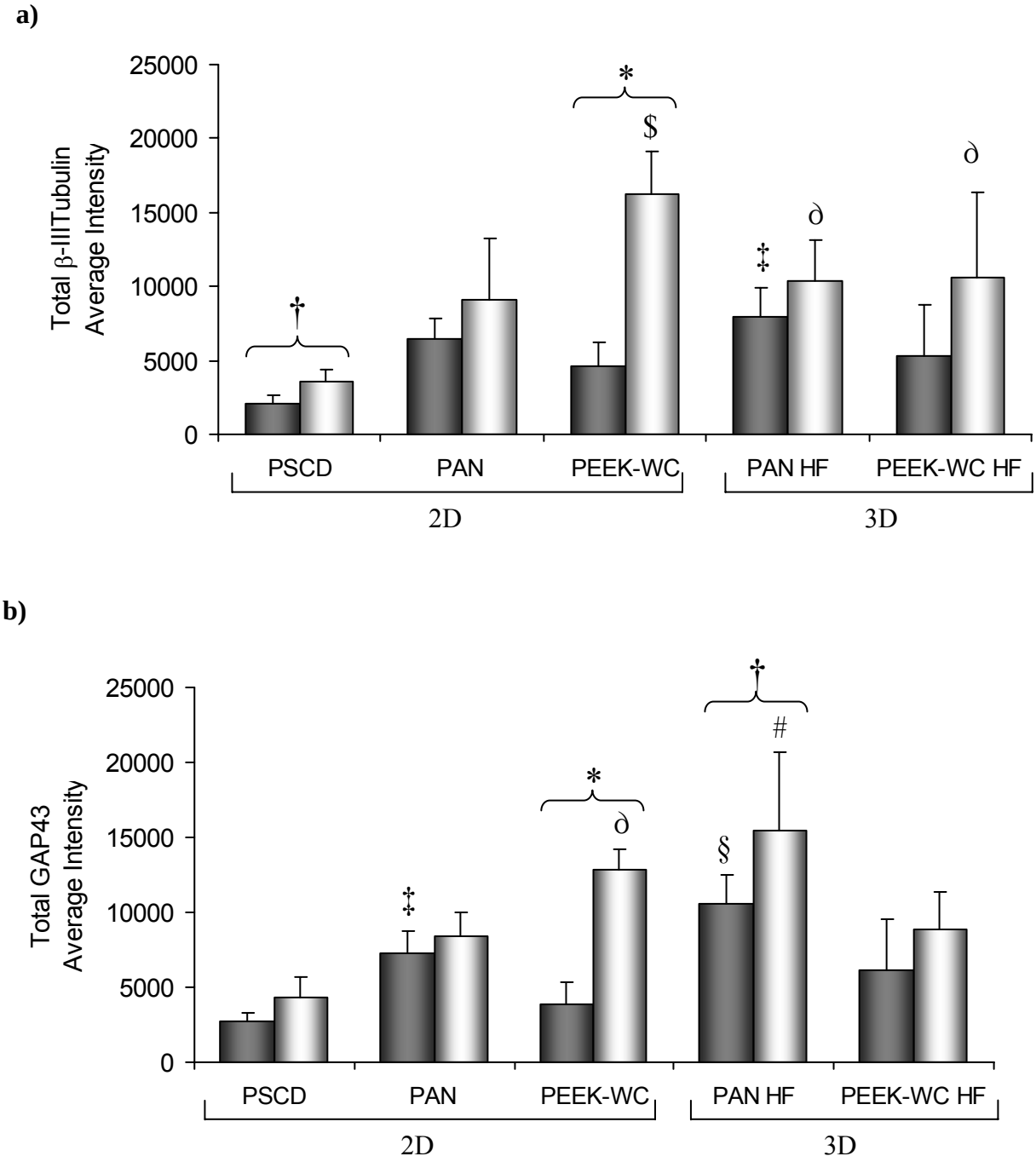


**Figure 6.9** Fluorescence average intensity for stained βIII-tubulin (a) and GAP43 (b) of hippocampal neurons at DIV8 (full bar) and DIV12 (empty bar) on the different membranes. Data statistically significant according to ANOVA followed Bonferroni and t-test. ‡$p < 0.05$ vs PSCD at DIV8; \$$p<0.05$ vs PSCD at DIV 12 and PAN at DIV12; ∂$p<0.05$ vs PSCD at DIV12; §$p<0.05$ vs PSCD at DIV8, PAN at DIV 8 and PEEK-WC HF at DIV8; #$p<0.05$ vs PSCD, PAN and PEEK-WC HF at DIV 12. Data statistically significant according to Student's t-test: †$p<0.05$ vs the same substrate at DIV8; *$p<0.001$ vs the same substrate at DIV8.

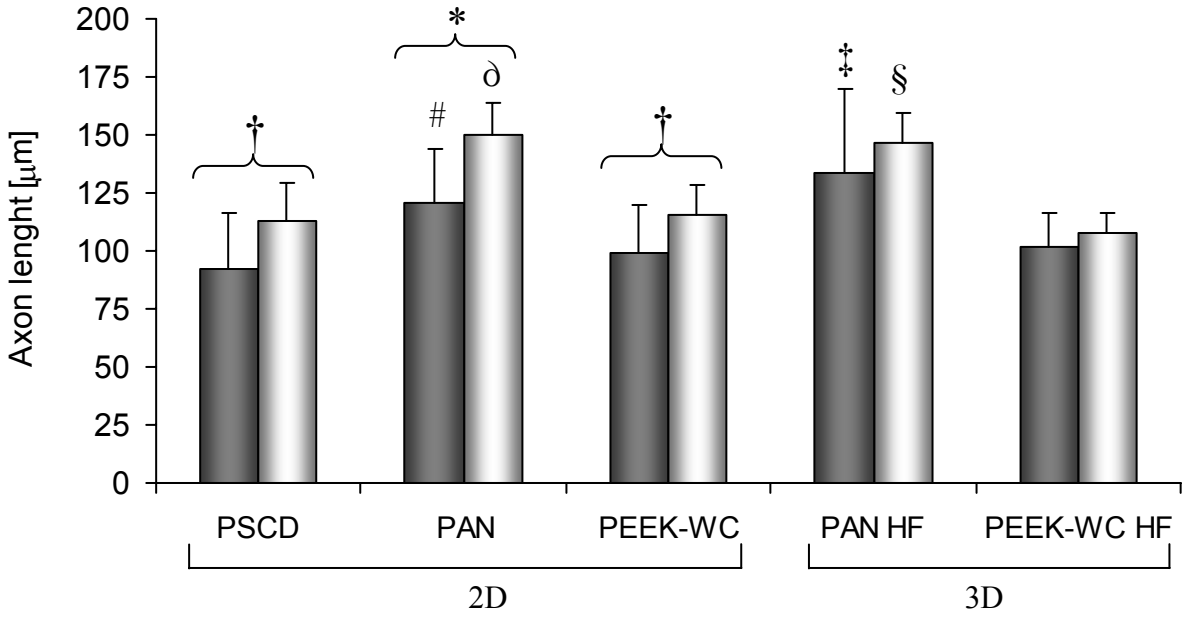


**Figure 6.10** Axon length of hippocampal neurons at DIV8 (full bar) and DIV12 (empty bar) for the different membranes. The values were expressed as average ± standard deviation. Data statistically significant according to ANOVA followed Bonferroni t-test and T-Student's test. ‡p < 0.05 vs PSCD, PEEK-WC and PEEK-WC HF at DIV8; #p<0.05 vs PSCD at DIV8; ðp<0.05 vs PSCD at DIV12, PEEK-WC DIV12 and PEEK-WC HF at DIV12; § p<0.05 vs PSCD, PEEK-WC and PEEK-WC HF at DIV 12; †p<0.05 vs the same substrate at DIV8. Data statistically significant according to Student's t-test: *p<0.001 vs the same substrate at DIV8.

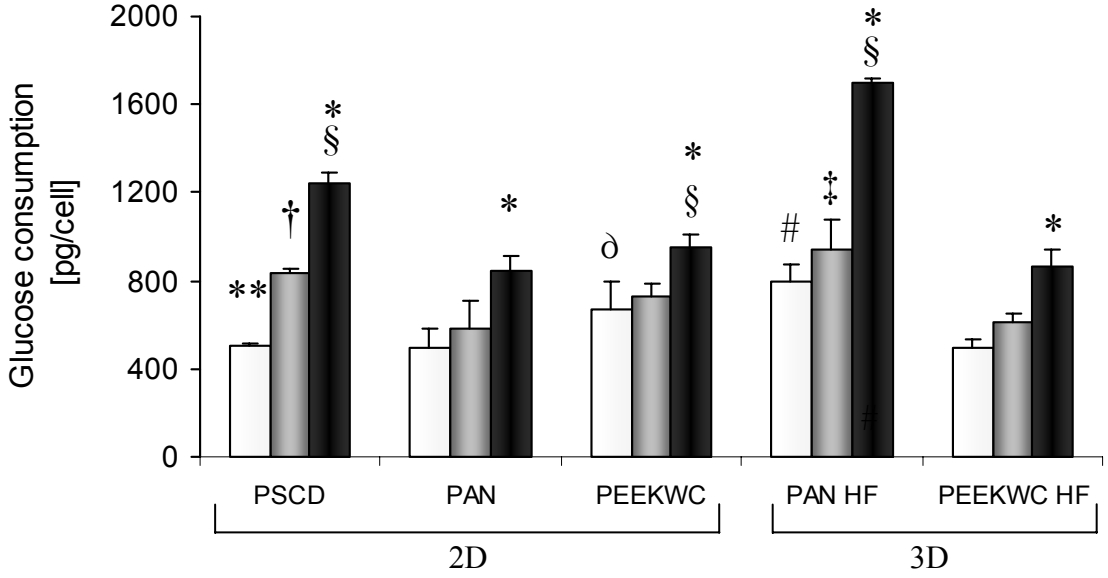


**Figure 6.11** Glucose consumption of hippocampal neurons at DIV4 (white bar), DIV8 (grey bar) and DIV12 (black bar) for the different membranes. The values expressed as average ± standard deviation are the mean of 6 experiments and evaluated according to ANOVA followed by Bonferroni *t*-test. #p<0.05 vs PSCD, PAN and PEEK-WC HF at DIV4; ðp<0.05 vs PAN at DIV4; †p < 0.05 vs PAN and PEEK-WC HF at DIV8; ‡p < 0.05 vs PAN, PEEK-WC and PEEK-WC HF at DIV8; §p<0.05 vs PAN at DIV12; *p<0.05 vs the same substrate at DIV4 and DIV8; **p<0.05 vs the same substrate at DIV4.

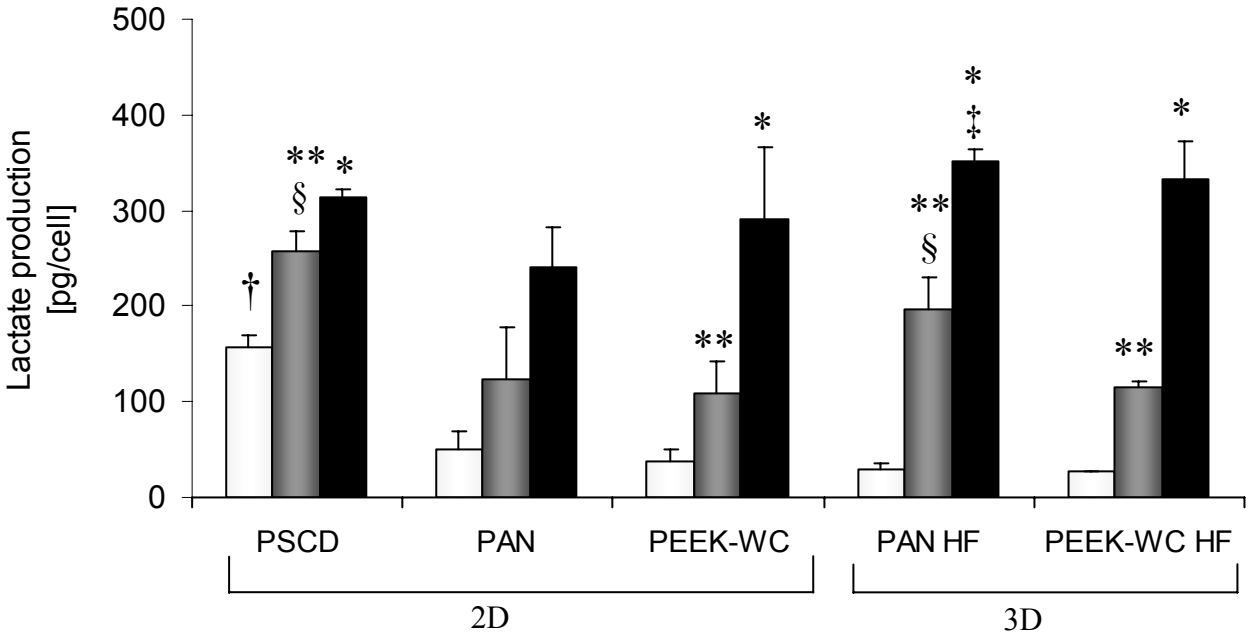


**Figure 6.12** Lactate production of hippocampal neurons at DIV4 (white bar), DIV8 (grey bar) and DIV12 (black bar) for the different membranes. The values expressed as average ± standard deviation are the mean of 6 experiments and evaluated according to ANOVA followed by Bonferroni *t*-test. †$p < 0.05$ vs PAN, PAN HF, PEEK-WC and PEEK-WC HF at DIV4; §$p<0.05$ vs PAN, PEEK-WC, PEEK-WC HF at DIV8; §$p<0.05$ vs PEEK-WC at DIV8; ‡$p < 0.05$ vs PAN at DIV12; *$p<0.05$ vs the same substrate at DIV4 and DIV8; **$p<0.05$ vs the same substrate at DIV4.

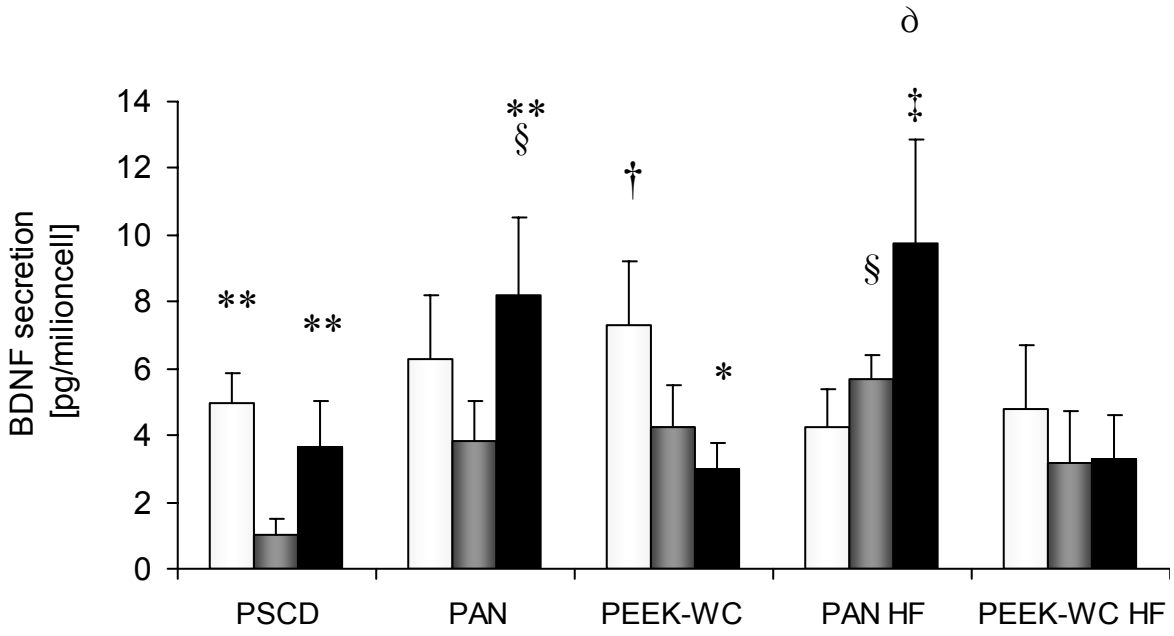


**Figure 6.13** BDNF secretion of hippocampal neurons at DIV4 (white bar), DIV8 (grey bar) and DIV12 (black bar) for the different membranes. The values expressed as average ± standard deviation are the mean of 6 experiments and evaluated according to ANOVA followed by Bonferroni *t*-test. †p <0.05 vs PAN HF at DIV4; §p<0.05 vs PSCD and PEEK-WC HF at DIV8; §p<0.05 vs PSCD, PEEK-WC and PEEK-WC HF at DIV 12; ‡p < 0.05 vs PSCD, PEEK-WC and PEEK-WC HF at DIV12; *p<0.05 vs the same substrate at DIV8 and DIV12; **p<0.05 vs the same substrate at DIV8; ∂p<0.05 vs the same substrate at DIV12.

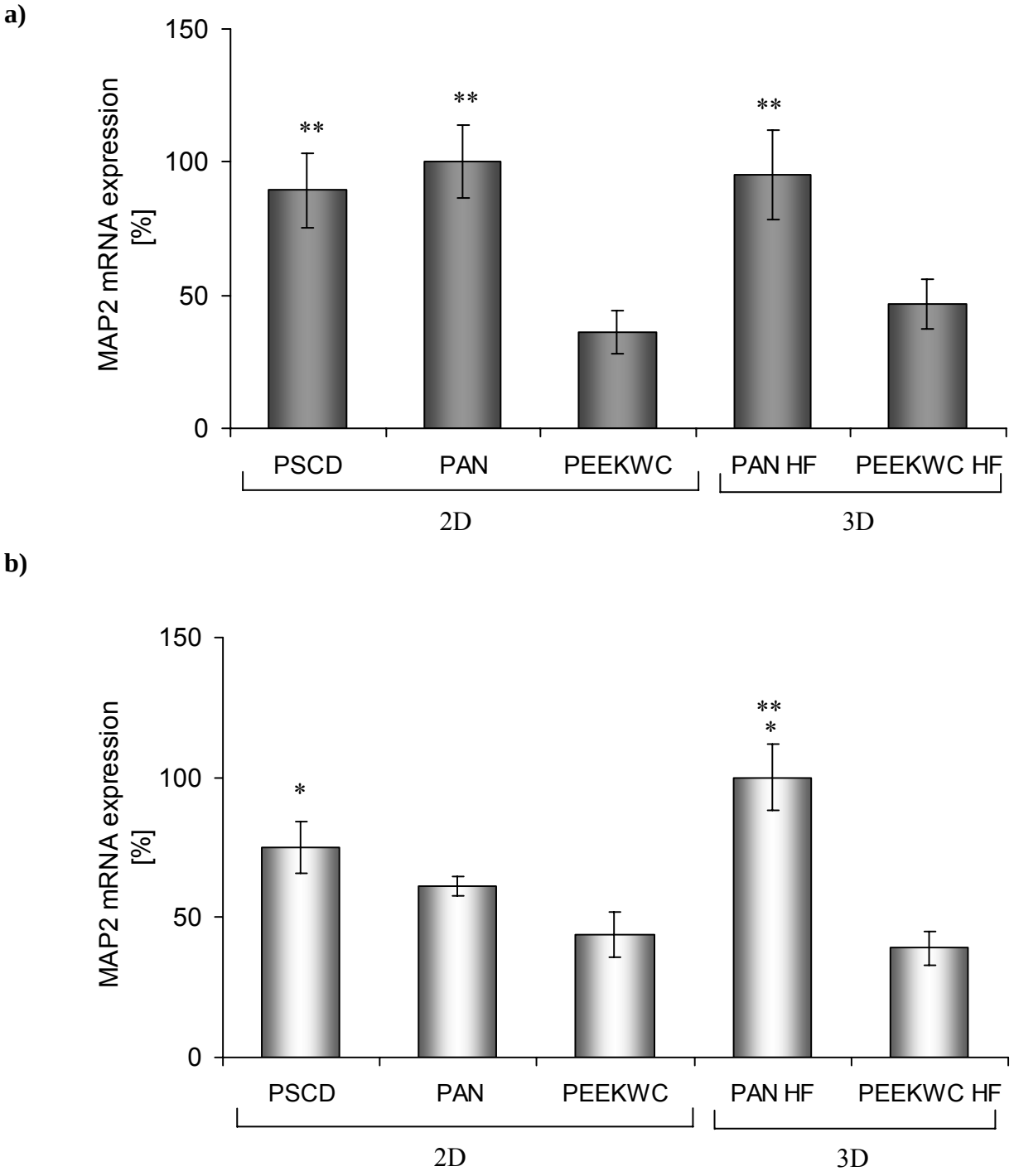


**Figure 6.14** MAP2 mRNA expression of hippocampal neurons at DIV8 (a) and DIV 12 (b) for the different membranes. The mRNA levels at A) 8 days and B) 12 days were evaluated in PSCD, PAN, PEEKWC, PAN HF and PEEKWC HF by qPCR. The results are expressed as a proportion of the highest value after normalization with respect to β-actin expression levels and represent the means ± s.e.m. of three independent biological replicates. Data were evaluated by a one-way ANOVA followed by Bonferroni test. a) **$p<0.01$ vs PEEKWC and PEEKWC HF; b) *$p<0.05$ vs PAN, **$p<0.01$ vs PEEKWC and PEEKWC HF.

**a)**

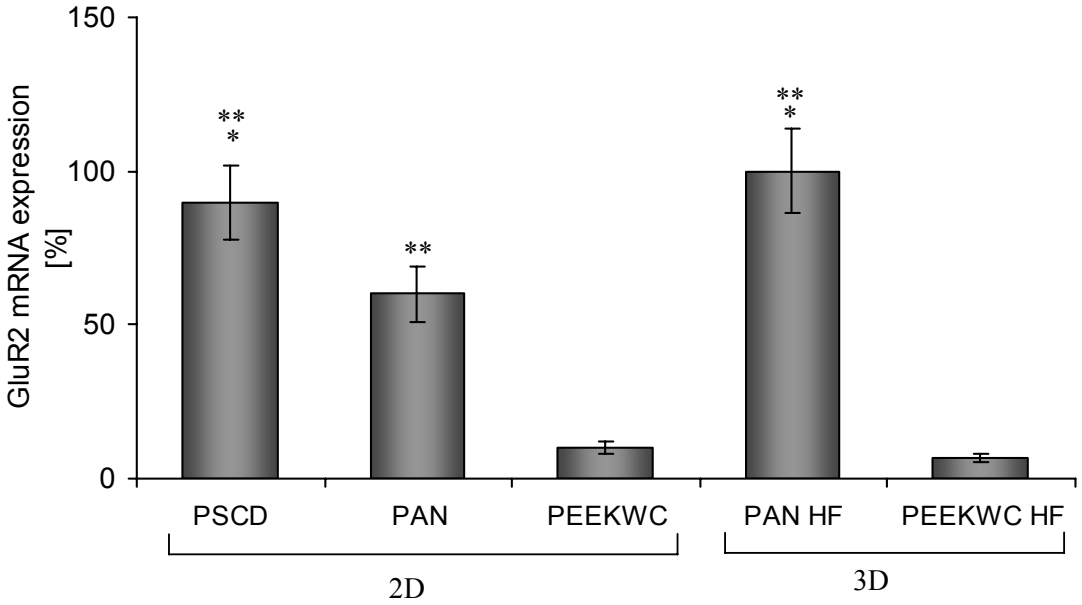


**b)**

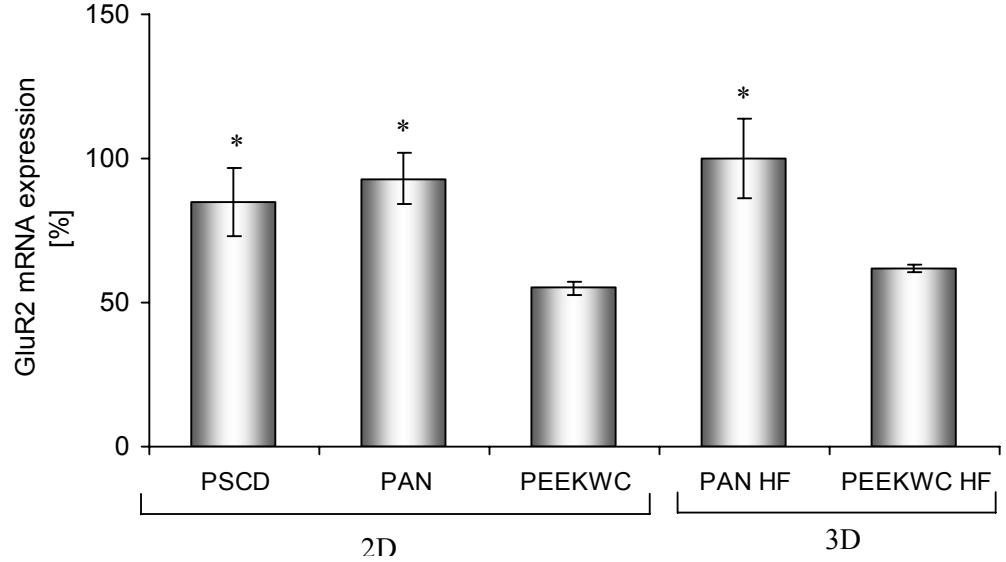


**Figure 6.15** GluR2 mRNA expression of hippocampal neurons at DIV8 (a) and DIV 12 (b) for the different membranes. The mRNA levels at A) 8 days and B) 12 days were evaluated on PSCD, PAN, PEEKWC, PAN HF and PEEKWC HF by qPCR. The results are expressed as a proportion of the highest value after normalization with respect to β-actin expression levels and represent the means ± s.e.m. of three independent biological replicates. Data were evaluated by a one-way ANOVA followed by Bonferroni test. a) *$p<0.05$ vs PAN, **$p<0.01$ vs PEEKWC and PEEKWC HF; b) *$p<0.05$ vs PEEKWC and PEEKWC HF.

**REFERENCES**

[1] Center for Disease Control and Prevention. Online, 2010. Available from URL: http://www.cdc.gov/health/default.html.

[2] Chau CH, Shum DK, Li H, et al. 2004, Chondroitinase ABC enhances axonal regrowth through Schwann cell-seeded guidance channels after spinal cord injury, *FASEB J*, **18**: 194–196

[3 ] Asada Y, Nakamura T, Kawaguchi S. 1998, Peripheral nerve grafts for neural repair of spinal cord injury in neonatal rat: aiming at functional regeneration, *Transplant Pro*, 30: 147– 148.

[4] Patist CM, Mulder MB, Gautier SE, et al. 2004, Freeze-dried poly(D,L-lactic acid) macroporous guidance scaffolds impregnated with brain-derived neurotrophic factor in the transected adult rat thoracic spinal cord, *Biomaterials*, 25: 1569-1576

[5] De Bartolo L, Rende M, Giusi G, et al. 2007, 'Membrane bio-hybrid systems: a valuable tool for the study of neuronal activities' in Evolutionary Molecular Strategies and Plasticity, eds. Canonaco M, Facciolo RM, Research Signpost, Kerala, India; 379-396

[6] De Bartolo L, Rende M, Morelli S, et al. 2008, Influence of membrane surface properties on the growth of neuronal cells isolated form hippocampus, *J Mem Sci,* 325: 139-149

[7] He Q, Zhang T, Yang Y, et al. 2009, In vitro biocompatibility of chitosan-based materials to primary culture of hippocampal neurons, J Mater Sci: Mater Med, 20:1457-1466

[8] Broadhead KW, Biran R, Tresco PA. 2002, Hollow fiber membrane diffusive permeability regulates encapsulated cell line biomass, proliferation, and small molecule release, *Biomaterials,* 23: 4689-4699

[9] Zhang N, Zhang C, Wen XJ. 2005, Fabrication of semipermeable hollow fiber membranes with highly aligned texture for nerve guidance, Biomed Mater Res, 75A: 941-49

[10] Liu VA, Bhatia SN. 2002, Three-dimensional photopatterning of hydrogels containing living cells, Biomed Microdevices, 4: 257–266

[11] Xu T, Molnar P, Gregory C, et al. 2009, Electrophysiological characterization of embryonic hippocampal neurons cultured in a 3D collagen hydrogel, Biomaterials, 30: 4377–4383

[12] O'Connor SM, Andreadis JD, Shaffer KM, et al 2000, Immobilization of neural cells in three-dimensional matrices for biosensor applications, Biosens Bioelectron, 14**:** 871–881.

[13] Frampton JP, Hynd MR, Williams JC, et al. 2007, Three-dimensional hydrogel cultures for modelling changes in tissue impedance around microfabricated neural probes, J Neural Eng, 4: 399–409.

[14] Ju YE, Janmeya PA, McCormick ME, et al. 2007, Enhanced neurite growth from mammalian neurons in three-dimensional salmon fibrin gels, Biomaterials, 28: 2097–2108

[15] Gingras M, Le Beaulieu M-M, Gagnon V, et al. 2008, In vitro study of axonal migration and myelination of motor neurons in a three-dimensional tissue-engineered model, Glia, 56:354–364.

[16] Canonaco M, Madeo M, Alò R, et al. 2005, The histaminergic signaling systems exerts a neuroprotective role against neurodegenerative-induced processes in the hamster, JPET, 315: 188-195.

[17] Dotti GC, Sullivan CA, Banker GA. 1988, The establishment of polarity by hippocampal neurons in culture, J Neurosci, 8: 1454-1468.

[18] Goslin K, Banker G. 1989, Experimental observations on the development of polarity by hippocampal neurons in culture, J Cell Biol, 108: 1507-1516.

[19] Kimmerle K, Strathmann H. 1990, Analysis of the structure-determining process of phase inversion membranes, *Desalination,* 79: 283-302.

[20] Zhang HC, Chen TL, Yuan YG. Synthesis of new type polyether ether ketone with phthalein lateral group. CN Patent No. 85108751; 1987.

[21] Tasselli F, Jansen JC, Sidari F, et al. 2005, Morphology and transport property control of modified poly(ether ether ketone) (PEEKWC) hollow fiber membranes prepared from PEEKWC/PVP blends: influence of the relative humidity in the air gap, Journal of Membrane Science, 255: 13–22.

[22] Mulder M. 1996, 'Transport in membranes' in Basic Principles of membrane technology, eds. Mulder M, Kluwer Academic Publishers, Netherland; 210-279.

[23] Xie C, Markesbery WR, Lovell MA. 2000, Acrolein a product of lipid peroxidation, inhibits glucose and glutamate uptake in primary neuronal cultures, Free Radic Biol Med, 29: 714-720

[24] Ahlemeyer B, Baumgart-Vogt E. 2005, Optimized protocols for the simultaneous preparation of primary neuronal cultures of the neocortex, hippocampus and cerebellum from individual newborn (P0.5) C57Bl/6J mice, J Neurosci Methods, 149: 110-120.

[25] Lekanne Deprez RH, Fijnvandraat AC, Ruijter JM, et al. 2002, Sensitivity and accuracy of quantitative real-time polymerase chain reaction using SYBR green I depends on cDNA synthesis conditions, Analytical Biochemistry, 307: 63-69

[26] Livak KJ, Schmittgen TD. 2001, Analysis of relative gene expression data using real-time quantitative PCR and the $^{2-\Delta\Delta CT}$ method, Methods, 25: 402-408

[27] Zhong H, Sia GM, Sato TR, et al. 2009, Subcellular dynamics of type II PKA in neurons, Neuron, 62: 363-374.

[28] Rainey-Smith SR, Andersson DA, Williams RJ, et al. 2010, Tumour necrosis factor alpha induces rapid reduction in AMPA receptor-mediated calcium entry in motor neurones by increasing cell surface expression of the GluR2 subunit: relevance to neurodegeneration, *J* Neurochem, 113:692-703.

[29] Gomez N, Lu Y, Chen S, et al. 2007, Immobilized nerve growth factor and microtopography have distinct effects on polarization versus axon elongation in hippocampal cells in culture, Biomaterials, 28: 271-284.

[30]Yang F, Murugan R, Wang S, et al. 2005, Electrospinning of nano/micro scale poly(L-lactic acid) aligned fibers and their potential in neural tissue engineering, Biomaterials, 26: 2603-2610.

[31] Li GN, Hoffman-Kim D. 2008, Tissue engineered models of axon guidance, Tissue Eng, 14: 33-51.

[32] Woerly S, Plant GW, Harvey AR.1996, Neural tissue engineering: from polymer to biohybrid organs, Biomaterials, 17: 301-313.

[33] Lo DC. 1995, Neurotrophic factors and synaptic plasticity, Neuron, 15: 979-98.

[34] Morelli S, Salerno S, Piscioneri A, et al. 2010, Influence of micro-patterned PLLA membranes on outgrowth and orientation of hippocampal neuritis, Biomaterials, 31: 7000-7011.

[35] Goslin K, Schreyer DJ, Skene JHP, et al. 1988, Development of neuronal polarity: GAP-43 distinguishes axonal from dendritic growth cones, Nature, 336: 672-674.

[36] Carre´ M, Andre´ N, Carles G, et al. 2002, Tubulin is an inherent component of mitochondrial membranes that interacts with the voltage-dependent anion channel, J Biol Chem, 277: 33664-33669.

[37]Gramowski A, Juugelt K, Weiss DG, et al. 2005, Substance identification by quantitative characterization of oscillatory activity in murine spinal cord networks on microelectrode arrays, Eur J Neurosci, 19: 2815–2825.

[38]van Pelt J, Wolters PS, Corner MA, et al. 2004, Long-term characterization of firing dynamics of spontaneous bursts in cultured neural networks, IEEE Trans Biomed Eng, 51:2051–2062.

[39] Giusi G, Facciolo RM, Rende M, et al. 2009, Distinct α subunits of the $GABA_A$ receptor are responsible for early hippocampal silent neuron-related activities, Hippocampus, 19: 1103-1114.

[40] Huber G, Matus A. 1984, Differences in the cellular distributions of two microtubule-associated proteins, MAP1 and MAP2, in rat brain, J Neurosci, 4:151–160

[41]Medvedev NI, Rodrìguez-Arellano JJ, Popov VI, et al. 2008, The glutamate receptor 2 subunit controls post-synaptic density complexity and spine shape in the dentate gyrus, Eur J Neurosci, 27: 315-325.

[42] Shafit-Zagardo B, Kalcheva N. 1998, Making sense of the multiple MAP-2 transcripts and their role in the neuron, *Mol Neurobiol*, **16**: 149-162

[43] Carrier RL, Maa TO, Obrietan K, et al. 2006, A sensitive and selective assay of neuronal degeneration in cell culture, J Neurosi Meth, 154: 239-244

[44] Grooms SY, Noh KM, Regis R, et al. 2006, Activity bidirectionally regulates AMPA receptor mRNA abundance in dendrites of hippocampal neurone, *J Neurosci*, **26**: 8339-8351.

[45] Leibrock J, Lottspeich F, Hohn A, et al. 1989, Molecular cloning and expression of brain-derived neurotrophic factor, Nature, 341:149 –152.

[46]McAllister AK, Katz LC, Lo DC. 1999, Neurotrophins and synaptic plasticity, Annu Rev Neurosci, 22:295–318.

[47]Gartner A, Polnau DG, Staiger V, et al. 2006, Hippocampal long-term potentiation is supported by presynaptic and postsynaptic tyrosine receptor kinase B-mediated phospholipase Cγ signalling, J Neurosci, 26:3496 –3504.

[48] Caldeira MV, Melo CV, Pereira DB, et al. 2007, Brain-derived neurotrophic factor regulates the expression and synaptic delivery of alpha-amino-3-hydroxy-5-methyl-4-isoxazole propionic acid receptor subunits in hippocampal neurons, J Biol Chem, 282:12619-12628.

[49] Geremia NM, Pettersson LME, Hasmatali JC, et al. 2010, Endogenous BDNF regulates induction of intrinsic neuronal growth programs in injured sensory neurons, Experimental Neurology, 223: 128–142.

# CHAPTER 7

## INFLUENCE OF MICROPATTERNED PLLA MEMBRANES ON OUTGROWTH AND ORIENTATION OF HIPPOCAMPAL NEURITES

Biomaterials 31 (2010) 7000–7011

Contents lists available at ScienceDirect

Biomaterials

journal homepage: www.elsevier.com/locate/biomaterials

# Influence of micro-patterned PLLA membranes on outgrowth and orientation of hippocampal neurites

Sabrina Morelli [a,1], Simona Salerno [a,1], Antonella Piscioneri [a], Bernke J. Papenburg [b], Anna Di Vito [c], Giuseppina Giusi [c], Marcello Canonaco [c], Dimitrios Stamatialis [b], Enrico Drioli [a], Loredana De Bartolo [a,*]

[a] Institute on Membrane Technology, National Research Council of Italy, ITM-CNR, C/o University of Calabria, via P. Bucci cubo 17/C, I-87030 Rende (CS), Italy
[b] Membrane Science & Technology, Faculty of Science and Technology, MIRA Institute for Biomedical Technology and Technical Medicine,, University of Twente, P.O. Box 217 7500 AE Enschede, The Netherlands
[c] Comparative Neuroanatomy Laboratory, Department of Ecology, University of Calabria, via P. Bucci, 87030 Rende (CS), Italy

ARTICLE INFO

*Article history:*
Received 4 May 2010
Accepted 27 May 2010
Available online 25 June 2010

*Keywords:*
Hippocampal neurons
Membranes
Orientation
Micropatterning
Neurite growth

ABSTRACT

In neuronal tissue engineering many efforts are focused on creating biomaterials with physical and chemical pathways for controlling cellular proliferation and orientation. Neurons have the ability to respond to topographical features in their microenvironment causing among others, axons to proliferate along surface features such as substrate grooves in micro-and nanoscales. As a consequence these neuronal elements are able to correctly adhere, migrate and orient within their new environment during growth. Here we explored the polarization and orientation of hippocampal neuronal cells on non-patterned and micro-patterned biodegradable poly(L-lactic acid) (PLLA) membranes with highly selective permeable properties. Dense and porous nonpatterned and micro-patterned membranes were prepared from PLLA by Phase Separation Micromolding. The micro-patterned membranes have a three-dimensional structure consisting of channels and ridges and of bricks of different widths. Nonpatterned and patterned membranes were used for hippocampal neuronal cultures isolated from postnatal days 1–3 hamsters and the neurite length, orientation and specific functions of cells were investigated up to 12 days of culture. Neurite outgrowth, length plus orientation tightly overlapped the pattern of the membrane surface. Cell distribution occurred only in correspondence to membrane grooves characterized by continuous channels whereas on membranes with interconnected channels, cells not only adhered to and elongated their cellular processes in the grooves but also in the breaking points. High orientation degrees of cells were determined particularly on the patterned porous membranes with channel width of 20 μm and ridges of 17 μm whereas on dense nonpatterned membranes as well as on polystyrene culture dish (PSCD) controls, a larger number of primary developed neurites were distributed. Based on these results, PLLA patterned membranes may directly improve the guidance of neurite extension and thereby enhancing their orientation with a consequently highly ordered neuronal cell matrix, which may have strong bearings on the elucidation of regeneration mechanisms.



## 1. Introduction

In neuronal network formation, neurite outgrowth and the orientation of cellular growth are two important processes that can be facilitated by designing a well-defined cellular pattern. The control of a neuronal network architecture can be utilized not only to reproduce structural features and signaling of the brain but also to study alterations of circuitry patterns. Neuronal microscale patterns have been shown to be useful in applications ranging from drug screening or tissue engineering, biosensors to neuronal culture platform serving basic research interests.

Neurons have the capacity of responding to topographical features in their microenvironment and they have been shown to adhere, migrate, and orient their axons in the same direction of surface features. Artificial substrates with microstructures (e.g., microchannels, ridges and grooves) have been designed in an attempt to mimic the natural physical cues of CNS elements represented by fibrous proteins, cell bodies and cell processes that direct the growth of developing neurites. To this purpose, recently several methods have been introduced with the intent of generating structural surfaces such as microfabrication technology,

* Corresponding author. Tel.: +39 0984 492036; fax: +39 0984 402103.
*E-mail addresses:* l.debartolo@itm.cnr.it, loredana.debartolo@cnr.it (L. De Bartolo).
[1] These authors contributed equally.

0142-9612/$ – see front matter © 2010 Elsevier Ltd. All rights reserved.
doi:10.1016/j.biomaterials.2010.05.079

photolithography and microcontact printing [1–3]. These approaches have successfully guaranteed neuronal growth on laminin, lysine, growth factor and other adhesive molecules patterned surfaces [4–7].

It is worthy to note that a wide range of patterns have been explored in the culture of neuronal cells. Mahoney studying the effects of polyimide microchannels of 20 and 60 μm in width and 11 μm in depth on PC-12 cells displayed that neurites were directed along the axis of the grooves [8]. In addition, micro-patterned polystyrene modified with grooves width of 16 μm and grooves spacing of 13 μm directed growth and differentiation of neural progenitor cells [9]. Similarly, polylactic acid in configuration of thin films guided PC-12 and chick sympathetic neurites by unidirectional grooves in 1 and 2 μm in width and 100 nm in height [10] and as nanofiber scaffold supported the growth and the alignment of dorsal root ganglion neurons (DRG) primary sensory neurons and E 15 primary motor neurons [11]. Another matrix and precisely protein micro-patterns of various widths have been applied to affect the outgrowth rates of DRG [12]. Moreover, combinations of topographical (e.g., microchannels) and molecular cues (e.g., NGF, laminin) proved to synergically effect neuronal polarization and neurite growth [9,13,14].

Aside the usual physical and biochemical cues, some specific physical parameters of the biomaterial such as permeability must be taken into consideration when designing a substrate to be used in tissue engineering. Among the recommended biomaterials that are used for neuronal regeneration, membranes with selective permeable properties have shown to be particularly advantageous because of the diffusion of nutrients and molecules, which are important for cell growth besides offering a large surface area for cell attachment. Previously we showed that synthetic polymeric membranes were able to support the axonal outgrowth and differentiation of neuronal cells [15,16]. Here we explored the polarization and orientation of hippocampal neuronal cells on nonpatterned and micro-patterned biodegradable poly(L-lactic acid) (PLLA) membranes, which are developed by Phase Separation Micromolding [17]. The micro-patterned membranes have a three-dimensional structure consisting of channels plus ridges and bricks whereas the nonpatterned membranes have a flat surface. This polymer offers distinct advantages in that its bio-compatibility as well as its sterilization procedures have been widely documented [18–20]. Furthermore, its degradation rate can be designed so that it matches that of the new neuronal tissue formation. In order to study these micro-patterned membranes, hippocampal neuronal cells were selected as our experimental model because they are the most common and best characterized model for investigating polarization events that usually occurs spontaneously during the first 48–72 h of culture [21,22]. Neurite length, orientation and specific functions of hippocampal cells were investigated on micro-patterned membranes with ridges and channels of different width and with bricks up to 12 days of culture. Changes in morphological and functional behaviours of cells were compared on the one hand with those of cells cultured on nonpatterned membranes characterized by porous and dense surfaces and on the other hand with polystyrene culture dish (PSCD) as a reference substrate.

## 2. Materials and methods

### 2.1. Preparation of patterned and nonpatterned membranes

The membranes were cast from poly(L-lactic acid) (PLLA) of $M_w = 1.6 \times 10^5$ g/mol. Both porous and dense membranes were manufactured. The porous PLLA films were cast from a 5 wt% PLLA in 1,4-dioxane solution using ethanol as nonsolvent at 3–4 °C. A 10 wt% PLLA in chloroform solution was used to prepare dense PLLA membranes. In fact, there the chloroform was allowed to evaporate for 30–60 s and then the membranes were immersed in ethanol bath.

For patterned membranes the initial casting thicknesses was 225 μm, whereas for nonpatterned ones it was 150 μm. The membranes were kept in a nonsolvent bath for 1 day and subsequently washed for 5–8 h in Milli-Q water, which was replaced 2–3 times. Finally, they were dried in a controlled atmosphere ($T = 18–21$ °C). All solvents and nonsolvent were purchased from Merck (Germany).

Samples were cut from the sheets to fit the specific well-plates. Sterilization was accomplished by samples being immersed in a 70% ethanol solution for 20–30 min, then the ethanol was allowed to evaporate and the samples were placed in well-plates. Isopropanol (70%) was sprayed on the samples within a laminar flow cabinet and left to evaporate. To ensure complete wetting of the sheets, the samples were kept in PBS for at least 4–8 h in an incubator (37 °C, humid atmosphere with 5% $CO_2$).

### 2.2. Membrane characterization

For the patterned membranes, 2 molds were used with distinct patterns. One pattern consisted of 30 × 20 × 20 μm channels (channel width × ridge width × channel dept). The second pattern consisted of interconnected channels with dimensions of 20 × 10 × 15 μm; every 100 μm the ridges are interrupted for 10 μm to create the interconnected pattern. Scanning electron microscopy (SEM, JEOL 5600LV) was used to visualize the sheet's pattern, dimensions and porosity. Prior to imaging, the samples were sputter-coated with a nm-thin gold layer. It is important to point out that during casting and phase separation the membranes shrunk and so the dimensions of these patterns resulted to be slightly smaller that the dimensions of the mold. Nonetheless, shrinkage is reproducible and uniform and is therefore taken into account with mold design.

The investigated membranes were identified on the basis of their characteristics: dense nonpatterned (d-np) and porous nonpatterned (p-np). The patterned membranes were distinguished on the basis of the measured channel width and ridge width (Table 1) in: d-p 20/25, p-p 20/17 and ic-p 17/7. FITC labelled Poly-L-lysine (PLL) (Sigma) was used for the visualization and quantification of the membrane coating. Imaging of the FITC labelled coated membranes were obtained by using an Olympus Fluoview FV300 Laser Confocal Scanning Microscope (LCSM) (Olympus Italia). Quantitative analysis was performed on the different areas of 3 samples of investigated coated membranes using Fluoview 5.0 software (Olympus Corporation) by measuring the fluorescence average intensity. A calibration curve of FITC labelled PLL was obtained by casting known quantities of the fluorescent protein on defined areas of polystyrene dishes calculating the surface concentrations and capturing confocal images of the dry samples. The thickness of the PLL coating resulted to be 1.2 ± 0.09 μm, as measured with FITC labelled PLL by *Z*-direction scanning at the LCSM.

### 2.3. Cell isolation and culture

The hippocampus of both hemispheres was dissected from the brain of postnatal days 1–3 (PND1-3) hamsters (*Mesocricetus auratus*), removed and collected in falcon tubes in Neurobasal medium A (Invitrogen Corporation, Milan, Italy) containing 0.02% BSA (Sigma, Milan, Italy). The tissue was digested in a Neurobasal medium A containing 0.1% papain (Sigma) and 0.02% BSA (Sigma) for 20 min at 37 °C [23]. Ten minutes after digestion, the tube containing the tissue was mixed and at the end of digestion, the supernatant containing papain was removed and Neurobasal medium A supplemented with B27 (2% v/v; Invitrogen Corporation, Milan, Italy) penicillin–streptomycin (100 U/mL), glutamine 0.5 mM (Biochrom AG), 5 ng/mL basic fibroblast growth factor (b-FGF; Sigma) was added to the remaining pellet. Samples were gently triturated mechanically by using a sterile Pasteur pipette with a wide opening to dissociate larger aggregates. After sedimentation of the aggregates the supernatant was removed and transferred into tubes containing 1% papain inhibitor in Neurobasal medium A and 1% BSA, as described elsewhere [15,16]. The samples were centrifuged at 1300 rpm for 10 min at room temperature and cell pellets were gently re-suspended in Neurobasal medium A containing B27 supplement, penicillin–streptomycin, 0.5 M glutamine, 5 ng/mL b-FGF. Serum-free B27

**Table 1**
Specificities of the micro-patterned polymer sheet replicas.

| | Channel width (μm) | Ridge width (μm) | Channel height (μm) | Remarks |
|---|---|---|---|---|
| d-np | – | – | – | Dense nonpatterned |
| p-np | – | – | – | Porous nonpatterned |
| d-p 20/25 | 20 | 25 | 20 | Dense continuous channels |
| p-p 20/17 | 20 | 17 | 17 | Porous continuous channels |
| ic-p 17/7 | 17 | 7 | 7 | Interconnected channels |

supplemented Neurobasal medium A seems to have a beneficial effect on the growth and differentiation of hippocampal neurons, as suggested by other researchers [24,25]. The viability of the cells after this isolation procedure was assessed by trypan blue test and resulted to be 97 ± 2%. Cells were seeded on the different membrane surfaces at 2.5 × $10^5$ cell/$cm^2$ density. Controls without cells were prepared for each kind of substrate. Cells and controls were incubated at 37 °C in an atmosphere containing 5% $CO_2$. Cultures were fed every 4 days replacing half of the medium at each feeding.

### 2.4. Immunostaining of neuronal cells

The morphological behaviour of neurons after 8 and 12 culture days of culture on the different membranes were investigated and compared to PSCD as controls with Laser Confocal Scanning Microscopy (LCSM, Fluoview FV300, Olympus, Milan, Italy) after the immunostaining of the neuronal cytoskeletric marker, βIII-tubulin, and axon marker, growth-associated protein-43 (GAP 43) [15]. Six samples for each substrate were analyzed. Specifically, the neuronal cells were rinsed with PBS, fixed for 15 min with paraformaldehyde (4%), permeabilized for 10 min with 0.25% Triton X-100 and subsequently blocked for 30 min with 1% BSA at room temperature. To visualize βIII-tubulin a rabbit polyclonal anti-βIII-tubulin (1:100; Sigma, Milan, Italy) and a goat anti rabbit IgG FITC-conjugated (1:100; Invitrogen) were used. To visualize GAP 43 a monoclonal mouse anti-GAP 43 (1:100; Sigma, Milan, Italy) and a goat anti mouse IgG TRICT-conjugated (1:100; Invitrogen) were used. Primary antibodies were incubated overnight at 4 °C, secondary antibodies for 60 min at room temperature. Nucleic acids were counterstained with DAPI (200 ng/mL; Sigma, Milan Italy). Finally samples were rinsed, mounted and observed with LCSM.

### 2.5. Sample preparation for SEM

Hippocampal neurons after 8 and 12 days of cultures on investigated surfaces were examined with scanning electron microscopy (SEM) (Quanta 200F ESM, FEI, USA). Samples were prepared by fixation for 30 min in 2.5% glutaraldehyde and 1% formaldehyde pH 7.4 phosphate buffer followed by post-fixation for 30 min in 1% osmium tetroxide and by progressive ethanol dehydration.

### 2.6. Neuronal morphology features of the different membranes

Representative images by LCSM displaying the distribution of βIII-tubulin and GAP 43 in hippocampal cell growth and by SEM displaying both neuronal structural features and adhesive properties on the different membrane surfaces were utilized for morphometric analysis at 8 and 12 days, periods in which the different neuronal elements and synaptic complexes respectively are fully formed. In particular SEM images were utilized to analyze the percentage of area surface covered by cells on different substrates by using Scion Image for Windows (National Institutes of Health, USA,) and for the identification of the number of primary neuritis emerging per cell. LSCM images were used to measure the axonal lengths, the neurite orientation and the cell location on different substrates. In particular the axonal lengths were measured on the neurons stained with the axon marker GAP 43 from the soma to the end of each axon by using Fluoview 5.0 software (Olympus Corporation) and averaged. Neurite orientation was defined as the angle of neuritis relative to the pattern direction calculated by using Geogebra-Dynamic Mathematics for Everyone (International GeoGebra Institutes): the direction of micropattern was represented as 0°, hence, the values between −10° and +10° represented highly oriented neurite outgrowth whereas values greater than 50° represent random neurite out growth [12]. To visualize cell location on different patterned and nonpatterned membranes a quantitative analysis was performed on acquired images by confocal microscopy of neurons after 8 days of culture and by using Fluoview 5.0 software (Olympus Corporation). The fluorescence average intensity for stained βIII-tubulin, GAP43 and DAPI was calculated on *in series* designated rectangular areas along a 200 μm wide range of the xy axis vs the *z* axis of acquired images of 0.5 μm optical thickness. For images of neurons cultured on PSCD and on nonpatterned membranes, a designed rectangle size of 10 × 145 μm was used. For micro-patterned membranes the rectangular areas were designed following the patterning of the different investigated samples according the size of the channels and ridges: for dense membranes with channel and ridges widths of 20 μm and 25 μm respectively, the rectangle sizes were alternatively 20 × 145 μm and 25 × 145 μm; for porous membranes with channel and ridges widths of 20 μm and 17 μm respectively, were alternatively 20 × 145 μm and 17 × 145 μm; for 17 μm wide interconnected channels membrane were alternatively 17 × 145 μm and 7 × 145 μm, respectively.

### 2.7. Metabolic assays

The metabolic activity of neuronal cells was determined by evaluating glucose, lactate and BDNF levels on neuronal cell medium previously collected and stored in tubes at −80 °C until assays from 6 different isolations and cultures on the different membranes of the two models systems. The glucose concentration was detected by using Accu-Chek Active (Roche Diagnostics, Monza Italy). Lactate content was determined using lactate oxidase enzymatic assay Lactate Dry-Fast (Sentinel, Milan, Italy) via spectrophotometer analysis. To assay the neuronal brain derived neurotrophic factor (BDNF) secretion (mammalian neurotrophin belonging to a family of structurally related dimeric proteins) a sensitive BDNF ELISA immunoassay (Promega Corporation, WI, USA) was carried out on samples collected from 6 different isolations. Ninety-six well plates were coated with 100 μL of anti-BDNF monoclonal antibody overnight at 4 °C. After 1 rinse, 100 μL of cell culture supernatant was added to the wells and incubated by shaking for 2 h at room temperature. After 5 rinses 100 μL of anti-human BDNF antibody were added to the wells and incubated with shaking for 2 h at room temperature. After 5 rinses, the wells were incubated by shaking with 100 μL of anti IgY horseradish peroxidase conjugated antibody for 1 h at room temperature and finally, after 5 additional rinses, were incubated with 100 μl of the enzymatic substrate Tetramethylbenzidine for 10 min. The reaction was blocked with 100 μl of 1 N HCl and absorbance was measured at 450 nm using a Multiskan Ex (Thermo Lab Systems).

The values of the different experimental tests were evaluated by using ANOVA followed, where appropriate by Bonferroni *t*-test ($p < 0.05$) according to the Student's *t*-test.

## 3. Results

Morphological behaviour of hippocampal neurons was evaluated by SEM and confocal microscopy after 8 and 12 days of culture on patterned, nonpatterned membranes and on PSCD (Figs. 1–3). After 8 days of culture, neuron cell bodies appeared slightly flattened and displayed a tight adhesion to the different substrates. Cells cultured on patterned membranes appeared to be localized in grooves whereas cells cultured on nonpatterned membranes and on PSCD distributed homogeneously and randomly on surface areas. Neurite outgrowth and polarization of the hippocampal neurons occurred on all investigated surfaces within the first 8 days of culture (Figs. 1 and 3). Active growth cones with filopodia and lamellipodia were observed and cells cultured on patterned membranes appeared to establish many contacts with the grooves (Fig. 1d'-f').

Neurites on all investigated patterned membranes linearly extended along the grooves of micro-patterns whereas no guidance of neurite outgrowths was observed on PSCD and on dense and porous nonpatterned membranes (Fig. 3). In particular hippocampal neurons grown on porous membranes with 20 and 17 μm channel and ridge width (p-p 20/17) after 8 days of culture exhibited highly elongated processes oriented parallel to the grooves of the patterned channels and not in communication with cells of adjacent grooves (Fig. 3e). On d-p 20/25 membranes with 20 μm and 25 channel and ridges width, respectively, hippocampal neurons appeared highly branched with numerous neuritis emerging and bridging also on ridges and in contact with cells of adjacent grooves of the patterned channels (Fig. 3d). Regarding interconnected channel membranes, the elongation of neuronal processes and the formation of synaptic communication between cells followed the typical topography and brick's geometry of interconnected channels (Fig. 3f). After 12 days of culture the neurons, displaying the typical bundle like arrangement, came into contact with each other and forming a complex network on all investigated substrates. In particular, on patterned membranes many bridging synaptic contacts were observed while the orientation of hippocampal neurons along patterned channels was maintained (Fig. 3a'-f').

In order to examine the neurite outgrowth orientation of hippocampal neurons cultured on patterned membranes, the angle between the wall pattern and neurite was measured and the frequency of each angle calculated (Fig. 4). Higher frequency of neuron orientation (35%) within ±10° was observed for hippocampal neurons cultured on p-p 20/17 membranes whereas for those cultured on d-p 20/25 membranes lesser frequencies of neuron orientation (25%) within ±10° was found. In contrast, the frequency profile of neurons cultured on 17 μm wide interconnected channel membranes exhibited lower frequencies of

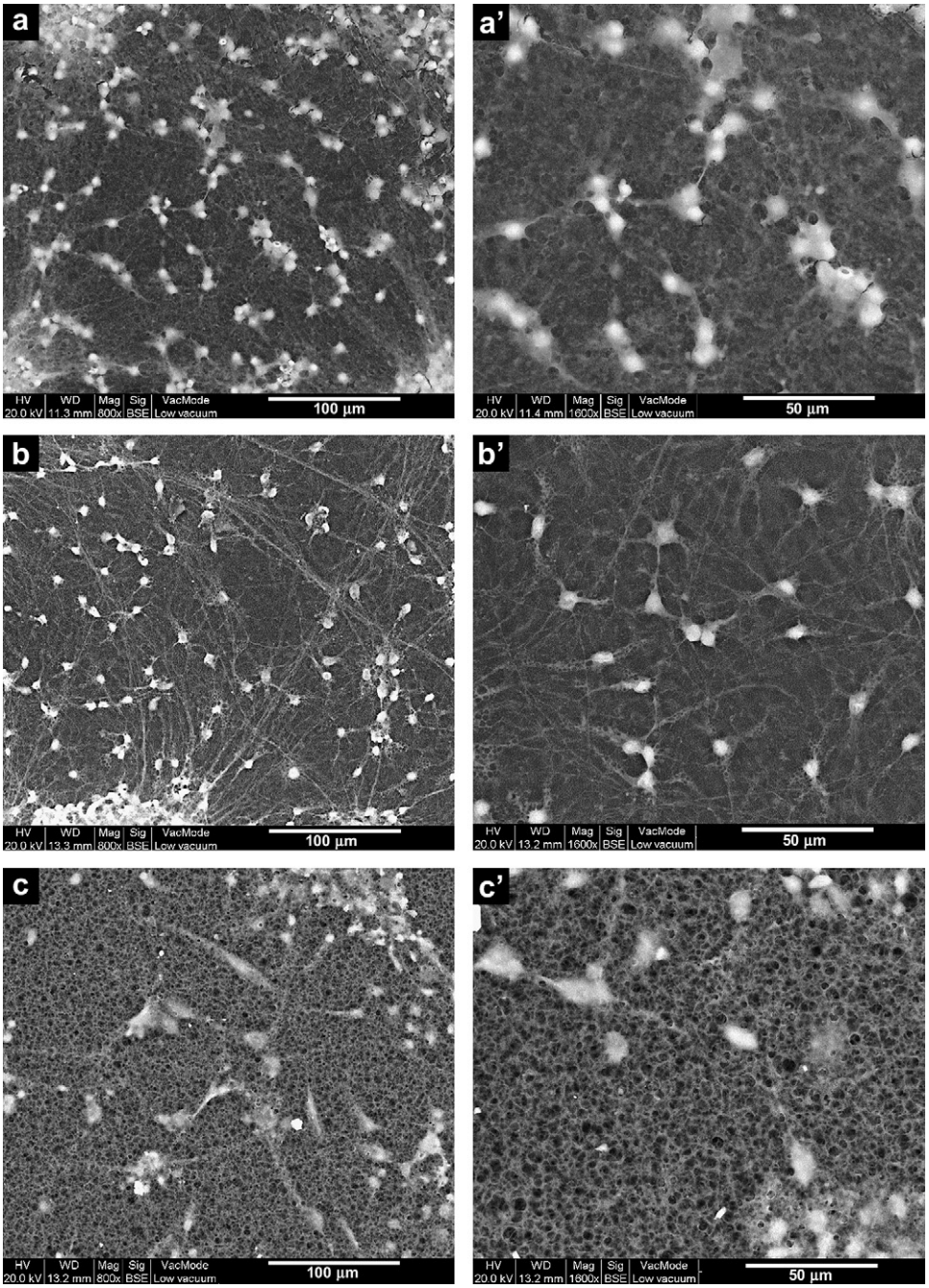


**Fig. 1.** SEM's images of hippocampal neurons after 8 days of culture on: (a, a') PSCD, (b, b') d-np, (c, c') p-np, (d, d') d-p 20/25, (e, e') 20/17 p-p and (f, f') ic-p 17/7 membranes.

neuronal orientation (20%) within ±10° and a more flat distribution within ±90° representing a more random growth.

A quantitative analysis of cell location on different patterned and nonpatterned membranes was performed on neurons after 8 days of culture by confocal microscopy. As reported in Fig. 5 on PSCD and on nonpatterned membranes, an average intensity of βIII-tubulin, GAP43 and DAPI were detected randomly along a 200 µm wide range on the xy axis (Fig. 5a–c). On the contrary, the fluorescence average intensity of stained proteins and acid nucleic were distributed according to the pattern fidelity with alternating high and low values in correspondence of channels and ridges, respectively, on micro-patterned membranes (Fig. 5d–f). It is interesting to note that on 20 µm wide channel porous membranes, the low values were distributed in a restricted range of average intensity, and namely: between 453.63 and 899.39 for βIII-tubulin, 1539.55 and 1915.04 for GAP43, 524.57 and 1020.81 for DAPI (Fig. 5e). On the other patterned membranes, the low values were distributed in a more complete range of average intensity. In particular, the fluorescence average intensity for βIII-tubulin ranged between 592.01 and 3193.51 on dense patterned membranes with continuous channels (d-p 20/25) and between 1205.59 and 3573.76 on wide interconnected channel membrane (ic-p 17/7) (Fig. 5d and f).

The percentage of covered area by hippocampal neurons cultured on different membranes at day 8 and 12 was evaluated on SEM images at different magnifications (Fig. 6). On day 8, neurons

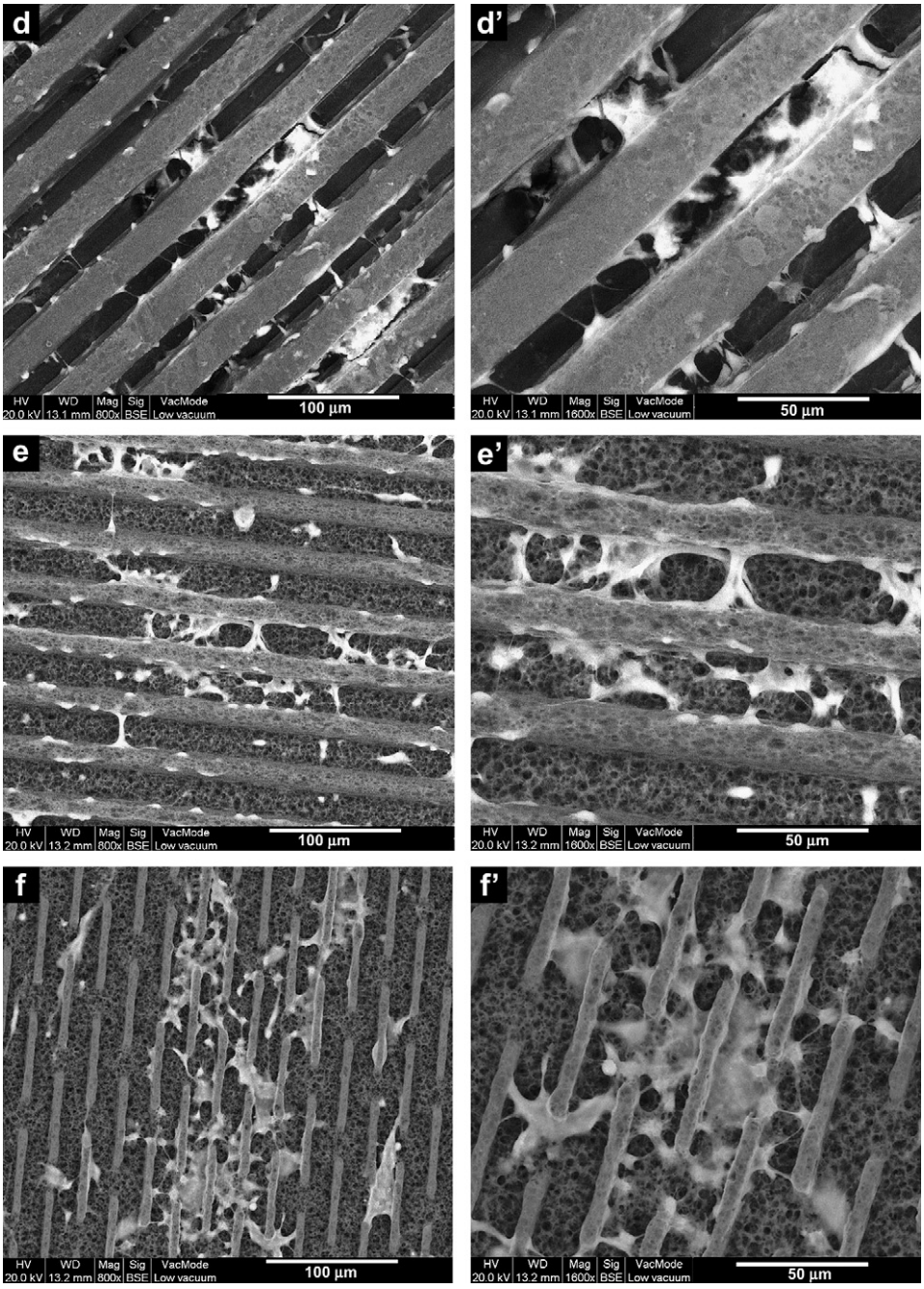


**Fig. 1.** (*continued*).

on PSCD adhered and covered a significantly higher surface area (61.5%) with respect to the nonpatterned and patterned membranes. Also neurons cultured on nonpatterned membranes (54.5%) covered larger surface area with respect to the patterned ones. The area covered by cells on all investigated surfaces increased significantly ($p < 0.01$) with time. An increase of a 19.3% was found on PSCD while on dense and porous nonpatterned membranes of a 30.1 and 29.3%, respectively. In the case of patterned membranes with continuous channels, the percentage of neuronal enriched area increased to about 18% whereas on membranes with interconnected channels increased to about 26.8% and this proved to be significantly higher with respect to the continuous channel patterned membranes. Even the number of primary neurites emerging per cell changed on the basis of the surface topography. As is reported in Table 2, the average neurite numbers per neurons ranged between $2.8 \pm 0.79$ and $3.12 \pm 0.8$ within the first 8 days of culture on all investigated micro-patterned membranes whereas a significant increase of the primary neurite number was found on neurons cultured on both PSCD ($4.29 \pm 1.1$) and on dense nonpatterned membranes ($4.25 \pm 0.91$).

Axonal length was evaluated on neurons stained with its specific protein (GAP43) involved with the regulation of axonal outgrowth on different acquired confocal images (Fig. 7). On day 8 of culture, all the hippocampal neurons exhibited an axonal growth without any significant differences on the different surfaces considered. After 12 days of culture, axonal growth continued at a moderately high significantly level ($p < 0.05$) for PSCD and porous

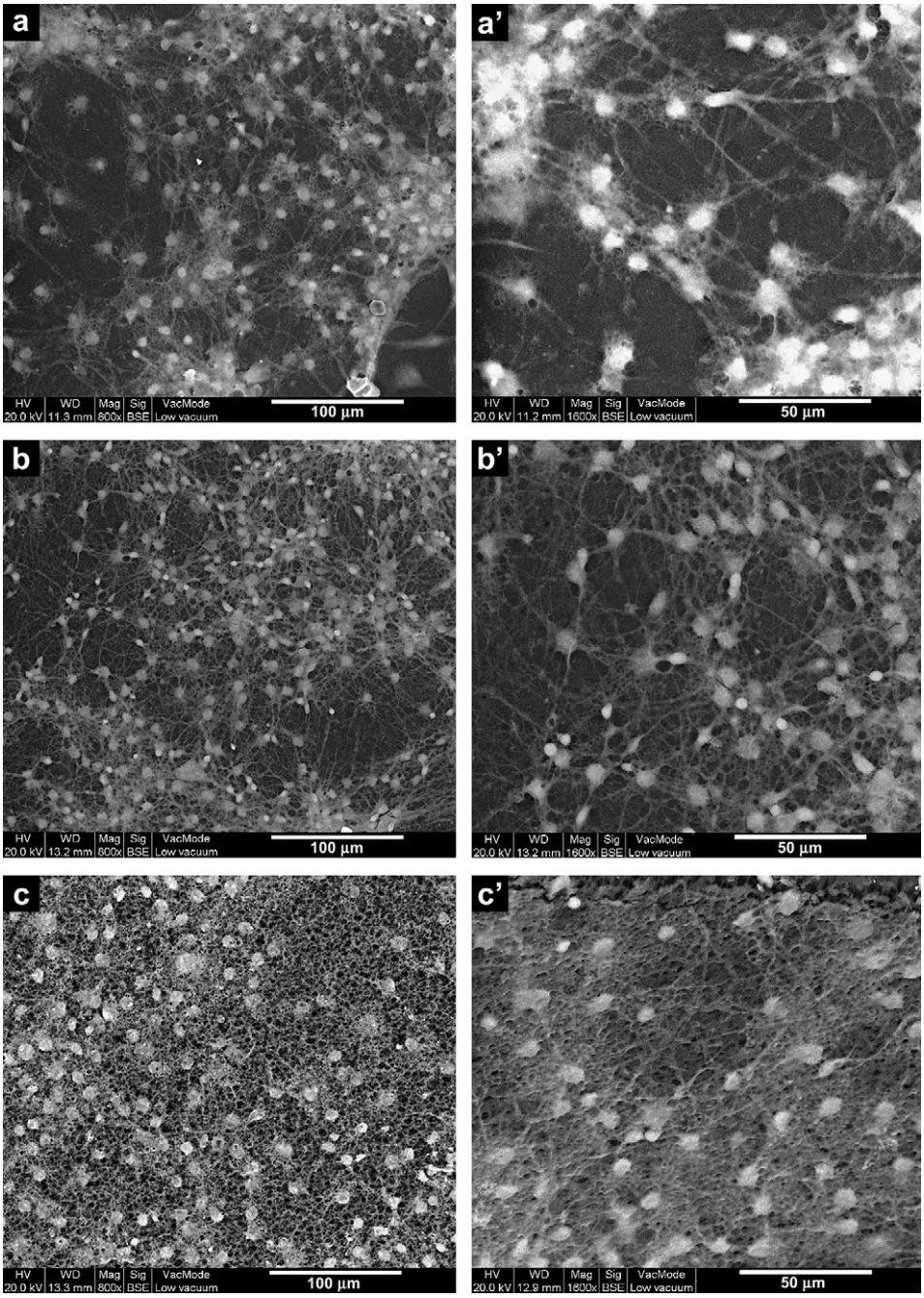


**Fig. 2.** SEM's images of hippocampal neurons after 12 days of culture on: (a, a') PSCD, (b, b') d-np, (c, c') p-np, (d, d') d-p 20/25, (e, e') 20/17 p-p, (f, f') and ic-p 17/7 membranes.

nonpatterned membranes, while a higher ($p < 0.01$) level was obtained for dense nonpatterned and all patterned membranes. The longest axons (164.1 ± 32 µm) were observed in neurons cultured on interconnected channel pattern, similarly to the neurons cultured on the other investigated surfaces, with the exception of neurons cultured on porous nonpatterned membrane that exhibited lower axonal growth.

When the metabolic activities of hippocampal neurons were evaluated after 4, 8 and 12 days of culture, it was possible to observe a comparable activity in all substrates considered with respect to PSCD. A significant increase of glucose consumption was shown to occur with time for the hippocampal neurons cultured on the membranes, with the exception of neurons cultured on continuous (p-p 20/17) and interconnected channel (ic-p 17/7) patterns (Fig. 8). The higher rates of glucose consumption were measured in neurons cultured on PSCD at day 8 and 12. Even lactate production increased with time at high rates for all the investigated surfaces (Fig. 9). Of noteworthy is the fact that neurons on PSCD and on porous nonpatterned membranes produced lactate to a larger extent with respect to the other surfaces on day 8, while lactate production only significantly increased on day 12 of patterned and dense nonpatterned membranes. In the case of BDNF secretion, the elevated levels of this factor appeared to be mostly typical of hippocampal neurons for all culture periods with the exception of 12 days of culture (Fig. 10). For the other substrates, significantly high levels were reached by neurons on day 4 and 8 of culture for only PSCD and interconnected channel patterns.

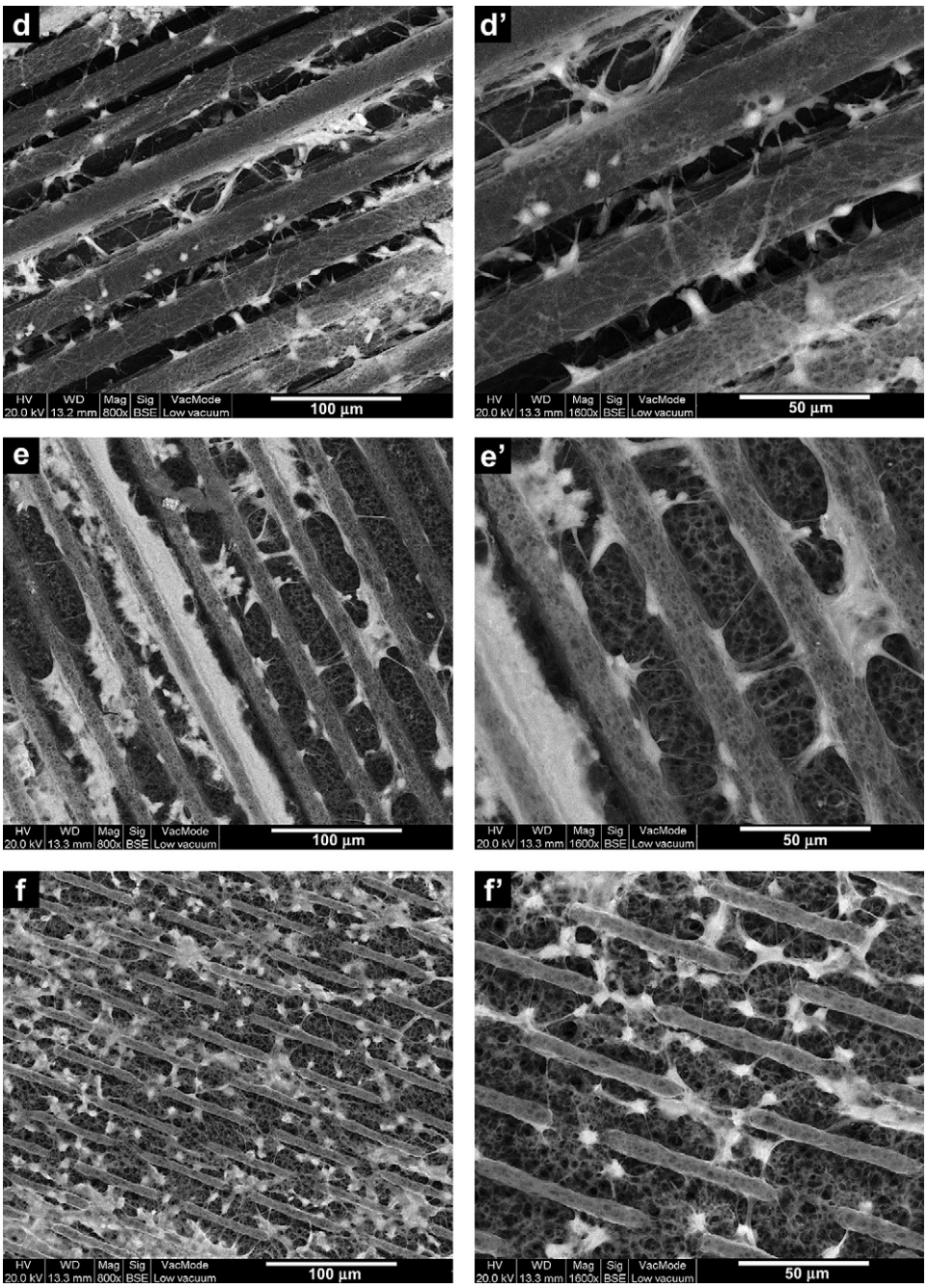


**Fig. 2.** (*continued*).

## 4. Discussion

The results of the present study favourably indicate that the spatial features of the micro-patterned PLLA membranes have profoundly different effects on cell morphology and adhesion features of cultured neurons. When presented as surface patterns, however, the channels, ridges and bricks induced cellular morphological changes that are determined by the shape of the pattern. Moreover, the quantitative analysis of branching patterns of newly formed axons demonstrated that neurons plated on micro-patterned membranes exhibited highly anisotropic outgrowth strongly based on the nature of the growth permissive surface pattern. The steering, turning and path findings of a growth cone seemed to be driven by filopodia protrusion and retraction as shown by cells growing on the membranes.

The advancing neurite filopodia and lamellipodia that emerged from the growth cone tend to exhibit an “exploring type” of reaction toward the surrounding extracellular environment including along with the vertical ridge wall. Consequently, the channel pattern is recognised by the cells in which cytoskeleton structures generate traction forces that push and pull the neurite forward. The direction of neurite extension is determined by the strength of the traction force exerted by a filopodia that depends on the ease in which the microtubules and actin filaments within the cytoskeleton structures can accumulate assemble and orient in the direction of a cell protrusion [26]. When cells were cultured on nonpatterned membranes, the strength of the traction force did not seem to rely on the angle at which the protrusion emerged from the cell soma, while neurites tended to emerge uniformly in all directions. When cells were cultured on patterned membranes with

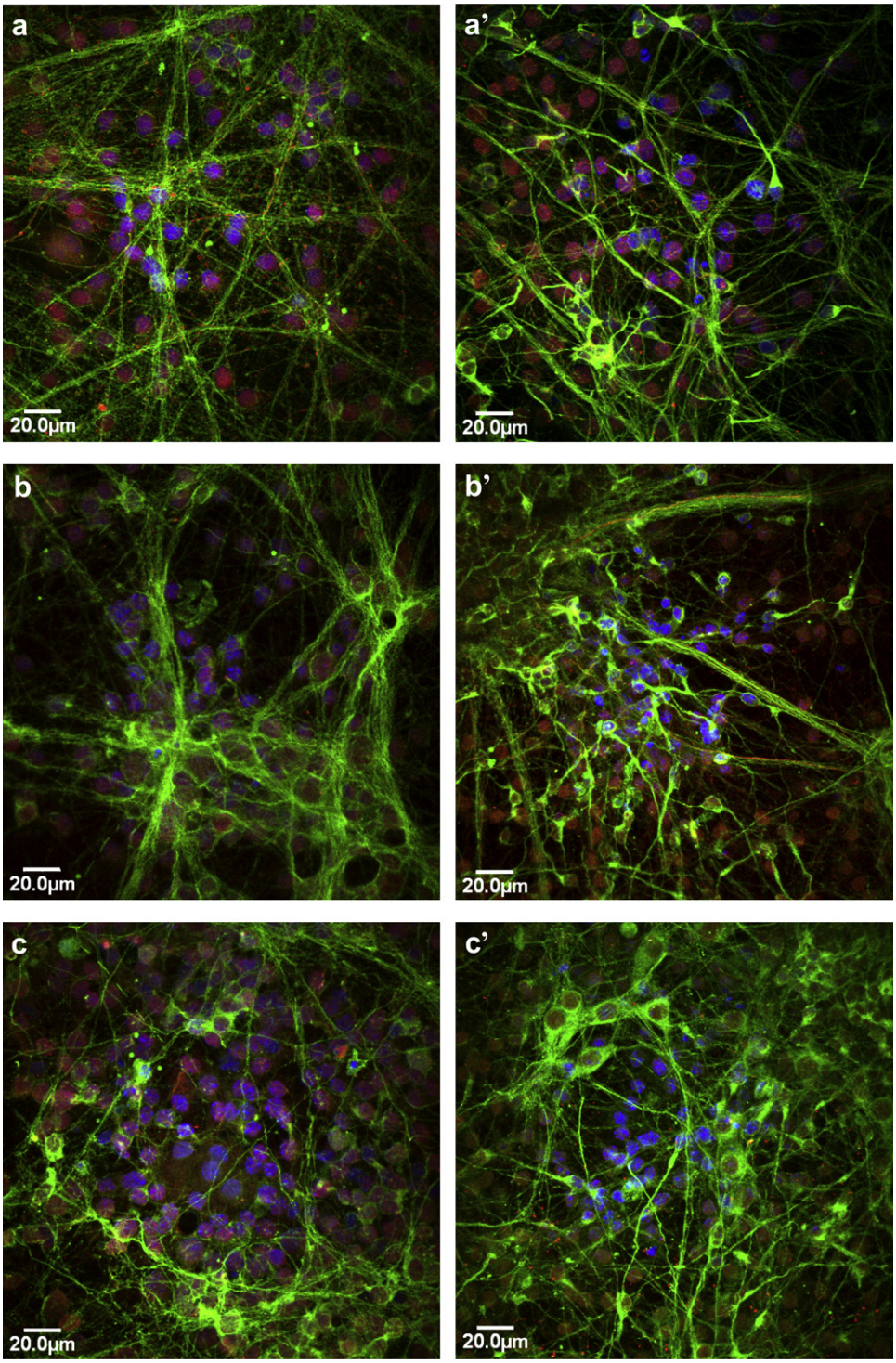


**Fig. 3.** Laser confocal micrographs of hippocampal neurons after 8 (a–f) and 12 (g–l) days of culture on: (a, a') PSCD, (b, b') d-np, (c, c') p-np, (d, d') d-p 20/25, (e, e') p-p 20/17 and (f, f') ic-p 17/7 membranes. Cells were stained for βIII-tubulin (green), GAP43 (red) and nuclei (blue).

channels and ridges, the height of the ridges limited their adhesion area and the directions over which the microtubules and actin filaments accumulated and oriented the filopodia. As a result, neuronal processes developed in the channels of the patterned membranes and cells at the end appeared to cover a lower membrane area.

Interestingly, micro-patterned membranes induced cell organization and outgrowth in a restricted area of the grooves of the membranes and as a consequence the complexity of neuronal architecture was reduced. In this case, cell distribution occurred only in correspondence to channels for the membranes with continuous channels whereas on membranes with interconnected channels, cells adhered and elongated their cellular processes not only at the grooves but also at the breaking points. Large channels allowed neurites to advance in a direction parallel to the wall as in the case of patterned membranes with 20 μm wide channels. A higher

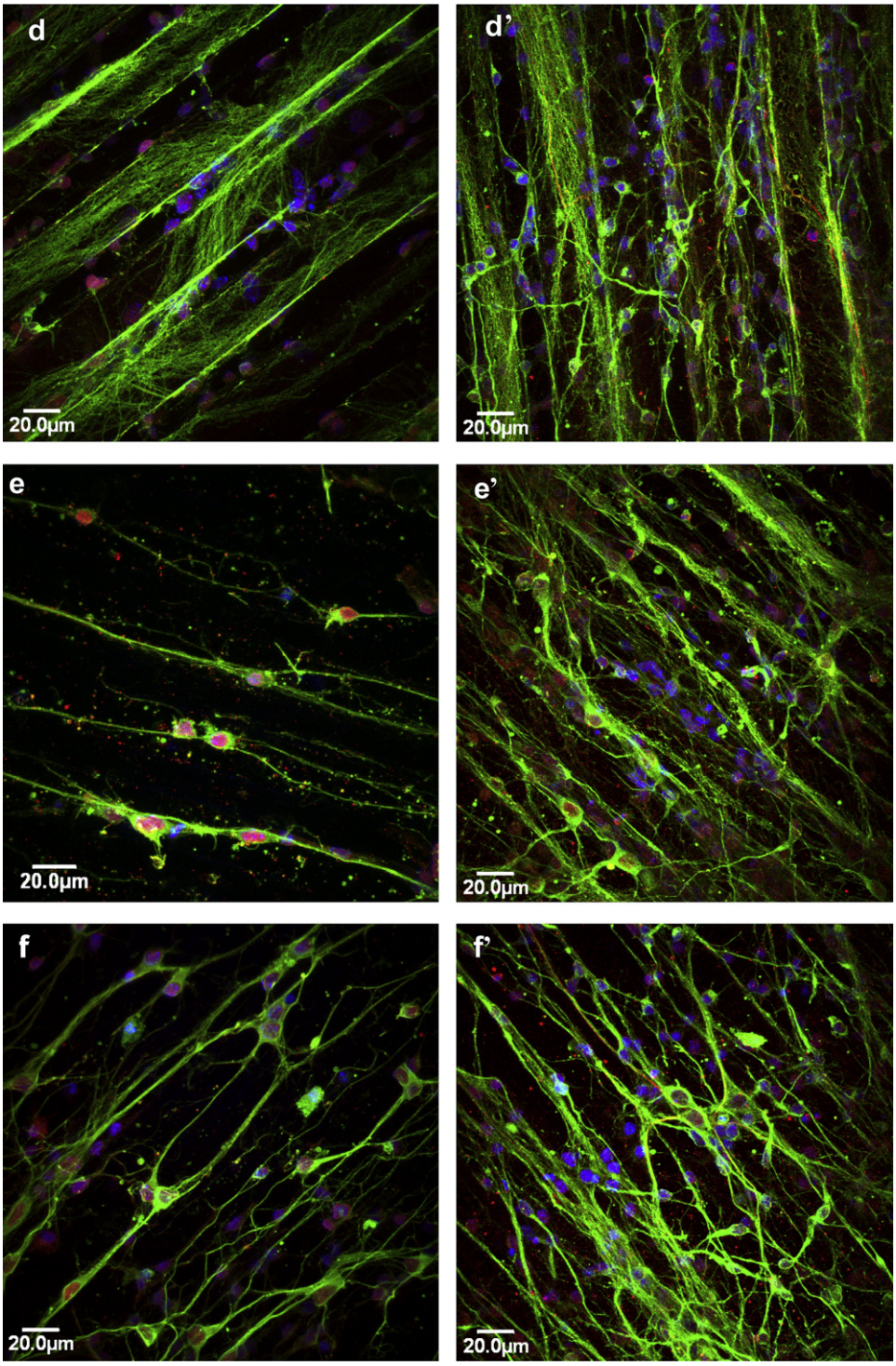


**Fig. 3.** (*continued*).

frequency of neurons orientation between −10° and 10° was found in the p-p 20/17 membranes. Hence, it is likely that the groove width plays an important role in the cell orientation as also shown by Miller et al. [27] on Schwann cells that established an optimal alignment by using poly(D,L-lactic acid) substrates with grooves in the same range. In the case of interconnected channels with a width of 17 μm cells, this parameter tends to extend neurites in the breaking points perpendicular to the short channels, thus reaching the neuronal processes of the cells located within the closer channels. In such cases, the outgrowth of neurites does not seem to be inhibited upon contact with the channel wall. Additionally, the smaller vertical wall (7 μm) of the bricks seems to also play a role on the orientation of neurite growth on these membranes, which is in agreement with other culture systems such as polystyrene and silicon [9,28]. The presence of microstructures and spatial features over the surface tend to strongly affect not only the orientation and emerging of primary neurites but also their direction of extension. We observed a larger number of primary neuritis cultured on dense

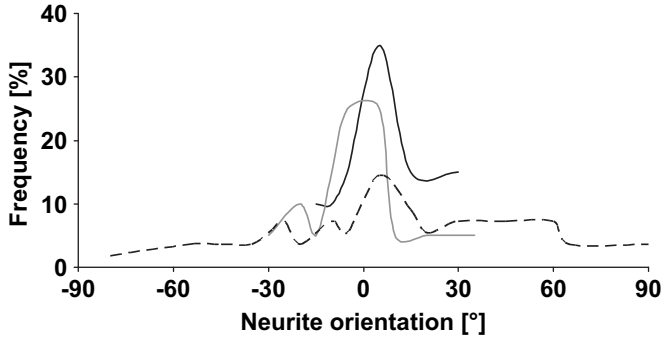


**Fig. 4.** Orientation frequency distribution of hippocampal neurons after 8 days of culture on d-p 20/25 (grey line), p-p 20/17 (black line) and ic-p 17/7 (dashed line) membranes.

nonpatterned membranes as well as on PSCD. It is possible that cells find the adequate amount of physical space to protrude from the soma neurite on these substrates with respect to patterned membranes where the presence of microchannels may be constraint and as a result only a lower number of neurites are able to spread out. At the same time even the presence of pores over the membrane surface appears to influence neurite outgrowth and thereby limiting the number of neuronal processes that emerge from the cell soma plus axonal extension on porous nonpatterned membranes. For such membranes, the number of primary emerging neurites and axonal outgrowth are significantly lower with respect to other investigated substrates. As a result, the neuronal network appears to be less developed with respect to the dense nonpatterned surface (Fig. 1b, c, and b', c'). This is in agreement with results obtained in a previous work that demonstrated a preference of cells to develop longer and highly branched neuritis on smooth membrane surfaces [15]. Otherwise, the observed preference in the orientation of neurite outgrowth on micro-patterned membranes and simplification of the

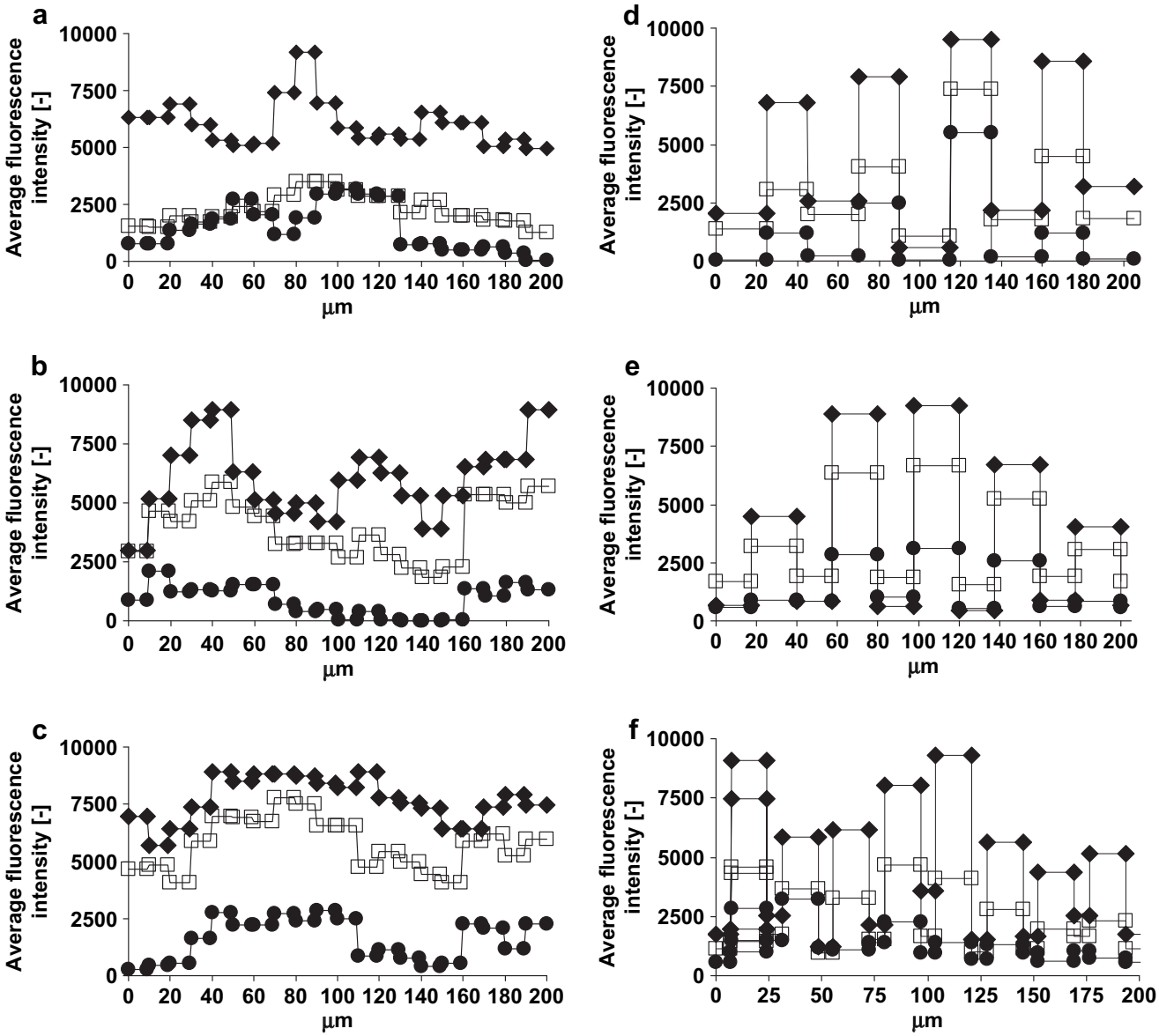


**Fig. 5.** Fluorescence average intensity for stained βIII-tubulin (◆), GAP43 (□), and DAPI (●) of hippocampal neurons after 8 days of culture on: (a) PSCD, (b) d-np, (c) p-np, (d) d-p 20/25, (e) p-p 20/17 and (f) ic-p 17/7 membranes.

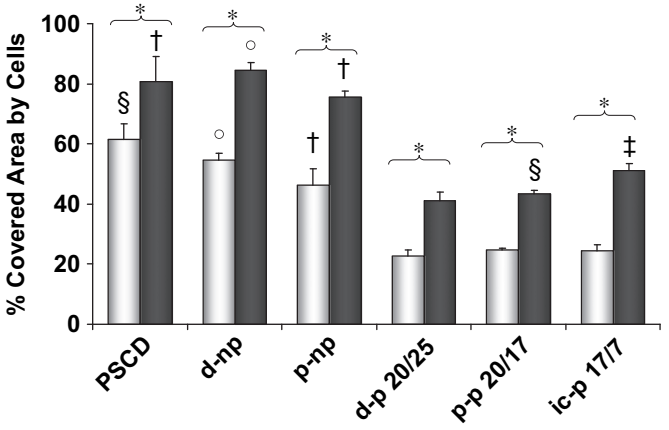


**Fig. 6.** Percentage extension of covered hippocampal neuronal areas after 8 (grey bar) and 12 (full bar) days of culture on the investigated substrates. Values, expressed as average ± standard deviation were evaluated by ANOVA followed, when appropriate by Bonferroni *t*-test ($p < 0.05$): (§) vs all substrates, (○) vs p-np, d-p 20/25, p-p 20/17 and ic-p 17/7 membranes, (†) vs d-p 20/25, p-p 20/17 and ic-p 17/7 membranes, (‡) vs d-p 20/25 and p-p 20/17 membranes. Data statistically significant according Student's *t*-test: (*) $p < 0.01$.

**Table 2**
Number of primary emerging neurites after 8 days of culture on all investigated substrates. Values, expressed as average±standard deviation were evaluated by ANOVA followed, where appropriate by Bonferroni *t*-test ($p < 0.05$), (§) vs all.

| | N° primary emerging neurites |
|---|---|
| PSCD | 4.29 ± 1.10 (§) |
| d-np | 4.25 ± 0.91 (§) |
| p-np | 2.39 ± 0.61 |
| d-p 20/25 | 3.12 ± 0.81 |
| p-p 20/17 | 2.8 ± 0.79 |
| ic-p 17/7 | 3.1 ± 0.74 |

cellular morphology indicates that spatial constraints exerted by the limited adhesion area of growth-guiding pattern serve as a primary factor in determining the morphology of neurons.

In addition, also the evaluation of the metabolic activity of neurons on membranes corroborated a functionally active cellular event that is prevalently specific for neurons grown for 12 days.

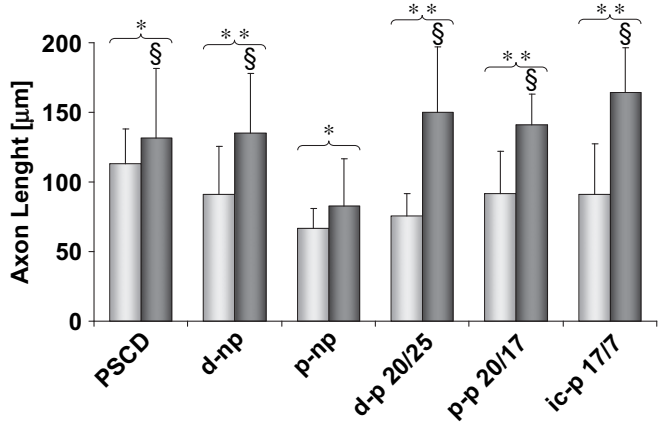


**Fig. 7.** Axonal length of hippocampal neurons after 8 (empty bar) and 12 (grey bar) days of culture were determined on the different substrates. The values are expressed as average ± standard deviation. Values, expressed as average ± standard deviation were evaluated by ANOVA followed, where appropriate by Bonferroni *t*-test ($p < 0.05$): (§) vs p-np membrane. Data statistically significant according Student's *t*-test: (*) $p < 0.05$, (**) $p < 0.01$.

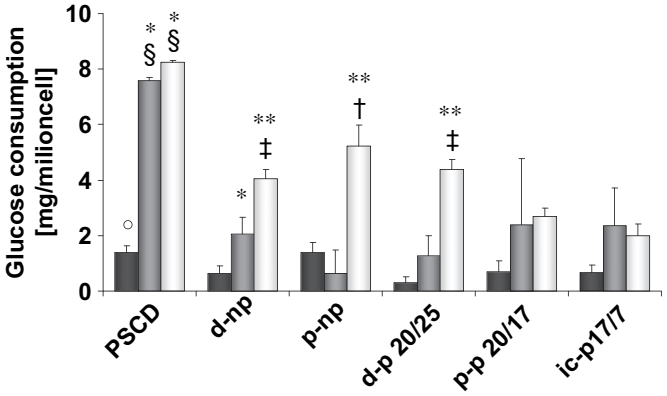


**Fig. 8.** Glucose consumption of hippocampal neurons after 4 (full bar), 8 (grey bar) and 12 (empty bar) days of culture were determined on the different substrates. The values were expressed as average ± standard deviation. Data statistically significant according to ANOVA followed by Bonferroni *t*-test ($p < 0.05$): (§) vs all substrates, (○) vs d-p 20/25, (†) vs p-p 20/17 and ic-p 17/7, (‡) vs ic-p 17/7, (*) vs 4 and (**) vs 4 and 8 days of culture.

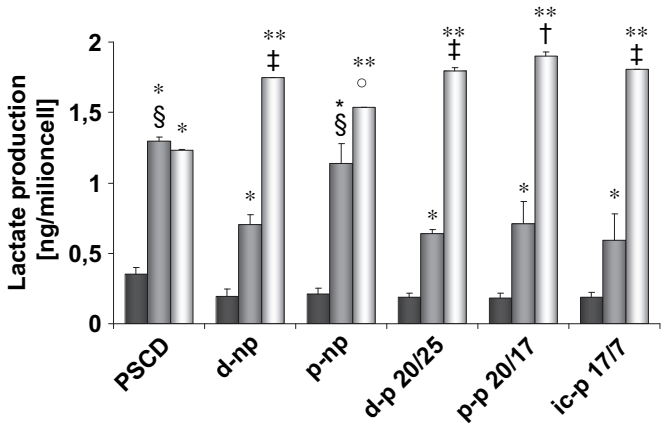


**Fig. 9.** Lactate production of hippocampal neurons after 4 (full bar), 8 (grey bar) and 12 (empty bar) days of culture were determined on the different substrates. The values are expressed as average ± standard deviation. Data statistically significant according to ANOVA followed by Bonferroni *t*-test ($p < 0.05$): (§) vs d-np and, d-p 20/25, p-p 20/17 and ic-p 17/7 membranes, (○) vs PSCD, (‡) vs PSCD and p-np, (†) vs PSCD, d-p 20/25 and ic-p 17/7, (*) vs 4 and (**) vs 4 and 8 days of culture.

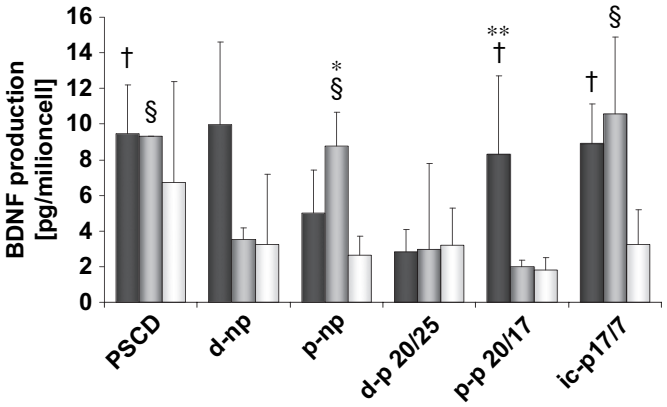


**Fig. 10.** BDNF secretion of hippocampal neurons after 4 (full bar), 8 (grey bar) and 12 (empty bar) days of culture were determined on the different substrates. Values, expressed as average ± standard deviation were evaluated by ANOVA followed, where appropriate by Bonferroni *t*-test ($p < 0.05$): (†) vs d-p 20/25, (§) vs d-np, d-p 20/25, p-p 20/17, (*) vs 4 and 8 days of culture, (**) vs 8 and 12 days of culture.

Indeed, during this period, glucose consumption and lactate production increased with time for most of the substrates investigated, especially for the high consumption of glucose supplied by cells grown on PSCD. In this context the secretion of BDNF tends to further underlie the viable status of hippocampal neurons despite a decrease in the late phase of neuronal development for all investigated substrates. This neurotrophin plays an important role in establishing synaptic connections and neuronal maturation. The high levels of BDNF observed during the first days of culture are related to the outgrowth of neurites and to the expression of synaptic proteins, which are required for establishing synaptic connections or functions during the development stage [29].

## 5. Conclusions

We have investigated the orientation and neurite outgrowth of hippocampal cells on the micro-patterned PLLA membranes that potentially can be applied in neuronal tissue engineering. Neuronal cells responded to the patterned and nonpatterned membrane surface as demonstrated by the variations of their morphology, neurite outgrowth and orientation. We found that the number of emerging neurites plus their direction and extension appeared to be tightly correlated to the topographical features of these new types of membranes. Neurons on PLLA membranes exhibited a preference for the orientation of neurite outgrowth following the pattern surface. Surprisingly, it seems that this morphological parameter also relies on both the width of channels and on the height of ridges such as the pattern continuity. Highly oriented neurons were observed specially on the patterned porous membranes with channel width of 20 μm and ridges of 17 μm, where a higher frequency of neuronal orientations between $-10^{\circ}$ and $10^{\circ}$ were observed. The induced cell orientation was maintained in time with an increase of neuronal bundle arrangements. Based on these results the PLLA patterned membranes may guide the neurite extension and enhance their orientation creating a highly ordered neuronal cell matrix, which may provide useful indications for studying regeneration processes of the different neurological disorders.

## Appendix

Figure with essential color discrimination. Fig. 3 in this article is difficult to interpret in black and white. The full color image can be found in the on-line version, at doi:10.1016/j.biomaterials.2010.05.079.

## References


[1] Goldner JS, Bruder JM, Li G, Gazzola D, Hoffman-Kim D. Neurite bridging across micorpatterned grooves. Biomaterials 2006;27:460–72.

[2] Wheeler BC, Corey JM, Brewer GJ, Branch DW. Microcontact printing for precise control of nerve cell growth in culture. J Biomech Eng 1999;121:73–8.

[3] Faid K, Voicu R, Bani-Yaghoub M, Tremblay R, Mealing G, Py C, et al. Rapid fabrication and chemical patterning of polymer microstructures and their applications as a platform for cell cultures. Biomed Microdevices 2005;7:179–84.

[4] Ruiz A, Buzanska L, Gilliland D, Rauscher H, Sirghi L, Sobanski T, et al. Microstamped surfaces for the patterned growth of neural stem cells. Biomaterials 2008;29:4766–74.

[5] Schamalenberg KE, Ulhrich KE. Micropatterned polymer substrates control alignment of proliferating Schwann cells to direct neuronal regeneration. Biomaterials 2005;26:1423–30.

[6] Foley JD, Grunwald EW, Nearley PF, Murphy CJ. Cooperative modulation of neuritogenesis by PC12 cells by topography and nerve growth factor. Biomaterials 2005;26:3639–44.

[7] Clark P, Britland S, Connolly P. Growth cone guidance and neuron morphology on micropatterned laminin surfaces. J Cell Sci 1993;105:203–12.

[8] Mahoney MJ, Chen RR, Tan J, Saltzman WM. The influence of microchannels on neurite growth and architecture. Biomaterials 2005;26:771–8.

[9] Recknor JB, Sakaguchi DS, Mallapragada SK. Directed growth and selective differentiation of neural progenitor cells on micropatterned polymer substrates. Biomaterials 2006;27:4098–108.

[10] Li J, McNally H, Shi R. Enhanced neurite alignment on micro-patterned poly-L-lactic acid films. J Biomed Mater Res 2008;87A:392–404.

[11] Corey JM, Gertz CC, Wang BS, Birrel LK, Johnson SL, Martin DC, et al. The design of electrospun PLLA nanofiber scaffold compatible with serum-free growth of primary motor and sensory neurons. Acta Biomater 2008;4:863–75.

[12] Song M, Uhrich KE. Optimal micropattern dimensions enhance neurite outgrowth rates, lengths, and orientations. Ann Biomed Eng 2007;35:1812–20.

[13] Gomez N, Lu Y, Chen S, Schmidt CE. Immobilized nerve growth factor and microtopography have distinct effects on polarization versus axon elongation in hippocampal cells in culture. Biomaterials 2007;28:271–84.

[14] Zhang J, Venkatarami S, Xu H, Song Y-K, Song H-K, Palmore GTR, et al. Combined topographical and chemical micropatterns for templating neuronal networks. Biomaterials 2006;27:5734–9.

[15] De Bartolo L, Rende M, Morelli S, Giusi G, Salerno S, Piscioneri A, et al. Influence of membrane surface properties on the growth of neuronal cells isolated form hippocampus. J Memb Sci 2008;325:139–49.

[16] Giusi G, Facciolo RM, Rende M, Alo R, Di Vito A, Salerno S, et al. Distinct α subunits of the GABAA receptor are responsible for early hippocampal silent neuron-related activities. Hippocampus 2009;19:1103–14.

[17] Papenburg BJ, Vogelaar L, Bolhuis-Versteeg LAM, Lammertink RGH, Stamtialis D, Wessling M. One-step fabrication of porous micropatterned scaffolds to control cell behaviour. Biomaterials 2007;28:1998–2009.

[18] Dotti GC, Sullivan CA, Banker GA. The establishment of polarity by hippocampal neurons in culture. J Neurosci 1988;8:1454–68.

[19] Fukata Y, Kimura T, Kaibuchi K. Axon specification in hippocampal cells. Neurosci Res 2002;43:305–15.

[20] Xie C, Markesbery WR, Lovell MA. Acrolein, a product of lipid peroxidation, inhibits glucose and glutamate uptake in primary neuronal cultures. Free Radic Biol Med 2000;29:714–20.

[21] Brewer GJ. Isolation and culture of adult rat hippocampal neurons. J Neurosci Methods 1997;71:143–55.

[22] Ahlemeyer B, Baumgart-Vogt E. Optimized protocols for the simultaneous preparation of primary neuronal cultures of the neocortex, hippocampus and cerebellum from individual newborn (P0.5) C57Bl/6J mice. J Neurosci Methods 2005;149:110–20.

[23] Dickson BJ. Molecular mechanisms of axon guidance. Science 2002;298:1959–64.

[24] Miller C, Shanks H, Witt A, Rutkowski G, Mallapragada S. Orientated Schwann cell growth on micropatterned biodegradable polymer substrates. Biomaterials 2001;22:1263–9.

[25] Russel P, Gasiorowski JZ, Nealy PF, Murphy CJ. Response of human trabecular meshwork cells to topographic cues on the nanoscale level. Invest Ophthalmol Vis Sci 2008;49:629–35.

[26] Ngo TTB, Waggoner PJ, Romero AA, Nelson KD, Eberhart RC, Smith GM. Poly (L-lactide) microfilaments enhance peripheral nerve regeneration across extended nerve lesions. J Neurosci Res 2003;72:227–38.

[27] Bini TB, Gao S, Xu X, Wang S, Ramakrishna S, Leong KW. Peripheral nerve regeneration by microbraided poly(L-lactide-co-glycolide)biodegradable polymer fibers. J Biomed Mater Res A 2004;68:286–95.

[28] Zhang X, Hua H, Shen X, Yang Q. In vitro degradation and biocompatibility of poly(L-lactic acid)/chitosan fiber composites. Polymer 2007;48:1005–11.

[29] Kumamaru E, Numakawa T, Adachi N, Yagasaki Y, Izumi A, Niyaz M, et al. Glucocorticoid prevents brain-derived neurotrophic factor-mediated maturation of synaptic function in developing hippocampal neurons through reduction in the activity of mitogen-activated protein kinase. Mol Endocrinol 2008;22:546–58.

# Conclusions

Biomaterials in tissue engineering and regenerative medicine should provide the necessary support for cell proliferation and the maintenance of their differentiated functions. This thesis showed how polymeric semipermeable membranes with different properties can be applied in tissue engineering and artificial organs. An important challenge in the field of regenerative medicine is to develop bioartificial systems that favor the reconstruction of tissues and modulate the behavior of cells. Therefore, the main goal of this thesis was the realization of different types of membrane biohybrid systems, through the use of synthetic and biodegradable membranes, for the growth and the differentiation of two different cell types, namely the progenitor liver cells and hippocampal neurons, giving rise to two specific applications in liver and neural tissue engineering.

The development of new culture models, such as these membrane biohybrid systems, made it possible to maintain cells perfectly vital for several days in a microenvironment that simulates in vivo conditions, thereby overcoming the limitations of the traditional culture systems.

It is very important to take into account that the use of membranes in tissue engineering and medical fields requires materials with high biocompatibility and bio-stability properties. With this aim, as the first step of the experimental design, a novel membrane of PEEK-WC-PU was realized and used for the cultivation of the progenitor liver cells. In order to enhance the cell-membrane interaction, the PEEK-WC-PU membrane was grafted with nitrogen functionalities by means of NH3 glow discharges. Native and plasma grafted membranes, used in a small scale gas permeable bioreactor, clearly supported the cell expansion and differentiation as evidenced by the results obtained. The cells cultured on the native and modified membranes exhibited a balanced cell-surface interaction exhibiting a three-dimensional spatial organization as revealed by the morphological analysis. The evaluation of the specific liver activity, in terms of urea synthesis and albumin production revealed that the highest metabolic rate was obtained by the cells cultured on the modified and unmodified with respect to the traditional culture system. High albumin and low AFP gene expression were found in the cells cultivated in both membranes. The analyses of cell cycle progression revealed that the

most of the cells grew on the membranes, exhibiting also the highest telomerase activity. From the combination of these results it is possible to conclude that the modified and unmodified membranes gave support to the expansion of rat embryonic liver cells and were able to guide the cells towards the acquisition of the functional differentiation as well.

The advantage of using a membrane biohybrid system rather than the traditional culture system consists in providing a threedimensional structure and template upon which the tissue-specific cells can attach, proliferate and produce ECM. A good strategy when designing these systems is the use of materials with controlled biodegradability or bioresorbability so that tissue will eventually replace the scaffold. With this purpose in mind, new membranes made of chitosan, a natural biodegradable material, were proposed. Therefore, membranes prepared from chitosan and modified polyetheretherketone were used for testing their ability to promote the expansion and functional differentiation of rat embryonic liver cells. The structural similarity of the chitosan to the glycosamminoglycans enhanced cell adhesion and proliferation with a complete coverage of the available space and the formation a cord-like structure typical of the liver parenchyma. Also on the PEEK-WC membrane the cells appeared well spread with the formation of tight cell-cell contact. The staining for actin and vinculin confirmed a maintenance of cell morphology similar to that in vivo, demonstrating that the membranes provide good microenvironments for the cells. The analyses of the specific liver metabolic activity assessed the suitability of the membranes, in particular of the chitosan, to commit the cell differentiation. In fact, the cells cultured on this membrane were able to perform urea synthesis, albumin production and to biotrasform the diazepam. Furthermore, the detection of the albumin protein through western blot analysis gave additional proof that the cells underwent to differentiation acquiring the main specific features of the mature liver cells.

To further asses the useful application of the membrane biohybrid systems in tissue engineering applications, membrane bio-hybrid systems of neuronal cells isolated from hippocampus and semipermeable membrase in flat (2D) and hollow fiber (3D) configurations were developed. In such neurobiotechnology application the membranes favor the adhesion and compartimentalization of cells and the regeneration of a highly branched neuronal network. On both bidimensional systems as well as on the reference

system, the cells were able to recreate the neuronal network, that appear more complex during the entire culture period. Concerning the use of bidimensional systems, the highest values of neurites length as well as of the area covered by the cells were obtained by using the PAN membranes. Moreover, the evaluation of the metabolic activity increased in a time dependent manner, showing that the systems supported the long term cells viability and the specific functionality. The use of hollow fiber membranes allowed the recreation of a three-dimensional system capable of mimicking in vitro the ultrastructural organization of the Nervous System. The morphological analysis showed that the threedimensional system strongly contributed to the recreation of a highly branched neural network especially on PAN HF. Also the highest rate of metabolic activity was observed on PAN HF membrane with respect to the PEEK-WC HF. Indeed, neuronal cells adhered outside HF membranes surface and developed a typical well defined shape, with a primary apical axon and many branched dendrites developing synaptic contacts.

Concluding, both 2D and 3D systems were able to support the cell adhesion and neurite outgrowth and alignment and the differences revealed in these two systems are strictly related to the intrinsic characteristics of the membranes in terms of transport and conformational properties.

Several studies in literature focus on investigating the behavior of neurons to specific topographical features for creating new biomaterials able to provoke particular cell responses.

In the last part of the experimental work neuronal hippocampal cells have been cultured on micropatterned and non patterned PLLA membranes, in order to evaluate the effect of different topographic features on neuron polarization, axon length, axon alignment and cell morphology.

The hippocampal neurons responded differently to topographies of different size and shape, and neurites on all investigated patterned membranes linearly extended along the grooves of micro-patterns whereas on the non patterned membrane were more randomly distributed.

The highest orientation degree was observed on the patterned porous membranes with channel width of 20 μm and ridges of 17 μm where the highest frequency of neuronal orientation was observed. In all the investigated patterned membranes the induced

orientation was maintained accompanied by an increasing number of synaptic contacts as shown shown by the confocal images.

The ability of the PLLA patterned membranes to induce the neuronal alignment determines the creation of an ordered neuronal cell matrix showing that specific biomaterials features can act at the interface cell-substrate modulating the cellular behavior. The role played by the topographic features might be used in providing new insight in the study of the regeneration process.

The main outcome of the whole experimental design was the ability to recreate different biohybrid systems to be used as in vitro models for testing new drugs as alternative to animal experimentation or as a platform for the study of pathophysiological events that may occur in tissue disease, representing a valuable tool for liver and neuronal tissue engineering applications and regenerative medicine.

*OTHER PUBBLICATIONS*

***List of other publications in international journals from December 2007:***

**1.** Morelli S., Salerno S., **Piscioneri A**., Rende M., Campana C., De Bartolo L., "Membrane approaches for liver and neuronal tissue engineering". In : Enrico Drioli and Lidietta Giorno, Comprehensive Membrane science and Engineering 2010, 3 :229-252 Oxoford: Academic Press.

**2.** Morelli S., Salerno S., **Piscioneri A.**, Campana C., Drioli E., De Bartolo L. "Membrane bioreactors for regenerative medicine: an example of the bioartificial liver", *Asia-Pacific Journal of Chemical Engineering* 2010, **5**: 146–159 .

**3.** Salerno S., **Piscioneri A.**, Laera S., Morelli S., Favia P., Bader A., Drioli E., De Bartolo L., "Improved functions of human hepatocytes on $NH_3$ plasma-grafted PEEK-WC-PU membranes", *Biomaterials.* 2009; 30(26):4348-4356.

**4.** Laera S., Lopez L.C., De Bartolo L., Morelli S., Salerno S., **Piscioneri A.**, Nardulli M., Gristina R., d'Agostino R., Favia P., "$H_2$-$NH_3$ Plasma-grafting of PEEK-WC-PU membranes to improve their cytocompatibility with hepatocytes. *Plasma Polymer and Processes* 2009; 6: S81–S84.

**5.** De Bartolo L., Salerno S., Curcio E., **Piscioneri A.**, Rende M., Morelli S., Tasselli F., Bader A., Drioli E., "Human hepatocyte functions in a crossed hollow fiber membrane bioreactor", *Biomaterials* 2009 , 30 (13) :2531-2543.

**6.** De Bartolo L., Rende M., Morelli S., Giusi G., Salerno S.**, Piscioneri A.**, Gordano A., Di Vito A., Canonaco M. , Drioli E., "Influence of membrane surface properties n the growth of neuronal cells isolated from hippocampus", Journal of Membrane Science 2008; 325: 139-149.

**7.** Morelli S., Salerno S., **Piscioneri A.,** Rende M., Campana C., Drioli E., De Bartolo L., "Membranes in regenerative medicine and tissue engineering", Membrane Operations; Wiley VCH, *E. Drioli, L. Giorno (eds.)*, 1st Ed. – April 2009; ISBN-10: 3-527-32038-5; 433-446.

***Proceedings***

1. Salerno S, Curcio E, **Piscioneri A**, Rende M, Morelli S, Tasselli F, Bader A., Drioli E. De Bartolo L . Nanostructured Membrane Bioreactor for liver tissue engineering as a tool for drug testing. Nanotec2009.it. Nanotechnologies: Competitiveness & Innovation for industrial growth, March 31-April 3, 2009 Rome, Italy; pp:201-2.

2.

3. De Bartolo L, **Piscioneri A.**, Campana C., Salerno S. , Bader A and Drioli E. Chitosan Membrane Bioartificial Systems for Liver Tissue Engineering. International Conference on Processing and Manufacturing of Advanced Materials. August 25-29, 2009 Berlin, Germany.

4. De Bartolo, Morelli S., Salerno S., Piscioneri A., Rende M., Campana C., Drioli E. Development of membrane biohybrid systems for liver and neuronal tissue engineering. XXXVI European Society for Artificial Organs Congress, Compiegne, France, 2-5 September 2009. Int J. Artif. Organns 2009; 32 (7):409.

5. De Bartolo L, Salerno S, Curcio E, **Piscioneri A**, Rende M, Morelli S, Tasselli F, Bader A and Drioli E.Crossed hollow fiber membrane bioreactor using human hepatocytes for in vitro study of drugs and metabolic disease. *Euromembrane* 2009, Montpellier -France, 6-10 september 2009.

6. **Piscioneri A**, Campana C, Salerno S, Morelli S, Tasselli F, Bader A, Drioli E and De Bartolo L. A chitosan membrane biohybrid system for liver progenitor cells. 4th World Congress on Regenerative Medicine, March 12-14, 2009, Bangkok, Thailand. Current Regenerative Medicine, 2009; pp:99.

7. De Bartolo L, Salerno S, Curcio E, **Piscioneri A**, Rende M, Morelli S, Tasselli F, Bader A and Drioli E. A crossed hollow fiber membrane bioreactor for liver tissue engineering. 4th World Congress on Regenerative Medicine, March 12-14, 2009, Bangkok, Thailand. Current Regenerative Medicine, 2009; pp:68.

8. Laera S, Lopez LC, De Bartolo L, Morelli S, Salerno S**, Piscioneri A**, Nardulli M, Gristina R, d'Agostino R, Favia P. *$H_2/NH_3$ plasma–grafted PEEK-WC-PU membranes improve the biological behaviour of* human hepatocytes. Eleventh International Conference on Plasma Surface Engineering, September 15-19, 2008, Garmisch-Patenkirchen, Germany.

9. Salerno S**, Piscioneri A**, Morelli S, Laera S, Rende M, Favia P, Drioli E, Bader A, De Bartolo L. *Behaviour of human hepatocyte in ammonia plasma-grafted PEEK-WC-PU membrane bio-hybrid system*, September 3-6 Geneve;. In Int J Artif Organs 2008; 31 (7): 586-7.

10. De Bartolo L, Salerno S**, Piscioneri A**, Morelli S, Rende M, Campana C, Drioli E. *Bioactive membranes for liver tissue engineering.* The International Congress on Membranes and Membrane Processes, July 12-18, 2008, Honolulu, Haway

11. De Bartolo L, Rende M, Morelli S, Giusi G, Salerno S, **Piscioneri A**, Gordano A, Canonaco M, Drioli E. *Morphological and functional features of neurons isolated*

*from hippocampus on different membrane surfaces*. The International Congress on Membranes and Membrane Processes, July 12-18, 2008, Honolulu, Haway.

12. Salerno S**, Piscioneri A**, Morelli S, Rende M, Campana C, Bader A, Drioli E, De Bartolo L. *Membrane biohybrid systems for liver tissue engineering.* TERMIS-EU 2008, June 22-26, 2008, Porto, Portugal. Tissue Engineering, 2008; 14(5A): 755.

13. Rende M, Morelli S., Giusi G, Salerno S. **Piscioneri A**., Gordano A. Canonaco M., Drioli E. *Effect of membrane surface on Hippocamapal neuronal cells differentiation.* TERMIS-EU 2008, June 22-26, 2008, Porto, Portugal. Tissue Engineering, 2008; 14(5A): 725-726.

14. De Bartolo L, Rende M, Giusi G, Morelli S, **Piscioneri A**, Salerno S, Canonaco M and Drioli E. *Hollow fiber membranes for neuronal cell differentiation*. 8th World Biomaterials Congress, May 28-June 1, 2008, Amsterdam RAI, The Nederlands.

*SCIENTIFIC ACTIVITY*

***Involved in the following projects***

- Research Project :"Membrane system in regenerative medicine, tissue engineering, and biotechnology", KACST-ITM-CNR, financed by KACST, SA.

- PRIN project prot. 2007SCPN4C_003, financed by the MIUR with the title "Studio dell'effetto dell'IL-6 sull'espressione dei recettori di membrana e trasduzione del segnale in epatociti umani in un sistema bioibrido a membrana". Period : (2008-2010).

- NanoMemPro, "The European Network of Excellence on Nanoscale-based Membrane Technologies", Project financed by the European Community in the FP6.

- Livebiomat project STREP NMP3-CT-013653 in the FP6, with the title: "Development of new polymeric biomaterials for in vitro and in vivo liver reconstruction" (2005-2008)

***Courses attended***

- NanoMemCourse: "Nano-structured materials and Membranes for Health and Sustainable Water", at University of Twente , 7-16 April, 2010.

- 4th World Congress on Regenerative Medicine, Marzo 12-14, 2009, Bangkok, Thailand (**Oral presentation)**.

# APPENDIX

Biomaterials 30 (2009) 4348–4356

Contents lists available at ScienceDirect

Biomaterials

journal homepage: www.elsevier.com/locate/biomaterials

# Improved functions of human hepatocytes on $NH_3$ plasma-grafted PEEK-WC–PU membranes

Simona Salerno [a], Antonella Piscioneri [a,b], Stefania Laera [c], Sabrina Morelli [a], Pietro Favia [c], Augustinus Bader [d], Enrico Drioli [a,e], Loredana De Bartolo [a,*]

[a] Institute on Membrane Technology, National Research Council of Italy, ITM-CNR, c/o University of Calabria, via P. Bucci cubo 17/C, I-87030 Rende (CS), Italy
[b] Department of Cell Biology, University of Calabria, via P. Bucci, 87030 Rende (CS), Italy
[c] Department of Chemistry, University of Bari, via Orabona 4, 70126 Bari, Italy
[d] Biomedical-Biotechnological Center, BBZ, University of Leipzig, Germany
[e] Department of Chemical Engineering and Materials, University of Calabria, via P. Bucci, I-87030 Rende (CS), Italy

ARTICLE INFO

*Article history:*
Received 1 April 2009
Accepted 29 April 2009
Available online 4 June 2009

*Keywords:*
Human hepatocytes
$NH_3$ plasma
Liver specific functions
Cell morphology
Membranes

ABSTRACT

PEEK-WC–PU membranes were modified with an $NH_3$ glow discharge process to graft N-containing functional groups at their surface in order to improve the maintenance of human hepatocytes. Native and modified membrane surfaces were characterized with XPS, ToF-SIMS and WCA measurements. We have investigated morphological behaviour and specific functions of primary human hepatocytes on native and modified PEEK-WC–PU membranes in a small-scale gas-permeable bioreactor. N-containing groups grafted at the surface of the membranes improved the initial steps of adhesion and the maintenance of phenotype and differentiated functions of cells. Confocal microscopy of cell morphology evidenced human hepatocytes exhibiting a polygonal shape and organizing a 3D structure. The presence of CK19 positive cells, a marker of biliary duct epithelium, was also found on native and modified membranes. Liver specific functions, investigated in terms of urea production, albumin synthesis and diazepam biotransformation, were maintained at high levels up to 19 days, particularly on surface-modified membranes.



## 1. Introduction

Biomaterials in tissue engineering and regenerative medicine should provide the necessary support for cell proliferation and maintenance of their differentiated functions. It is well known that cells interact *in vivo* among each other and with their microenvironment, e.g., with the proteins of the extracellular matrix (ECM), through receptors present over their membrane. This communication integrates and coordinates the various gene expression patterns that are crucial for tissue function and homeostasis. Various natural and synthetic materials have been used for culture of anchorage-dependent cells such as hepatocytes. Natural materials including components purified by ECM such as proteoglycan, fibronectin, laminin and collagens have been proposed as substrates for hepatocyte adhesion [1–3]. These materials have the advantages to favour interactions with cells through the integrins, but on the other hand their availability is limited, their costs are high and their composition is variable from batch to batch.

Synthetic polymeric materials are attractive because of their reproducible composition and their well defined and characterized nano and micro-structure. Polymeric semipermeable membranes with different physico-chemical and transport properties are appealing in tissue engineering and bioartificial organs since they share similarities with biomembranes, such as selective molecules transport, resistances and protection [4]. Furthermore, synthetic membranes can easily be mass produced with modulated morphological and physico-chemical properties for specific applications. We have developed a membrane from a polymeric blend of modified polyetheretherketone (PEEK-WC) and polyurethane (PU) as support for hepatocyte culture [5]. This membrane combines advantageous properties of both polymers (biocompatibility, thermal and mechanical resistance, elasticity) with those of membranes (permeability, selectivity and well defined geometry). Human hepatocytes cultured on such PEEK-WC–PU membranes showed adhesion efficiency comparable with that of cells cultured on natural substrates such as collagen [5].

* Corresponding author. Tel.: +39 0984 492036; fax: +39 0984 402103.
*E-mail addresses:* l.debartolo@itm.cnr.it, loredana.debartolo@cnr.it (L. De Bartolo).

0142-9612/$ – see front matter © 2009 Elsevier Ltd. All rights reserved.
doi:10.1016/j.biomaterials.2009.04.052

For this study we have modified PEEK-WC–PU membranes with an $NH_3$ glow discharge plasma aiming to graft nitrogenated functionalities at their surface, in order to investigate whether the maintenance of differentiated functions of human hepatocytes could be enhanced. Among several surface modification strategies, grafting of N-containing functional groups allows to increase the polarity of the surface and to have chemical groups typical also of proteins that could support cell adhesion and functions.

Low-temperature plasma modification (etching, deposition and grafting) processes are widely used to modify the surface of biomaterials, including membranes, with tunable density of surface functional groups, without altering their bulk [6,7]. Plasma treatments (grafting) with $NH_3$ or $N_2$ feeds and plasma deposition processes with N-containing monomer feeds (e.g., allylamine), can provide polymer surfaces with N-containing functional groups, whose distribution and density can be tuned with the plasma parameters, and depend also on ageing processes (hydrophobic recovery, surface oxidation, etc.). The surface density of $-NH_2$ groups plasma-grafted on polyethylene, for example, can be tuned among all other N-groups by changing $NH_3/H_2$ feed ratio, power input, sample position (glow-afterglow) and process duration [8]. Polar O- and N-groups generated on polymer surfaces are pursued to confer and improve "biological activity" and cell adhesion to materials [9–15].

We have plasma-grafted N-groups at the surface of PEEK-WC–PU membranes to improve adhesion and functions of human hepatocytes. Cell morphology and adhesion of hepatocytes were investigated on native and modified PEEK-WC–PU membranes, as well as cell phenotype and liver functions relevant in the case of organ replacement or regeneration.

## 2. Materials and methods

### 2.1. Membrane preparation

Native membranes were prepared from a blend of modified PEEK-WC (patented by Zhang et al. [16] and provided by the Institute of Applied Chemistry, Changchun, China) i.e., poly(oxa-1,4-phenylene-oxo-1,4-phenylene-oxa-1,4-phenylene-3,3-(isobenzofurane-1,3-dihydro-1-oxo)-diyl-1,4-phenylene) and PU by means of the inverse phase technique by using the direct immersion-precipitation method as previously described [5]. The PEEK-WC is obtained by polycondensation reaction between 4,4-dichlorobenzophenone and phenolphthalein [16].

### 2.2. Membrane modification

#### 2.2.1. Plasma processes

Plasma pre-treatments with $H_2$ and treatments with $NH_3$ processes were performed in a pyrex plasma reactor, described in detail elsewhere [17], equipped with two internal steel electrodes in parallel plate configuration. The $H_2$ pre-treatment was found efficient to slow down the ageing of the modified membranes after the N-grafting process, as it will be explained in the next. Discharges were ignited between the radiofrequency (RF, 13.56 MHz; ENI-ACG-10 generator, and impedance matching network) driven upper electrode and the flat lower internal electrode, 7 cm far, ground, used as substrate holder. $H_2$ generated with a HG200 Claind Hydrogen Generator and 99.999 % purity $NH_3$ (Air Liquide) was fed trough electronic MKS mass flowmeters. A rotative pump was used to keep the pressure constant during the processes (base pressure $10^{-3}$ Torr); the pressure was controlled with an MKS baratron. The two plasma processes were performed in sequence, without opening the reactor in between, in the following experimental conditions: pre-treatment: 10 sccm $H_2$ flow rate; 200 m Torr pressure; 30 W power; 1 min; treatment 10 sccm $NH_3$ flow rate; 200 m Torr pressure; 20 W power; 1 min.

Plasma parameters of both processes were optimized in order to maximize the grafting extent of N-groups, measured by the N/C ratio of the modified PEEK-WC–PU surface, and to slow down the hydrophobic recovery of the modified polymer and retain with time the surface properties gained [17]. Soon after the plasma modification, processed membranes were stored in polystyrene boxes and used for cell culture experiments within 8 days.

#### 2.2.2. Surface characterization

The surface composition of the membranes was examined within 1 h after the plasma process and 7–15 days after by means of X-ray photoelectron spectroscopy (XPS), in order to evaluate their ageing. A Thermo VG Scientific XPS instrument (monochromatic AlKα X-rays source; 1486.6 eV, 100 W, 400 μm spot size) was used, at a take-off angle of 53° with respect to the normal to the sample surface (sampling depth $6 \pm 2$ nm). Survey (0–1100 eV Binding Energy, BE) and high-resolution spectra (C1s, N1s, O1s) were recorded. Error bars resulted from measurements performed on 3–5 different spots on the same substrate, on 3–5 substrates of the same kind. C1s spectra were best-fitted with 6 components: C0 (BE $285.0 \pm 0.2$ eV, reference; C–C, C–H); C1 (BE $286.4 \pm 0.2$ eV; C–O–C, C–OH, C–N); C2 (BE $287.6 \pm 0.2$ eV; C═O, O–C–O, N–C═O); C3 (BE $289.2 \pm 0.2$ eV; COOH, COOR, O–CONH); C4 (BE $289.9 \pm 0.2$ eV; shake up, aromatic structures) and C5 (BE $291.8 \pm 0.2$ eV; shake up, C═O).

Sessile drop water contact angle (WCA) measurements were performed in static mode with a CAM 200 contact angle instrument (KSV Instruments LTD, Helsinki, Finland) equipped with a photocamera. 2 ml drops of double distilled water were used. WCA values were measured within 1 h after the surface modification process, and many times during 2–3 weeks. The CAM software of the instrument was utilized to fit the shape of the drop and determine the WCA tangent with the Young–Laplace equation. Error bars resulted from measurements performed on 3–5 different spots per substrate, on 2–4 substrates of the same kind.

ToF-SIMS analysis was performed with an ION-TOF (IV) ToF-SIMS system equipped with a 25 keV cluster metal ion source operating with $Bi^{3+}$ primary ions. Spectral analyses have been obtained from $250 \times 250\ \mu m^2$ spots in high mass resolution burst mode (resolution $M/\Delta M > 6000$). The total ion beam dose was limited to less than $1 \times 10^{12}$ ions/cm$^2$, within the static SIMS regime.

### 2.3. Human hepatocytes culture

Primary human hepatocytes (Lonza Sales Ltd, Basel, Switzerland) isolated from non-transplantable tissue of young single donors were used for cell culture experiments. The purity of isolated hepatocytes is 95% and nonparenchymal cells are present in a very low percentage (5%). Cryopreserved human hepatocytes were quickly thawed in a 37 °C water bath with gentle shaking. Then, the cell suspension was transferred slowly into a tube containing 30 ml of cold hepatocyte culture medium (HCM™, Lonza Sales Ltd, Basel, Switzerland), and centrifuged at 50g at 4 °C for 5 min. The HCM™ is constituted of hepatocyte basal medium (HBM™, Lonza Sales Ltd, Basel, Switzerland) together with all the components provided in HCM™ bulletkit® (Lonza Sales Ltd, Basel, Switzerland): epidermal growth factors, insulin, ascorbic acid, transferrin, hydrocortisone 21-hemosuccinate, bovine serum albumin–fat acid free 2% (BSA–FAF) and gentamicin sulphate 50 μg/ml amphotericin B 50 ng/ml. The cell pellet was suspended in HCM™ and tested for the cell viability by Trypan blue exclusion.

Human hepatocytes were seeded at a final concentration of $2.5 \times 10^5$ cells/cm$^2$ on native and plasma-grafted PEEK-WC–PU membranes previously conditioned with hepatocyte culture medium supplemented with bovine serum albumin–fat acid free 2% (BSA–FAF), in a small-scale gas-permeable bioreactor system [18]. Native and modified membranes were located in tight contact with the gas-permeable membrane of the bioreactor, to ensure optimal transfer of $CO_2$, $O_2$ and $H_2O$ vapour in the culture chamber. Cells were incubated at 37 °C in a 5% $CO_2$; 20% $O_2$ atmosphere (v/v) with 95% relative humidity in hepatocyte culture medium containing 2% BSA–FAF for the first 24 h, thereafter under serum-free conditions for the total culture time. Experiments were performed in the presence of diazepam 10 μg/ml in the culture medium to evaluate the ability of cells to perform drug biotransformation functions, in particular the elimination of diazepam and the formation of its metabolites.

The morphology of the cells cultured on native and modified membranes was assessed by means of Scanning Electron Microscopy (SEM) and Laser Confocal Scanning Microscopy (LCSM).

Liver specific cellular functions were investigated in terms of albumin production and urea synthesis.

### 2.4. Hepatocyte fixation for SEM

Cells cultured for 19 days on native and modified membranes were prepared for SEM analysis by fixation in 3% glutaraldehyde and 1% formaldehyde in PBS, followed by post-fixation in 1% osmium tetroxide and progressive ethanol dehydration.

### 2.5. Hepatocyte staining for LCSM

The morphological behaviour of human hepatocytes cultured on native and modified membranes was investigated at 7, 13 and 19 days of culture with Laser Confocal Scanning Microscopy (LCSM) after cytoskeleton and ECM protein immunostaining. Samples were rinsed with PBS, fixed for 15 min in 3% paraformaldehyde in PBS at room temperature (RT), permeabilized for 5 min with 0.5 % Triton-X100 and saturated for 15 min with 2% Normal Donkey Serum (NDS).

To visualize vinculin, a mouse monoclonal antibody raised against human vinculin (Santa Cruz Biotechnology, Santa Cruz, CA) and a Cy™3-conjugated AffiniPure donkey anti-mouse IgG (Jackson ImmunoResearch Europe Ltd, Cambridge, UK) was used. Actin was stained with phalloidin Alexa 488 conjugated (Molecular Probes, Inc, Eugene, OR). To visualize laminin a rabbit polyclonal antibody raised against laminin α-4 of human origin (Santa Cruz Biotechnology, Santa Cruz, CA) and a Cy™2-conjugated AffiniPure donkey anti-rabbit IgG (Jackson ImmunoResearch Europe Ltd,

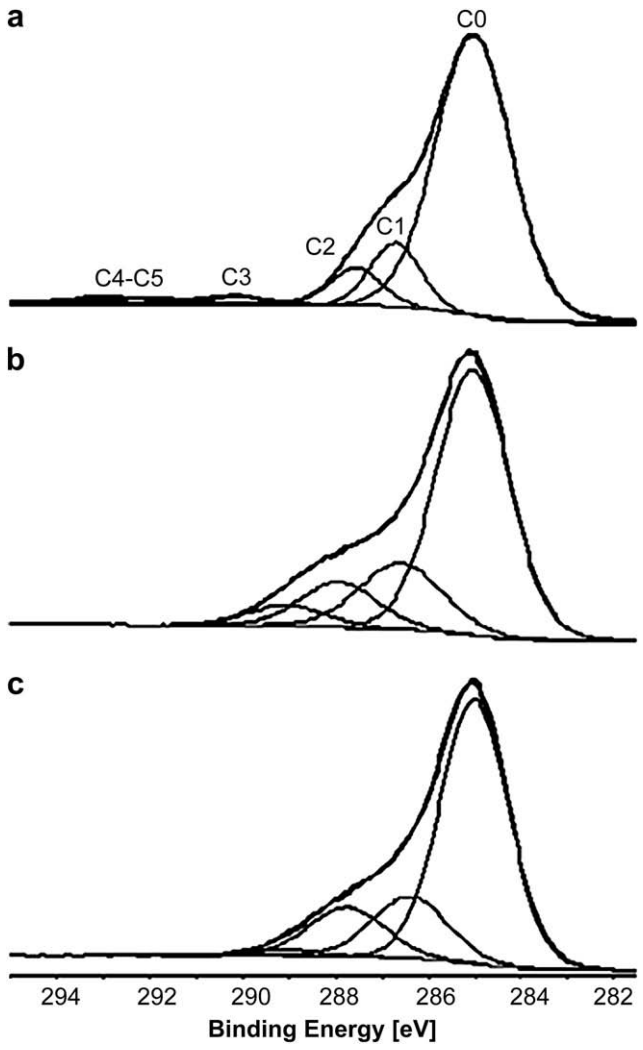


**Fig. 1.** C1s spectra of the PEEK-WC–PU membrane (a) native, (b) just after the $H_2/NH_3$ plasma process and (c) after 8 days of ageing in air.

Cambridge, UK) was used. To visualize fibronectin a mouse monoclonal antibody raised against human fibronectin (Santa Cruz Biotechnology, Santa Cruz, CA) and a Cy™3-conjugated AffiniPure donkey anti-mouse IgG (Jackson ImmunoResearch Europe Ltd, Cambridge, UK) was used.

The hepatic bile duct marker Cytokeratin 19 (CK19) was stained with a goat polyclonal antibody raised against human CK19 (Santa Cruz Biotechnology, Santa Cruz, CA) and Cy™5-conjugated AffiniPure donkey anti-goat IgG (Jackson ImmunoResearch Europe Ltd, Cambridge, UK). All primary and secondary antibodies were incubated for 2 and 1.5 h at RT, respectively. Counterstaining for nuclei was performed with DAPI 0.2 μg/ml (Molecular Probes Inc, Eugene, OR) incubated for 30 min. Finally samples were rinsed, mounted and observed with a Laser Confocal Scanning Biological Microscope (Fluoview FV300, Olympus Italia).

### 2.6. Biochemical assays

Samples from the culture medium were collected in pre-chilled tubes and stored at −20 °C until assayed. Albumin secretion was measured with the immunoenzymatic ELISA method. 96 well plates were coated with chromatographically purified human albumin (Sigma, Milan, Italy) 50 μg/ml and left overnight at 4 °C. After 4 rinses, 100 μl of cell culture supernatant were added to the wells and incubated overnight at 4 °C with 100 μl of anti human albumin monoclonal antibody conjugated with horseradish peroxidase (Bethyl Laboratories, Inc., USA). After 4 rinses, the substrate buffer containing Tetramethylbenzidine and $H_2O_2$ (Sigma, Milan, Italy) was added for 7 min and the reaction was stopped with 100 μl of 8 N $H_2SO_4$. Absorbance was measured at 450 nm using a Multiskan Ex (Thermo Lab Systems).

The urea concentration was determined by the quantitative colorimetric urea assay kit QuantiChrom™ (Gentaur, Brussels, Belgium).

The statistical significance of the experimental results was established according to the Unpaired Statistical Student's *t*-test ($p < 0.05$).

### 2.7. HPLC analysis of diazepam and metabolites

Hepatocytes were incubated with 10 μg/ml diazepam; HPLC was used to monitor the biotransformation of diazepam [19] in its metabolites. Aliquots of the culture medium were alkalinized with 20% of 4 M NaOH, precipitated with isopropanol (1:10) and extracted with ethyl acetate (5:1) by gentle rocking for 10 min and subsequent centrifugation at 200*g* for 15 min at RT. The ethyl acetate phase was then evaporated and dried under vacuum, and the pellet dissolved in 96 μl mobile phase consisting of acetonitrile/methanol/0.04%triethylamine pH 7.04 at proportion of 25/35/40 respectively. The samples were HPLC analysed using a $C_{18}$-RP Purosphere Star 5 μm, 250 × 4,6 mm column, equipped with a precolumn (Merck KGaA, Darmstadt, Germany). The sample injection volume was 20 μl. The mobile phase was delivered at 0.8 ml/min and the column was operated at room temperature. Effluents were monitored with a UV detector at 236 nm. Besides diazepam its metabolites temazepam, oxazepam and nordiazepam were detected. For all substances calibration curves were regularly run between 10 ng/ml and 10 μg/ml.

## 3. Results

PEEK-WC–PU membranes were pre-treated in a $H_2$ glow discharge in order to cross-link and stabilize the surface of the membrane before grafting the N-groups, and reduce their hydrophobic recovery ageing [17]; soon after the membranes were plasma-treated in an $NH_3$ discharge in order to graft N-containing functionalities at their surfaces.

XPS spectra and compositional data in Fig. 1 and Table 1 show the surface composition evolution of the PEEK-WC–PU membranes after the $H_2/NH_3$ plasma-process and after 8 days of ageing in air. Since PU is part of the PEEK-WC–PU blend, nitrogen was found at the surface of the native membrane. After the plasma process both the percentage of N surface atoms and the N/C surface ratio increased remarkably, due to the grafting of N-containing active species from the $NH_3$ plasma. Tof-SIMS and WCA data, shown in the next, are in agreement with this finding. After 8 days of ageing a slightly lower density of N-groups was stabilized at the surface of the membranes, that remained stable with time. These last data are representative of the membrane surface utilized in contact with cells during the biological experiments.

C1s spectra in Fig. 1 refer to the PEEK-WC–PU membrane (a) native; (b) within 1 h after the $H_2/NH_3$ plasma process; and (c) after 8 days of ageing in air. Spectra were best-fitted with the C0–C5 components described in the Materials and methods section. In spectrum (a) component C0 refers to aromatic carbon atoms in PEEK-WC; C1 to ether groups in PEEK-WC and PU; C2 to carbonyl moieties in PEEK-WC; C3 to carboxyl groups in PEEK-WC and to urethane in PU; C4 and C5 shake-up structures are related to aromatic structures and C═O double bonds. Fragmentation and recombination plasma reactions generate several nitrogen species in the $NH_3$ discharge (NH radicals and $N_2$ molecule were detected,

**Table 1**
XPS atomic percentages and relative percentages of the C0–C6 components (see Materials and methods section for the assignments) to each C1s signal. The error estimated is within ±10%.

| PEEK-WC–PU | C% | O% | N% | O/C | N/C | C0 | C1 | C2 | C3 | C4 | C5 |
|---|---|---|---|---|---|---|---|---|---|---|---|
| Native | 80.9 ± 4.0 | 17.0 ± 1.0 | 2.1 ± 0.1 | 0.21 ± 0.02 | 0.026 ± 0.003 | 77.3 | 12.1 | 7.0 | 1.3 | 1.6 | 0.7 |
| Within 1 h after the process | 67.2 ± 3.4 | 12.9 ± 0.6 | 19.9 ± 1.0 | 0.19 ± 0.02 | 0.296 ± 0.030 | 64.8 | 18.3 | 11.6 | 5.3 | – | – |
| 8 days after the process | 67.5 ± 3.4 | 12.3 ± 0.6 | 17.5 ± 0.9 | 0.18 ± 0.02 | 0.259 ± 0.026 | 67.5 | 17.2 | 13.8 | 1.5 | – | – |

for examples, by Favia et al. [8]), that react with the polymers exposed and generate N-containing groups at their surface. Surface amine, imide, cyano and other functional groups can be produced in this way, whose distribution is highly dependent on the nature of the polymer and on the conditions of the discharge. Interactions with air modify further the surface of the treated polymer through oxidation reactions (e.g., formation of amides, and of O-containing functionalities) and hydrophobic recovery (grafted N-polar groups tend to rotate underneath, untreated polymer chains tend to rotate toward the polymer–air interface [9,17]). The composition of the final surface of the material can be stabilized and tailored after careful optimization of the experimental parameters. After the plasma process (Fig. 1b), nitrogen groups are grafted and, at the same time, the aromatic structures are fragmented at the surface of the membrane, due to the chemical action of the species present in the plasma, and to the positive ion bombardment associated to the plasma process. As a consequence, components C1, C2 and C3, which grafted nitrogen- (amine, amide, etc.) and oxygen- (ether, carbonyl, alcohol, etc.) containing groups contribute to, become more important in trace (b) respect to trace (a), and the shake-up signals C4 and C5 disappear. The ageing after 8 days induces some lowering of peak components C1, C2 and C3, as evident in Fig. 1c, and the overall N/C and O/C surface ratios results only slightly lowered (see Table 1) compared to trace (b), thus attesting that grafted polar groups are still present at the surface of the processed material after 8 days, at the moment of the cell culture experiments. The situation does not change (data not shown) after 15 days of ageing.

The grafting of N-containing polar groups is confirmed also by ToF-SIMS analysis, as reported in Fig. 2, where a comparison of the positive ion SIMS spectra of native and $H_2/NH_3$ plasma-processed and aged PEEK-WC–PU membrane is shown between 10 and 50 $m/z$ units. New and more intense mass peaks appear at 18 ($NH_4^+$), 28 ($CH_2N^+$), and 30 ($CH_4N^+$) $m/z$ on the modified surface. WCA values of $80 \pm 8^\circ$ were measured on native membrane, the large error bar is likely due to pore size distribution and roughness of the membrane surface, as well as of its surface composition (e.g., uneven surface segregation of PU). Much lower values were found after the plasma modification, $41 \pm 9^\circ$, attesting for the grafting of polar groups. After 8 days of ageing in air, during which the hydrophobic recovery took place to some extent, WCA values were found stabilized at $61 \pm 3^\circ$. WCA values of $51 \pm 5^\circ$ were measured, instead, for membranes modified without the $H_2$ pre-treatment; after 8 days such substrates recovered WCA values of $75 \pm 3^\circ$, almost the original WCA value of the native surface.

Primary human hepatocytes were cultured on native and on modified PEEK-WC–PU membranes in the gas-permeable bioreactor system. After the seeding cells adhered rapidly on both kind of membranes, reaching a confluent layer with the establishment of cell–cell contacts. Morphological SEM and LCSM observations show human hepatocytes slightly flattened and spread at the surface of the membrane, where cell–material contacts were established (Figs. 3 and 4). Cells exhibited several tight junctions with neighbour cells, and assumed a polygonal shape on both native and processed membranes. Several cells tended to develop pseudopodia which were anchored in the pores of the membrane (Fig. 3d). The surface of the plasma-processed membrane, in particular, appeared completely covered by cells with a more homogeneous surface distribution (Fig. 3c) with respect to the native membranes (Fig. 3a–b). Further structural morphological investigations were performed with LCSM after cytoskeleton and ECM protein immunostaining, at 7, 13 and 19 days of culture. The staining for actin displayed the overall morphology of cells cultured on native and N-grafted membranes, and the organization of their cytoskeleton actin. Cells on both membranes appeared well spread, with typical longitudinal actin fibres developed (Fig. 4a–b). After 19 days of culture thin filament bundles of actin were observed radially oriented in the area of cell–cell contact, likely to establish concave active arcs along the expanding contacts. Spreading cells were detected in the basal level very close to the membranes, showing that adhesion occurred. In particular, after 19 days, cells grown on modified membranes developed only a limited number of longitudinal stress fibers, and displayed an evident polyhedral shape (Fig. 4b).

Fluorescence staining for vinculin revealed the formation of focal adhesion complexes with a dot-like distribution (Fig. 4a–b). The formation of lumen-like structures is also visible, where surrounding cells were positive for the biliar duct marker CK19 (Fig. 4a–b). Confocal images demonstrated the presence of secreted ECM proteins such as laminin and fibronectin on both membrane surfaces (Fig. 5a–b).

The ability of human hepatocytes to perform their specific functions was investigated up to 19 days of culture. The rate of albumin synthesis was maintained for all culture times with values ranging from $1.50 \pm 0.29$ to $4.11 \pm 1.20$ ng/h$\times 10^6$ cells (Fig. 6). A remarkable difference was observed for albumin produced on modified with respect to native membranes, which was statistically significant on days 7 and 9 ($p < 0.05$), on day 13 ($p < 0.01$) and on day 17 of culture ($p < 0.01$).

Human hepatocytes cultured on native membrane were able to synthesize urea with a rate ranging from $1.97 \pm 0.12$ to $5.52 \pm 1.01$ μg/h$\times 10^6$ cells (Fig. 7); their metabolic activity was found improved on modified membranes. Statistically significant differences ($p < 0.05$) were observed on days 5 and 7.

The ability of the cells to perform drug biotransformation was evaluated after providing 10 μg/ml of diazepam over the whole culture time, and evaluating its elimination and the formation of its metabolites over time. Also the liver biotransformation functions of primary human hepatocytes were maintained for all culture time. The rate of diazepam elimination ranged between $156.8 \pm 14.15$ and $332.46 \pm 55.47$ ng/h$\times 10^6$ cells (data not shown). The diazepam metabolites of the phase I reactions that include oxazepam, nordiazepam and temazepam were detected. Statistically significant differences were observed for the rate of metabolite formation from hepatocytes cultured on plasma-modified membranes with respect to those cultured on native ones (Fig. 8), particularly for temazepam

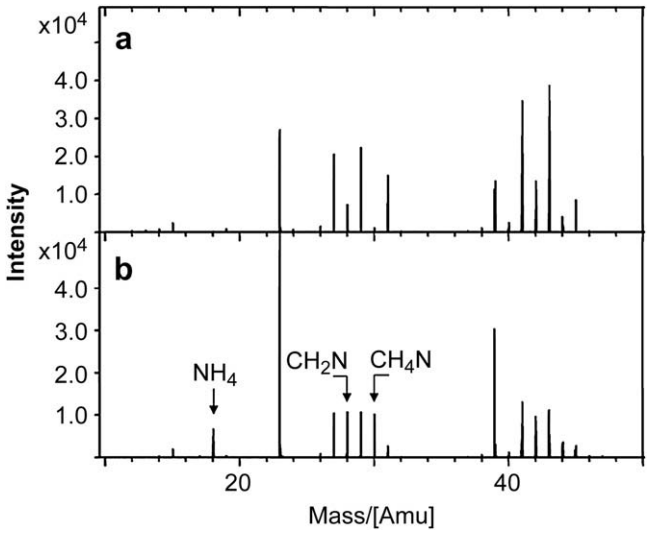


**Fig. 2.** Positive ion SIMS spectra of (a) native and (b) $H_2/NH_3$ plasma-processed and aged PEEK-WC–PU membrane in the 10–50 $m/z$ region.

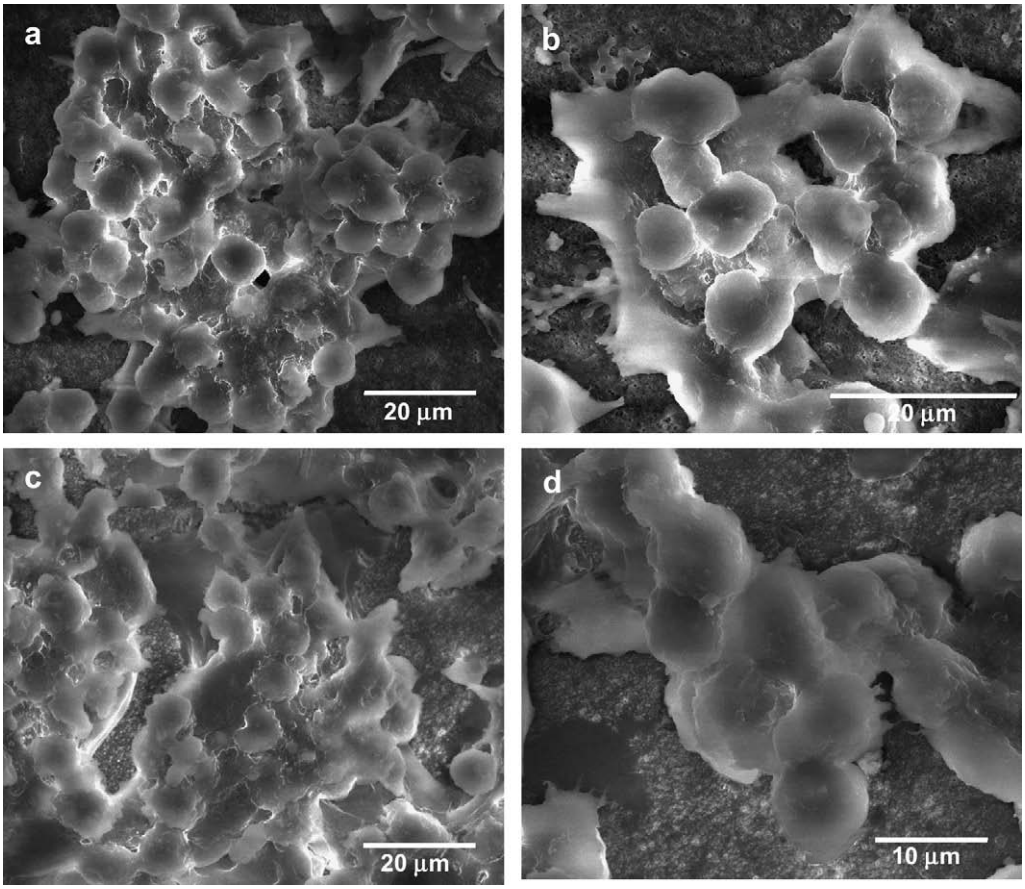


**Fig. 3.** SEM images of primary human hepatocytes after 19 days of culture on native (a,b) and plasma-processed (c,d) PEEK-WC–PU membranes at different magnification.

formation on days 11 and 13 ($p < 0.05$) and on days 7, 15 and 17 ($p < 0.01$), for nordiazepam on days 7 and 15 ($p < 0.01$) and for oxazepam on day 5 ($p < 0.01$) (Fig. 8b). Independently on the type of membranes on which cells were cultured, the clearance of diazepam occurred with the formation of temazepam metabolite to a larger extent with respect to oxazepam and nordiazepam. In particular, an average of 71.2% of temazepam was produced with respect to 7.6% of oxazepam and 21.1% of nordiazepam on modified membranes.

## 4. Discussion

PEEK-WC–PU membranes plasma-grafted with N-groups were investigated in order to improve the adhesion of human hepatocytes and the maintenance of their differentiated functions. Beside grafting N-groups (amines, imines, cyano, etc.), $NH_3$ plasma-treatments, are known to leave polymer surfaces prone to oxidation upon exposure to air due to long-living free radicals; so, as a general effect, the surface of $NH_3$ plasma-treated polymers is usually enriched of both N- and O-containing chemical groups [8,20], all responsible for increasing wettability and improving cell adhesion. Such groups likely influence positively the adsorption of proteins (enhanced and/or selective adsorption, favorable conformation of adsorbed proteins, etc.) from the culture medium first, then the interactions of adhering cells with the adsorbed protein layer. Surface –NH2 groups for example, known to be grafted on $NH_3$-plasma-treated polymers [8], could easily be ionized at physiological pH, and bind negatively charged proteins.

The *ageing* of plasma-treated polymer surfaces is often crucial for applications. When polar groups are covalently bound to surface chains (0–2 nm below the interface) of a hydrophobic polymer, a dynamic polymer/air interface is created which experiences, at different extents, the so called *hydrophobic recovery* of the original moieties of the polymer underneath. Rotational/translational motions, when permitted, allow the original hydrophobic polymer moieties to emerge at the interface to minimize the air–polymer interfacial energy, while polar groups are rotated below. As a consequence, the WCA polymer value lowered by the plasma treatment increases back toward its original value loosing, partially or totally, the properties conferred by the process [17,21–25].

For this work PEEK-WC–PU membranes were first pre-treated in a $H_2$, then in an $NH_3$ RF glow discharge; the pre-treatment cross-links and stabilizes the surface of the membrane before grafting N-groups [17], so the hydrophobic recovery of the final surface is reduced. Ar discharge pre-treatments were also performed, but they were found less efficient in reducing the ageing of N-grafted PEEK-WC–PU. Very likely, the better performance of $H_2$ with respect to Ar is due to the higher UV emission of $H_2$ plasmas, that cross-links deeper layers of the membrane.

Morphology and liver specific functions of primary human hepatocytes were investigated in a small-scale gas-permeable membrane bioreactor, with cells cultured on native and on $NH_3$ plasma-grafted PEEK-WC–PU membranes. Due to the high $O_2$ dependence of primary hepatocytes in long-term cultures, mostly for cell attachment and spreading activities, oxygenating supports offer beneficial culture conditions, close to physiologic ones [26,27]. A membrane permeable to $O_2$, $CO_2$ and water vapor was used to provide oxygen to adherent cells directly, not only through the medium. As shown in previous works, this bioreactor allows to preserve the differentiated state of primary porcine and human

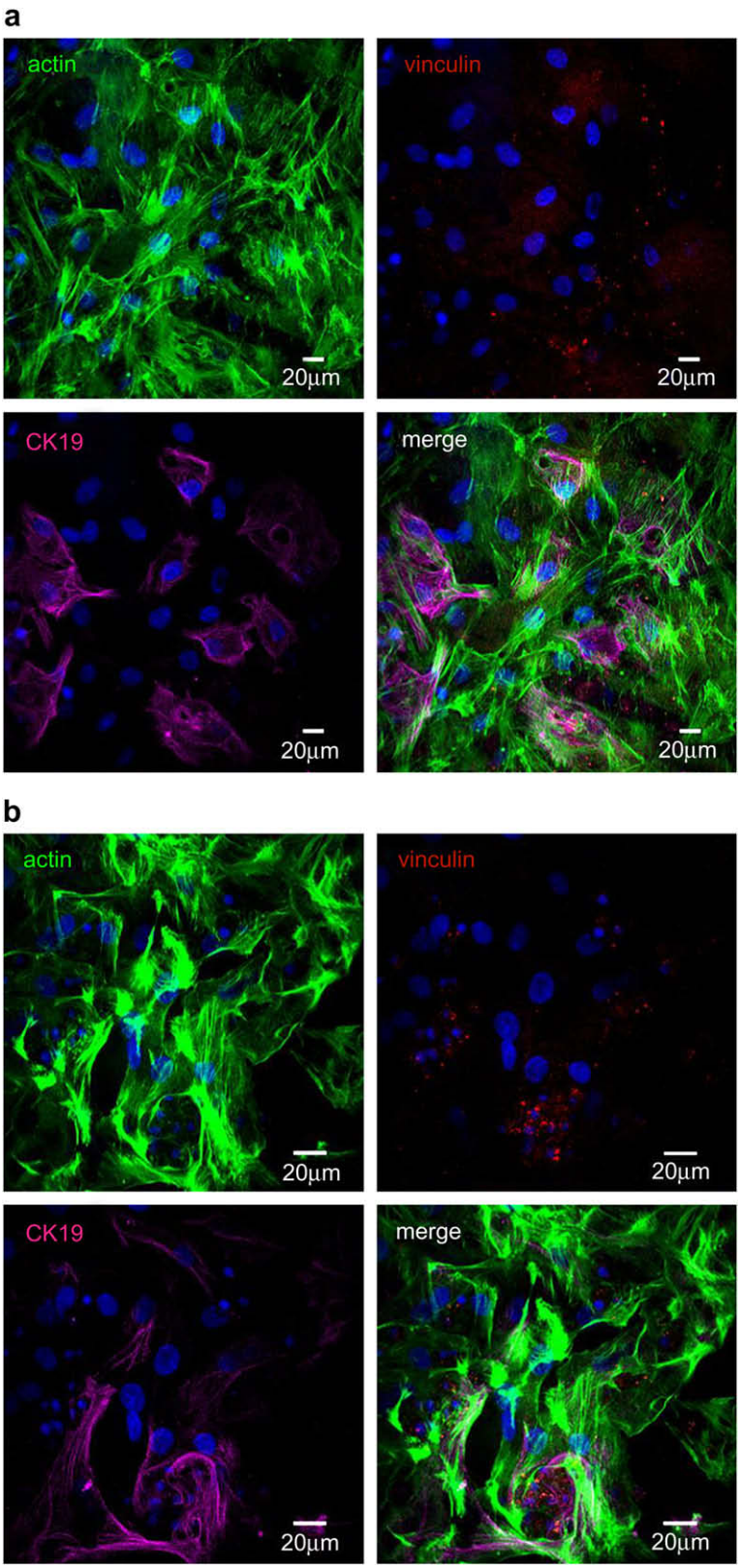


**Fig. 4.** Confocal images of primary human hepatocytes after 19 days of culture on native (a) and modified (b) PEEK-WC–PU membranes. Cells were stained for actin (green), vinculin (red), CK19 (violet) and nuclei (blue).

hepatocytes, as well to maintain their liver specific functions of albumin synthesis, urea synthesis and drug biotransformation [27–29]. The direct delivery of $O_2$ was particularly helpful for maintaining metabolic functions of mouse hepatocyte spheroids [30].

Our $NH_3$ plasma-treatment grafted surface polar N-groups at the PEEK-WC–PU membrane, amines among them, that not only increase its hydrophilicity, but probably also boost the initial protein-mediated cell-membrane interactions and adhesion

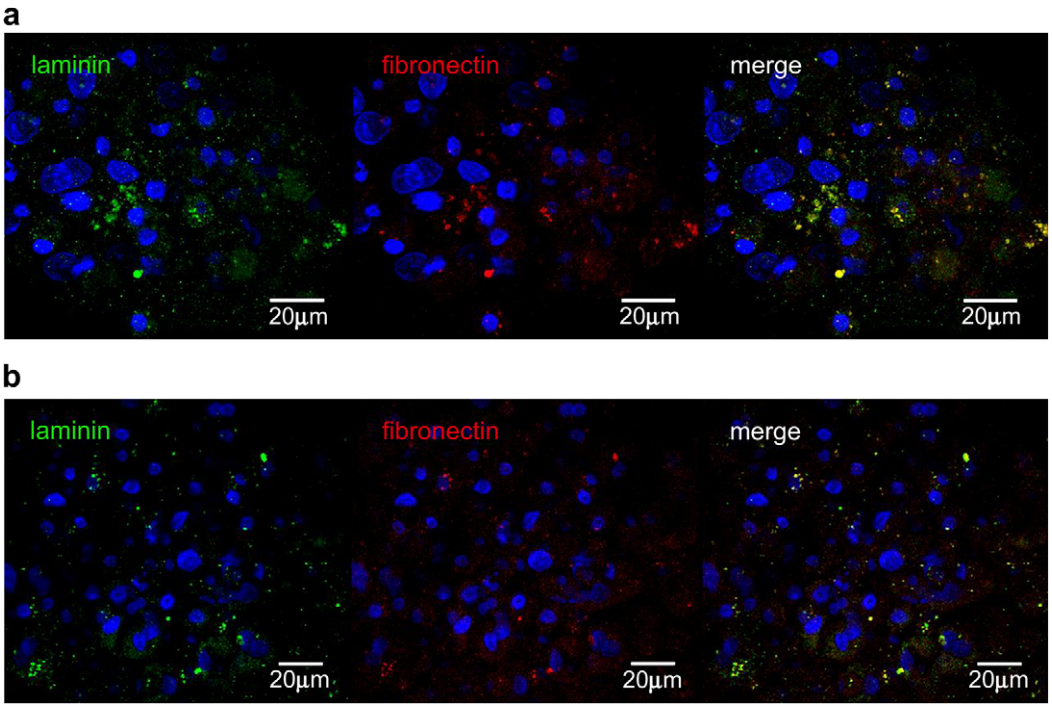


**Fig. 5.** Confocal images of primary human hepatocytes after 19 days of culture on native (a) and modified (b) PEEK-WC–PU membranes. Cells were stained for laminin (green), fibronectin (red) and nuclei (blue).

through improved protein adsorption. Cell–substrate adhesion is a multistep process that involves, in sequence: adsorption of ECM proteins onto the surface; recognition of ECM components by cell receptors; cytoskeletal rearrangements; cell spreading [31,32]. N-groups grafted over the membrane trigger initial adhesion until cells synthesize ECM proteins able of mediating the contact with the membranes through integrins. Amino groups, for example, positively charged at physiological pH, probably interact with negatively charged carboxylated groups of medium proteins in the early-attachment phase, and/or with proteoglycans of the pericellular membranes. These receptors are involved in signal transduction pathways for activating kinases, growth factors, protein synthesis genes, cell proliferation and cytoskeleton organization. ECM proteins interacting with specific cell receptors could, thus, improve cell adhesion at substrates, and support long-term cultures with maintained differentiated functions.

SEM revealed hepatocytes adhering on both native and modified membranes (Fig. 3). In particular, many cells were imaged to adhere and spread on modified membranes through direct interactions with the material, with pseudopodia protruded to find anchor points on the membrane surface, probably to activate cell migration (Fig. 3b).

LCSM observations confirmed that cells on native and modified membranes are engaged in secreting ECM proteins such as laminin and fibronectin, which are both involved in cell adhesion processes through interactions with integrins [33,34].

Further LCSM investigations (Fig. 4) clearly show reorganized cytoskeleton proteins up to 19 days of culture, with the presence of concave active arcs of thin longitudinal actin filament bundles. This arc-like span conformation with bundles of actin filaments radially oriented is usually formed at the edge of expanding cell–cell contacts, while circumferential bundles become discontinuous

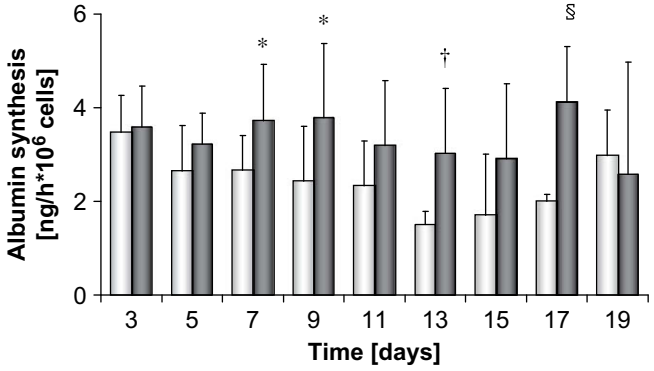


**Fig. 6.** Albumin synthesis of primary human hepatocytes on native (shade bar) and on plasma-processed (full bar) PEEK-WC–PU membranes. The values are the mean of six experiments ± standard deviation. Data statistically significant with respect to native membranes: *($p < 0.05$), † ($p < 0.01$), § ($p < 0.001$).

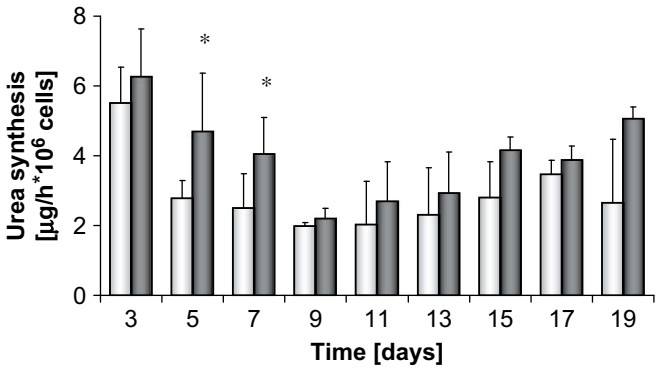


**Fig. 7.** Urea synthesis of primary human hepatocytes on native (shade bar) and plasma-processed (full bar) PEEK-WC–PU membranes. The values are the mean of six experiments ± standard deviation. Data statistically significant with respect to native membranes: *($p < 0.05$).

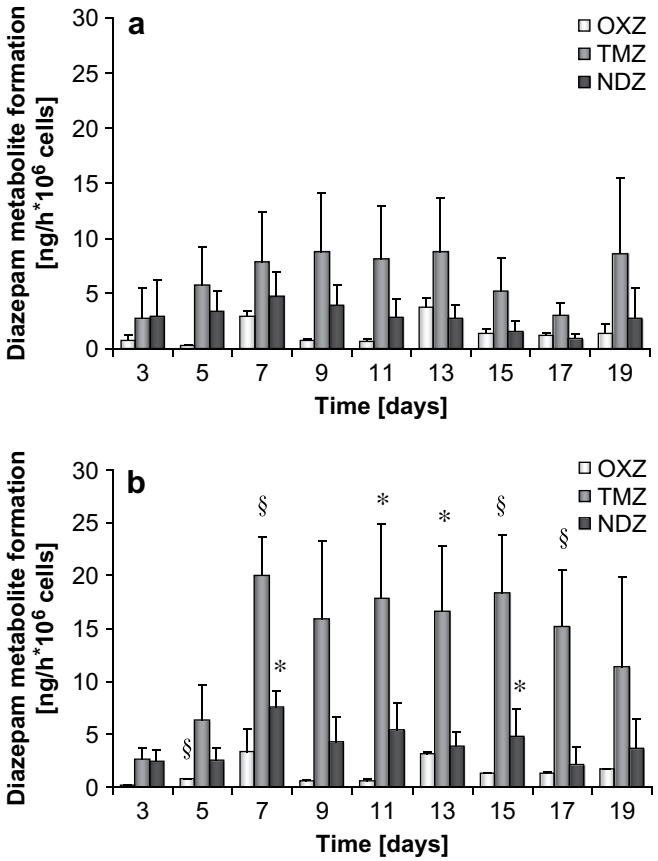


**Fig. 8.** Diazepam metabolite formation of primary human hepatocytes on native (a) and on plasma-processed (b) PEEK-WC–PU membranes. The values are the mean of six experiments ± standard deviation. Data statistically significant with respect to native membranes: *($p < 0.05$), § ($p < 0.001$).

[35]. Hepatocytes cultured on modified membranes appeared slightly flattened with more condensed and circumferentially organized actin with typical polyhedral shape with respect to those cultured on native membranes. This cytoskeletal organization could be due to the more hydrophilic character of the modified membranes, as found also by Krasteva et al. [36] for human C3A hepatoblastoma cells cultured on polyacrylonitrile-*N*-vinyl-pyrrolidone and polyvinylidendifluoride.

Hepatocytes developed enough focal adhesions on both membranes. Vinculin is associated with focal adhesion and regulates both cell–cell and cell–matrix junctions, and binds adhesion complexes to the actin cytoskeleton. Dot-like adhesion foci were evidenced by a punctuate distribution of vinculin staining on hepatocytes cultured on both membranes. The punctuate vinculin distribution could be due to membrane pores where cell protrusions are inserted [3].

LCSM images evidenced also many CK19 epithelial cells displaying reorganized histological architecture with lumen-like structures (Fig. 4). Such cells indicate the formation of biliary ducts, expression of the histological architecture of the liver [37]. The small percentage (5%) of contaminant nonparenchymal cells in the cell suspension obtained during the isolation process would help hepatocytes to organize a characteristic and differentiated histologic architecture; Michalopoulos et al. [38] demonstrated the possibility of phenotypic transition of hepatocytes to biliary epithelial cells in organoid cultures of only hepatocytes in the presence of hepatocyte (HGF) and epidermal (EGF) growth factors [39,40]. Finding CK19 positive cells in our study confirmed that the membranes support, like in the liver, the formation of highly differentiated structures.

Urea synthesis and albumin production were maintained at high levels up to 19 days; in particular hepatocytes cultured on modified membranes expressed such liver specific functions at significantly higher levels with respect to those on native ones (Figs. 6 and 7). Also biotransformation functions were probed; cells were able to clear diazepam up to 19 days of culture, at a larger extent on modified with respect to native membranes (Fig. 8). Diazepam is metabolised in human through 3-hydroxylation by CYP2C19, 3A4 and 3A5 to temazepam and trough *N*-demethylation by CYP2B6, 2C8, 2C9, 2C18, 2C19, 3A4 and 3A5 to nordiazepam [41,42]. These first generation metabolites are then *N*-demethylated by CYP2B6, 2C8, 2C9, 2C19, 3A4 and 3A5 and 3-hydroxylated by CYP2C19, 3A4 and 3A5 respectively to the final metabolite oxazepam [42]. Cell dedifferentiation that may occur in unfavorable culture conditions is accompanied by the loss of some liver specific enzymes, especially cytochrome P450 monooxygenases, affecting the biotransformation capacity of the system [27,43]. The production of all three metabolites on both kind of membranes demonstrated the activity and inducibility maintenance of the phase I CYP isoenzymes achieved in these culture conditions. Our findings are in agreement with those of other authors that observed the improvement of the initial osteoblast functions on titanium surfaces functionalized with amino groups [44]. The presence of positively charged amino groups allowed to significantly improve the initial steps of cellular contacts of the osteoblasts at the surface of the material. Also in our case an improvement of the adhesion process of human hepatocytes and of their following cell organization at the surface of the membrane results in improved maintenance of liver cell functions.

## 5. Conclusions

Plasma grafting of N-groups on PEEK-WC–PU membranes has increased their hydrophilicity and improved interactions with adhering human hepatocytes, probably through improved adsorption of proteins from the culture medium. Specific metabolic functions were sustained at all investigated culture times, thus demonstrating the maintenance of functional integrity of hepatocytes in the membrane bioreactor used. Tissue architecture and parenchymal cell morphology reflected the maintenance of the functional differentiation of hepatocytes cultured on both native and plasma-treated membranes. Cells reconstituted many of the liver features active *in vivo*; when cultured on $NH_3$ plasma-grafted membranes they displayed higher metabolic activity in terms of albumin synthesis, urea production as well as for the biotransformation of diazepam as model drug.

## Acknowledgements

This work was supported by grants from the European Commission through the Livebiomat project STREP NMP3-CT-013653 in the FP6. The authors acknowledge Dr. Francois Rossi and Dr. Douglas Gilliland (Joint Research Center, Ispra (VA), Italy) for SIMS analysis.

## Appendix

Figures with essential colour discrimination. Figs. 4 and 5 in this article are difficult to interpret in black and white. The full colour images can be found in the on-line version, at doi:10.1016/j.biomaterials.2009.04.052.

## References


[1] Yang J, Bei J, Wang S. Enhanced cell affinity of poly (D,L-lactide) by combining plasma treatment with collagen anchorage. Biomaterials 2002;23:2607–14.
[2] Hersel U, Dahmen C, Kessler H. RGD modified polymers: biomaterials for stimulated cell adhesion and beyond. Biomaterials 2003;24:4385–415.
[3] Ma Z, Mao Z, Gao C. Surface modification and property analysis of biomedical polymers used for tissue engineering. Colloids Surf B 2007;60:137–57.
[4] Drioli E, De Bartolo L. Membrane bioreactor for cell tissues and organoids. Artif Organs 2006;30:793–802.
[5] De Bartolo L, Morelli S, Gallo MC, Campana C, Statti G, Rende M, et al. Effect of isoliquiritigenin on viability and differentiated functions of human hepatocytes maintained on PEEK-WC–polyurethane membranes. Biomaterials 2005;26:6625–34.
[6] Sardella E, Favia P, Gristina R, Nardulli M, d'Agostino R. Plasma-aided micro- and nanopatterning processes for biomedical applications. Plasma Process Polym 2006;3:456–69.
[7] Favia P, Sardella E, Lopez LC, Laera S, Milella A, Pistillo B, et al. Plasma assisted surface modification processes for biomedical materials and devices. In: Guceri S, Fridman A, editors. Plasma assisted decontamination of biological and chemical agents, NATO science for peace and security series; 2008. p. 203–26.
[8] Favia P, Stendardo MV, d'Agostino R. Selective grafting of amine groups on polyethylene by means of $NH_3$–$H_2$ RF glow discharges. Plasma Polym 1996;1:91–112.
[9] Siow KS, Brichter L, Kunar S, Griesser HJ. Plasma methods for the generation of chemically reactive surfaces for biomolecule immobilization and cell colonization. Plasma Process Polym 2006;3:392–418.
[10] Daw R, O'Leary T, Kelly J, Short RD, Cambray-Deakin M, Devlin AJ, et al. Molecular engineering of surfaces by plasma copolymerization and enhanced cell attachment and spreading. Plasma Polym 1999;4:113–32.
[11] Hsiue GH, Lee SD, Wang CC, Chang PCT. ppHEMA-modified silicone rubber film towards improving rabbit corneal epithelial cell attachment and growth. Biomaterials 1993;14:591–7.
[12] Sipheia R, Martucci G, Barbarosie M, Wu C. Enhanced attachment and growth of human endothelial cells derived from umbilical veins on ammonia plasma modified surfaces of PTFE and ePTFE synthetic vascular graft biomaterials. Biomater Artif Cell Immobil Biotechnol 1993;21:455–68.
[13] Ben Rejeb S, Tatoulian M, Khonsari FA, Durand FA, Martel A, Lawrence JF, et al. Functionalization of nitrocellulose membranes using ammonia plasma for the covalent attachment of antibodies for use in membrane-based immunoassays. Anal Chim Acta 1998;376:133–8.
[14] Puleo DA, Kissling RA, Sheu MS. A technique to immobilize bioactive proteins, including bone morphogenetic protein-4 (BMP-4), on titanium alloy. Biomaterials 2002;23:2079–87.
[15] Griesser HJ, Chatelier RC, Gengenbach TR, Johnson G, Steele JG. Growth of human cells on plasma polymers: putative role of amine and amide groups. J Biomater Sci Polym Ed 1994;5:531–54.
[16] Zhang HC, Chen TL, Yuan YG. CN Patent No. 85108751; 1987.
[17] Favia P, Milella A, Iacobelli L, d'Agostino R. Plasma pre-treatment and treatments on polytetrafluorethylene for reducing the hydrophobic recovery. In: d'Agostino R, Favia P, Wertheimer MR, Oehr C, editors. Plasma processes and polymers. Weinheim: Wiley-VCH; 2005. p. 271–80.
[18] Schmitmeier S, Langsch A, Jasmund I, Bader A. Development and characterization of a small-scale bioreactor based on a bioartificial hepatic culture model for predictive pharmacological in vitro screenings. Biotechnol Bioeng 2006;95:1198–206.
[19] Bader A, De Bartolo L, Haverich A. High level benzodiazepine and ammonia clearance by flat membrane bioreactors with porcine liver cells. J Biotechnol 2000;81:95–105.
[20] Lopez LC, Buonomenna MG, Fontananova E, Iacoviello G, D'Agostino R, Favia P, et al. New generation of catalytic PVDF membranes: coupling plasma treatments with chemical immobilization of W-based catalysts. Adv Funct Mater 2006;16:1417–24.
[21] Chatelier RC, Xie X, Gengenbach TR, Griesser HJ. Quantitative analysis of polymer surface restructuring. Langmuir 1995;11:2576–84.
[22] Chatelier RC, Xie X, Gengenbach TR, Griesser HJ. Effects of plasma modification conditions on surface restructuring. Langmuir 1995;11:2585–91.
[23] Everaert EP, Chatelier RC, van der Mei HC, Busscher HJ. A quantitative model for the surface restructuring of repeatedly plasma treated silicone rubber. Plasma Polym 1997;2:41–51.
[24] Xie X, Gengenbach TR, Griesser HJ. Changes in wettability with time on plasma modified perfluorinated polymers. J Adhes Sci Technol 1992;6:1411–31.
[25] Randall S, Holmes-Farley SR, Reamey RH, Nuzzo R, Mc Carthy TJ, Withesides GM. Reconstruction of the interface of oxidatively functionalized polyethylene and derivatives on heating. Langmuir 1987;3:799–815.
[26] Rotem A, Toner M, Bhatia S, Foy BD, Tompkins RG, Yarmush ML. Oxygen is a factor determining in vitro tissue assembly: effects on attachment and spreading of hepatocytes. Biotechnol Bioeng 1994;43:654–60.
[27] Bader A, Fruhauf N, Tiedge M, Drinkgern M, De Bartolo L, Borlak JT, et al. Enhanced oxygen delivery reverses anaerobic metabolic states in prolonged sandwich rat hepatocytes culture. Exp Cell Res 1999;246:221–32.
[28] De Bartolo L, Jarosch-Von Schweder G, Haverich A, Bader A. A novel full-scale flat membrane bioreactor utilizing porcine hepatocytes: cell viability and tissue-specific functions. Biotechnol Prog 2000;16:102–8.
[29] De Bartolo L, Salerno S, Morelli S, Giorno L, Rende M, Memoli B, et al. Long-term maintenance of hepatocytes in oxygen-permeable membrane bioreactor. Biomaterials 2006;27:4794–803.
[30] Curcio E, Salerno S, Barbieri G, De Bartolo L, Drioli E, Bader A. Mass transfer and metabolic reactions in hepatocytes spheroids cultured in rotating wall gas-permeable membrane system. Biomaterials 2007;28:5487–97.
[31] Clark EA, Brugge JS. Integrins and signal transduction pathways: the road taken. Science 1995;268:233–9.
[32] Ben-Ze'ev AG, Robinson S, Bucher NL, Farmer SR. Cell–cell and cell matrix interactions differentially regulate the expression of hepatic and cytoskeletal genes in primary cultures of rat hepatocytes. Proc Natl Acad Sci U S A 1988;85:1–6.
[33] Timpl R, Brown JC. The laminins. Matrix Biol 1994;14:275–81.
[34] Pankov R, Yamada KM. Fibronectin at a glance. J Cell Sci 2002;115:3861–3.
[35] Gloushankova NA, Alieva NA, Krendel MF, Bonder EM, Feder HH, Vasiliev JM, et al. Cell–cell contact changes the dynamics of lamellar activity in non-transformed epitheliocytes but not in their ras-transformed descendants. Proc Natl Acad Sci U S A 1997;94:879–83.
[36] Krasteva N, Harms U, Albrecht W, Seifert B, Hopp M, Altankov G, et al. Membranes for biohybrid liver support systems – investigations on hepatocytes attachment, morphology and growth. Biomaterials 2002;23:2467–78.
[37] Marceau N, Loranger A. Cytokeratin expression, fibrillar organization and stable functions in liver cells. Biochem Cell Biol 1995;73:619–25.
[38] Michalopoulos GK, Bowen WC, Mule K, Lopez-Talavera JC, Mars W. Hepatocytes undergo phenotypic transformation to biliary epithelium in organoid cultures. Hepatology 2002;36:278–83.
[39] Michalopoulos GK, Bowen WC, Mule K, Stolz DB. Histological organization in hepotocyte organoid cultures. Am J Pathol 2001;159:1877–87.
[40] Block GD, Locker J, Bowen WC, Petersen BE, Katyal S, Strom SC, et al. Population expansion, clonal growth and specific differentiation patterns in primary cultures of hepatocytes induced by HGF/SF, EGF and TGF alpha in a chemically defined (HGM) medium. J Cell Biol 1996;132:1133–49.
[41] Jung F, Richardson TH, Raucy JL, Johnson EF. Diazepam metabolism by cDNA-expressed human 2C P450s: identification of P4502C18 and P4502C19 as low K(M) diazepam *N*-demethylases. Drug Metab Dispos 1997;25:133–9.
[42] Ono S, Hatanaka T, Miyazawa S, Tsutsui M, Aoyama T, Gonzales FJ, et al. Human liver microsomal diazepam metabolism using cDNA-expressed cytochrome P450s: role of CYP2B, 2C19 and the 3A subfamily. Xenobiotica 1996;26:1155–66.
[43] Guillouzo A, Morel D, Ratanasasavanh C, Chesne C, Guguen-Guillouzo C. Long-term cultures of functional hepatocytes. Toxicol In Vitro 1990;4:415–27.
[44] Nebe B, Finke B, Luthen F, Bergemann C, Schroder K, Rychly J, et al. Imporved initial osteoblast functions on amino-functionalized titanium surfaces. Biomol Eng 2007;24:447–54.

# $H_2/NH_3$ Plasma-Grafting of PEEK-WC-PU Membrane to Improve their cyto-Compatibility with Hepatocytes

Stefania Laera,* Linda C. Lopez, Loredana De Bartolo, Sabrina Morelli, Simona Salerno, Antonella Piscioneri, Marina Nardulli, Roberto Gristina, Riccardo d'Agostino, Pietro Favia

Plasma treatments in $H_2$ and $NH_3$ RF (13.56 MHz) glow discharges have been used for modifying the surface of PEEK-WC-PU membranes. Water contact angle (WCA) and X-Ray photoelectron spectroscopy (XPS) analyses were performed to study the compositional changes of PEEK-WC-PU membranes after grafting. Cell culture experiments with human hepatocytes clearly show that grafting N-containing groups improves the cyto-compatibility of the membranes.

## Introduction

Low-temperature plasma modification (etching, deposition, and grafting) processes are extensively used in biomedical applications[1–3] to modify the surface of materials with tunable density of surface functional groups without altering their bulk. In particular, plasma treatment (grafting) processes with non-depositing gas feeds such as $H_2$, $O_2$, $NH_3$, $N_2/H_2$, and others enhance the surface density of N- and/or O-containing functional groups (e. g. $-NH_2$, COOH, OH) which might confer "biological activity" to the material, i.e. improved protein adhesion and improved adhesion, spreading and growth of cells.[4–7] In particular, some authors reported that surface N-containing groups may affect the cyto-compatibility of materials by adjusting the surface hydrophilicity and through interactions with cell peptides.[8–10]

In this study we have investigated the grafting of N-groups from $NH_3$ fed RF glow discharges as surface modification strategy on a new polymer membrane to improve its cyto-compatibility. Among several biomaterials that may be used for improving cell adhesion, new membranes made of modified polyetheretherketone (PEEK-WC) and polyurethane (PU) revealed to be suitable substrates for the adhesion and growth of liver cells,[11] e.g., in bioreactor applications. Such membranes combine many advantageous properties of polymers (biocompatibility, thermal and mechanical resistance, elasticity, etc.) with those of membranes (permeability, selectivity, well-defined geometry, etc.). It has been shown that human hepatocytes cultured on PEEK-WC-PU exhibit synthetic and detoxification functions comparable to those expressed by cells on natural substrates such as collagen.[11]

PEEK-WC-PU membranes were first plasma pre-treated in a $H_2$ RF glow discharge, and then in a $NH_3$ RF glow discharge. $H_2$ plasma pre-treatments were used to cross-link and stabilize the surface of the membranes before the plasma-grafting of N-groups, in order to reduce their hydrophobic recovery ageing.[12] After surface characterization, native and modified membranes were used as substrates to culture *in vitro* human hepatocytes.

S. Laera, L. C. Lopez, M. Nardulli, R. d'Agostino, P. Favia
Department of Chemistry, University of Bari, via Orabona 4, 70126, Bari, Italy
Fax +39 080 5443405; E-mail: laera.s@chimica.uniba.it
R. Gristina, R. d'Agostino, P. Favia
CNR Institute on Membrane Technology, University of Calabria, via P. Bucci cubo 17/C, I-87036 Rende (CS), Italy
R. d'Agostino, P. Favia
CNR Institute of Inorganic Methods and Plasmas, IMIP-Bari, Italy
L. De Bartolo, S. Morelli, S. Salerno, A. Piscioneri
CNR Institute of Inorganic Methods and Plasmas, IMIP-Bari, Italy



DOI: 10.1002/ppap.200930307

## Experimental Part

### Plasma Processes

PEEK-WC-PU membranes prepared with the phase inversion technique[11] were used as substrates. Plasma pre-treatments ($H_2$) and treatment ($NH_3$) processes were performed in a Pyrex glass plasma reactor, described elsewhere,[13] equipped with two internal "parallel plate" steel electrodes. Discharges were ignited between the upper electrode, connected to a radiofrequency (RF, 13.56 MHz) generator (ENI-ACG-10) through an impedance matching network, and the flat lower internal electrode, 7 cm far, ground, used as a substrate holder. $H_2$ was generated with a HG200 Claind Hydrogen Generator, 99.999% purity $NH_3$ (Air Liquide) was used. The gases were fed into the chamber through electronic MKS mass flowmeters. A rotative pump was used to keep the pressure constant during the processes; the pressure was controlled with a MKS baratron. A base pressure of $10^{-3}$ Torr was obtained. Plasma pre-treatment and treatment processes were performed in sequence, without opening the reactor in between, in the following conditions:

$-$ pre $-$ treatment($H_2$): 10 sccm flow rate;
200 mTorr pressure;
30 Watt power;
1 min.

$-$treatment($NH_3$): 10 sccm flow rate;
200 mTorr pressure;
20 Watt power;
1 min.

Plasma parameters above were previously optimized (data not shown) to maximize the extent of grafting of N-groups, measured with the XPS N/C ratio of the modified PEEK-WC-PU surface, and to minimize their hydrophobic recovery ageing, probed with WCA measurements.

### Surface Characterization

The chemical composition of unmodified and modified surfaces was determined with a Thermo VG Scientific XPS instrument, using monochromatic Al$K\alpha$ X-rays radiation (1486.6 eV, 100 W), with a spot size of 400 $\mu$m. A take-off angle of 53° was used with respect to the normal to the sample surface, for a sampling depth of about $6 \pm 2$ nm. Survey (0–1100 eV of Binding Energy, BE) and high resolution spectra (C1s, N1s, O1s) were recorded. Error bars resulted from measurements on 3–5 different spots of the same substrate, on 3–5 substrates of the same kind. C1s spectra were best-fitted with six components: C0 (BE $285.0 \pm 0.2$ eV, reference, C$-$C, C$-$H); C1 (BE $286.4 \pm 0.2$ eV, C$-$O$-$C, C$-$OH, C$-$N); C2 (BE $287.6 \pm 0.2$ eV, C=O, O$-$C$-$O, N$-$C=O); C3 (BE $289.2 \pm 0.2$ eV, COOH, COOR, O$-$CONH); C4 (BE $289.9 \pm 0.2$ eV, shake up, aromatic structures); and C5 (BE $291.8 \pm 0.2$ eV, shake up, C=O).

$NH_3$ plasma treatments, besides grafting N-groups, leave the treated polymer surface more reactive to oxidation (oxygen uptake) after exposure to air due to long-living surface free radicals; so, as a general effect, the surface of $NH_3$ plasma-treated polymers is generally found to be rich both in Nitrogen- and Oxygen-containing chemical groups.[13,14] $H_2$ plasma treatments were selected, among possible others (e.g., Ar), to cross-link the membrane before the grafting of the N-groups. This happens through the UV emission of $H_2$ plasmas that penetrates deep and causes bond cleavage and rearrangements in polymers, as well as through other mechanisms (abstraction of species by H atoms, ion bombardment, rearrangements).[13,15,16] Exposing $H_2$ plasma-treated membranes to air (before the $NH_3$-process) resulted in massive surface oxidation and limited N-groups grafting (after the $NH_3$ process), so it was decided to perform the two treatments in sequence, without opening the reactor.

Sessile drop WCA measurements were performed in a static mode with a CAM 200 contact angle instrument equipped with a photo camera. Two milliliter drops of double distilled water were used. The CAM software of the instrument was utilized to fit the shape of the drop and determine the WCA tangent with the Young–Laplace equation. Measurements were performed on 3–5 different spots per substrate, on 2–4 substrates of the same kind.

### Cell Culture

Cryopreserved primary human hepatocytes (BD Bioscience, Milan, Italy) with 95–98% viability, assessed by Trypan blue exclusion, were cultured on native and modified membranes in William's medium E (Sigma–Aldrich, Milan, Italy) supplemented with prednisolone 0.762 $\mu g \cdot ml^{-1}$, glucagone 0.133 $\mu g \cdot ml^{-1}$, and insulin 0.18 $U \cdot ml^{-1}$ (Sigma–Aldrich, Milan, Italy), L-glutammine 5.4 mM and penicillin/streptomycin 272 $\mu g \cdot ml^{-1}$ (Biochrom, Berlin, Germany).[17] The maintenance of liver specific functions was evaluated in terms of urea synthesis. The concentration of urea in the culture medium was assayed with the enzymatic urease method (Sentinel, Milan, Italy).

## Results and discussion

A WCA value of $80 \pm 8°$ was measured on native membranes. The quite high deviation of WCA values is due to non-homogeneity of porosity and roughness of the membrane, as well as of surface chemical composition (e.g., due to uneven surface segregation of PU). Soon after the $H_2/NH_3$ plasma modification, a much lower WCA value of $41 \pm 9°$ was found, attesting for the grafting of polar groups. After 8 days of ageing in air, during which the hydrophobic recovery of the material takes place to some extent, the WCA value of the samples reaches a stable value of $61 \pm 3°$. A WCA value of $51 \pm 5°$ was found, instead, for $NH_3$-treated membranes, without any pre-treatment; after 8 days such substrates recovered almost completely the WCA value of the unprocessed surface, with WCA values of $75 \pm 3°$.

The grafting of N-containing groups on $H_2/NH_3$ plasma processed PEEK-WC-PU membranes is evident after XPS analysis (within one day after the process), as shown in Table 1. Nitrogen atoms are found at the surface of the



DOI: 10.1002/ppap.200930307

*Table 1.* XPS analysis of PEEK-WC-PU plasma–processed in $H_2$ (pre-treatment) and $NH_3$ (treatment) RF Glow discharges.

| PEEK-WC-PU | C% | O% | N% | O/C | N/C |
|---|---|---|---|---|---|
| As received | 80.9 ± 4.0 | 17.0 ± 1.0 | 2.1 ± 0.1 | 0.21 ± 0.02 | 0.026 ± 0.003 |
| After $H_2/NH_3$ grafting | 67.2 ± 3.4 | 12.9 ± 0.6 | 19.9 ± 1.0 | 0.19 ± 0.02 | 0.296 ± 0.030 |

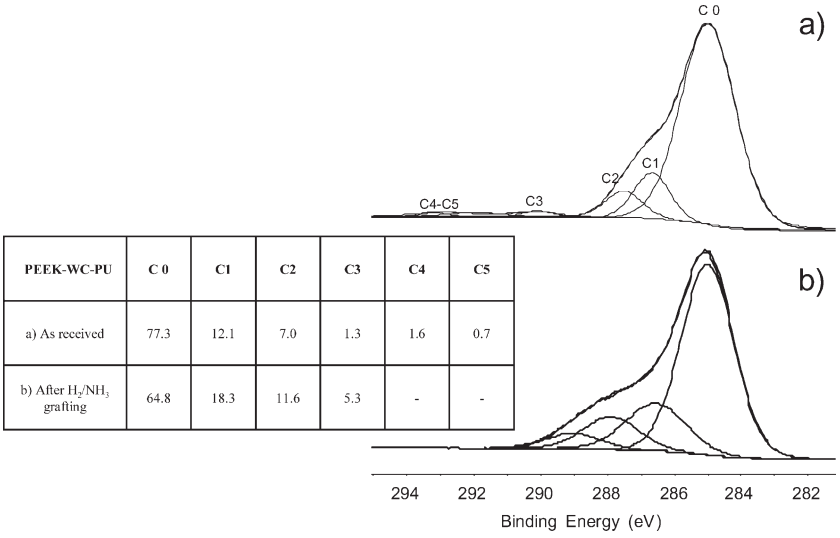


| PEEK-WC-PU | C 0 | C1 | C2 | C3 | C4 | C5 |
|---|---|---|---|---|---|---|
| a) As received | 77.3 | 12.1 | 7.0 | 1.3 | 1.6 | 0.7 |
| b) After $H_2/NH_3$ grafting | 64.8 | 18.3 | 11.6 | 5.3 | - | - |

*Figure 1.* C1s spectra of the PEEK-WC-PU membrane (a) untreated, (b) after the $H_2/NH_3$ plasma process. The inset reports the relative percent of the Co–C5 components (see experimental section for assignments) in each C1s signal. The error estimated is within ± 10%.

untreated membrane due to the presence of PU in PEEK-WC-PU; after the $H_2/NH_3$ plasma process both the percent of N surface atoms and the N/C surface ratio increase remarkably, in agreement with the increased wettability of the modified membranes. After 8 days of ageing a ~15% reduction of the N/C ratio was recorded, also in agreement with the wettability data.

The C1s spectra of the untreated and $H_2/NH_3$ plasma processed PEEK-WC-PU membrane are shown in Figure 1. Spectra have been best-fitted with the C0–C5 components listed in the experimental section. The C1s spectrum (a) refers to untreated PEEK-WC-PU; in detail, the C0 component refers to aromatic carbons in PEEK and WC, C1 to ether groups in PEEK and PU, C2 to carbonyl moieties in PEEK, C3 to carboxyl groups in WC and to urethane groups in PU, C4 and C5 shake-up structures are related to aromatic structures and to C=O double bonds. Nitrogen groups are grafted after the $H_2/NH_3$ plasma process (spectrum b), at the same time the aromatic surface structures of the membrane are fragmented, due to the positive-ion bombardment associated to the plasma process. In fact components C1, C2, and C3, which grafted N- (amine, imine, nitrile, amide, etc) and O- (ether, carbonyl, alcohol, etc.) containing groups contribute to, become more important with respect to trace a), and the shake-up signals C4 and C5 disappear. It is not straightforward at all to quantify exactly the distribution of grafted N-groups on PEEK-WC-PU due to the complexity of the substrate and the overlap of N-groups contributions ($-NH_x$, $-CN$, $-C{=}NH$, $-CONH$, etc.) in 286–288 eV BE region of the C1s spectra, so accurate best-fitting procedures were not attempted in this sense, neither derivatization procedures.

Primary human hepatocytes were cultured on membranes within 8 days after the treatment; cells adhered on native and modified membranes. No morphological differences were found among cells cultured on the two different surfaces. Cells, though, were found to exhibit slightly different liver specific functions in terms of urea synthesis; quantitative results normalized per cell density are shown in Figure 2 as a function of culture time. It is interesting to note that cells cultured on N-grafted membranes synthesize at all times urea at higher level with respect to native membranes. Statistically significant differences ($p < 0.05$), in particular, were observed on day 5 and 7. Also, the normalized synthesis of total proteins was found increased of 22%[18] on the modified membranes on day 5.

Grafted N-groups at the membrane surface, likely coupled with increased wettability, clearly induced an

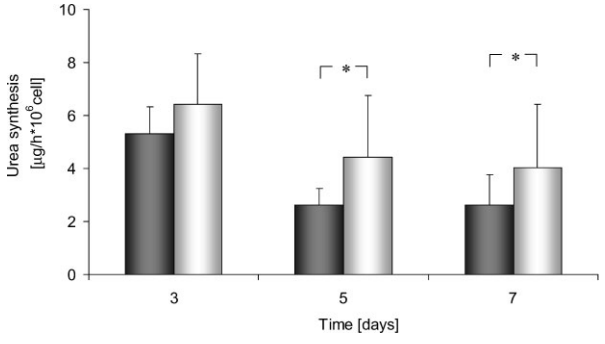


*Figure 2.* Rate of urea synthesis of human hepatocytes cultured on native (full bar) and modified (empty bar) PEEK-WC-PU membranes. The values are expressed as μg/h $10^6$ cell ± standard deviation, and evaluated according to *t*-test. $^*p < 0.05$.

enhancement of the cell metabolic functions due to peculiar surface-cell interactions, whose nature needs to be clarified. These are probably related to the increased surface polarity of the membranes (WCA $= 61 \pm 3^{\circ}$) as well as to specific interactions between N-grafted groups, proteins in the culture medium, and cell receptors. This is not completely unexpected considering that several evidence in literature shows that cells adhere well on moderately wettable surfaces due to the adsorption of adhesive proteins present in the culture medium and/or secreted by cells.[19,20]

## Conclusions

$H_2/NH_3$ glow discharges were found to graft N-containing groups at the surface of PEEK-WC-PU membranes and to increase their wettability; $H_2$ pre-treatments were found to improve the efficiency of the grafting process, and to slow down the hydrophobic recovery of the membranes. Surface modified membranes improved the *in vitro* growth of primary human hepatocytes, as it was checked by measuring their urea and total protein synthesis; likely, $H_2/NH_3$ plasma treatments turned membranes more susceptible to positive interactions with proteins and cell membranes, resulting in a positive cell response and improved cell metabolic functions.

Acknowledgements: The "LIVEBIOMAT" 6$^{th}$FP STREP European project is acknowledged for funding this research. Mr. Savino Cosmai (Department of Chemistry, University of Bari) is acknowledged for technical assistance.

Received: October 6, 2008; Accepted: February 2, 2009; DOI: 10.1002/ppap.200930307

Keywords: ammonia discharges; biocompatibility; membranes; plasma treatment

[1] Special issue devoted to "*Plasma Processes for Biomedical Applications*", Vol 3, P. Favia, Ed., Plasma Processes & Polymers, 2006, 6/7.
[2] S. Ben Rejeb, M. Tatoulian, F. A. Khonsari, F. A. Durand, A. Martel, J. F. Lawrence, et al. *Anal. Chim. Acta* **1998**, *376*, 133.
[3] D. A. Puleo, R. A. Kissling, M. S. Sheu, *Biomaterials* **2002**, *23*, 2079.
[4] K. S. Siow, L. Brichter, S. Kunar, H. J. Griesser, *Plasma Proc. Polym.* **2006**, *3*, 392–418.
[5] R. Daw, T. O'Leary, J. Kelly, R. D. Short, M. Cambray-Deakin, A. J. Devlin, I. M. Brook, A. Scutt, S. Kothari, *Plasmas and Polymers* **1999**, *4*, 113.
[6] G. H. Hsiue, S. D. Lee, C. C. Wang, M. H. I. Shiue, P. C. T. Chang, *Biomaterials* **1993**, *14*(8), 591.
[7] R. Sipheia, G. Martucci, M. Barbarosie, C. Wu, *Biomater. Artif. Cell. Im.* **1993**, *21*(4), 455.
[8] P. B. Van Wachem, A. H. Hogt, T. Beugeling, *Biomaterials* **1987**, *8*, 323.
[9] H. J. Griesser, R. C. Chatelier, T. R. Gengenbach, J. G. Steele, *J. Biomater. Sci. Polymer Edn.* **1994**, *5*, 531.
[10] S. I. Ertel, B. D. Ratner, T. A. Horbett, *J. Biomed. Mat. Res.* **1990**, *24*, 1637.
[11] L. De Bartolo, S. Morelli, M. C. Gallo, C. Campana, G. Statti, M. Rende, S. Salerno, E. Drioli, *Biomaterials* **2005**, *26*, 6625–6634.
[12] P. Favia, A. Milella, L. Iacobelli, R. d'Agostino, in: *Plasma Processes and Polymers*, R. d'Agostino, P. favia, C. Oehr, M. R. Werheimer, Eds., Wiley-VCH, Weinheim, Germany **2004**, 271.
[13] L. C. Lopez, M. G. Buonomenna, E. Fontananova, G. Iacoviello, E. Drioli, R. d'Agostino, P. Favia, *Advanced Functional Materials* **2006**, *16*, 1417.
[14] P. Favia, M. V. Stendardo, R. d'Agostino, *Plasmas and Polymers* **1996**, *1*, 91.
[15] A. Hollander, R. Wilken, J. Behnisch, *Surf. Coat. Technol.* **1999**, 116–119, 788.
[16] A. Hollander, J. E. Klemberg-Sapieha, M. R. Wertheimer, *J. Polym. Sci. A: Polym. Chem.* **1995**, *33*, 2013.
[17] L. De Bartolo, S. Salerno, S. Morelli, L. Giorno, M. Rende, B. Memoli, A. Procino, V. E. Andreucci, A. Bader, E. Drioli, *Biomaterials* **2006**, *27*, 4794–4803.
[18] S. Salerno, A. Piscioneri, S. Laera, S. Morelli, P. Favia, A. Bader, E. Drioli, L. De Bartolo, submitted, 2009.
[19] L. De Bartolo, S. Morelli, A. Bader, E. Drioli, *Biomaterials* **2002**, *23*, 2485–2497.
[20] Y. Arima, H. Iwata, *Biomaterials* **2007**, *28*, 3074–3082.



DOI: 10.1002/ppap.200930307

Biomaterials 30 (2009) 2531–2543

Contents lists available at ScienceDirect

Biomaterials

journal homepage: www.elsevier.com/locate/biomaterials

# Human hepatocyte functions in a crossed hollow fiber membrane bioreactor

Loredana De Bartolo [a,*], Simona Salerno [a], Efrem Curcio [b], Antonella Piscioneri [a,c], Maria Rende [a,b], Sabrina Morelli [a], Franco Tasselli [a], Augustinus Bader [d], Enrico Drioli [a,b]

[a] Institute on Membrane Technology, National Research Council of Italy, ITM-CNR, c/o University of Calabria, Via P. Bucci, Cubo 17/C, I-87030 Rende (CS), Italy
[b] Department of Chemical Engineering and Materials, University of Calabria, Via P. Bucci, I-87030 Rende (CS), Italy
[c] Department of Cell Biology, University of Calabria, Via P. Bucci, 87030 Rende (CS), Italy
[d] Biomedical-Biotechnological Center, BBZ, University of Leipzig, Germany

ARTICLE INFO

*Article history:*
Received 13 October 2008
Accepted 6 January 2009
Available online 31 January 2009

*Keywords:*
Hollow fiber
Membrane bioreactor
Mass transport
Hepatocytes
Liver functions
Diazepam biotransformation

ABSTRACT

An important challenge in liver tissue engineering is the development of bioartificial systems that are able to favour the liver reconstruction and to modulate liver cell behaviour.
A crossed hollow fiber membrane bioreactor was developed to support the long-term maintenance and differentiation of human hepatocytes. The bioreactor consists of two types of hollow fiber (HF) membranes with different molecular weight cut-off (MWCO) and physico-chemical properties cross-assembled in alternating manner: modified polyetheretherketone (PEEK-WC) and polyethersulfone (PES), used for the medium inflow and outflow, respectively. The combination of these two fiber set produces an extracapillary network for the adhesion of cells and a high mass exchange through the cross-flow of culture medium. The transport of liver specific products such as albumin and urea together with the transport of drug such as diazepam was modelled and compared with the experimental metabolic data. The theoretical metabolite concentration differed 7.5% for albumin and 5% for urea with respect to experimental data. The optimised perfusion conditions of the bioreactor allowed the maintenance of liver functions in terms of urea synthesis, albumin secretion and diazepam biotransformation up to 18 days of culture. In particular the good performance of the bioreactor was confirmed by the high rate of urea synthesis (28.7 μg/h $10^6$ cells) and diazepam biotransformation. In the bioreactor human hepatocytes expressed at high levels the individual cytochrome P450 isoenzymes involved in the diazepam metabolism. The results demonstrated that crossed HF membrane bioreactor is able to support the maintenance of primary human hepatocytes preserving their liver specific functions for all investigated period. This device may be a potential tool in the liver tissue engineering for drug metabolism/toxicity testing and study of disease pathogenesis alternatively to animal experimentation.


## 1. Introduction

Liver tissue constructs consisting of functional cells and artificial materials are being greatly studied for their applications in the clinical field for organ replacement and in the in vitro studies for drug development and metabolic diseases. The impact will be increasing for the coming decade in the design of in vitro physiological models to study disease pathogenesis and in the development of molecular therapeutics alternatively to animal experimentation. Animal models suffer from serious shortcomings regarding the prediction for a human situation as significant species differences in enzyme expression exist between man and animals. Isolated hepatocytes represent a good model of liver metabolism because they are able to perform the full range of known in vivo biotransformation, synthetic and detoxification functions [1,2]. However, hepatocytes rapidly lose their liver specific functions when maintained under standard in vitro culture conditions. In fact, static culture methods are characterized by an unstirred medium layer overlying cells attached to a gas impermeable substratum and are exposed to changes of nutrient concentration and catabolite accumulation on time. For liver cells, which are highly perfused in vivo, such conditions are susceptible to oxygen and nutrient limitations with consequent reduction of cell viability and functionality. A variety of culture methods have been developed to foster retention of hepatocyte functions including co-culture with nonparenchymal cells [3], culture in a sandwich collagen gel [4], synthetic extracellular

* Correspondence to: Loredana De Bartolo, Institute on Membrane Technology, National Research Council of Italy, ITM-CNR, c/o University of Calabria, Via P. Bucci, Cubo 17/C, I-87030 Rende (CS), Italy. Tel.: +39 0984 492036; fax: +39 0984 402103.
*E-mail addresses:* l.debartolo@itm.cnr.it, loredana.debartolo@cnr.it (L. De Bartolo).

0142-9612/$ – see front matter © 2009 Elsevier Ltd. All rights reserved.
doi:10.1016/j.biomaterials.2009.01.011

matrix [5], in three-dimensional systems in spheroids [6,7] or scaffolds [8], and in a variety of dynamic systems such as bioreactors [9–13]. Bioreactors allow the culture of cells under tissue specific mechanical forces (e.g., pressure, shear stress and interstitial flow) augmenting the gas and nutrient exchange under complete fluid dynamics control that ensure the long-term maintenance of cell viability and functions [14,15]. Various bioreactor configurations have been explored for hepatocyte culture including membrane bioreactors (hollow fiber, flat, fiber network, spiral) [16–21] and by using several adhesive substrates [22–26]. Among the bioreactors hollow fiber membrane bioreactors meet the main requirements for cell culture: wide area for cell adhesion, oxygen and nutrient transfer, removal of catabolites and protection from shear stress [14,15]. Furthermore, hollow fiber membranes may serve as scaffolding material guiding the spatial organisation and microarchitecture of the liver tissue. Critical issues in the hollow fiber (HF) membrane bioreactors are the configuration of the bioreactor, the fluid dynamics and the membrane properties which depend on the cell adhesion and mass transport. Mass transfer across the membrane occurs by diffusion and/or convection in response to existing transmembrane concentration or pressure gradients. Both mechanisms of transport should be taken into account in the design of HF membrane bioreactors [14]. In the case of hepatocytes which are anchorage-dependent cells the membrane properties are critical not only for the transport but also for their interaction with cells. Surface properties favouring the cell functional and phenotypic maintenance [27–29] are required. Previously we have developed modified polyetheretherketone (PEEK-WC) membranes in flat configuration for hepatocyte culture [30]. This polymer owing to the presence of an isobenzofurane-1,3-dihydro-1-oxo- group in the polymer chain is soluble in common solvents and it can be used for preparing membranes with different properties by an inexpensive and flexible method [31]. Our studies demonstrated that PEEK-WC flat membranes are able to support the adhesion and metabolic functions of hepatocytes. PEEK-WC in hollow fiber (HF) configuration has been used also for lymphocytes culture [32].

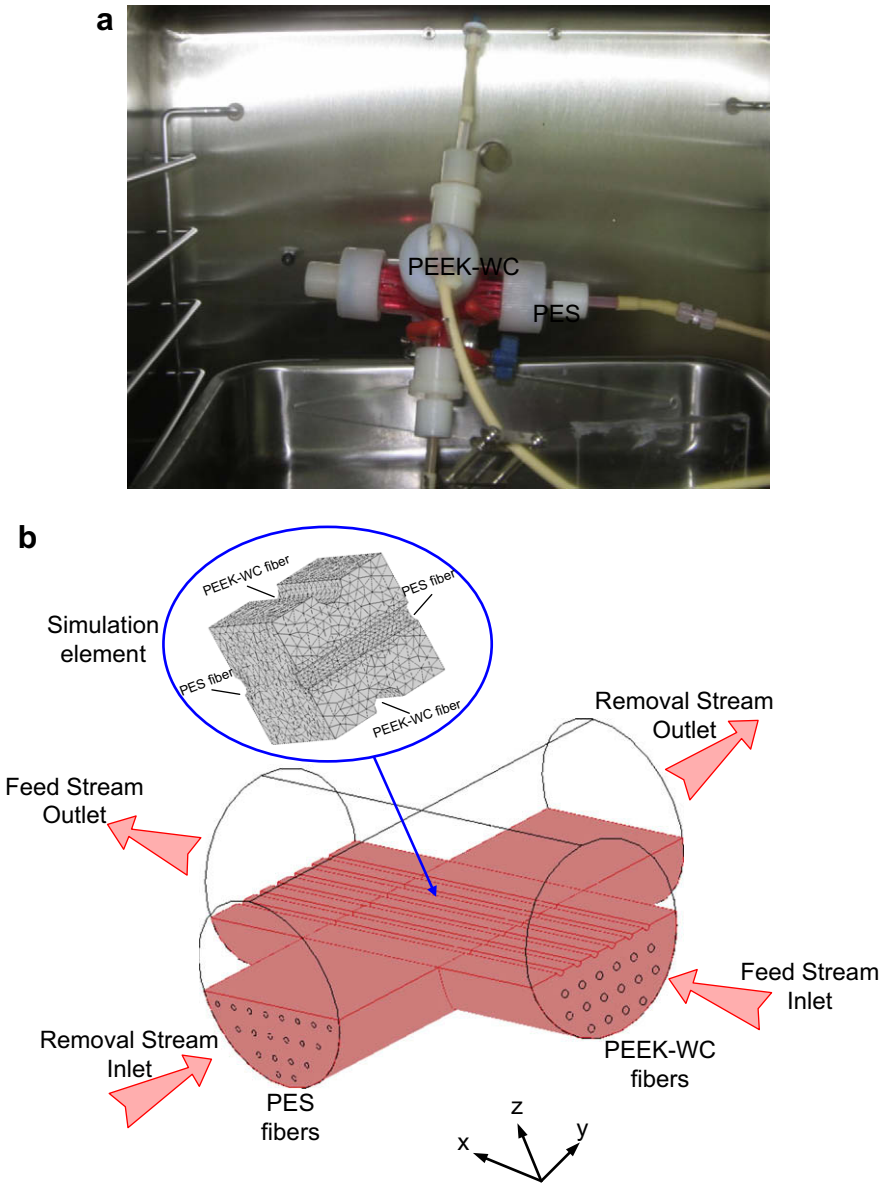


**Fig. 1.** Membrane bioreactor: (a) photograph. (b) Vertical section scheme of the crossed hollow fiber membrane bioreactor.

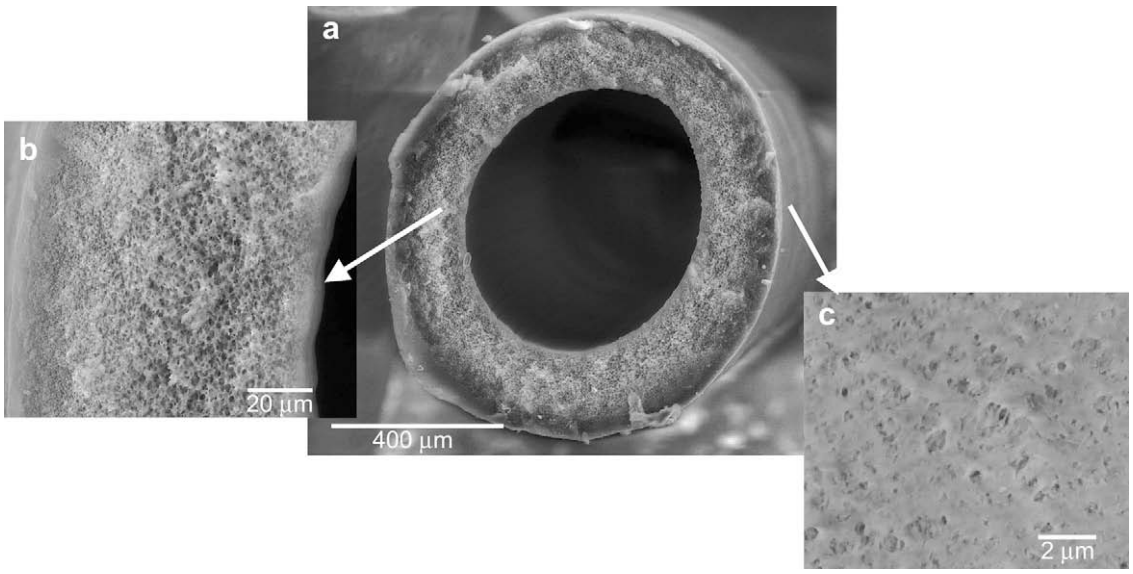


**Fig. 2.** Representative Scanning Electron Micrographs of (a) cross-section, (b) wall thickness and (c) external surface of polyether-sulphone (PES) hollow fiber membranes.

We hypothesize that the differentiated functions of primary human hepatocytes can be maintained in a crossed HF membrane bioreactor in which cells are cultured in the extraluminal compartment among different kinds of fibers. The bioreactor is based on the use of two types of HF membranes with different molecular weight cut-off (MWCO) and physico-chemical properties cross-assembled in alternating manner: PEEK-WC and polyethersulfone (PES). The different HF membranes in the bioreactor have different functions: PEEK-WC HFs are devoted to provide the cells oxygenated medium containing nutrients and metabolites while PES HFs are devoted to remove from cell compartment catabolites and cell specific products. In this way the two HF membrane systems mimic the in vivo arterious and venous blood vessels. Mass transport through each type of fiber is evaluated and modelled and the fluid dynamics of the bioreactor is optimised.

## 2. Materials and methods

### 2.1. Crossed HF membrane bioreactor

The bioreactor consists of crossed membrane system of 40 independent PEEK-WC HF and 40 PES HF membranes used for the medium inflow and outflow, respectively. The two fiber systems were assembled in alternating manner and potted with polyurethane adhesive (Polaris Polymers, OH, USA) within glass housing (Fig. 1). The fibers were potted at each end in order to establish three separate compartments: two intraluminal compartments within the PEEK-WC and PES fibers, and an extraluminal compartment or shell outside of the fibers. The intraluminal and extraluminal compartments communicate through the pores in the fiber wall. Fig. 1a illustrates the bioreactor (volume: 40 ml) that is connected to the perfusion circuit consisting of micro-peristaltic pump, gas-permeable silicone tubing, reservoir of medium and glass medium waste.

The oxygenated medium enters from the reservoir to the membrane bioreactor with a flow rate $Q_f$ of 1.5 ml/min that was set on the basis of average retention time. Fresh medium was perfused in single-pass and the stream leaving the bioreactor

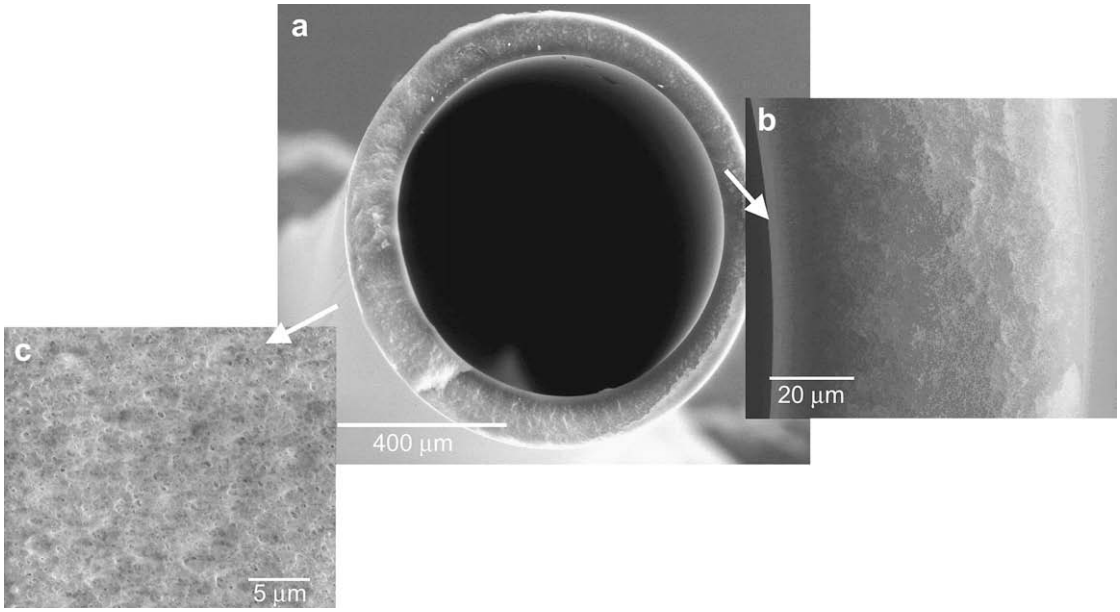


**Fig. 3.** Representative Scanning Electron Micrographs of (a) cross-section, (b) wall thickness and (c) external surface of modified polyetheretherketone (PEEK-WC) hollow fiber membranes.

**Table 1**
Morphological and physico-chemical properties of PEEK-WC and PES HF membranes.

| | PEEK-WC HF | PES HF |
|---|---|---|
| Inner diameter | $572 \pm 6$ μm | $300 \pm 40$ μm |
| Wall thickness | $51 \pm 10$ μm | $100 \pm 25$ μm |
| Mean pore size | – | 0.2 μm |
| MWCO | 190 kDa | – |
| $J$ [L/m$^2$ h mbar] | 0.758 | 15.2 |
| Contact angle | $69.7 \pm 2.7°$ | $43 \pm 3.5°$ |

$Q_{out}$ was collected as waste until approaching the steady state. When the system reached the steady state, the stream leaving the bioreactor was recycled ($Q_r$) in order to obtain the accumulation of products.

### 2.2. RTD characterization

Residence time distribution (RTD) was investigated through the introduction of tracer (step input) at the entrance of PEEK-WC fibers and recording it in time at the exit of the PES fibers. The tracer, consisting in a solution of Williams' medium E, was sent to the bioreactor with flow rate of 1.5 ml/min and continuously monitored by online spectrophotometer (UV Cord Pharmacia, Uppsala, Sweden).

The fluid dynamics was characterized without the cells by tracer experiments using Williams' medium E. The bioreactor was challenged by changing the tracer concentration stepwise in the feed stream ($C_{in}$) and the outlet concentration ($C_{out}$) was continuously monitored by online spectrophotometer (UV Cord Pharmacia, Uppsala, Sweden). The fluid dynamics of the bioreactor was characterized in terms of the cumulative residence time distribution (RTD) to step inputs:

$$F(t) = c_{out}/c_{in} \quad (1)$$

where $t$ is the actual time. The theoretical mean retention time was calculated as:

$$\tau = \frac{V}{Q} \quad (2)$$

where $Q$ is the perfusion flow rate and $V$ is the volume of the bioreactor [33].

### 2.3. PEEK-WC HF membrane preparation

PEEK-WC HF membranes were prepared according to the well-known dry-wet spinning method. In order to prepare highly porous membranes, poly-(vinylpyrrolidone) (PVP K17 by BASF) was used as a pore forming additive. Membranes were prepared from solutions of PEEK-WC and PVP both at 15 wt.% in dimetylformamide (DMF) under continuous mechanical stirring at room temperature as described elsewhere [32].

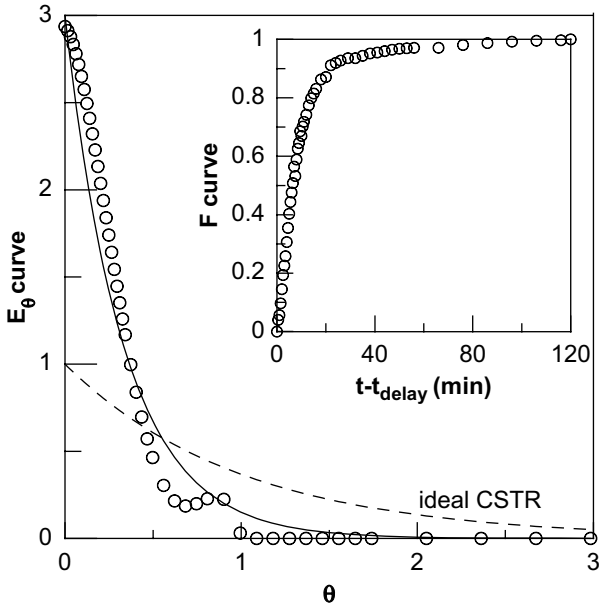


**Fig. 4.** RTD analysis of the bioreactor (○: experimental points; solid line: CSTR + dead zone model; dotted line: ideal CSTR).

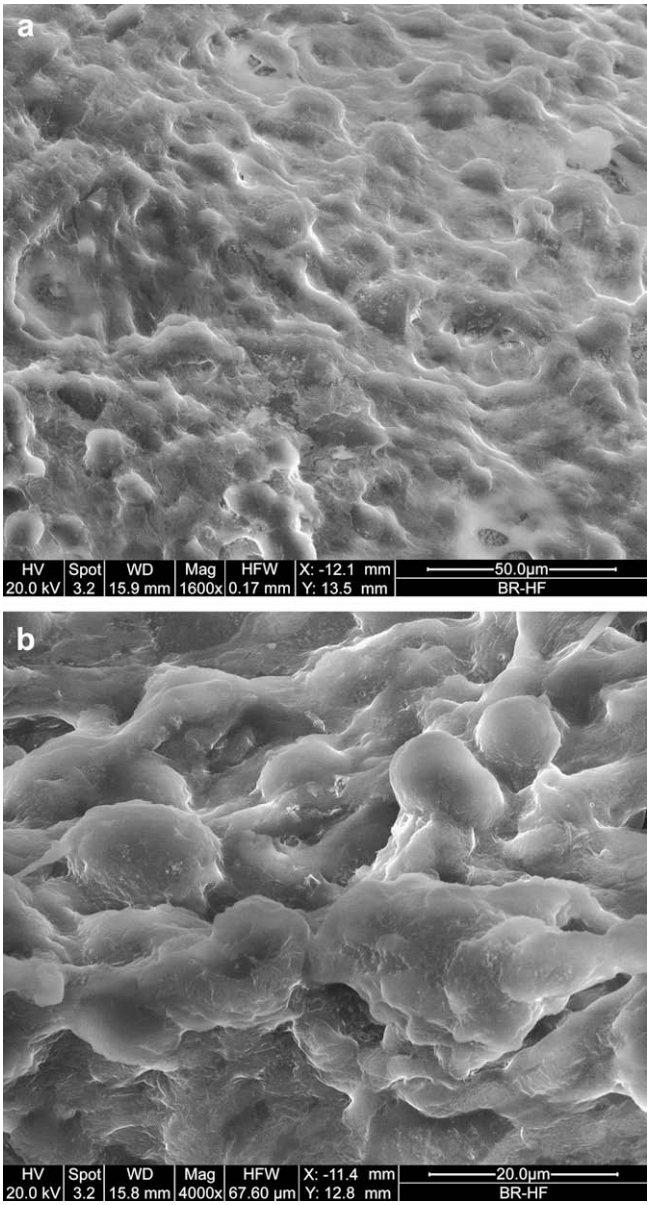


**Fig. 5.** SEM images of human hepatocytes after 18 days of culture in the crossed HF membrane bioreactor; a) and b) different magnifications.

### 2.4. Characterization of membrane properties

Dried PEEK-WC HF membranes were cut in cross-section, mounted with double-faced conductive adhesive tape, and analysed by Scanning Electron Microscope (SEM) (ESEM FEG QUANTA 200, FEI Company, Oregon, and USA) in order to obtain information about the cross-sectional structure and thickness, intra- and extra-lumen morphology and diameters, and the shape and size of the membrane pores.

The hydrophobic/hydrophilic character of the investigated membranes was estimated by contact angle technique. Water contact angles were measured using the sessile drop method at ambient temperature by CAM 200 contact angle meter (KSV Instruments LTD, Helsinki, Finland), depositing the liquid on the membrane surface using an automatic microsyringe.

For the characterization of mass transport properties, the membranes were potted inside glass modules (length: 20 cm, inner diameter: 1.5 cm) that allowed access to both the intraluminal and extraluminal compartments [14]. A peristaltic pump (ISMATEC, General Control, Milan, Italy) circulated the metabolite solution by pumping the fluid (feed) from the reservoir into the inlet port of the module. Pressures were monitored at inlet and outlet of the module by online manometers (Allemano, accuracy $\pm 0.98$ mbar). Inlet pressures were varied in order to obtain transmembrane pressures ($\Delta P^{TM}$) from 0 to 80 mbar. The extraluminal flow (permeate) was measured continuously, and the concentration of the metabolite

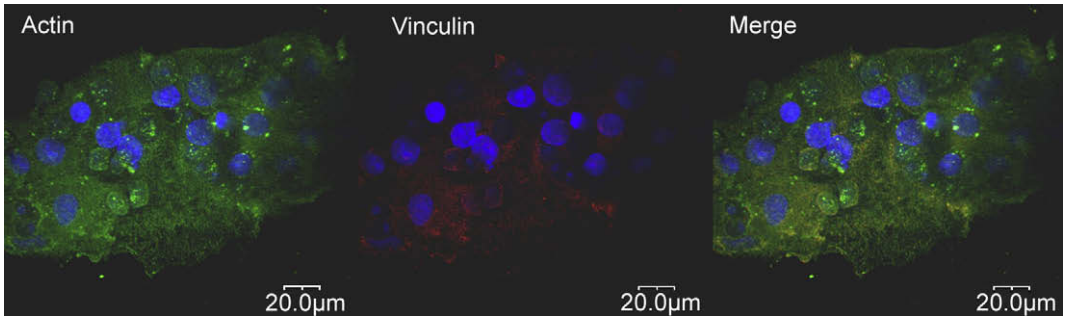


**Fig. 6.** Confocal Laser Scanning Micrographs of hepatocytes after 18 days of culture in the crossed HF membrane bioreactor. Hepatocytes were immunostained for actin (green) and vinculin (red). DAPI (blue) counterstaining was used to detect nuclei.

permeating through the membranes was monitored by an online UV-spectrophotometer (LKB Uvicord SII, Pharmacia). Diffusive transport of albumin and urea from the fiber lumen to the shell of PES HF membranes was evaluated by assessing the concentration changes of metabolites in the shell with time. Diffusive transport of diazepam from the lumen to the shell of PEEK-WC HF membranes was also evaluated by the same procedure. Albumin (MW 67 kDa) (Sigma), urea (MW 60.06 Da) (Sigma) and diazepam (MW 284.74 Da) (Sigma) solutions were prepared by dissolving separately 0.5 mg/ml for albumin, 50 μg/ml for urea and diazepam 10 μg/ml in phosphate buffer at pH 7.4.

The PEEK-WC and PES HF membrane modules were initially fed with water to evaluate the hydraulic permeance, and then it was filled with metabolite solutions for solute permeation measurements. For each type of metabolite a new module was used. In order to ensure a high reproducibility of permeance data, transmembrane flux ($J$) vs. transmembrane pressure ($\Delta P^{TM}$) was evaluated on four modules and the average hydraulic permeance was reported.

### 2.5. The human hepatocytes

Cryopreserved primary human hepatocytes (BD Bioscience, Milan, Italy), isolated from human tissue, were thawed in a 37 °C water bath with gentle shaking. Cell suspension was slowly transferred into pre-heat 50 ml of isolation media from the One Step Purification Kit (BD Bioscience), and centrifuged at 50g RT for 5 min. the cell pellet was then suspended in the Williams' medium E (Sigma Aldrich, Milan, Italy) supplemented with prednisolone 0.762 μg/ml, glucagone 0.133 μg/ml and insulin 0.18 U/ml (Sigma Aldrich, Milan, Italy), L-glutammine 5.4 mM and penicillin/streptomycin 272 μg/ml (Biochrom, Berlin, Germany). The viability of the hepatocytes (assessed by Trypan blue exclusion) ranged between 95 and 98%.

The human hepatocytes were then seeded in the extralumen compartment of the bioreactor on the outer surface of and between the HF membranes. After the liver cells adhered, the bioreactor was perfused with oxygenated medium.

Hepatocytes were cultured also in batch system on collagen. This latter was used as reference substratum. Collagen from calf skin (Sigma, Milan, Italy) was dissolved with sterile acetic acid (0.1 M) to the final concentration of 1 mg/ml. Solution of collagen gel was added to obtain a coating density of 10 μg/cm$^2$. Cells and controls were incubated at 37 °C in a 5% $CO_2$; 20% $O_2$ atmosphere (v/v) with 95% relative humidity for the duration of the experiments.

### 2.6. Sample preparation for SEM

Specimens of cell cultures were prepared for Scanning Electron Microscopy (SEM) by fixation in 2.5% glutaraldehyde, pH 7.4 phosphate buffer, followed by post-fixation in 1% osmium tetroxide and by progressive dehydration in ethanol.

### 2.7. Hepatocyte staining for Laser Confocal Scanning Microscopy

The morphological behaviour of human hepatocytes cultured in the membrane bioreactor was investigated after 48 h of culture by Laser Confocal Scanning Microscopy (LCSM). Samples were washed with PBS, fixed for 15 min in 3% paraformaldehyde in PBS at room temperature, permeabilized for 5 min with 0.5% Triton-X100 and saturated for 15 min with 2% Normal Goat Serum (NGS). To visualize vinculin, a specific monoclonal anti-vinculin antibody (Sigma, St. Louis, MO, USA), diluted 1:50 in 1% NGS, was incubated for 30 min at room temperature [23]. Then samples were washed twice in PBS and incubated for 30 min with goat anti-mouse IgG TRITC conjugated (Sigma, Milan, Italy), diluted 1:100 in PBS. To visualize the actin, the samples were incubated in phalloidin conjugated with FITC (50 μg/ml) (Fluka, Milan, Italy) in PBS. Then samples were washed twice in PBS and incubated for 20 min with DAPI (Sigma, Milan, Italy) to visualize nucleic acid. Finally, the samples were washed, mounted and viewed with Laser Confocal Scanning Biological Microscope (Fluoview FV300, Olympus, Milan, Italy).

### 2.8. Biochemical and ELISA assays

Samples of the culture medium were collected from the bioreactor in pre-chilled tubes and stored at −80 °C until assayed. The protein content in the samples was determined by protein assay using bicinchoninic acid solution (Sigma, Milan, Italy) by spectrophotometer analysis. The urea concentration was assayed by the enzymatic urease method (Sentinel, Milan, Italy).

Albumin production in the samples was measured by the immunometric method (ELISA) using antibodies against human albumin (Sigma, St. Louis, MO, USA). ELISA assays were done from cells of six different isolations. Chromatographically purified human albumin and the monoclonal antibody for human albumin were from Bethyl (Bethyl Laboratories Inc., USA). Ninety-six well plates were coated with 50 μg/ml of albumin and left overnight at 4 °C. After washing the plate 4 times, 100 μl of cell culture supernatant was added to the wells and incubated with 100 μl of anti-human albumin antibody conjugated with horseradish peroxidase (Bethyl Laboratories, Inc.). After 24 h at 4 °C, the substrate buffer containing tetramethylbenzidine and $H_20_2$ (Sigma, St. Louis, MO, USA) was added for 7 min. The reaction was stopped with 50 μl of 8 N $H_2SO_4$. Absorbance was measured at 450 nm using a Multiskan Ex (Thermo Lab Systems).

### 2.9. HPLC analysis of diazepam and metabolites

Diazepam analysis was performed as reported previously [34]. HPLC was used to assess the diazepam and metabolite concentrations in medium samples [35]. The samples from the culture medium were alkalinized with 20% of 4 M NaOH, precipitated with isopropanol (1:10) and extracted with ethyl acetate (5:1) by gentle rocking for 10 min and subsequent centrifugation at 200g for 15 min at RT. Thereafter the ethyl acetate phase was evaporated and exsiccated under vacuum condition and the pellet was dissolved in 96 μl mobile phase consisting of acetonitrile/methanol/0.04%triethylamine pH 7.04 at proportion of 25/35/40 respectively. Then samples were HPLC analysed using a $C_{18}$-RP Purospher Star 5 μm, 250 × 4.6 mm column, equipped with a precolumn (Merck KGaA, Darmstadt, Germany). The sample injection volume was 20 μl. The mobile phase was delivered at 0.8 ml/min and the column was operated at ambient temperature. The effluents were monitored with a UV detector at 236 nm. Besides diazepam its metabolites temazepam, oxazepam and *N*-desmethyl-diazepam were detected. For all substances calibration curves were regularly run between 10 ng/ml and 10 μg/ml. Diazepam biotransformation was followed by the formation of the metabolites temazepam, oxazepam and *N*-desmethyl-diazepam. Diazepam elimination and its metabolite formation were assessed by incubating hepatocytes with 10 μg/ml diazepam.

### 2.10. Modelling

The purpose of the modelling study is to verify the performance of the proposed bioreactor device in terms of metabolites/catabolites mass transport (diffusion/perfusion), by determining the concentration profiles of albumin and urea (synthesized by hepatocyte) and diazepam (fed to the cells) in the extraluminal region of the central body of the bioreactor, where PEEK-WC and PES HFs cross-each other.

In order to decrease the geometrical and computational complexity of the system and to improve the clarity of the modelling output, the simulation space was divided in three-dimensional unit elements, each one representing the extraluminal region between two adjacent PEEK-WC fibers and two adjacent PES fibers. According to momentum and continuity equations, the analytical solutions for the velocity profiles in a single fiber of PEEK-WC are:

$$v_{ax} = \frac{2Q_f}{\pi R^2 N}\left(1 - \frac{Q_p}{Q_f}\frac{x}{L}\right)\left(1 - \frac{r^2}{R^2}\right) \quad (3)$$

$$v_{rad} = \frac{Q_p}{2\pi RLN}\left(\frac{2r}{R} - \frac{r^3}{R^3}\right) \quad (4)$$

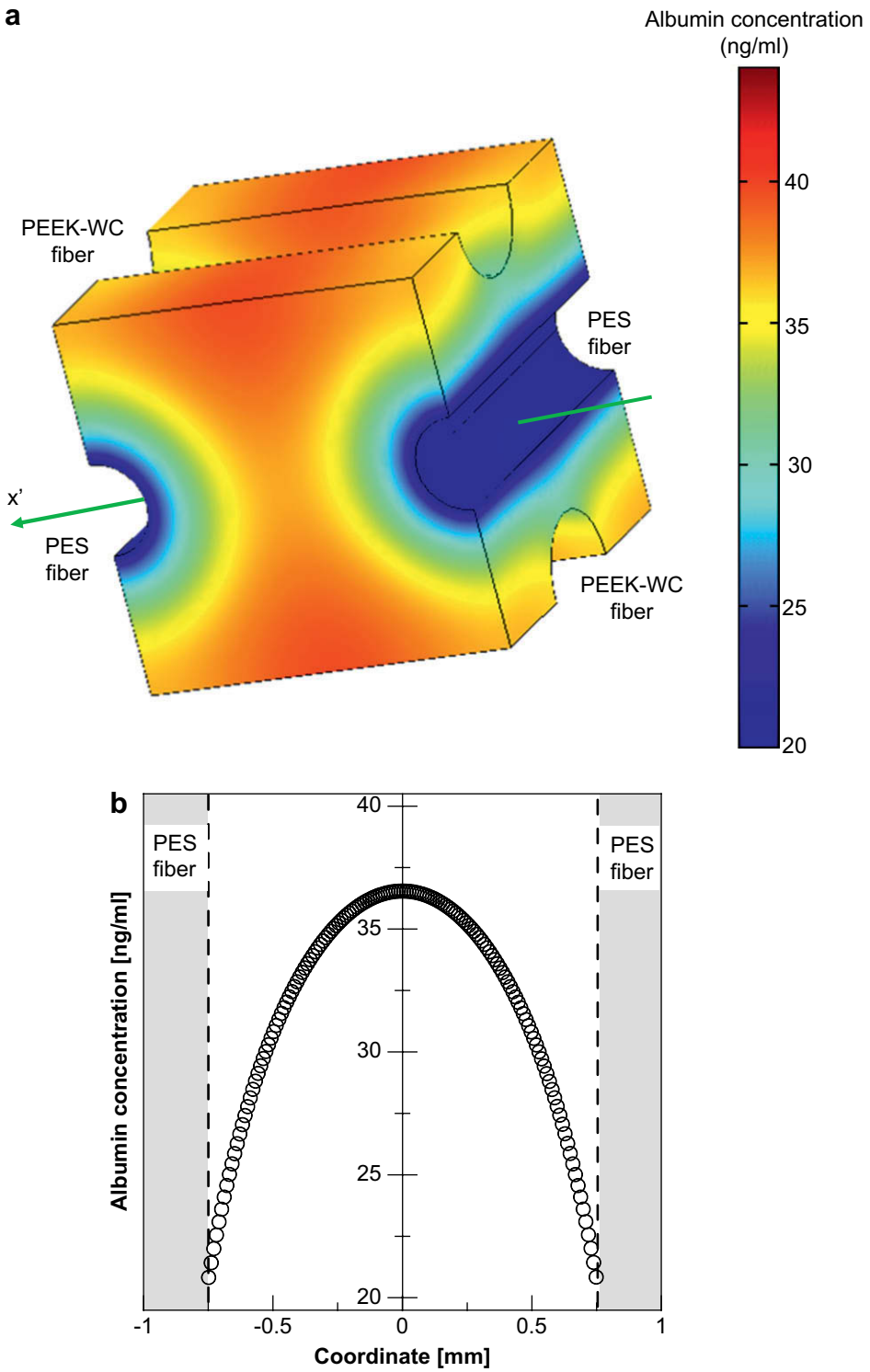


**Fig. 7.** a) Simulated distribution profile of albumin concentration (ng/ml) after 2 days; b) simulated concentration profile of albumin along the longitudinal direction between PES fibers (axis $x'$) at day 2.

The validity of Equations (3) and (4), when written along the axial coordinate $y$, is extended to PES fibers.

Focussing on the extraluminal space, the mass balance equation for the generic i-th component – written under the assumption that both density and diffusion coefficient $D_i$ are constant – is:

$$\frac{\partial c_i}{\partial t} + (v \cdot \nabla c_i) = D_i \nabla^2 c_i + \Psi_i \tag{5}$$

The reaction term $\Psi_i$ was assumed negative for the consumption of diazepam, and positive for the production of albumin and urea. Equation (5) was solved for the following boundary conditions:

$$c_i(t = 0) = 0 \text{ throughout the whole element} \tag{6a}$$

$$-D_i \nabla c_i + \nu_{radial} c_i = J_i \text{ at the membrane/extralumen interfacies, where } J_i \text{ is the transmembrane flux} \tag{6b}$$

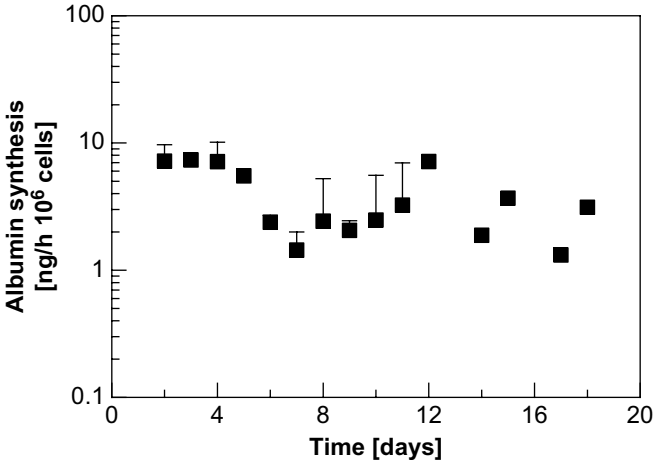


**Fig. 8.** Rate of albumin synthesis of human hepatocytes cultured in the crossed HF membrane bioreactor. The values are expressed as ng/h $10^6$ cells ± s.e.m. and are the mean of 6 experiments.

$$\nabla c_i = 0 \text{ in the remaining boundary surfaces} \quad (6c)$$

Due to the relatively low hydraulic permeance of PEEK-WC HFs ($2.1 \times 10^{-7}$ m/s mbar), the transport of diazepam (MW = 284.74 Da) was prevalently diffusive at the low working transmembrane pressure (<2 mbar). On the other hand, the measured hydraulic permeance of $4.2 \times 10^{-6}$ m/s mbar through PES HFs was 20 folds higher (more permeable HF membranes were used in order to assure an efficient removal of catabolites for the cellular compartment), thus determining a significant contribution of the convective transport mechanism.

The set of differential equations was numerically integrated by COMSOL MULTIPHYSICS® v3.3 Chemical Engineering Module, using a finite element method (FEM). Each simulation element in the extraluminal compartment was discretized into 23,266 nodes gradually thicker towards the hollow fibers and boundary surfaces. Because of the intensive memory request of the time-dependent computational process, the theoretical analysis has been protracted from the beginning until the second day of culture, and results compared to the corresponding experimentally measured data. On a 1.8 GHz Intel Personal Computer running under Windows XP v. 2000, the problem solution was reached – on average – within 30 min.

## 3. Results

Fig. 1 shows the crossed HF membrane bioreactor used for the hepatocyte culture. The bioreactor consists of two separate bundles of hollow fibers assembled in perpendicular at 250 μm distance each other. The four ends of the bioreactor are sealed by polyurethane potting. The medium entering the bioreactor via PEEK-WC permeates into the extracapillary space where cells are seeded before leaving the bioreactor via PES membranes, which exhibit high permeability and hydrophilicity. The structure and morphology of PES and PEEK-WC HF membranes are shown in Figs. 2 and 3 respectively. The PES HF membranes appeared to have an external porous structure, an internal diameter and wall thickness respectively of 300 ± 40 μm and 100 ± 25 μm. Differently the PEEK-WC HF membranes have an external surface less porous, an internal diameter and wall thickness respectively of 572 ± 6 μm and 51 ± 10 μm. This membrane has a moderate wettability although has a contact angle value higher with respect to the PES HF (Table 1).

The combination of these two fiber set produces and extracapillary network for the adhesion of cells and a high mass exchange through the cross-flow of culture medium.

Tracer experiments were performed in order to investigate the bioreactor fluid dynamics. According to the cumulative density function *F*, illustrated in the right-up corner of Fig. 4, the response of the system reached a uniform condition after 60 min; then remained constant throughout the duration of the experiment at operating flow rate $Q_f$ of 1.5 ml/min.

The residence time distribution function *E*, providing the age distribution of the non-ideal flow in the reactor, has been mathematically derived as:

$$E = \frac{dF}{dt} \quad (7)$$

For comparative purposes, the dimensionless variable $\theta$ has been defined as the ratio between the fluid residence time ($t$) and the mean retention time ($\tau$), and:

$$E_\theta = \tau E \quad (8)$$

In order to describe the deviation from ideality of the bioreactor (presumably caused by the existence of dead zones in the edge of the device and of active zones where PES and PEEK-WC fibers intersect each others), it has been assumed a model consisting in a continuous stirred tank reactor (CSTR) with active volume $V_m$ connected to a tank with volume $V_d$ under stagnant flow.

The response of this model in terms of $E_\theta$ is [33]:

$$E_\theta = \frac{V}{V_m} e^{-(V/V_m)\theta} \quad (9a)$$

where:

$$V = V_m + V_d \quad (9b)$$

The good agreement of the RTD response curve with that resulting from the model (Equations (9a) and (9b)), obtained assuming $V/V_m = 3$, can be deduced from Fig. 4. Under the chosen operating conditions, the bioreactor can be considered well mixed in the central part of its body, where hepatocytes are cultured in the extra-lumen side of crossing fibers.

After fluid dynamics characterization, the bioreactor was used for human hepatocyte culture.

Hepatocytes were cultured in the bioreactor in the medium containing serum only for the first 24 h thereafter they were cultured throughout the period with serum free medium. The appearance of the hepatocytes after 18 days of culture in the bioreactor was examined by SEM. Apparently the membranes induced a high level of cell adhesion as we can see in Fig. 5: a dense layer of cells was observed on the fibers. Hepatocytes appeared to be mostly polygonal in shape and surrounded by an extracellular matrix-like structure. Confocal images show the localization and organisation of two cytoskeleton proteins such as actin (green) and vinculin (red), which are major cytoskeletal proteins involved in integrin-mediated signaling and cell spreading. The cells appeared to establish cell–cell contacts and actin microfilaments are clearly displayed in hepatocytes adhered to the HF membranes. In Fig. 6 the staining for vinculin (red) shows a localization of the protein at the sites of cell–cell contact and cell membrane adhesion.

Functional maintenance of hepatocytes is crucial in assessing the performance of the crossed HF membrane bioreactor. The transport of liver specific products such as albumin and urea together with the transport of drug such as diazepam was modelled and compared with the experimental metabolic data.

The graphical output of FEM simulation at day 2 for the concentration profile of albumin in the extraluminar space comprised between PES and PEEK-WC fibers is shown in Fig. 7a. As expected, albumin concentration (produced by hepatocytes cultured in the shell of the bioreactor) increases at higher distance from PES fibers. A difference of 75% was predicted between the value of albumin concentration in the core of the simulated element and at the interface of the extraction fibers; this value confirms the interesting ability of the cross-fibers configuration to efficiently transfer this protein from the cell compartment to the medium compartment.

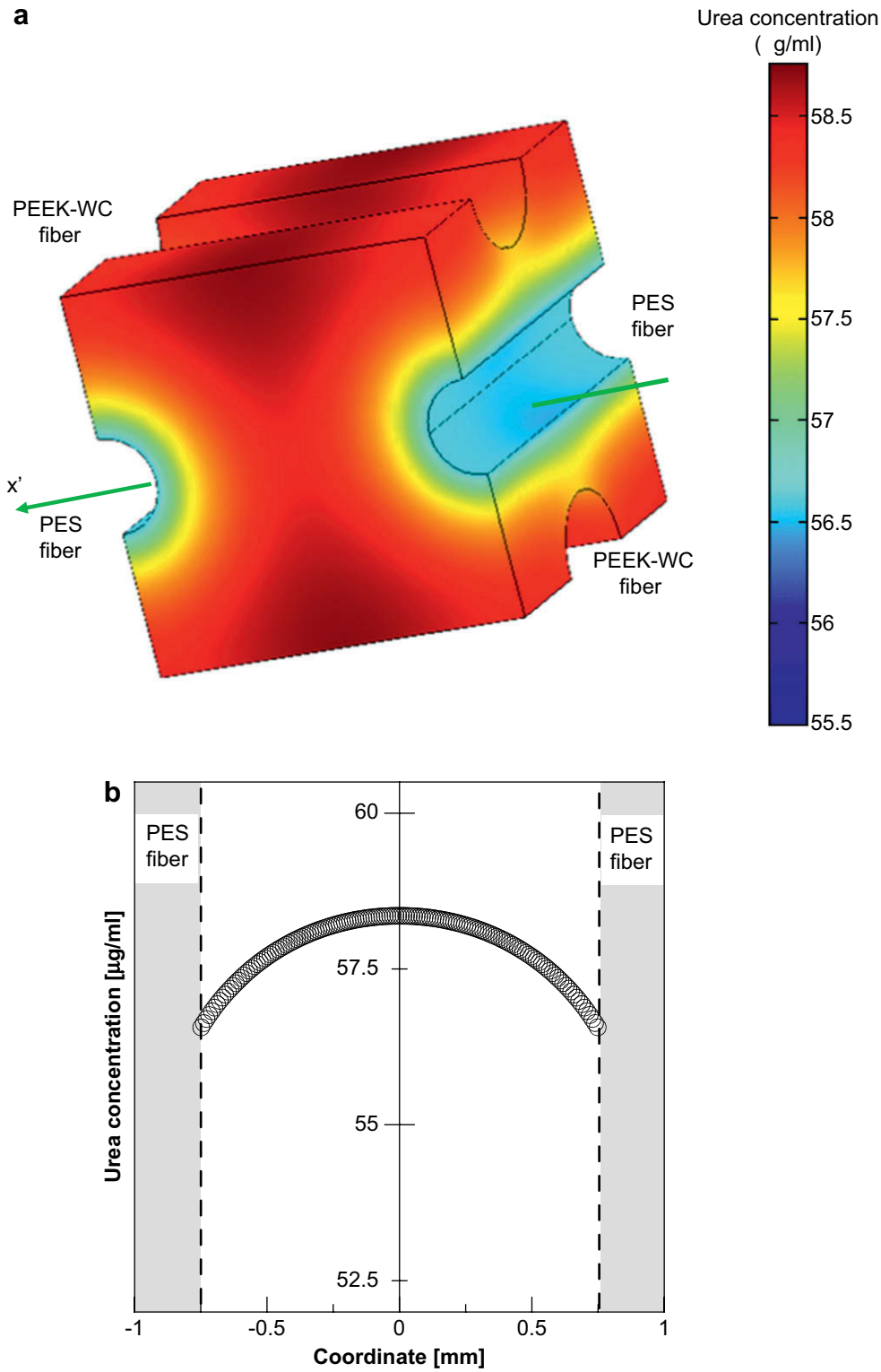


**Fig. 9.** a) Simulated distribution profile of urea concentration (μg/ml) after 2 days; b) simulated concentration profile of urea along the longitudinal direction between PES fibers (axis $x'$) at day 2.

The concentration profile along the longitudinal direction between PES fibers (axis $x'$ in Fig. 7a) appears symmetric and parabolic, as reported in Fig. 7b, reaching a maximum value of 36.5 ng/ml in the middle of the compartment. According to reaction kinetic measurements, over the first 4 days albumin is synthesized by hepatocyte cells cultured in the bioreactor with an average rate of $7.2 \pm 2.7$ ng/h $10^6$ cells. This value then decreases to $2.4 \pm 0.3$ ng/h $10^6$ cells at day 6 and remains almost constant over the entire second week (Fig. 8).

Interesting it is to note that the human hepatocytes maintained their differentiated functions with respect to the albumin secretion up to 18 days although they expressed a low activity of albumin synthesis. This is probably due to the use of cryopreserved human hepatocytes.

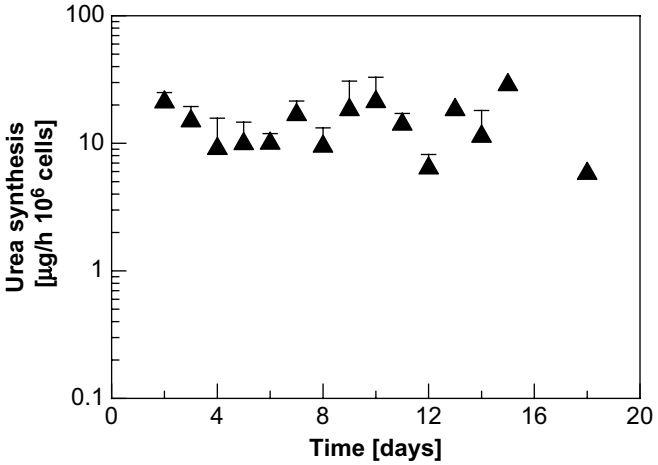


**Fig. 10.** Rate of urea synthesis of human hepatocytes cultured in the crossed HF membrane bioreactor. The values are expressed as μg/h $10^6$ cells ± s.e.m. and are the mean of 6 experiments.

In order to validate the model, the predicted value of metabolite concentration in correspondence of the PES fiber was compared to the experimental value read in the intraluminal solution. For albumin, the theoretical value at day 2 (20.82 ng/ml, read at coordinates ±0.75 mm in Fig. 7b) differed by 7.5% with respect to the experimental one (19.25 ng/ml), thus confirming the good consistency of the FEM model.

The theoretical concentration gradients of urea in the extraluminal space of the bioreactor appears quite smooth, as shown in Fig. 9a, with a difference between the core of the cellular compartment and the interface at PES fibers of about 5%. This behaviour is determined by both kinetic and diffusion aspects. The observed production rate of urea is more than 3 orders of magnitude higher than the production rate of albumin (Fig. 10), and from the value of 21.0 ± 3.9 μg/h $10^6$ cells measured at day 2 it decreases down to an average value of 9.9 ± 3.3 μg/h $10^6$ cells observed from day 4 to day 5. In addition, the diffusional rate of urea is one order of magnitude higher than albumin, as a result of ~1000-times lower MW. The synthesis rate increased to ~16 μg/h $10^6$ cells in the subsequent days, scattering around this average value by ±15%. Also for urea, the concentration value predicted at day 2 (56.56 μg/ml, read at coordinates ±0.75 mm in Fig. 9b) well agreed with the experimentally observed one (53.43 μg/ml, difference of 5.8%).

The liver is the most important organ concerning biotransformation of xenobiotics. Benzodiazepine biotransformation was evaluated by use of the synthetic compound diazepam. The modelled concentration profile at day 2 of diazepam, fed through PEEK-WC fibers (~10 μg/ml in the medium), metabolised by hepatocyte cells and removed through PES fibers is shown in Fig. 11. Diazepam is consumed with steadily decreasing reaction rate, from 4.88 ± 2.42 μg/h $10^6$ cells measured at day 2 to 1.65 ± 0.75 μg/h $10^6$ cells measured at day 5; this behaviour has been also observed, with regularity after changing medium, in the successive days of culture (Fig. 12a).

The concentration profile along the longitudinal direction between PEEK-WC fibers (axis $y'$ in Fig. 11a) reaches the minimum value in proximity of the central part of the extraluminal space (2.66 μg/ml), corresponding to a reduction of 73% with respect to the diazepam concentration in the feed (Fig. 11).

Fig. 12a displays the comparison between the diazepam concentration present in the inlet culture medium and in the outlet medium after incubation with cells into the bioreactor. The metabolic pathway of diazepam includes the metabolites temazepam, oxazepam and *N*-desmethyl-diazepam; all these metabolites were generated in the bioreactor, as shown in Fig. 12b.

In particular, the synthesis rate of temazepam was bigger than production rates experimentally observed for the other metabolites, passing from 373.5 ± 73.4 ng/h $10^6$ cells (day 2) to 182.8 ± 94.3 ng/h $10^6$ cells (day 18) through a maximum of 731.4 ± 91 ng/h $10^6$ cells at day 6. *N*-desmethyl-diazepam and oxazepam were produced for all culture time at averaged rates of about 17 ng/h $10^6$ cells and 11.3 ng/h $10^6$ cells respectively.

According to Fig. 12a, the agreement between theoretical concentration of diazepam at day 2 (1.80 μg/ml) and the experimentally observed one (1.56 ± 0.33 μg/ml) is satisfactory. Moreover, the model results can be extended over the first 5 days of culture with reasonable accuracy, thus representing a powerful predictive tool for evaluating the performance of the crossed fibers membrane bioreactor.

The results of the theoretical analysis examined in terms of the squared observed Thiele modulus $\phi^2_{obs}$, defined as the ratio between the observed chemical reaction rate ($r_{obs}$) to the rate of diffusion in the extraluminar space ($D_{eff}$):

$$\phi^2_{obs} = \frac{r_{obs}}{D_{eff} c_b} \left(\frac{l}{2}\right)^2 \quad (10)$$

show the different impact of diffusional phenomena and reaction kinetics [33]. In Equation (10), $c_b$ is the bulk concentration of the metabolite or drug, and $l$ the packing distance of fibers.

For albumin, the value of $\phi^2_{obs}$ within the first 4 days is around 0.1, thus evidencing a moderate prevalence of the production rate over the transport rate. For urea, the squared observed Thiele modulus is 0.006, confirming a tendency towards a kinetic control due to the higher diffusional rate of this catabolite (MW = 60.06 Da, $D_{eff} = 8.6 \times 10^{-4}$ mm$^2$/s) with respect to albumin (MW = 60.6 kDa, $D_{eff} = 6.4 \times 10^{-5}$ mm$^2$/s). An analogous result ($\phi^2_{obs} = 0.011$) was found for diazepam, having a molecular weight (284.74 Da) closer to urea.

## 4. Discussion

Optimization of culture conditions for maintenance of hepatocyte function and phenotype is necessary for the development of clinical device or in vitro cell-based tissue construct. Several researchers have shown that the substrate, neighbouring cells, nutrients and oxygen transfer can influence the viability and functions of hepatocytes [36–38]. The substrate where cells are cultured not only provide a surface for cell adhesion but also have profound influence on modulating the cell shape and gene expression relevant to cell growth and liver specific functions [39].

In this study we describe the morphological and functional maintenance of human hepatocytes in a crossed HF bioreactor whose configuration and fluid dynamics were optimised in order to ensure an adequate mass transfer of nutrients and drug to the cell compartment and a removal of specific products and catabolites from the cell compartment. The two-fiber system with different morphological and physico-chemical properties has a constant distance of 250 μm inside the bioreactor. This geometry allows achieving a homogeneous and small size cell aggregates, which facilitate mass transfer and therefore the perfusion of cells cultured inside the network of the fibers and the necessary turnover of the medium in the cell compartment. Both for nutrient supply and waste elimination, mass transfer to and from cells is a critical issue in any bioreactor design especially when cells are cultured in three-dimensional multicellular aggregates where mass transfer limitation of oxygen and metabolism may occur in the core of aggregates [6]. In the case of the design of bioartificial liver besides the catabolites (e.g., lactate, ammonium, carbon dioxide) removal, the accumulation of toxins and toxic metabolites produced by drug biotransformation must be

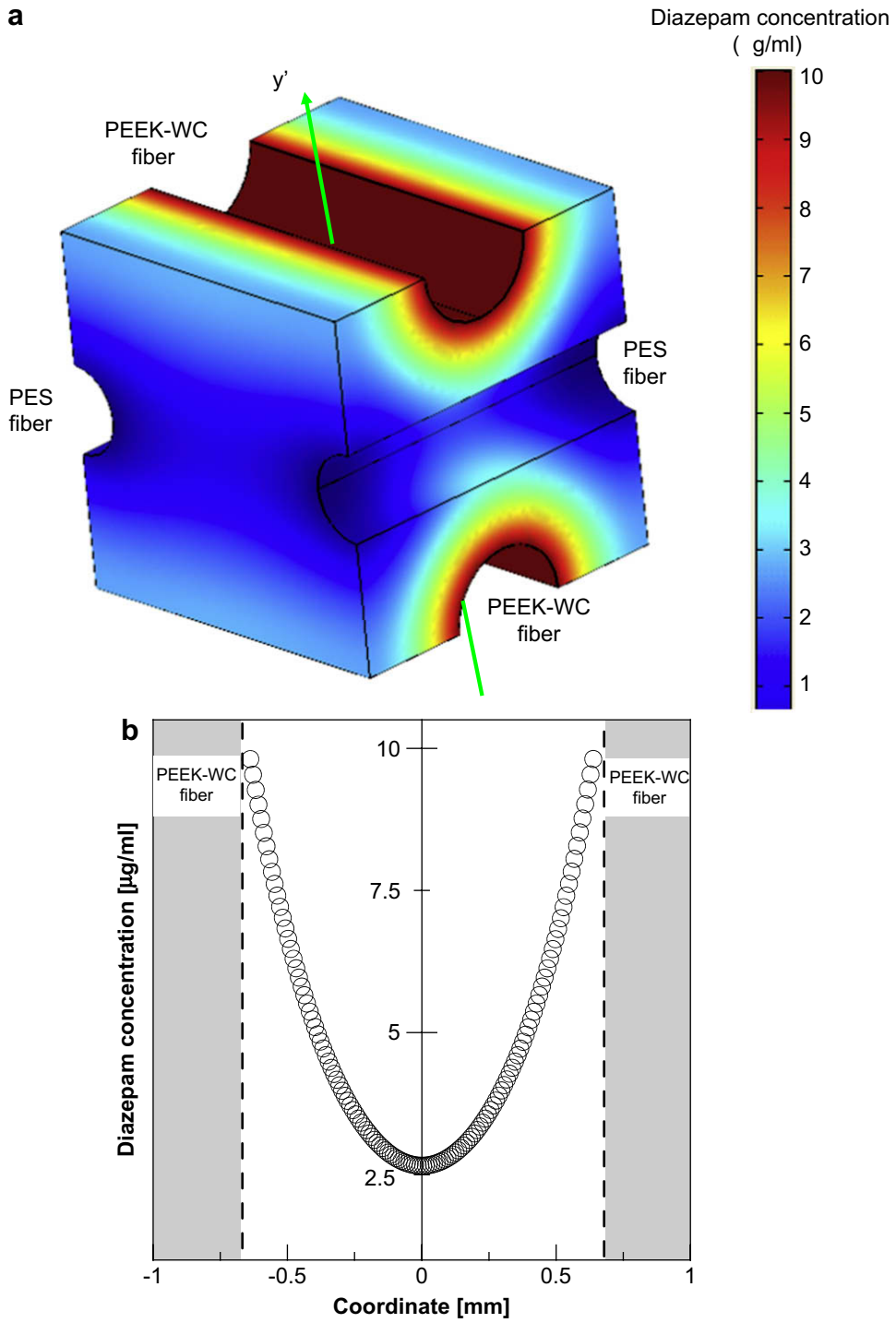


**Fig. 11.** a) Simulated distribution profile of diazepam concentration (μg/ml) after 2 days; b) simulated concentration profile of diazepam along the longitudinal direction between PEEK-WC fibers (axis *y'*) at day 2.

avoided in order to maintain viable and functional cells inside the bioreactor environment. Furthermore, the delivery of plasma proteins as well as large MW proteins (e.g., clotting factors) and drug metabolites must be ensured in both clinical and in vitro devices.

The efficient mass transfer of nutrients, metabolites and toxins appear to be a key point in all bioreactor designs varied from classical (hemodyalisers) to more complicated geometry. In this paper the transport phenomena related to diffusion and reaction of liver metabolites such as albumin and urea and of diazepam are mathematically described and experimentally verified.

Differently from the most of papers present in literature that reported the morphological and functional changes of rat liver cells, pig hepatocytes, hepatoma cell lines or immortalized cell lines [8,11–13,24,40], we investigated the liver specific and biotransformation functions of primary human hepatocytes in a crossed HF bioreactor. It is well-known, in fact, that hepatoma cells, although easier to culture, have important functional differences: they may express only a set of hepatic functions and at levels different from those exhibited by normal hepatocytes, as compared to primary hepatocytes [41,42]. Hepatocytes isolated from animals have

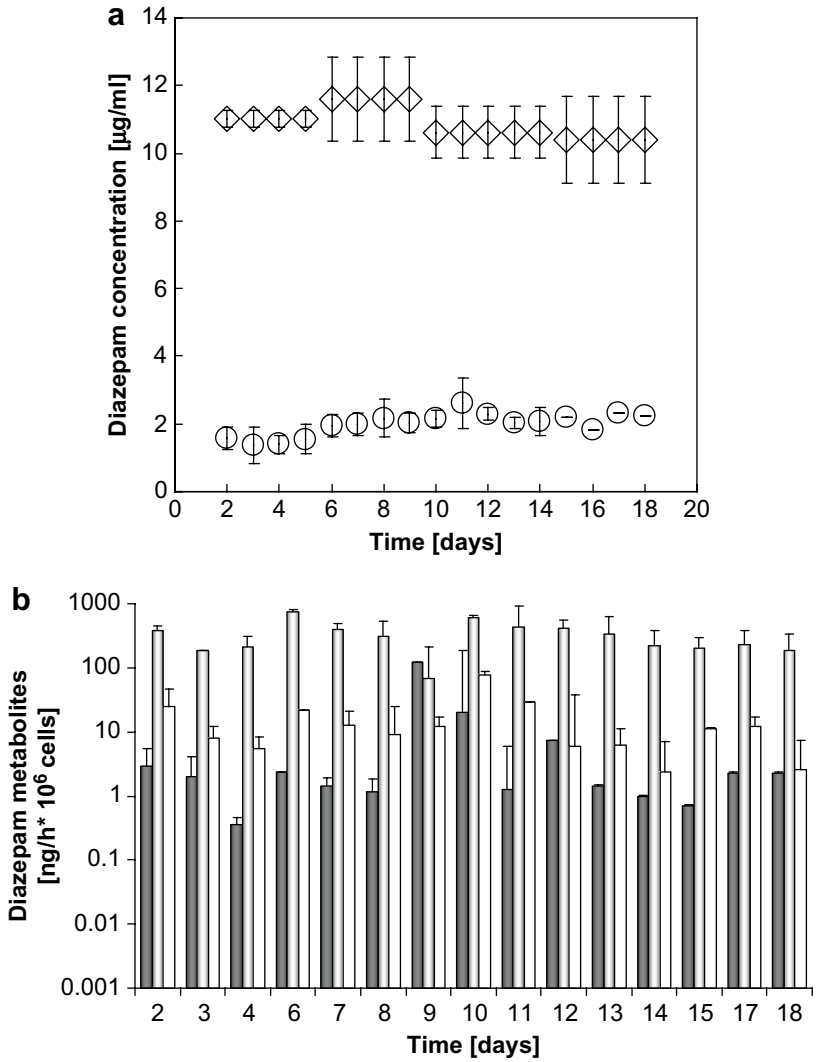


**Fig. 12.** a) Diazepam concentration in the inlet medium (◇) and in outlet medium from bioreactor loaded with cells (○) in presence of 10 μM diazepam added to the culture medium. b) Formation of diazepam metabolites: (full bar) oxazepam, (grey bar) temazepam and (white bar) *N*-desmethyl-diazepam. The values are expressed as ng/h $10^6$ cells ± s.e.m. and are the mean of 6 experiments.

different drug metabolising enzymes especially those related to cytochrome P450. Thus, results obtained from other cells cannot be directly transferred to humans. Primary human hepatocytes are preferred particularly in drug metabolism studies since they are the closest model to the human liver and therefore reflect its functionality in vivo [43].

As reported in literature, important shortcomings in the use of hollow fiber membrane reactors related the limitation to the mass transport of nutrients and metabolites, were faced by arranging fibers in cell plates with sinusoidal structures located on both sides. A particularly interesting approach was undertaken by Gerlach et al. [17] by using a multicompartment bioreactor with four different capillary membranes, each one serving a specific function: a) plasma inflow, b) plasma outflow, c) decentralised oxygen supply and carbon dioxide removal, and d) sinusoidal endothelial co-culture. This complex geometry was proven to ensure adequate perfusion of cells with medium/plasma, oxygen and removal of catabolites and liver specific products.

In our work, the two different kinds of HF membranes used to facilitate the mass exchanges between medium/cells compartments, mimic the in vivo arterious and venous blood vessels. Moreover, this approach reduces the complexity of the bioreactor analysis, thus obtaining a satisfactory control of the operational parameters (including fluid dynamics optimization) and of the system performance, as confirmed by the good correspondence between the experimental results and simulation data.

The ability to support cell metabolic functions using PEEK-WC hollow fibers (190 kDa MWCO), by supplying nutrients and drugs contained in the medium according to a transport mechanism prevalently diffusive, has been demonstrated in previous studies [32].

PES HF membranes, because of their high pore size (0.2 μm), show high permeability and provide unhindered transport of molecules which result in a facilitated and efficient removal of molecules from cell compartments through a predominantly convective mechanism. These benefits are particularly evident for albumin, a high MW macromolecule: according to simulation results, the concentration at PES fiber interface is reduced by 75% with respect to the concentration in the bulk of the bioreactor.

The long-term stability of human liver cells in a biohybrid system is required for in vitro and clinical applications. Perfusion bioreactor conditions allowed the maintenance of human hepatocytes into the bioreactor. The liver specific functions expressed in terms of urea synthesis and albumin production were maintained at high levels for 18 days (Figs. 8 and 10). Also the

biotransformation functions were performed by cells in the bioreactor for all culture time (Fig. 12).

In particular, the good performance of the reactor in terms of detoxification functions is confirmed by the high urea synthesis rate, that reaches the maximum value of 28.7 μg/h $10^6$ cells at day 15, remarkably higher with respect to the values of: 3.8 μg/h $10^6$ cells reported in literature by Gerlach in a hybrid liver support system [44], 1.7 μg/h $10^6$ cells found by Flendrig et al. using a spirally wound nonwoven polyester matrix [16], ~2.5 μg/h $10^6$ cells reported by Mizumoto et al. for hepatocyte (from Wistar rat) organoids cultured in the lumen of highly permeable hollow fibers [45], 6.0 μg/h $10^6$ cells determined by Jasmund et al. in a oxygenating hollow fiber bioreactor cultivated with primary porcine hepatocytes [46]; ~3 μg/h $10^6$ cells observed by Lu et al. in a galactosylated poly(vinylidene difluoride) hollow fiber bioreactor [24]; 9.2 μg/h $10^6$ cells measured by Park and colleagues (2008) in a stacked microfabricated grooved-substrate bioreactor [11].

Also the biotransformation functions were performed by cells in the bioreactor for all culture time. Diazepam is metabolised by cytochrome P450 activities. In the bioreactor about 87% of the administered diazepam was metabolised during the first days of culture. Diazepam in human is metabolised through 3-hydroxylation to temazepam and *N*-desmethylation to *N*-desmethyldiazepam, Both metabolites are then hydroxylated to oxazepam the main metabolite found in the urine as a glucuronide. Diazepam 3-hydroxylation activity is catalysed mostly by CYP3A4 enzyme whereas the diazepam *N*-desmethylation is catalysed by both CYP3A4 and 2C19 and partly by the *S*-mephenytoin hydroxylase. Oxazepam is formed either by Cyp 3A4 or to a lesser extent by CYP 2C19 and 3A5 via the 3-hydroxylation of *N*-desmethyldiazepam or via the *N*-demethylation of temazepam [47]. We have shown previously that human polarized hepatocytes in vitro can form phase II metabolites such as sulfonation and glucuronidation [48]. Such metabolites are end products of biotransformation following initial phase I biotransformation. Out of the 3 diazepam CYP450 phase I metabolites the phase II glucuronidation has been reported also previously [49]. In the recirculating mode of the bioreactor we could measure daily metabolic activity and used the available standards of these metabolites for validation.

Our results indicate that temazepam is produced to a larger extent with respect to *N*-desmethyldiazepam and oxazepam. The high cell specific activity found in this study and the high synthesis rate of the all diazepam metabolites is a clear proof for the workability of the device concept. As a term of comparison, the synthesis rate of oxazepam measured by De Bartolo et al. in a flat membrane bioreactor using porcine hepatocytes [21] was found almost constant during 18 days of culture time, with values lower, ranging within 0.58 and 0.62 ng/h $10^6$ cells.

The cross-fiber reactor is able to sustain the diazepam metabolism through the formation of intermediates desmethyldiazepam and temazepam and the subsequent conversion to the final metabolite. For primary porcine hepatocytes cultivated in an oxygenating HF bioreactor, Jasmund et al. [46] observed a lower production of diazepam metabolites (estimated synthesis rate for oxazepam ~0.2 ng/h $10^6$ cells, for desmethyldiazepam ~0.5 ng/h $10^6$ cells, for temazepam ~1 ng/h $10^6$ cells) with respect to our experimental results, due to the specific differences in the rate of metabolism and expression of enzymes involved in the drug metabolism between animal and humans.

These results demonstrate that the diazepam is completely metabolised as occur in humans where each of metabolites is finally converted to oxazepam. In the bioreactor the human hepatocytes expressed at high levels the individual CYP isoforms involved in the diazepam biotransformation. These enzymes are among the most sensitive and fragile found in hepatocytes, responding quickly by loss of activities to unfavourable culture conditions. The high cell specific activity found in this study demonstrates the good performance of the bioreactor to maintain viable and functional integrity of human hepatocytes.

## 5. Conclusions

We described the functional behaviour of human hepatocytes cultured in a crossed HF membrane bioreactor. In this device cells were cultured in an extracapillary network formed by two fiber set that allow a high mass exchange through the cross-flow of culture medium. The fluid dynamics and mass transport of metabolites through the fibers were characterized and optimised in order to closely mimic the perfusion conditions found in vivo hepatic tissue. The transport phenomena related to diffusion and reaction of liver metabolites such as albumin, urea and diazepam, which were mathematically described, was in good agreement with experimental metabolic data. As a result of the adequate perfusion conditions, human hepatocytes maintained their metabolic functions for all investigated period. Diazepam was completely metabolised as occur in vivo where each of metabolites is finally converted to oxazepam. The crossed HF membrane bioreactor can potentially be used to address the mass transfer limitations currently seen in liver tissue engineered constructs.

## Acknowledgements

This work was supported by grants from the European Commission through the Livebiomat project STREP NMP3-CT-013653 in the FP6.

## Appendix

Figures with essential colour discrimination. Certain figures in this article, in particular Figs. 6, 7, 9 and 11, are difficult to interpret in black and white. The full colour images can be found in the online version, at doi:10.1016/j.biomaterials.2009.01.011.

## References

[1] Berry MN, Edwards AM. The hepatocyte review. Dordrecht, Boston, London: Kluwer Academic Publishers; 2000. p. 365–85.
[2] Guillozo A, Begue JM, Campion JP, Gascoin MN, Guguen-Guillozo C. Human hepatocyte culture: a model of pharmaco-toxicological studies. Xenobiotica 1985;15:635–41.
[3] Donato MT, Castell JV, Gomez-Lechon MJ. Co-cultures of hepatocytes with epithelial-like cell lines: expression of drug biotransformation activities by hepatocytes. Cell Biol Toxicol 1991;7:1–14.
[4] Dunn JC, Tompkins RG, Yarmush ML. Long-term in vitro function of adult hepatocytes in a collagen sandwich configuration. Biotechnol Prog 1991;7:237–45.
[5] Nozaki T, Yamato M, Nishida K, Okano T. Transportation of transplantable cell sheets fabricated with temperature-responsive culture surfaces for regenerative medicine. J Tissue Eng Regen Med 2008;2:190–5.
[6] Curcio E, Salerno S, Barbieri G, De Bartolo L, Drioli E, Bader A. Mass transfer and metabolic reactions in hepatocyte spheroids cultured in rotating wall gas-permeable membrane system. Biomaterials 2007;28:5487–97.
[7] Yarmush ML, Toner M, Dunn JC, Rotem A, Hubel A, Tompkins RG. Hepatic tissue engineering. Development of critical technologies. Ann N Y Acad Sci 1992;665:238–52.
[8] Park TG. Perfusion culture of hepatocytes within galactose-derivatized biodegradable poly(lactide-*co*-glycolide) scaffolds prepared by gas foaming of effervescent salts. J Biomed Mater Res 2002;59:127–35.
[9] Allen JW, Hassanein T, Bathia SN. Advance in bioartificial liver devices. Hepatology 2001;34:447–55.
[10] Strain AJ, Neuberger JM. A bioartificial liver – state of the art. Science 2002;295:1005–9.
[11] Park J, Li Y, Berthiaume F, Toner M, Yarmush ML, Tilles AW. Radial flow hepatocyte bioreactor using stacked microfabricated grooved substrates. Biotechnol Bioeng 2008;99(2):455–67.

[12] Powers MJ, Janigian DM, Wack KE, Baker CS, Beer Stolz D, Griffith LG. Functional behaviour of primary rat liver cells in a three-dimensional perfused microarray bioreactor. Tissue Eng 2002;8:499–513.
[13] Schmitmeier S, Langsch A, Jasmund I, Bader A. Development and characterization of a small-scale bioreactor based on a bioartificial hepatic culture model for predictive pharmacological in vitro screenings. Biotech Bioeng 2006;95/6:1198–206.
[14] Curcio E, De Bartolo L, Barbieri G, Rende M, Giorno L, Morelli S, et al. Diffusive and convective transport through hollow fiber membranes for liver cell culture. J Biotechnol 2005;117:309–21.
[15] Martin Y, Vermett P. Bioreactors for tissue mass culture: design, characterisation, and recent advances. Biomaterials 2005;26:7481–503.
[16] Flendrig LM, La Soe JW, Joerning GGA, Steenbeck A, Karlsen OT, Bovée WMM, et al. In vitro evaluation of a novel bioreactor based on an integral oxygenator and a spirally wound nonwoven polyester matrix for hepatocyte culture as small aggregates. J Hepatol 1997;26:1379–92.
[17] Gerlach J, Trost T, Ryan CJ, Meissler M, Hole O, Müller C, et al. Hybrid liver support system in a short term application on hepatectomized pigs. Int J Artif Organs 1994;17:549–53.
[18] Jauregui HO, Mullon CJP, Trenkler D, Naik S, Santangini H, Press P, et al. In vivo evaluation of a hollow fiber liver assist device. Hepatology 1995;21:460–9.
[19] Nyberg SL, Shatford RA, Peshwa MW, White JG, Cerra FB, Hu WS. Evaluation of a hepatocyte-entrapment hollow fiber bioreactor: a potential bioartificial liver. Biotechnol Bioeng 1992;41:194–203.
[20] Patzer JF. Advances in bioartificial liver assist devices. Ann N Y Acad Sci 2001;944:320–33.
[21] De Bartolo L, Jarosch-Von Schweder G, Haverich A, Bader A. A novel full-scale flat membrane bioreactor utilizing porcine hepatocytes: cell viability and tissue-specific functions. Biotechnol Prog 2000;16:102–8.
[22] Dunn JC, Tompkins RG, Yarmush ML. Hepatocytes in collagen sandwich: evidence for transcriptional and translational regulation. J Cell Biol 1992;116:1043–53.
[23] Sanchez A, Alvarez Pagan R, Roncero C, Vilaro S, Benito M, Fabregat I. Fibronectin regulates morphology, cell organization and gene expression of rat fetal hepatocytes in primary culture. J Hepatol 2000;32(2):242–50.
[24] Lu H-F, Lim WS, Zhang PC, Chia SM, Yu H, Mao HQ, et al. Galactosylated poly(vinylidene difluoride) hollow fiber bioreactor for hepatocyte culture. Tissue Eng 2005;11:1667–77.
[25] De Bartolo L, Morelli S, Lopez L, Giorno L, Campana C, Salerno S, et al. Biotransformation and liver specific functions of human hepatocytes in culture on RGD-immobilised plasma-processed membranes. Biomaterials 2005;26(21):4432–41.
[26] Watanabe Y, Liu X, Shibuya I, Akaike T. Functional evaluation of poly-(*N*-*p*-vinylbenzyl-*O*-*b*-D-galactopyranosyl-[1-4]-D-gluconamide) (PVLA) as a liver specific carrier. J Biomater Sci Polym Ed 2000;11:833–48.
[27] De Bartolo L, Morelli S, Bader A, Drioli E. Evaluation of cell behaviour related to physico-chemical properties of polymeric membranes to be used in bioartificial organs. Biomaterials 2002;23(12):2485–97.
[28] Krasteva N, Harms U, Albrecht W, Seifert B, Hopp M, Altankov G, et al. Membranes for biohybrid liver support systems – investigations on hepatocyte attachment, morphology and growth. Biomaterials 2002;23:2467–78.
[29] De Bartolo L, Catapano G, Della Volpe C, Drioli E. The effect of surface roughness of microporous membranes on the kinetics of oxygen consumption and ammonia elimination by adherent hepatocytes. J Biomater Sci Polym Ed 1999;10(6):641–55.
[30] De Bartolo L, Morelli S, Rende M, Gordano A, Drioli E. New modified polyetheretherketone membrane for liver cell culture in biohybrid systems: adhesion and specific functions of isolated hepatocytes. Biomaterials 2004;25:3621–9.
[31] Kimmerle K, Strathmann H. Analysis of the structure-determining process of phase inversion membranes. Desalination 1990;79:283–302.
[32] De Bartolo L, Piscioneri A, Cotroneo G, Salerno S, Tasselli F, Campana C, et al. Human lymphocyte PEEK-WC hollow fiber membrane bioreactor. J Biotechnol 2007;132:65–75.
[33] Levenspiel O. Chemical reaction engineering. New York: Wiley; 1972.
[34] Karim N, Allmeling C, Hengstler J-G, Haverich A, Bader A. Diazepam metabolism and albumin secretion of porcine hepatocytes in collagen-sandwich after cryopreservation. Biotechnol Lett 2000;22:1647–52.
[35] Bader A, De Bartolo L, Haverich A. High level benzodiazepine and ammonia clearance by flat membrane bioreactors with porcine liver cells. J Biotechnol 2000;81(2–3):95–105.
[36] Fiegel HC, Havers J, Kneser U, Smith MK, Moeller T, Kluth D, et al. Influence of flow conditions and matrix coatings on growth and differentiation of three-dimensionally cultured rat hepatocytes. Tissue Eng 2004;10:165–74.
[37] Bathia SN, Balis UJ, Yarmush ML, Toner M. Effect of cell–cell interactions in preservation of cellular phenotype: co-cultivation of hepatocytes and non-parenchymal cells. FASEB J 1999;13:1883–900.
[38] Yamada KM, Clark K. Survival in three dimensions. Nature 2002;419:790–1.
[39] Mooney DJ, Hansen L, Vacanti JP, Langer R, Farmer S, Ingber D. Switching from differentiation to growth in hepatocytes: control by extracellular matrix. J Cell Physiol 1992;151:497–505.
[40] Du Y, Han R, Wen F, San SNS, Xia L, Wohland T, et al. Synthetic sandwich culture of 3D hepatocyte monolayer. Biomaterials 2008;29:290–301.
[41] Wilkening S, Stahl F, Bader A. Comparison of primary human hepatocytes and hepatoma cell line HEPG2 with regard to their biotransformation properties. Drug Metab Dispos 2003;31:1035–42.
[42] Guillozo A, Morel F, Langouet S, Maheo K, Rissel M. Use of hepatocyte cultures for study of hepatotoxic compounds. J Hepatol 1997;26(Suppl. 2):23–80.
[43] Gomez-Lechon MJ, Donato MT, Catsell JV, Jover R. Human hepatocytes as a tool for studying toxicity and drug metabolism. Curr Drug Met 2003;4:292–312.
[44] Gerlach JC. Development of a hybrid liver support system: a review. Int J Artif Organs 1996;19:645–54.
[45] Mizumoto H, Ishihara K, Nakazawa K, Ijima H, Funatsu K, Kajiwara T. A new culture technique for hepatocyte organoid formation and long-term maintenance of liver specific functions. Tissue Eng Part C 2008;14:167–75.
[46] Jasmund I, Langsch A, Simmoteit R, Bader A. Cultivation of primary porcine hepatocytes in an OXY-HFB for use as a bioartificial liver device. Biotechnol Prog 2002;18:839–46.
[47] Ono S, Hatanaka T, Miyazawa S, Tsutsui M, Aoyama T, Gonzales FJ, et al. Human liver microsomal diazepam metabolism using cDNA-expressed cytochrome P450s: role of CYP2B6, 2C19 and the 3A subfamily. Xenobiotica 1996;26:1155–66.
[48] Kern A, Bader A, Pichlmayr R, Sewing K-F. Drug metabolism in hepatocyte sandwich cultures of rats and humans. Biochem Pharmacol 1997;54:761–72.
[49] Court MH, Hao Q, Krishnaswamy S, Bekaii-Saab T, Al-Rohaimi A, von Moltke LL, et al. UDP-glucuronosyltransferase (UGT) 2B15 pharmacogenetics: UGT2B15 D85Y genotype and gender are major determinants of oxazepam glucuronidation by human liver. J Pharmacol Exp Ther 2004;310(2):656–65.

## List of symbols

| | |
|---|---|
| *c:* | concentration, μg/ml |
| *E:* | RTD function, – |
| *F:* | RTD cumulative function, – |
| $J_i$: | transmembrane flux, μg/(mm)$^2$min |
| *l:* | Distance between fibers, mm |
| *L:* | fiber length, mm |
| *N:* | number of fibers, – |
| *Q:* | flowrate, ml/min |
| *r:* | radial coordinate, – |
| *R:* | fiber radius, mm |
| *t:* | time, min |
| *v:* | velocity, mm/min |
| *V:* | volume, ml |
| *x:* | *x*-axis coordinate |
| *y:* | *y*-axis coordinate |
| *z:* | *z*-axis coordinate |

*Greek symbols*

| | |
|---|---|
| $\tau$: | mean retention time, min |
| $\theta$: | dimensionless time, – |
| $\Psi_i$: | reaction term, μg/ml min |

*Subscripts*

| | |
|---|---|
| *ax:* | axial |
| *b:* | bulk |
| *d:* | dead (volume) |
| *f:* | feed |
| *in:* | inlet |
| *eff:* | effective |
| *m:* | active (volume) |
| *obs:* | observed |
| *out:* | outlet |
| *p:* | permeate |
| *r:* | recycle |
| *rad:* | radial |

*Acronyms*

| | |
|---|---|
| *CSTR:* | Continuous stirred tank reactor |
| *DMF:* | Dimetylformamide |
| *FEM:* | Finite element method |
| *HF:* | Hollow Fiber |
| *MWCO:* | Molecular weight cut-off |
| *PEEK-WC:* | Polyetheretherketone with cardo group |
| *PES:* | Polyethersulfone |
| *PVP:* | Polyvinylpyrrolidone |
| *RTD:* | Residence time distribution |

Journal of Membrane Science 325 (2008) 139–149

Contents lists available at ScienceDirect

Journal of Membrane Science

journal homepage: www.elsevier.com/locate/memsci

# Influence of membrane surface properties on the growth of neuronal cells isolated from hippocampus

Loredana De Bartolo[a,*], Maria Rende[a,b], Sabrina Morelli[a], Giuseppina Giusi[c], Simona Salerno[a], Antonella Piscioneri[a,d], Amalia Gordano[a], Anna Di Vito[c], Marcello Canonaco[c], Enrico Drioli[a,b]

[a] Institute on Membrane Technology, National Research Council of Italy, ITM-CNR, via P. Bucci Cubo 17/C, Rende (CS), Italy
[b] Department of Chemical Engineering and Materials University of Calabria, via P. Bucci, Rende (CS), Italy
[c] Comparative Neuroanatomy Laboratory, Department of Ecology, University of Calabria, via P. Bucci, 87030 Rende (CS), Italy
[d] Department of Cell Biology, University of Calabria, via P. Bucci, 87030 Rende (CS), Italy

ARTICLE INFO

*Article history:*
Received 28 April 2008
Received in revised form 27 June 2008
Accepted 8 July 2008
Available online 17 July 2008

*Keywords:*
Hippocampal neurons
Membranes
Roughness
Morphology
BDNF secretion

ABSTRACT

Membranes have become of great interest for tissue engineering application, since they offer the advantage of developing neuronal tissue that may be used in implantable or *in vitro* hybrid systems for the simulation of brain function. The behaviour of neurons isolated from the hippocampus on membranes with different surface properties was investigated.

The different membranes used as substrates for cell adhesion consisted of polyester (PE), modified polyetheretherketone (PEEK-WC), fluorocarbon (FC) and polyethersulfone (PES), all of which coated with poly-L-lysine (PLL) in order to have the same functional groups interacting with cells. The membranes exhibited different morphological surface properties in terms of pore size, porosity and roughness.

Hippocampal neurons exhibited a different morphology in response to varying the properties of the membrane surface. Indeed, cells grown on the smoother membranes and namely FC and PES membranes displayed a large number of neurites with consequent formation of bundles. As a consequence while a very complex network was formed on these membranes, cells tend to, instead, form aggregates and most of the processes are developed inside the pores of the membranes when rougher PEEK-WC surfaces were used. In addition, the secretion of brain-derived neurotrophic factor (BDNF) was expressed at high levels in neurons grown on FC membranes with respect to the other membranes. Taken together these results suggest the pivotal role played by membrane surface properties in the adhesion and growth of the hippocampal neurons, which must be considered in the development of tailored membranes for neural tissue engineering.



## 1. Introduction

Advances in neural tissue engineering require a comprehensive understanding of neuronal behaviour on biomaterials, which provide mechanical support and guide cell growth in a new tissue or organ. Current interest is focused on attempts to find new biomaterials and new cell sources as well as novel designs of tissue-engineered neuronal devices to generate healthy and more efficacious recovered neuronal elements [1,2]. Among the biomaterials that have been successfully applied in the manufacture of neuronal tissue, polymeric semi-permeable membranes can be used as support for the adhesion of neurons and as a selective barrier for the transport of nutrients to the cells and for the removal of catabolism waste products in implantable or *in vitro* hybrid system [3]. Advances in polymer chemistry have facilitated the engineering of synthetic membranes that can be specifically manipulated with regard to their physical and mechanical characteristics, which may affect the interactions with cells.

In particular, surface properties of polymeric membranes such as surface free energy parameters, roughness and pore size seem to play an important role since they have been shown to influence the viability and metabolic rates of other cells such as isolated hepatocytes [4,5]. With respect to the neural engineering applications, the wettability of the membrane surface has proved to be a factor that affects the growth of neurons from PC-12 cells and meningeal cells [6,7], modulating the adsorption of adhesion proteins contained in the culture medium or secreted by cells that mediate the adhesion of cells to the substrate. The influence of topographical features

* Corresponding author at: Institute on Membrane Technology, National Research Council of Italy, ITM-CNR, C/o University of Calabria, via P. Bucci Cubo 17/C, I-87030 Rende (CS), Italy. Tel.: +39 0984 492036; fax: +39 0984 402103.
*E-mail address:* l.debartolo@itm.cnr.it (L. De Bartolo).

0376-7388/$ – see front matter © 2008 Elsevier B.V. All rights reserved.
doi:10.1016/j.memsci.2008.07.022

on neuronal cell adhesion and differentiation has been studied by using patterned adhesive areas that provide only a fraction of the surface for cell adhesion while the rest is cell-repellent or by using contact guidance cues in combination with also nerve growth factors or electric field [8–10]. Topographic guidance of neuritis outgrowth has been explored *in vitro* with culture substrate containing etches, microchannels, nanotubes or microgrooves [11–15]. Although the topographical influence on the neuronal adhesion and orientation has been investigated by using designed artificial substrates, the effect of microporous membrane surface properties on the growth of primary hippocampal neurons has not still been studied.

In this paper we describe our efforts to investigate how the membrane surface properties influence the behaviour of neuronal cells. We used neurons isolated from hippocampus, which is an important brain area owing to its vital role in the consolidation of several forms of learning and memory and especially during the formation of declarative memories [16,17]. Hippocampal neurons, which are well known for their plasticity and regeneration properties [18], are the best-characterised model for investigating polarization that occurs spontaneously during the first days of culture [19–21].

Polymeric membranes consisted of polyester (PE), modified polyetheretherketone (PEEK-WC), fluorocarbon (FC) and polyethersulfone (PES), with different morphological properties (e.g., pore size, pore size distribution, porosity and roughness) were coated with poly-L-lysine (PLL), in order to have surfaces with the same functional groups but with different morphological properties. PLL was chosen for coating because is the substrate that allows the *in vitro* growth of neuronal cells [22]. The membranes were tested to compare neuronal growth and metabolic behaviour of cells aimed to establish the membrane properties capable of reconstructing the neural network *in vitro*.

In this context, the quantification of brain-derived neuronal factor (BDNF) secretion in these bio-hybrid systems constitutes a key functional marker for developmental hippocampal properties, since this neurotrophic factor with specific cytoskeletal functions appeared to be also responsible for pre-synaptic dendritic arborization of embryonic hippocampal neurons [23]. The properties of membrane surface could be important elements for the application of the membrane bio-hybrid system in neuronal tissue engineering for *in vitro* investigation of *in vivo* environment. The membrane bio-hybrid systems could be potential valuable tools aimed to study and understand cellular mechanisms of neurodegenerative processes and for drug testing.

## 2. Experimental

### 2.1. Membranes

Among the available commercial membranes we have chosen those membranes that were tested previously for culture of other anchorage-dependent cells [5]. Commercial microporous membranes such as PE (Osmonics, USA) and PES (Pall, USA) were used together with dense membranes such as FC (In Vitro Systems & Services, Germany) membranes permeable to oxygen, carbon dioxide and aqueous vapour.

Membranes were also prepared from PEEK-WC or poly(oxa-1,4-phenylene-oxo-1,4-phenylene-oxa-1,4-phenylene-3,3(isobenzofurane-1,3-dihydro-1-oxo)diyl-1,4-phenylene) by inverse phase techniques using the direct immersion precipitation method [24]. PEEK-WC is a chemically stable polymer with excellent thermal and mechanical resistance [25]. PEEK-WC membranes were prepared from 10% (w/w) PEEK-WC polymer, 24% (w/w) PEG (w/w) in dimethylformamide (DMF). After casting, the polymeric films were coagulated in a water bath at $T = 40\,^{\circ}C$. The membranes were washed extensively with water and dried at room temperature [26].

The membranes were modified by coating with PLL (MW 30,000–70,000), dissolved in a boric acid/sodium tetraborate solution (1:1) to a final concentration of 0.1 mg/mL, in order to have the same functional groups over the surfaces with a density of $40\,\mu g/cm^2$. The membranes were coated with poly-L-lysine in PBS and incubated for 3 h and then the excess of PLL solution was removed and dried. Poly-L-lysine-coated polystyrene culture dishes (PSCD) were used as controls. FITC-labelled PLL (Sigma) was used for the visualization and quantification of the membrane coating. Imaging of the FITC-labelled coated membranes were obtained by using an Olympus Fluoview FV300 laser confocal scanning microscope (LCSM) (Olympus Italia). Quantitative analysis was performed on different area of three samples of each investigated coated membrane using Fluoview 5.0 software (Olympus Corporation) by measuring the average intensity of fluorescence. A calibration curve of FITC-labelled PLL was obtained by casting known quantities of the fluorescent protein on defined areas of polystyrene dishes calculating the surface concentrations and capturing confocal images of the dry samples. The thickness of the PLL coating resulted to be $1.2 \pm 0.09\,\mu m$, as measured with FITC-labelled PLL by *Z*-direction scanning at the LCSM.

### 2.2. Membrane characterisation

The morphological properties of the membranes were characterised in terms of mean pore size, pore size distribution, thickness and roughness.

Dried membrane samples were cut and mounted with double-faced conductive adhesive tape and analyzed by environmental scanning electron microscope (Quanta 200F ESEM, FEI, USA). From some selected representative images it was possible to observe the typical morphology of the membranes and namely, the shape and size of membrane pores as well as the pore size distribution.

The roughness of the membrane surfaces after PLL coating was evaluated by using atomic force microscopy (AFM), Nanoscope III (Digital Instruments, VEECO Metrology Group). Tapping Mode™ AFM operated by scanning a tip attached to the end of an oscillating cantilever across the sample surface. The cantilever was oscillated at or near its resonance frequency with amplitude ranging typically from 20 to 100 nm. Silicon probes were used. Surface roughness was estimated with respect to the mean absolute value difference, Ra, and the root mean squared difference, RMS, between the actual surface height and that of the line dividing the surface of the investigated profile into two equal areas. The reported roughness values are the average of 20 measurements on different membrane samples.

The wettability of the membrane, which is an important parameter for cell adhesion, was characterised by means of water dynamic contact angle (DCA) measurements. The contact angle of water droplets was measured at room temperature with a CAM 200 contact angle meter (KSV Instruments, Ltd., Helsinki, Finland). DCA measurements were performed under standardised conditions, which take into account various parameters (e.g., temperature, cleanliness of sample, drop volume). The instrument supported by video camera and software permits precise drop measurements and evolution in time. DCA measurements were performed on native and PLL-coated membranes. At least 30 measurements on different regions of each membrane sample were averaged for each DCA value. Standard deviations are indicated as error bars.

The permeability properties of the membranes were characterised by pure water flux measurements in the absence of solutes

and at different transmembrane pressure ($\Delta P^{TM}$). For each membrane the hydraulic permeance $L_p$, was evaluated before and after modification process with PLL by the following equation [27]:

$$L_P = \left(\frac{J_{Solvent}}{\Delta P^{TM}}\right)_{\Delta c=0}$$

This equation assumes a linear correlation between water flux and the convective driving force.

### 2.3. Cell isolation and culture

The hippocampus of both hemispheres was dissected from the brain of postnatal days 1–3 (PND1–3) hamsters (*Mesocricetus auratus*), removed and collected in falcon tubes in Neurobasal medium A (Invitrogen Corporation, Milan, Italy) containing 0.02% BSA (Sigma, Milan, Italy). The tissue was digested in a Neurobasal medium A containing 0.1% papain (Sigma) and 0.02% BSA (Sigma) for 20 min at 37 °C [28]. Ten minutes after digestion, the tube containing the tissue was mixed and at the end of digestion, the supernatant containing papain was removed and Neurobasal medium A supplemented with B27 (2%, v/v; Invitrogen Corporation, Milan, Italy) penicillin–streptomycin (100 U/mL), glutamine 0.5 mM (Biochrom AG), 5 ng/mL basic fibroblast growth factor (b-FGF; Sigma) was added to the remaining pellet. Samples were gently triturated mechanical by using a sterile Pasteur pipette with a wide opening to dissociate larger aggregates. After sedimentation of the aggregates the supernatant was removed and transferred into tubes containing 1% papain inhibitor in Neurobasal medium A and 1% BSA, as described elsewhere [29]. The samples were centrifuged at 1300 rpm for 10 min at room temperature and cell pellets were gently re-suspended in Neurobasal medium A containing B27 supplement, penicillin–streptomycin, 0.5 mM glutamine, 5 ng/mL b-FGF. Serum-free B27 supplemented Neurobasal medium A seems to have a beneficial effect on the growth and differentiation of hippocampal neurons, as suggested by other researchers [22,30]. The viability of the cells after this isolation procedure was assessed by trypan blue test and resulted to be 97 ± 2%. Cells were seeded on the different membrane surfaces at $2.5 \times 10^5$ cell/cm$^2$ density. Controls without cells were prepared for each kind of substrate. Cells and controls were incubated at 37 °C in an atmosphere containing 5% $CO_2$. Cultures were fed every 4 days replacing half of the medium at each feeding.

### 2.4. Immunofluorescence of neuronal cell cultures

The morphological behaviour of neurons cultured on the different membranes were investigated and compared to PSCD as controls. Representative images of 4 and 16 culture days displaying the distribution of the neuronal cytoskeletric marker, βIII-tubulin, and axon marker, growth-associated protein-43 (GAP-43) that were observed *in vitro* by a LCSM (Fluoview FV300, Olympus, Milan, Italy). Six samples for each substrate were analyzed.

The immunofluorescence method specific for hippocampal cell cultures was conducted by using primary anti-βIII-tubulin followed by secondary antibody conjugated with FITC fluorochrome on samples previously fixed and permeabilized [21,29]. Specifically, the neuronal cells were fixed in paraformaldehyde (4%) for 15 min. Fixed cells were permeabilized with 0.25% Triton X-100 in PBS for 10 min and subsequently blocked with 1% BSA for 30 min at room temperature. The cultures were then rinsed three times with PBS and incubated with the monoclonal antibodies anti-βIII-tubulin (1:100; Sigma, Milan, Italy) and anti-GAP-43 (1:100; Sigma, Milan, Italy) overnight at 4 °C. Afterwards, neuronal cells were rinsed with PBS and incubated with fluorescently labelled secondary antibodies FITC-conjugated (1:100; Invitrogen) and TRICT-conjugated (1:100; Invitrogen) in PBS for 60 min at room temperature. The cells were counterstained with DAPI (200 ng/mL; Sigma, Milan, Italy), mounted by using a fluorescent mounting medium and observed at LCSM.

### 2.5. Neuronal morphology features of the different membranes

The immunofluorescence samples displaying the distribution of βIII-tubulin and GAP-43 in hippocampal cells grown on the different membranes were used in order to analyze *in vitro* some morphological parameters such as the area filled by neurons and axonal length especially at 4 and 16 days, periods in which the different neuronal elements and synaptic complexes, respectively, are fully formed. Quantitative evaluations of these morphological parameters were determined for distinct cell fields (100 μm × 100 μm) at the two different developmental stages. NIH-Scion Image software was used in order to quantify the area filled by neurons, expressed as percentage of the total membrane area, and the axonal length (μm ± S.E.M.).

### 2.6. Sample preparation for SEM

Samples of cell cultures were prepared for scanning electron microscopy (SEM) (Quanta 200F ESEM, FEI, USA) by fixation in 2.5% glutaraldehyde, pH 7.4 phosphate buffer, followed by post-fixation in 1% osmium tetroxide and by progressive dehydration in ethanol. Samples were examined at SEM and representative images displaying both neuronal structural features and adhesive properties on the different membrane surfaces were obtained at 8 days *in vitro.*

### 2.7. Biochemical assays

Neuronal medium was collected from the different cell culture membranes in pre-chilled tubes at critical developmental *in vitro* stages and stored at −80 °C until assays.

The glucose concentration in the medium was detected by using Accu-Chek Active (Roche Diagnostics, Monza, Italy). To assay the neuronal brain-derived neurothrophic factor (BDNF) secretion, a sensitive BDNF ELISAs immunoassay (Promega Corporation, WI, USA) was carried out on samples collected from six different isolations. BDNF Elisa was performed as follows: ELISA plates were coated with 100 μL of anti-BDNF monoclonal antibody overnight at 4 °C. After washing, 100 μL of cell culture supernatant was added to the wells and left for 2 h at room temperature. Thereafter the wells were washed five times and incubated with 100 μL of anti-human BDNF for 2 h at room temperature. After washing five times the wells were covered for 1 h with anti-BDNF antibody horseradish peroxidase conjugate and then 100 μL of tetramethylbenzidine were added for 10 min. The reaction was blocked with 100 μL of 1N HCl and absorbance was measured at 450 nm using a Multiskan Ex (Thermo Lab Systems).

The statistical significance of the experimental results was established according to the ANOVA test followed by Bonferroni *t*-test ($p < 0.05$).

## 3. Results

The membranes displayed a different surface morphology as Fig. 1 shows. All membrane parameters are reported in Table 1. FC membrane exhibits a dense structure without any pore (Fig. 1a). This membrane is permeable to oxygen, carbon dioxide and aqueous vapour. PES membrane surface shows pores with mean size of 0.1 μm (Fig. 1b) and with homogeneous pore distribution. The membrane has a porosity of 74.4 ± 1.6% and a thickness of

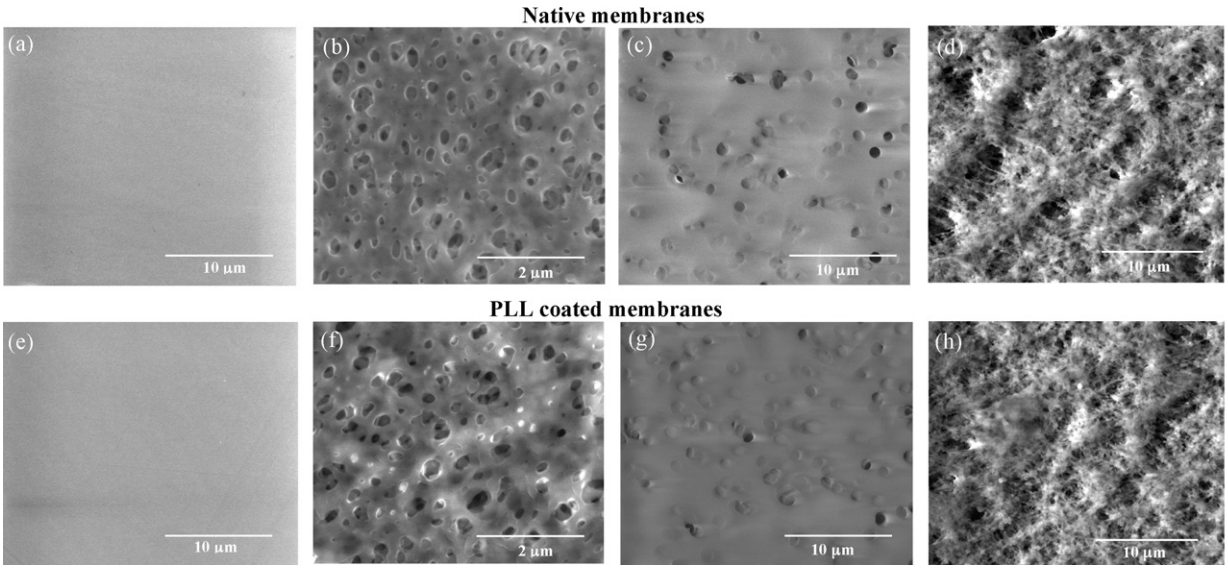


**Fig. 1.** Scanning electron micrographs of native (a–d) and modified (e–h) membrane surfaces: (a, e) FC, (b, f) PES, (c, g) PE and (d, h) PEEK-WC.

**Table 1**
Properties of the investigated membranes

| Membrane | Pore diameter | Porosity (%) | Thickness (μm) | Ra (nm) | Hydraulic permeance (L/(m$^2$ h mbar)) | |
|---|---|---|---|---|---|---|
| | | | | | Native | Modified |
| FC | – | – | 47 ± 6.5 | 6.26 ± 0.91 | – | – |
| PES | 0.1 | 74.4 ± 1.6 | 140 ± 0.5 | 49.38 ± 1.15 | 6.48 ($R^2$ = 0.99) | 6.3 ($R^2$ = 0.99) |
| PE | 0.1 | 79.6 ± 3.6 | 23.86 ± 2.5 | 87.22 ± 1.25 | 126.9 ($R^2$ = 0.98) | 45.2 ($R^2$ = 0.98) |
| PEEK-WC | 0.2 | 71.2 ± 3.1 | 44 ± 2.0 | 199.21 ± 1.05 | 4.0 ($R^2$ = 0.97) | 3.2 ($R^2$ = 0.98) |

140 ± 0.5 μm (Table 1). Pores with round shape and mean diameter of 0.1 μm are regularly distributed over the PE membrane surface (Fig. 1c). These membranes are very thin as evidenced by the thickness value (Table 1). On the other hand PEEK-WC membranes have pores with an elongated shape and mean size of 0.2 μm (Fig. 1d). The porosity of this membrane is also similar to that of the PES membrane. Membrane surfaces seem to maintain their morphological features after coating with poly-L-lysine as we can see from the SEM's images (Fig. 1e–h).

The effective coating of the membranes with PLL was evaluated in the absence of cells by a quantitative analysis using FITC-labelled PLL for detection purposes only. As observed in Fig. 2, the amount of PLL on the different membranes determined by measurements of the average fluorescence intensity was in the range of 40 μg/cm$^2$ and not statistically different among them confirming the similar coating level of all membranes with PLL.

The PLL coating of the membranes modified their native physico-chemical properties as expected (Fig. 3). The advancing and receding contact angles for native FC membranes and PEEK-WC decreased after PLL coating to values, respectively, of

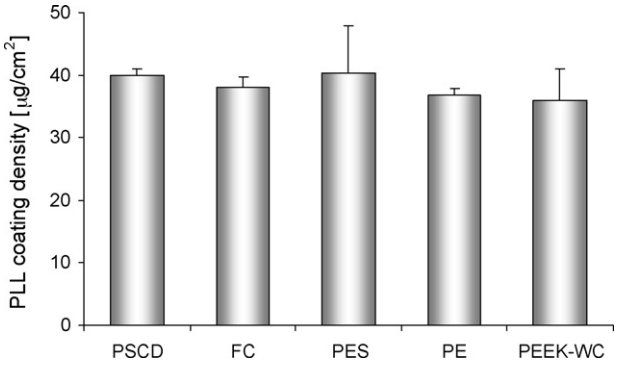


**Fig. 2.** Poly-L-lysine (PLL) density measured on the different substrates after coating with FITC labeled PLL. The values were expressed as μg/cm$^2$ ± S.E.M. and determined with respect to the fluorescence average intensity measured on PLL-coated PSCD. Data were expressed as μg/cm$^2$ ± S.E.M.

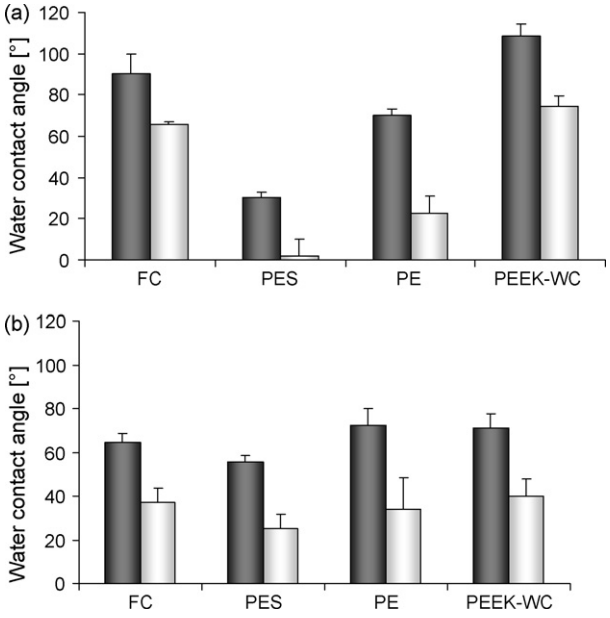


**Fig. 3.** Advancing (full bar) and receding (empty bar) contact angle measured on: (a) native membranes and (b) PLL-coated membranes.

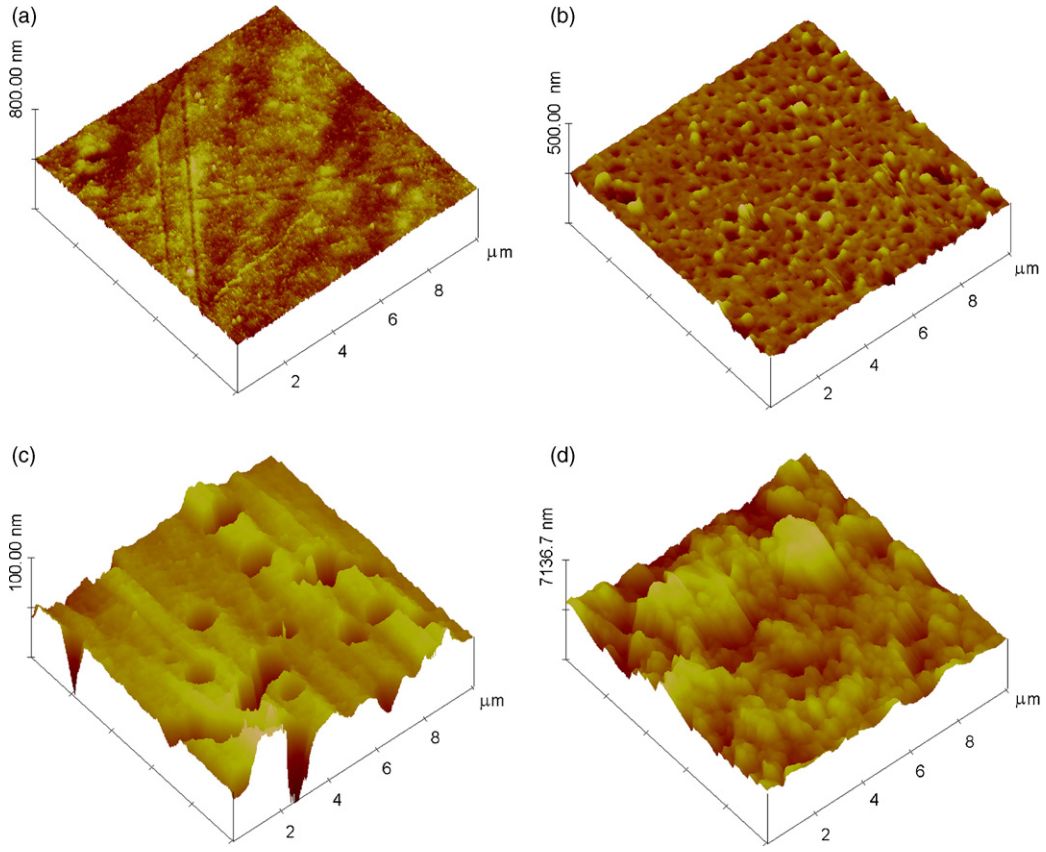


**Fig. 4.** AFM micrographs of the modified membrane surfaces: (a) FC, (b) PES, (c) PE and (d) PEEK-WC.

$\theta_{adv} = 64.3 \pm 4.1^\circ$ and $\theta_{rec}$ $36.9 \pm 6.4^\circ$ for FC and $\theta_{adv} = 71.3 \pm 6.1^\circ$ and $\theta_{rec}$ $40.2 \pm 7.5^\circ$ for PEEK-WC. Native PES membranes have a very high hydrophilic surface character in fact the water contact angle measured on this membrane was $30.6 \pm 1.2^\circ$. Also the modified membranes display a marked wettability even if, in this case, the PLL coating induced a reduction in the surface hydrophilic character. The wettability of the PE membranes did not change significantly after PLL coating as show the values of water contact angles.

The topographical images of the modified membranes show surfaces with nanostructures, which confer rougher profile to the surfaces (Fig. 4). The FC (Fig. 4a) and PEEK-WC membranes (Fig. 4d) appeared to be respectively smoother and rougher with respect to the other membranes. The evaluation of the average roughness reported in Table 1 confirmed the rougher profiles of the AFM images: in fact membranes have different values of average roughness ranging from 6 to 200 nm.

The membranes exhibited also different permeability properties, which are important for the transport through the membranes (Table 1). The observed steady-state hydraulic permeance of the investigated membranes was calculated accordingly as the slope of the flux $J$ versus the transmembrane pressure ($\Delta P^{TM}$) straight line. PE membrane was more permeable with respect to PES and PEEK-WC membranes. This result is in a good agreement with the small value of membrane thickness that for porous membranes is inversely related to the water flux. The coating reduced the hydraulic permeance of 64% for PE membranes and 20% for PEEK-WC membranes. No significant changes were observed in the hydraulic permeance of the PES membranes after coating.

After characterization of morphological and permeability properties, the membranes were used for cell culture experiments. It is particular interesting to note that the isolated hippocampal neurons adhered successfully to the different surfaces. In Figs. 5 and 6 are reported the micrographs of hippocampal neurons on FC membranes and on PSCD (control). Both substrates have characteristics of transparency therefore permitted the online observation of the cells with time by an inverse light microscope. During the first hours of culture a flattening of the cells was observed as well as minor processes starting to emerge from several sites along the circumference of the cells (Figs. 5a and 6a ). With the progress of their growth period (Figs. 5b and 6b), the tiny neuronal filaments begin to acquire the definite characteristics of dendrites and axons and subsequently the formation of synaptic contacts develop into a rich neuronal network (Figs. 5c and 6c). The complexity of the neuronal network increased with time: dendrites emerging from the cell body became highly branched (Figs. 5d and 6d).

Fig. 7 shows the adhesion of the isolated hippocampal neurons to the different surfaces. On day 4 of culture the area covered by cells was moderately ($p < 0.05$) higher for FC, PES membranes as well as PSCD, whereas neurons grown on PE and PEEK-WC substrates adhered to a lesser extent than that of the other membranes. Neurons on the FC membranes (Fig. 8b) as well as on PSCD (control) (Fig. 8a) developed axons and highly branched dendrites and formed a complex network of neurite bundles. A similar morphology was also displayed by cells on PES membranes: the cells formed an axonal network at high density and highly branched processes plus the development of large neurite bundles (Fig. 8c). On the PE membrane surface, cells adhered forming processes over the membrane surface that established intercellular contacts (Fig. 8d). Conversely, on the PEEK-WC membranes cells developed short neurites with the tendency to grow into the pores of the membrane surface (Fig. 8e). The area covered by cells increased with time

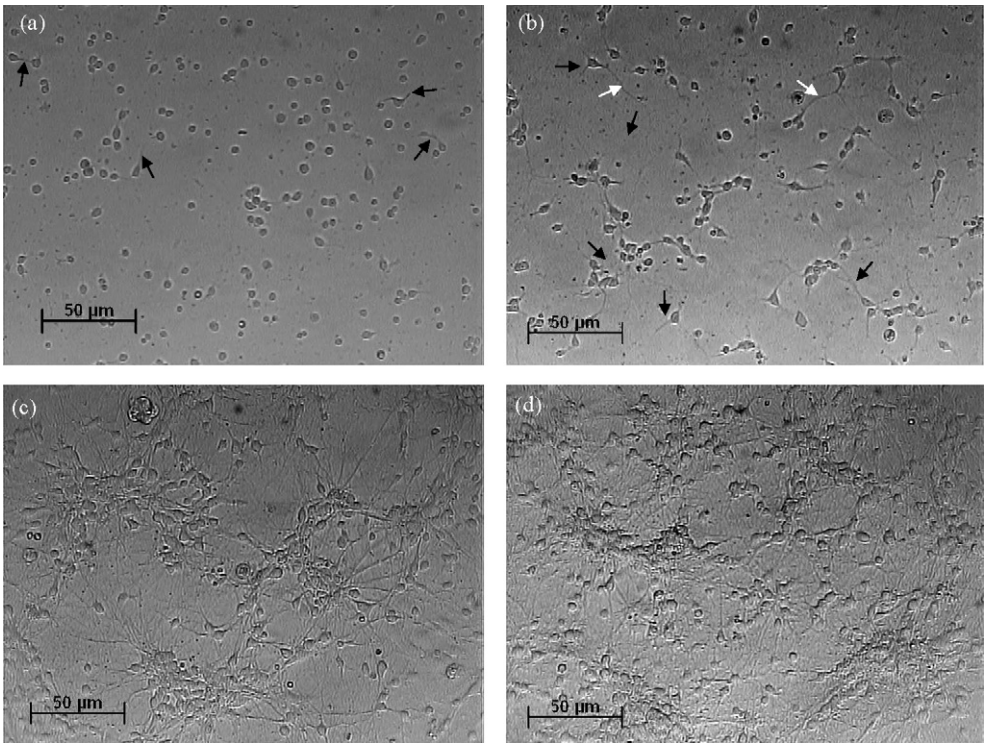


**Fig. 5.** Micrographs of hippocampal neurons on FC membrane after: (a) 4 h, (b) 3 days, (c) 8 days and (d) 16 days of culture. The arrows in (a) indicate the emerging processes from the cell circumference; the arrows in (b) indicate the axon (black) and the dendrites (white).

and after 16 days the FC and PES membranes similarly to PSCD supported the growth of hippocampal neurons (Fig. 7).

The confocal images of the neurons on the different surfaces showed the localization of βIII-tubulin (green) in the neuronal network (Fig. 9). This cytoskeletal protein was present in the soma and in all neuronal processes, while the axonal growth cones were visualized through the localization of GAP-43 (red), a specific protein involved in the regulation of axonal outgrowth. On FC (Fig. 9c and d) and PES membranes (Fig. 9e and f) cells tended to show a somatic morphology that was comparable to that of neurons grown

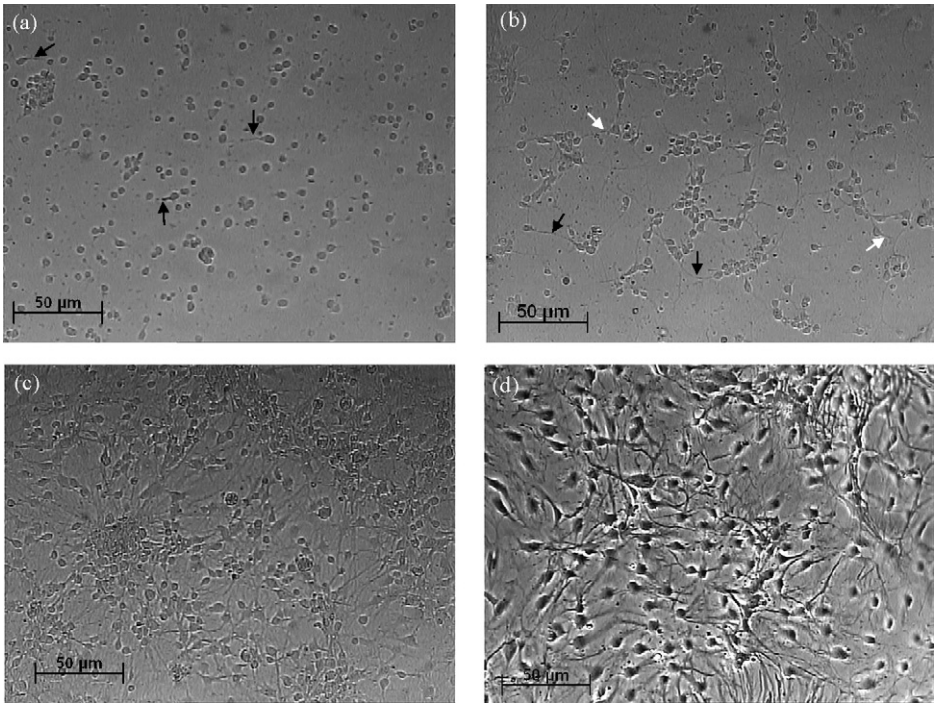


**Fig. 6.** Micrographs of hippocampal neurons on PSCD after: (a) 4 h, (b) 3 days, (c) 8 days and (d) 16 days of culture. The arrows in (a) indicate the emerging processes from the cell circumference; the arrows in (b) indicate the axon (black) and the dendrites (white).

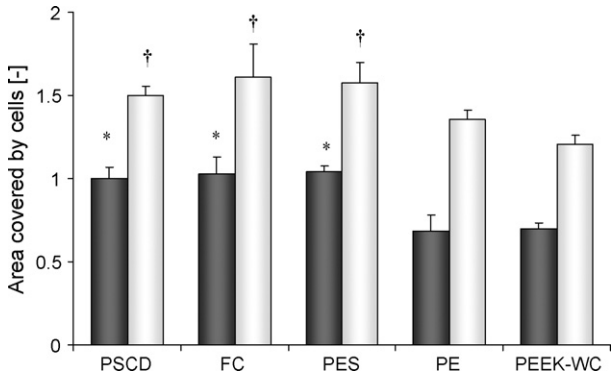


**Fig. 7.** Area covered by hippocampal neurons after 4 days (full bar) and 16 days (empty bar) of culture on the different surfaces. The data normalised with respect to the value of PSCD were expressed as average ± S.E.M. and evaluated according to ANOVA followed by Bonferroni *t*-test. $^{*}p < 0.05$ versus PE and PEEK-WC membranes; $^{\dagger}p < 0.05$ versus PEEK-WC membranes.

on PSCD substrates in spite of longer axons developed at 4 days of culture (Fig. 9a and e). Quantitative analysis confirmed that hippocampal axons were moderately longer on FC and PES membranes along with PSCD than those developed on the other two substrates after 4 days (Fig. 10). Interestingly axonal growth continued in time above all for smooth surfaces as demonstrated by moderately longer axons with respect to rougher substrates after 16 days of culture (Fig. 10). A complex neuronal network was achieved after 16 days of culture, as demonstrated by moderately longer axons measured on smoother membranes with respect to rougher substrates (Fig. 9d and f). In the case of PE (Ra = 87.2 nm), neuronal formations only developed above the membrane surface and the cells exhibited a good neurite outgrowth but a lower degree of fasciculation with respect to FC and PES membranes (Fig. 9g and h). Conversely, in the case of PEEK-WC membranes (Ra = 200 nm), the smaller cells with respect to other membranes tended to aggregate and develop their processes into the pores of the membrane surface (Fig. 9i–l).

It is worthy to note that the altered levels of some of the major metabolic activities and namely glucose consumption and BDNF secretion support the conservation of vital cell function at different growth periods (Fig. 11a and b). A comparison of the glucose consumption of cells among the membranes showed high level of glucose consumption on day 4 of *in vitro* culture on FC, PES and PE membranes as well as on PSCD. Cells on PEEK-WC displayed low rate of glucose consumption. The glucose uptake decreased with time for all substrates reaching on day 16 values of 256 and 242 μg/mL millioncell on FC and PES membranes respectively (Fig. 11a). The evaluation of the metabolic activity showed that cells maintained their function in terms of BDNF secretion at different levels throughout the entire culture period, depending on the membrane surface (Fig. 11b). The production of cellular BDNF was detected up to 16 days of culture. On FC membranes as well as on PSCD, cells exhibited significantly high levels of BDNF on days 4 and 8 of *in vitro* culture. The synthesis of BDNF on PSCD decreased from 51.8 pg/mL millioncell (day 4) to 3.9 pg/mL millioncell (day 16) whereas on FC the secretion of BDNF on day 16 was 17.55 pg/mL millioncell on day 16 of culture (Fig. 11b).

## 4. Discussion

The main objective of this study was to compare the adhesion and growth of primary neurons isolated from the hippocampus on membranes with different surface properties. The membranes were modified by coating with PLL in order to minimize their native different physico-chemical properties and to have the same functional groups interacting with cells. Membranes after coating displayed different morphology in terms of pore size, porosity and roughness.

The dynamic contact angles of the native membranes evidenced the different physico-chemical properties of these substrates. As the advancing and receding contact angles are respectively a measure of the apolar and polar aspect of the surfaces, it is interesting to note the difference of these properties among the investigated membranes. The PLL coating led significant changes in the wettabilities of the membranes yielding more homogenous surfaces with respect to their native character. An appreciable hysteresis was also observed on the membrane surface, which is caused by the surface roughness, microporosity, the heterogeneous distribution of polar and apolar domains over the surface as well as reorientation of groups in the surface under the influence of the liquid phase.

The results of the membrane characterisation displayed the effective PLL coating performed on all investigated surfaces that shown a similar PLL density (Fig. 2).

Neurons shown the capacity to respond to the different membranes, they adhered, polarised and developed neurites differently on the basis of the topographical characteristics of the surface. Neurons are unpolarised cells after isolation they polarised and establish axons and dendrites during the first days of culture (Figs. 5 and 6). Neuronal cells on the different membranes used in the present study displayed the typical morphology of hippocampal neurons that included a primary apical dendrite with multiple ramifications, very thin axons plus a discretely flattened soma. On membranes with surface roughness of 6–50 nm such as FC (Ra = 6.26 nm) and PES membranes (Ra = 49.38 nm), neurons reached a well-developed state as shown by their large soma and ramification of their extending processes (Figs. 8b and c and 9c–f). The density of axonal network increases the neuritis become more elaborate and highly branched on the smooth surfaces. In the case of PE and PEEK-WC membranes, the neurons were less developed as demonstrated by the round-shaped soma and poorly branched processes. Therefore the smooth membranes seem to be more supportive of neurite outgrowth modulating the development process of the neurons. Probably the roughness of the surface may either influence cell motility or hinder the extension and ramification of neuronal processes that emerge from the cell soma or guide the adsorption of adhesion proteins necessary for the interaction with membrane surfaces. Other studies *in vitro* support the importance of topography in the nerve growth and regeneration [31,32]. Neurons have been shown to adhere, migrate and orient their axons to navigate surface features such as grooves in substrates in the micro- and nano-scales [33]. Aebischer et al. [34] observed that smooth inner walls of polymeric channels induced the formation of discrete nerve cables with a number of myelinated axons within an organized fibrin matrix in contrast with rough inner walls that elicited the formation of scattered nerve fascicles in an organized fibrin matrix. Other authors found an optimal surface with roughness in the range of 50 nm for the attachment of primary neurons isolated from the substantia nigra [35]. Our results obtained with hippocampal cells show an improved neuronal growth on smooth surfaces such as FC and PES membranes.

The correct and stable hippocampal neuronal formation is supported by the evaluation of some major cytoskeletal markers such as βIII-tubulin and GAP-43. Indeed, the constantly intense distribution of βIII-tubulin, specific for neuronal processes and soma, up to 16 days of culture, underlies the strong capability of FC and PES membranes to assure well defined plus, above all, orderly structured neuronal networks for a greater period of time more than that supplied by other substrates [36]. This constant expression of βIII-tubulin turns out to be very important since like others have reported cytoskeletal proteins are involved in basic cellular activi-

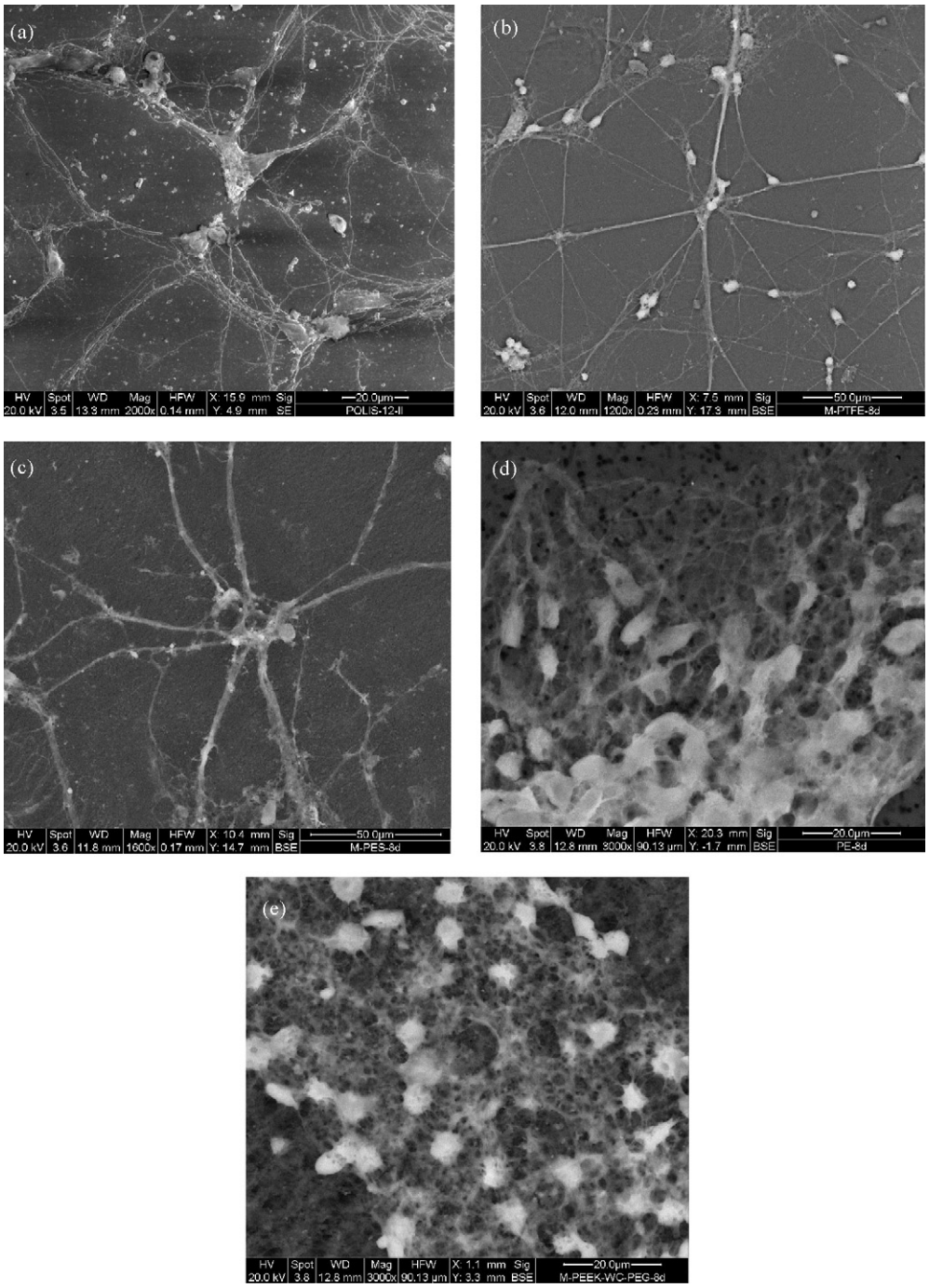


**Fig. 8.** SEM's images of hippocampal neurons on: (a) PSCD, (b) FC, (c) PES, (d) PE and (e) PEEK-WC after 8 days of culture.

ties that include cell–cell interaction, cell adhesion and migration and any eventual damage may lead to the total degradation of neuronal processes [37,38]. It is worthy to note that even the axonal marker GAP-43, noted for the stabilization of actin in both long axons as well as the growth cone [39], resulted to be very intensely and specifically distributed in the axon along with its growth cone, which further confirms its highly application value.

The evaluation of the metabolic activity of neurons on membranes demonstrated that cells adhered on the membranes are functionally active for 16 days of culture. Differences in cell metabolism in terms of glucose consumption and BDNF secretion were measured among the investigated membranes. Notable levels of glucose consumption considered throughout the entire culture period in this study, demonstrate that the cells adhering to the membranes are also functionally active. A low ability to uptake glucose was measured on PEEK-WC membrane on days 4 and 8 of *in vitro* culture. Indeed, both at the beginning of neuronal growth (day 4) and at the later phases (day 16), cells on FC, PES and PE membranes exhibited high glucose consumption. In this context the secretion of BDNF, mammalian neurotrophin belonging to a family of structurally related dimeric proteins, is a further confirmation of the viable status of hippocampal neurons throughout the culture period. Hippocampal neurons exhibited high levels of BDNF secretion on FC membranes where cells formed highly branched neurites

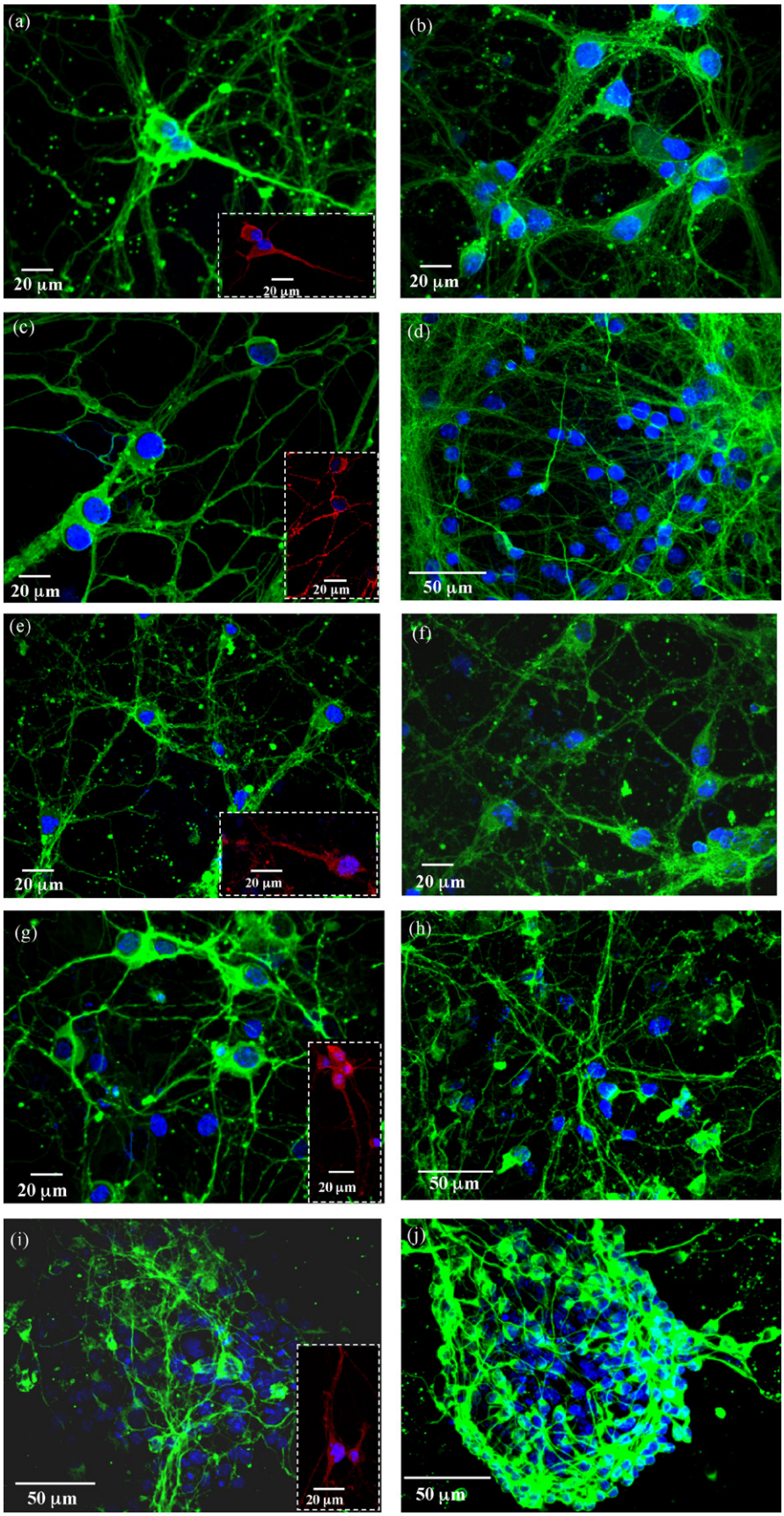


**Fig. 9.** Confocal laser micrographs of hippocampal neurons traced for entire culture period and from representative images after 4 days (a, c, e, g and i) and 16 days (b, d, f, h and l) of culture it was possible to evaluate the distribution of βIII-tubulin (green) and the axonal marker GAP-43 (red) on: (a and b) PSCD, (c and d) FC, (e and f) PES (g and h) PE and (i–l) PEEK-WC membranes. Cell nuclei were labeled with DAPI (blue). (For interpretation of the references to color in this figure legend, the reader is referred to the web version of the article.)

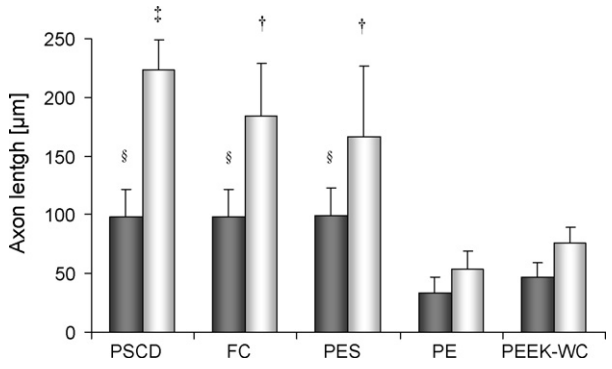


**Fig. 10.** Axonal length of hippocampal neurons after 4 (full bar) and 16 days (empty bar) of culture on the different surfaces. Data were expressed as µm ± S.E.M. and evaluated according to ANOVA followed by Bonferroni *t*-test. §$p < 0.05$ versus PE and PEEK-WC membranes; †$p < 0.05$ versus PE and PEEK-WC membranes; ‡$p < 0.05$ versus all.

and a more complex network. The secretion of BDNF was high up to 8 days of culture, which corresponds to the maturation stage of hippocampal cells. It is widely known that this class of mammalian neurotrophins expressed at the central nervous system level plays a critical role in the survival, differentiation and maintenance of specific neuronal populations [40]. As a consequence, the elevated production of such a cellular protein at the brain level accounts for its involvement in processes such as the enhancement of synaptic transmission and the expression of other neurotrophins [41]. Moreover this neurotrophin is distributed not only along dendrites and therefore located postsynaptically but also presynaptically along the axon.

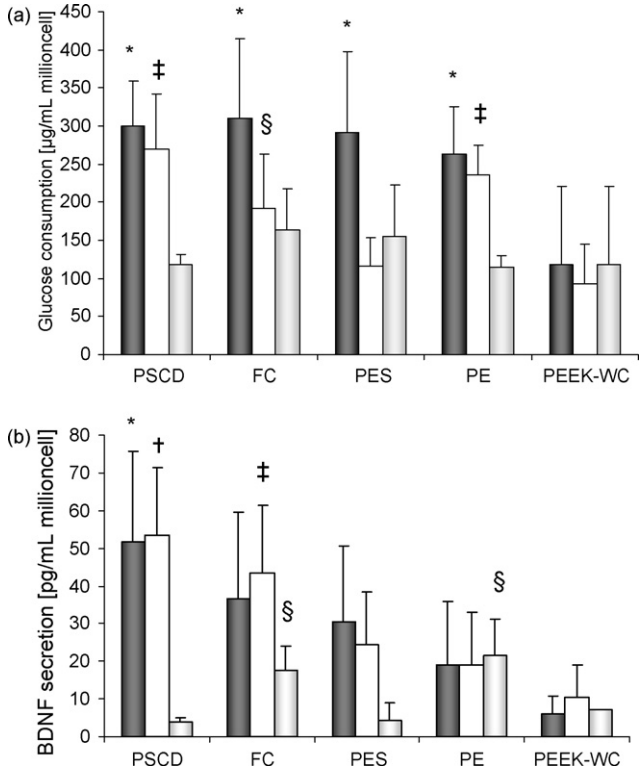


**Fig. 11.** Metabolic activity of hippocampal neurons cultured on the different membranes. (a) Glucose consumption of hippocampal neurons on the different membranes on day 4 (black bar), day 8 (white bar) and day 16 (grey bar) of culture. The values expressed as µg/mL millioncell ± S.E.M. are the mean of 6 experiments and evaluated according to ANOVA followed by Bonferroni *t*-test. *$p < 0.05$ versus PEEK-WC; ‡$p < 0.05$ versus PES and PEEK-WC; §$p < 0.05$ versus PEEK-WC. (b) BDNF secretion of hippocampal neurons on the different membranes on day 4 (full bar), day 8 (empty bar) and day 16 (grey bar) of culture. Data were expressed as pg/mL millioncell ± S.E.M. and evaluated according to ANOVA followed by Bonferroni *t*-test. *$p < 0.05$ versus PE and PEEK-WC; †$p < 0.05$ versus PES, PE and PEEK-WC; ‡$p < 0.05$ versus PE and PEEK-WC; §$p < 0.05$ versus PSCD, PES and PEEK-WC.

## 5. Conclusions

This study reports the effect of the membrane surface properties on the development of neurons isolated from hippocampus and on the potentiality of applying membrane bio-hybrid system in neural tissue engineering. Neuronal cells respond to the different membrane surface by changing their morphology and neurite outgrowth. Smooth membranes tend to strongly favor the formation of well-polarised neuronal structures as confirmed by βIII-tubulin immunoreactivity, which specifically points to the unaltered cytoskeletal features of cells throughout their development processes. In agreement with morphologically integral neurons, the specific metabolic functions as displayed by the elevated secretion of BDNF corroborate the high expression of neurotrophin secretion on a smoother membrane surface up to maturation stage of hippocampal cells (8 days). The main finding of this study encourages the development of a membrane engineering system of hippocampal neurons, which is able to remodel and regenerate neural tissue in a well-controlled microenvironment. From a future perspective view, the surface characteristics of the membrane to be used in a neural tissue engineered construct have to be precisely engineered to combine physical and chemical stimuli aimed to develop neuronal network.

## Acknowledgement

This work was supported by grants from the European Commission through the Livebiomat project STREP NMP3-CT-013653 in the FP6.

## References

[1] C.E. Schmidt, J.B. Leach, Neural tissue engineering: strategies for repair and regeneration, Annu. Rev. Biomed. Eng. 5 (2003) 293.
[2] N. Zhang, H. Yan, X. Wen, Tissue-engineering approaches for axonal guidance, Brain Res. Rev. 49 (2005) 48.
[3] E. Drioli, L. De Bartolo, Membrane bioreactor for cell tissues and organoids, Artif. Organs 30 (2006) 793.
[4] L. De Bartolo, G. Catapano, C. Della Volpe, E. Drioli, The effect of surface roughness of microporous membranes on the kinetics of oxygen consumption and ammonia elimination by adherent hepatocytes, J. Biomater. Sci.: Polym. Edn. 10 (1999) 641.
[5] L. De Bartolo, S. Morelli, A. Bader, E. Drioli, Evaluation of cell behaviour related to physico-chemical properties of polymeric membranes to be used in bioartificial organs, Biomaterials 23 (2002) 2485.
[6] A.J. Lee, G. Knang, Y.M. Lee, H.B. Lee, The effect of surface wettability on induction and growth of neuritis from the PC-12 cell on a polymer surfaces, J. Colloid Interf. Sci. 259 (2003) 228.
[7] M.E. Manwaring, R. Biran, P.A. Tresco, Characterisation of rat meningeal cultures on materials of differing surface chemistry, Biomaterials 22 (2001) 3155.
[8] N. Gomez, Y. Lu, S. Chen, C.E. Schmidt, Immobilized nerve growth factor and microtopography have distinct effects on polarization versus axon elongation in hippocampal cells in culture, Biomaterials 28 (2007) 271.
[9] N.M. Dowell-Mesfin, M.-A. Abdul-Karim, A.M.P. Turner, S. Schanz, H.G. Craighead, B. Roysam, J.N. Turner, W. Shain, Topographically modified surfaces affect orientation and growth of hippocampal neurons, J. Neural Eng. 1 (2004) 78.
[10] C.E. Schmidt, V.R. Shastri, J.P. Vacanti, R. Langer, Stimulation of neurite outgrowth using an electrically conducting polymer, Proc. Natl. Acad. Sci. U.S.A. 94 (1997) 8948.
[11] I. Ahmed, H.Y. Liu, P.C. Mamiya, A.S. Ponery, A.N. Babu, T. Weik, M. Schindler, S. Meiners, Three-dimensional nanofibrillar surfaces covalently modified with tenascin-C-derived peptides enhance neuronal growth *in vitro*, J. Biomed. Mater. Res. A 76 (2006) 851.
[12] F. Yang, R. Murugan, S. Wang, S. Ramakrishna, Electrospinning of nano/micorscale poly(L-lactic acid) aligned fibers and their potential in neural tissue engineering, Biomaterials 26 (2005) 2603.

[13] V. Lovat, D. Pantarotto, L. Lagostena, B. Cacciari, M. Gandolfo, M. Righi, G. Spalluyo, M. Prato, L. Ballerini, Carbon nanotube substrates boorst neuronal electrical signaling, Nano Lett. 5 (2005) 1107.
[14] J. Norman, T. Desai, Methods for fabrication of nanoscale topography for tissue engineering scaffolds, Ann. Biomed. Eng. 34 (2006) 89.
[15] G.N. Li, D. Hoffman-Kim, Tissue-engineered platforms of axon guidance, Tissue Eng. B 14 (2008) 33.
[16] M.A. Linch, Long-term potentiation and memory, Physiol. Rev. 84 (2004) 87.
[17] D. Gaffan, What is a memory system? Horel's critique revisited, Behav. Brain Res. 127 (2001) 5.
[18] M. Canonaco, M. Madeo, R. Alò, G. Giusi, T. Granata, A. Carelli, A. Canonaco, R.M. Facciolo, The histaminergic signaling systems exerts a neuroprotective role against neurodegenerative-induced processes in the hamster, JPET 315 (2005) 188.
[19] G.C. Dotti, C.A. Sullivan, G.A. Banker, The establishment of polarity by hippocampal neurons in culture, J. Neurosci. 8 (1988) 1454.
[20] Y. Fukata, T. Kimura, K. Kaibuchi, Axon specification in hippocampal cells, Neurosci. Res 43 (2002) 305.
[21] K. Goslin, G. Banker, Experimental observations on the development of polarity by hippocamapl neurons in culture, J. Cell Biol. 108 (1989) 1507.
[22] B. Ahlemeyer, E. Baumgart-Vogt, Optimized protocols for the simultaneous preparation of primary neuronal cultures of the neocortex, hippocampus and cerebellum from individual newborn (P0.5) C57Bl/6J mice, J. Neurosci. Methods 149 (2005) 110.
[23] M.J. Chen, T.V. Nguyen, C.J. Pike, A.A. Russo-Neustadt, Norepinephrine induces BDNF and activates the PI-3K and MAPK cascades in embryonic hippocampal neurons, Cell Signal 19 (2007) 114.
[24] K. Kimmerle, H. Strathmann, Analysis of the structure-determining process of phase inversion membranes, Desalination 79 (1990) 283.
[25] H.C. Zang, T.L. Chen, Y.G. Yuan. Chin. Patent CN 85, 108, 1987, 751.
[26] L. De Bartolo, S. Morelli, M.C. Gallo, C. Campana, G. Statti, M. Rende, S. Salerno, E. Drioli, Effect of isoliquiritigenin on viability and differentiated functions of human hepatocytes on PEEK-WC-polyurethane membranes, Biomaterials 26 (2005) 6625.
[27] M. Mulder, Basic Principles of Membrane Technology, Kluwer Academic Publishers, Dordrecht/Boston/London, 1991.
[28] C. Xie, W.R. Markesbery, M.A. Lovell, Acrolein a product of lipid peroxidation, inhibits glucose and glutamate uptake in primary neuronal cultures, Free Radic. Biol. Med. 29 (2000) 714.
[29] L. De Bartolo, M. Rende, G. Giusi, S. Morelli, A. Piscioneri, M. Canonaco, E. Drioli, Membrane bio-hybrid systems: a valuable tool for the study of neuronal activities, in: M. Canonaco, R.M. Facciolo (Eds.), Evolutionary Molecular Strategies and Plasticity Research Signpost, 2007, pp. 379–396.
[30] G.J. Brewer, Isolation and culture of adult rat hippocampal neurons, J. Neurosci. Methods 71 (1997) 143.
[31] M.J. Mahoney, R.R. Chen, J. Tan, W.M. Saltzman, The influence of microchannels on neurite growth and architecture, Biomaterials 26 (2005) 771.
[32] C.J. Peng, K.D. Nelson, R. Eberhart, G.M. Smith, Permeable guidance channels containing microfilament scaffolds enhance axon growth and maturation, J. Biomed. Mater. Res. A 75 (2005) 374.
[33] N.M. Dowell-Mesfin, M.A. Abdul-Karim, J.N. Turner, W. Shain, Topographically modified surfaces affect orientation and growth of hippocampal neurons, J. Neural Eng. 1 (2004) 78.
[34] P. Aebischer, V. Huenard, R.F. Valentini, The morphology of regenerating peripheral nerves is modulated by the surface microgeometry of polymeric guidance channels, Brain Res. 531 (1990) 211.
[35] Y.W. Fan, F.Z. Cui, L.N. Chen, Y. Zhai, Q.Y. Xu, I.S. Lee, Adhesion of neural cells on silicon wafer with nanotopographic surface, Appl. Surf. Sci. 187 (2002) 213.
[36] T.H. Young, W.W. Hu, Covalent bonding of lysine to EVAL membrane surface to improve survival of cultured cerebellar granule neurons, Biomaterials 24 (2003) 1477.
[37] C.A. Blizzard, M.A. Haas, J.C. Vickers, T.C. Dickson, Cellular dynamics underlying regeneration of damaged axons differs from initial axon development, Eur. J. Neurosci. 26 (2007) 1100.
[38] R.S. Chung, G.H. McCormack, A.E. King, A.K. West, J.C. Vickers, Gluatamate induces rapid loss of axonal neurofilamnet proteins from cortical neurons *in vitro*, Exp. Neurol. 193 (2005) 481.
[39] R. Kowara, M. Ménarda, L. Browna, B. Chakravarthya, Co-localization and interaction of DPYSL3 and GAP43 in primary cortical neurons, Biochem. Biophys. Res. Commun. 363 (2007) 190.
[40] G.R. Lewin, Y.A. Barde, Physiology of the neurotrophins, Annu. Rev. Neurosci. 19 (1996) 289.
[41] D.C. Lo, Neurotrophic factors and synaptic plasticity, Neuron 15 (1995) 979.